

https://dspace.org/

Removal of toxic metals and recovery of acid from acid mine drainage using acid retardation and adsorption processes

Nleya, Yvonne

2016

http://hdl.handle.net/10539/21051

Nleya, Yvonne (2016) Removal of toxic metals and recovery of acid from acid mine drainage using acid retardation and adsorption processes University of Witwatersrand, Johannesburg, <http://wiredspace.wits.ac.za/handle/10539/21051>

Downloaded from a DSpace repository. https://dspace.org/



REMOVAL OF TOXIC METALS AND RECOVERY OF ACID FROM ACID MINE DRAINAGE USING ACID RETARDATION AND ADSORPTION PROCESSES

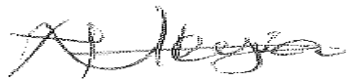
Yvonne Nleya

A dissertation submitted to the Faculty of Engineering and the Built Environment, University of Witwatersrand, Johannesburg, in fulfillment of the requirements for the degree of Master of Science in Engineering.

Johannesburg, 2016

DECLARATION

I declare that this dissertation is my own unaided work. It is being submitted to the degree of Master of Science in Engineering to the University of the Witwatersrand, Johannesburg. It has not been submitted before for any other degree or examination in any other University.



15th day of April, 2016

ABSTRACT

The remediation of acid mine drainage (AMD) has received much attention over the years due to the environmental challenges associated with its toxic constituents. Although, the current methods are able to remediate AMD, they also result in the loss of valuable products which could be recovered and the financial benefits used to offset the treatment costs. Therefore, this research focused on the removal of toxic heavy metals as well as the recovery of acid using a low cost adsorbent and acid retardation process, respectively. In the first aspect of the study, three low cost adsorbents namely zeolite, bentonite clay and cassava peel biomass were evaluated for metal uptake. The adsorption efficiencies of zeolite and bentonite, was found to be less than 50% for most metal ions, which was lower compared to the 90% efficiency obtained with cassava peel biomass. Subsequently, cassava peel biomass was chosen for further tests.

The metal removal efficiency using the cassava biomass was in the order Co^{2+}> Ni^{2+}> Ca^{2+}> Mn^{2+}> Fe^{3+}> Mg^{2+}. The highest metal removal was attained at 2% adsorbent loading and 30 ˚C solution temperature. Amongst the equilibrium models tested, the experimental data was found to fit well with the Langmuir isotherm model. Column studies using the immobilized cassava waste biomass suggested that the breakthrough curves of most metal ions did not resemble the ideal breakthrough curve, due to the competitive nature of the ions present in the AMD used in this study. However, the experimental data from the column tests was found to correlate well with the Adam-Bohart model. Sulphuric acid recovery from the metal barren solution was evaluated using Dowex MSA-1 ion exchange resins. The results showed that sulphuric acid can be recovered by the resins via the acid retardation process, and could subsequently be upgraded to near market values of up to 70% sulphuric acid using an evaporator. Water of re-usable quality could also be obtained in the acid upgrade process. An economic evaluation of the proposed process also showed that it is possible to obtain revenue from sulphuric acid which could be used to offset some of the operational costs.

PUBLICATIONS AND PRESENTATIONS

Journal Publications

1. Nleya, Y., Simate, G.S., Ndlovu, S., 2015. Sustainability assessment of the recovery and utilisation of acid from acid mine drainage. Journal of Cleaner Production 113, pp 17 – 27.
2. Nleya, Y., Ndlovu, S., Simate, G.S., 2015. Removal of toxic metals and recovery of acid from acid mine drainage using adsorption and acid retardation processes. Water Research, *Submitted for publication*

Conference Proceedings

1. Nleya, Y; Ndlovu, S; Simate, G.S., 2014. The recovery of valuable materials from acid mine drainage using adsorption and acid retardation processes. SAMMRI Hydrometallurgy Symposium, University of Cape Town, South Africa, 3rd – 6th August, 2014.

ACKNOWLEDGEMENTS

I would like to extend my most heartfelt gratitude to my supervisors Professor S. Ndlovu and Dr. G.S. Simate for their willingness to impart valued knowledge and constant motivation in carrying out this research.

I would also like to express my appreciation to the Dow Chemical Company and Ecca (a member of IMERYS Minerals Ltd) Holdings for supplying the ion exchange resins and bentonite samples used in this project. Mr E. du Toit and Mr V. Donnelly are gratefully acknowledged for facilitating the supply of the samples. Much appreciation also goes to Mr E.M. Peters for his insightful comments on this project. I would also like to acknowledge the financial support I received from the National Research Foundation (NRF) and the University of the Witwatersrand (Wits)'s postgraduate merit award (PMA), which gave me the opportunity to carry out this project.

I am grateful to my family for their support, love and encouragement. To my mother for continually challenging me and reminding me to give it my best all the time. I am immensely grateful to my friends for their love, support and company without which this project would have been very difficult. My regards also go to the support staff in the School of Chemical and Metallurgical Engineering for their technical assistance. My colleagues in the Metal Extraction and Recovery group are also greatly acknowledged for their unwavering support and help throughout the project and life at Wits.

Finally, I would like to give my heartfelt thanks to God for blessing me with the wonderful people that surrounded me during my study and also for blessing me with favour, strength and good health to complete it.

TABLE OF CONTENTS

DECLARATION ii

ABSTRACT iii

PUBLICATIONS AND PRESENTATIONS iv

ACKNOWLEDGEMENTS v

TABLE OF CONTENTS vi

LIST OF FIGURES xi

LIST OF TABLES xv

CHAPTER ONE 1

INTRODUCTION 1

1.1 General Introduction 1

1.2 Problem statement 4

1.3 Aim and Objectives 4

1.4 Key research questions 5

1.5 Research methodology 5

1.6 Dissertation layout 6

CHAPTER 2 8

LITERATURE REVIEW 8

2.1 General introduction 8

2.2 Formation and constituents of AMD 8

2.3 Environmental and ecological impact of AMD 11

2.3.1 Impact of low pH 12

2.3.2 Effect of high sulphate levels 13

2.3.3 Impact of dissolved metals 14

2.3.4 Impact of solid precipitate from AMD 17

2.4 Source control of AMD 18

2.4.1 Flooding/sealing of underground mines 19
2.4.2 Underground storage of mine tailings 19
2.4.3 Depyritization 20
2.4.4 Mine Capping 20
2.4.5 Blending of mineral wastes 21
2.4.6 Application of anion surfactants 21
2.5 Treatment options for AMD 22
2.5.1 Active treatment methods 22
2.5.2 Passive treatment technologies 24
2.6 Recently developed methods 27
2.6.1 CSIR Alkali-Barium-Calcium (ABC) Process 27
2.6.2 SAVMIN Process 29
2.6.3 SPARRO process 30
2.6.4 GYP-CIX Process 31
2.6.5 THIOPAQ Process 32
2.6.6 The Rhodes BioSURE Process 32
2.6.7 Tshwane University of technology Magnesium-Barium-Alkali (MBA) Process 32
2.6.8 HiPRO (High Pressure Reverse Osmosis) Process 33
2.6.9 EARTH (Environmental and Remedial Technology Holdings) Ion Exchange Process 33
2.7 Adsorption of AMD 35
2.7.1 Adsorption process 37
2.7.2 Biosorption 47
2.7.3 Adsorption isotherms 53
2.7.4 Mathematical models for fixed bed columns 56

2.8 Sulphuric acid recovery from AMD 58
2.8.1 Acid retardation process 59
2.9 Summary 64
CHAPTER THREE 65
MATERIALS AND METHODS 65
3.1 General introduction 65
3.2 Materials and sample preparations 65
3.2.1 Materials 65
3.2.2 Adsorbent preparation 67
3.3 Experimentation 69
3.3.1 Batch adsorption tests 69
3.3.2 Column adsorption tests 70
3.3.3 Ion exchange column tests 72
3.4 Analytical techniques 73
3.4.1 Determination of surface morphology, area and pore structure 73
3.4.2 Determination of functional groups 73
3.4.3 Determination of chemical composition of adsorbents 73
3.4.4 Sulphate and pH measurements 74
3.4.5 Determination of total solids (TS), total suspended solids (TSS) and total dissolved solids (TDS) 74
3.4.6 Determination of the metal ion concentration 75
3.4.7 Determination of the acid content 75
3.4.8 Determination of the point of zero charge (pH_{PZC}) 75
3.5 Summary 76
CHAPTER FOUR 77
RESULTS AND DISCUSSIONS 77

4.1 Characterization results 77
4.1.1 XRD analysis 77
4.1.2 Chemical composition of adsorbents 79
4.1.3 Fourier transform infrared spectroscopy (FTIR) 81
4.1.4 Point of zero charge (pH_{PZC}) 84
4.1.5 Physicochemical properties 86
4.1.6 Surface morphology 87
4.2 Batch adsorption studies 92
4.2.1 Metal removal results 93
4.2.2 Solution acidity and sulphate content 121
4.2.3 Selection of a low cost adsorbent 124
4.3 Adsorption isotherms 126
4.4 Column adsorption studies 129
4.4.1 Introduction 129
4.4.2 Surface chemistry structure of immobilized cassava waste biomass 129
4.4.3 Fixed bed adsorption studies 131
4.4.4 Column dynamics studies 146
4.4.5 Summary of column studies 153
4.5 Acid retardation tests 154
4.5.1 Properties of Dowex MSA-1 resins 155
4.5.2 Acid retardation test 155
4.5.3 Elution studies 160
4.5.4 Evaporation 162
4.6 Economic evaluation of the process 164
4.6.1 Estimation of the proposed process costs 165
4.7 Summary 173

CHAPTER FIVE 175

CONCLUSION AND RECOMMENDATIONS 175

5.1 Conclusion 175

5.1.1 Introduction 175

5.1.2 Batch adsorption studies 176

5.1.3 Column tests 177

5.1.4 Acid retardation tests 179

5.1.5 Acid upgrade 180

5.1.6 Economic evaluation 181

5.2 Recommendations 181

REFERENCES 183

Appendix A 208

Appendix B.....217

Appendix C.....221

LIST OF FIGURES

Figure 1.1: Dissertation Layout…….……7

Figure 2.1: A picture of water affected by AMD in the West Rand……...18

Figure 2:2: Passive treatment technologies……..……25

Figure 2.3: Process flow diagram for the CSIR-ABC process…….....28

Figure 2.4: SAVMIN Process flow diagram……30

Figure 2.5: Proposal flow sheet for remediation of AMD……...35

Figure 2.6: Structure of (a) zeolite and (b) bentonite clay……...38

Figure 3.1: Experimental set up for column tests……71

Figure 4.1: X-Ray Diffraction chart for (a) zeolite and (b) bentonite powder……78

Figure 4.2: FTIR spectra of (a) zeolite (b) bentonite clay (c) cassava peel biomass before and after modification……..82

Figure 4.3: SEM images of (a) mobilized zeolite (b) immobilized zeolite (c) bentonite powder (d) bentonite beads (e) untreated cassava (f) acid treated cassava (g) immobilized cassava waste biomass before metal adsorption, all at 3000 times magnification……...89

Figure 4.4: SEM images of (a) mobilized zeolite (b) immobilized zeolite (c) bentonite powder (d) bentonite beads (e) untreated cassava (f) acid treated cassava (g) immobilized cassava waste biomass after metal adsorption, all at 3000 times magnification ……..….91

Figure 4.5: Effect of contact time on metal ion adsorption using (a) Mobilized and (b) Immobilized zeolite [Adsorbent dosage: 5g, Agitation speed= 150rpm, Temperature = 30 ˚C, Contact time = 1h]……..……...94

Figure 4.6: Effect of contact time on metal ion adsorption using (a) Bentonite powder and (b) Bentonite beads [Adsorbent dosage: 5 g, Agitation speed= 150 rpm, Temperature = 30 ˚C, Contact time = 24 hrs]……99

Figure 4.7: Effect of contact time on metal ion adsorption using (a) Untreated cassava (b) 0.5M treated cassava and (c) 1M treated cassava [Adsorbent dosage= 5g, Agitation speed= 150rpm, Temperature = 30 ˚C, Contact time = 1h]……...102

Fig 4.8: Effect of adsorbent loading on metal ion adsorption using (a) Mobilized and (b) Immobilized zeolite (c) Bentonite powder and, (d) beads (e) Untreated (f) 0.5M treated and (g) 1M treated cassava [Agitation speed= 150 rpm, temperature = 30 ˚C, contact time = 1h for zeolite and cassava peel; 24 hrs for bentonite]……108

Figure 4.9: Effect of temperature on metal ion adsorption using (a) Mobilized and (b) Immobilized zeolite (c) Bentonite powder and, (d) beads (e) Untreated (f) 0.5M treated and (g) 1M treated cassava waste [Adsorbent dosage: 5g, Agitation speed= 150rpm, Contact time = 1h for zeolite and cassava peel; 24 hrs for bentonite]……...113

Figure 4.10: Effect of agitation speed on metal ion adsorption using (a) mobilized and, (b) immobilized zeolite beads (c) bentonite powder and, (d) beads (e) Untreated, (f) 0.5M treated and (g) 1M treated cassava peel [Adsorbent dosage: 5g ; Temperature = 30˚C, Contact time = 1h for zeolite and cassava peel; 24 hrs. for bentonite]……119

Figure 4.11: Sulphate ion trends in the effluent with time for (a) zeolite (b) bentonite clay (c) cassava peel biomass adsorbents [Adsorbent dosage: 5g, Agitation speed= 150rpm, Temperature = 30 ˚C, Contact time = 1h for zeolite and cassava peel; 24 hrs. for bentonite]……...…..122

Figure 4.12: FTIR spectra of cassava peel biomass beads before and after metal loading……130

Figure 4.13: Breakthrough curves for heavy metals in AMD at different flow rates (Adsorbent size= 3mm, Bed height =30cm, Temp. = 25˚C)…….……134

Figure 4.14: Breakthrough curves for heavy metals in AMD at different adsorbent bed height (Adsorbent size= 3 mm, Flow rate =0.89 mL/s, Temp. = 25˚C)……....139

Figure 4.15: Breakthrough curves for acid uptake from AMD at different flow rates (Bed height =20cm, Temp. = 25˚C)……...……156

Figure 4.16: Breakthrough curves for acid uptake from AMD at different bed heights (Flow rate =0.89mL/s, Temp. = 25˚C)……...……159

Figure 4.17: Elution cycles of sulphuric acid from Dowex MSA-1 resins (Bed height =30cm, Temp. = 25˚C)……...…161

Figure 4.18: EDS spectra of precipitate formed during the evaporation process……..162

Figure A1: Mass titration results for mobilized zeolite…….208

Figure A2: Mass titration results for immobilized zeolite…….208

Figure A3: Mass titration results for bentonite powder…….209

Figure A4: Mass titration results for bentonite beads……209

Figure A5: Mass titration results for untreated cassava waste biomass…….210

Figure A6: Mass titration results for 0.5M cassava waste biomass…….……..210

Figure A7: Mass titration results for 1M cassava waste biomass…….…….211

Figure A8: Effect of adsorbent loading on solution acidity using (a) zeolite (b) bentonite (c) cassava peel biomass adsorbents……..213

Figure A9: Effect of temperature on solution acidity using (a) zeolite (b) bentonite (c) cassava peel biomass adsorbents……215

Figure A10: Effect of agitation speed on solution acidity using (a) zeolite (b) bentonite (c) cassava peel biomass adsorbents……..216

Figure B1: Breakthrough curves for heavy metals in AMD at different biomass bead size (Adsorbent bed height= 45cm, Flow rate =0.89mL/s, Temp. = 25˚C)……...218

Figure B2: Breakthrough curves for heavy metals in AMD using single and double columns (Adsorbent bed height= 45cm, Flow rate =0.89mL/s, Temp. = 25˚C, adsorbent size= 1.5mm)…….220

Figure C1: SEM image of iron precipitate formed during evaporation of acid solution…….221

Figure C2: Mass balance of proposed process….....222

LIST OF TABLES

Table 2:1: Chemical characteristics of ground water of Witwatersrand basin collected in April 2002……10

Table 2:2: Recommended maximum sulphate levels……..……13

Table 3.1: AMD chemical composition……...66

Table 3.2: Experimental conditions for column adsorption studies……71

Table 3.3: Experimental condition for ion exchange column adsorption studies……72

Table 4.1: Chemical composition of zeolite and bentonite…….80

Table 4.2: Mass titration results of bentonite, cassava peel and bentonite adsorbents85

Table 4.3: Physicochemical properties of bentonite, cassava peel biomass and zeolite adsorbents……...….86

Table 4.4: Solution pH changes with time for mobilized and immobilized zeolite adsorbents……... 96

Table 4.5: Concentration of Al ions in the effluent with time….....104

Table 4.6: Linear Langmuir and Freundlich isotherm parameters for the adsorption of heavy metals from AMD by cassava peel biomass……...…127

Table 4.7: Langmuir and Freundlich isotherm error function values of different metals ……128

Table 4.8: Parameters of the breakthrough curves for metals in AMD at different flow rates (Adsorbent size= 3 mm, Bed height =30 cm, Temp. = 25˚C)……...136

Table 4.9: Breakthrough times for metals in AMD effluent at different bed height (Adsorbent size= 3 mm, Flow rate =0.89 mL/s, Temp. = 25˚C)……...141

Table 4.10: Breakthrough parameters for heavy metals in AMD at different conditions (Adsorbent bed height (single column) = 45 cm, Flow rate = 0.89 mL/s, Temp. = 25˚C)…….…..144

Table 4.11: Adam-Bohart parameters for heavy metals in AMD at different conditions using regression analysis……..……147

Table 4.12: Thomas parameters for heavy metals in AMD at different conditions using regression analysis…….……..150

Table 4.13: Dowex MSA-1 properties……..…155

Table 4.14: Breakthrough parameters for acid uptake by Dowex MSA-1 at different flow rates……...158

Table 4.15: Breakthrough parameters for acid uptake by Dowex MSA-1 at different bed heights…….160

Table 4.16: Chemical composition of the acid and water product obtained in the evaporation process……...163

Table 4.17: Assumptions used in economic evaluation calculations……164

Table 4.18: A summary of the mass balance of the proposed process…….165

Table 4.19: Proposed AMD plant costing…….168

Table A1: Data for solution pH changes with time for bentonite powder and beads211

Table A2: Data for solution pH changes with time for untreated and acid treated cassava waste biomass……...212

CHAPTER ONE

INTRODUCTION

1.1 General Introduction

South Africa is a water stressed country and the presence of acid mine drainage (AMD) in water streams threatens the security of this scarce resource. The AMD is normally formed when sulphide minerals such as pyrite are oxidized forming ferrous iron and sulphuric acid (Singer and Stumm, 1970, Evangelou, 1995). The initial products provide an acidic and oxidizing environment which promotes the leaching of other metal sulphides such as galena, sphalerite, chalcopyrite, etc., which are normally found in association with pyrite. As a result, water that has a low pH and enriched with sulphate ions as well as heavy metals such as iron, aluminum, nickel, manganese, cobalt, lead, etc., is formed. This water is highly corrosive and toxic, and thus poses serious environmental challenges when discharged into the biosphere. The deaths of aquatic life, plant poisoning, deterioration of the ecosystem and, scaling and corrosion of process equipment are some of the risks associated with AMD (Jennings et al., 2008). Therefore, it is imperative that the AMD is remediated before discharge to reduce its negative impact on the receiving environment.

Several studies have been conducted to solve the AMD issue (Juby, 1989; Du plesis, 1992; Fripp et al., 2000; Blueprint, 2009). Traditionally, acid neutralization using limestone and lime has been used to remediate AMD. The process neutralizes the acid and is able to remove noxious heavy metals through precipitation as metal carbonates and hydroxides. However, the challenge to this technique is the huge amount of sludge produced which is difficult to dispose as well as the failure to remove other harmful contaminants such as the sulphate ion (Novhe, 2012). In addition, sulphuric acid which could otherwise be recovered is lost in the process.

Other active treatment methods such as reverse osmosis, adsorption and ion exchange have also been used, but the high costs associated with their operation limits their application (Johnson and Hallberg, 2005). Therefore, passive methods such as constructed wetlands, diversion wells containing crushed limestone, or open ditches filled with limestone have also been applied in an effort to reduce cost and possibly the sulphate ion content in the product water, a challenge which most active treatment technologies have failed to address. However, passive treatment systems are costly to set up and require a lot of working space (Johnson and Hallberg, 2005; Novhe, 2012). Furthermore, the coating of limestone by iron precipitates (armouring) also presents serious operational challenges.

As already stated, current passive and active treatment often suffer from lack of economic sustainability. For example, valuable products such as iron oxides, sulphuric acid and many other metal values are lost in the treatment processes. Moreover, the recovery of valuable and saleable products from AMD can have a major impact on the economics of the operation since the financial benefits can be used to offset the treatment costs. Therefore, in the recent years research interests have shifted towards the recovery of valuable materials from AMD in addition to its remediation.

In fact, studies have revealed that valuable materials such as iron oxides, sulphuric acid and water can be successfully recovered using conventional methods such as diffusion dialysis and electro-dialysis (Hedin, 2003; Martí-Calatayud et al., 2013). The recovery of sulphuric acid and metals has, however, generated considerable research interests recently most likely due to the appreciable sulphuric acid market in the industry, as well as the environmental benefits derived from the removal of these toxic components from the water. Although, various methods have been used for acid and metal recovery from AMD most of them have financial constraints and other associated operational problems such the fouling potential of membranes, ineffectiveness of adsorbents at low metal concentrations, etc. Furthermore, most of the studies have been conducted on simulated AMD solutions; therefore, the

performance of the treatment methods on real AMD solutions is also an issue which has not been adequately addressed.

The present study, is therefore, aimed at testing the feasibility of using the adsorption and acid retardation processes for heavy metal removal and sulphuric acid recovery from real AMD solution, respectively. The study was divided into two aspects, the metal removal and acid recovery. In the first aspect of the study, three low cost adsorbents (i.e., cassava peel biomass, zeolite and bentonite clay) were tested on real AMD solution. Cassava peel biomass is a waste and has no economic value associated with it and hence its potential applicability to AMD treatment could render it a useful material. Furthermore, cassava peel biomass is degradable, and this could significantly reduce the quantity of the solid waste to be disposed of. Zeolite and bentonite clay are also found abundantly in nature and South Africa has a large reserves of both materials (Kapanji, 2009). Therefore, the use of these low cost and readily available materials to deal with an environmental problem could be an attractive AMD remediation option.

The second aspect of the study involved the recovery of the sulphuric acid from the metal barren solution. Feasibility studies were conducted on the solution using acid retardation process. Acid retardation separates acid and its associated salts by slowing down the movement of the acid while allowing the salts to pass through (Hatch and Dillon, 1963; Parujen, 1997; Sheedy and Parujen, 2012). The process has been widely used in the metal finishing industry for the recovery of sulphuric acid and many other acids from pickling solutions (Parujen, 1997; Sheedy and Parujen, 2012). Presently, there is no published work on the recovery of sulphuric acid from AMD using the process. Hence, in the present work, feasibility tests were conducted using a laboratory column packed with fine mesh Dowex MSA-1 ion exchange resins to recover sulphuric acid from metal barren AMD.

1.2 Problem statement

The lack of economic sustainability by the current AMD remediation technologies has spurred interests in the research of technologies for recovering of valuable products from AMD in addition to its remediation. The financial benefits could be used to offset some of the operational costs. Therefore, the present work was focused on the removal of metals, and recovery of the acid from AMD using adsorption on low cost adsorbents and acid retardation process, respectively. Although numerous studies exist for metal adsorption on low cost adsorbents, most of the studies have been conducted on simulated AMD, and little attention has been paid to real AMD solutions. Therefore, the present study evaluated metal adsorption from a real AMD solution. The acid retardation process was also proposed in this study for the recovery of acid from the metal barren AMD. Although, the acid retardation process has a wide spread application in the recovery of acids from waste metal pickling solutions, no published work is available on the recovery of sulphuric acid from real AMD solutions.

1.3 Aim and Objectives

The main aim of this research was to investigate the feasibility of the adsorption and acid retardation processes as alternative methods for the treatment of AMD. The developed process should:

- Create value from the AMD through recovery of the acid constituent and other possible by-products
- Reduce solid waste material (by-products such as unwanted sludge) through recovery of valuable products from AMD.

The specific objectives are:

- To identify the best low cost adsorbent amongst zeolite, bentonite clay and cassava peel biomass based on metal adsorption efficiency.
- To obtain scale up information using the column adsorption studies.
- To recover the remaining sulphuric acid using acid retardation process.
- To recover water of re-usable quality through the acid upgrade process.

1.4 Key research questions

The various questions that were addressed in this study included the following:

- How effective are low cost adsorbents such as cassava peel, bentonite clay and zeolite in the removal of toxic heavy metals from a real AMD solution?
- What process parameter levels give the highest metal adsorption efficiency using the chosen adsorbents?
- Can sulphuric acid be recovered from an AMD solution and is it possible to upgrade the concentration of the acid to market values?
- Can water of re-usable quality be obtained during the treatment process?

1.5 Research methodology

The research methodology for this study involved the following major tasks: literature review, experimental design, laboratory testing, analysis of results, drawing conclusions from results, recommendations and documentation.

1.6 Dissertation layout

This dissertation consists of five chapters including this chapter (Chapter One) that provides the motivation for the research, the problem statement, and the overall objective of this study. The layout is schematically represented in Figure 1.1.

Chapter Two is the literature review, which includes the general overview of the formation of AMD and problems associated with it, the current technologies for AMD remediation, and the general knowledge on adsorption and acid retardation processes.

Chapter Three describes the materials and methods used in the study.

Chapters Four describes the results of laboratory tests and discussions of the findings.

Chapter Five concludes the dissertation with a summary of the findings and recommendations.

References to all articles used in the study are provided at the end of the dissertation. An appendix section provides relevant laboratory test results and other important data.

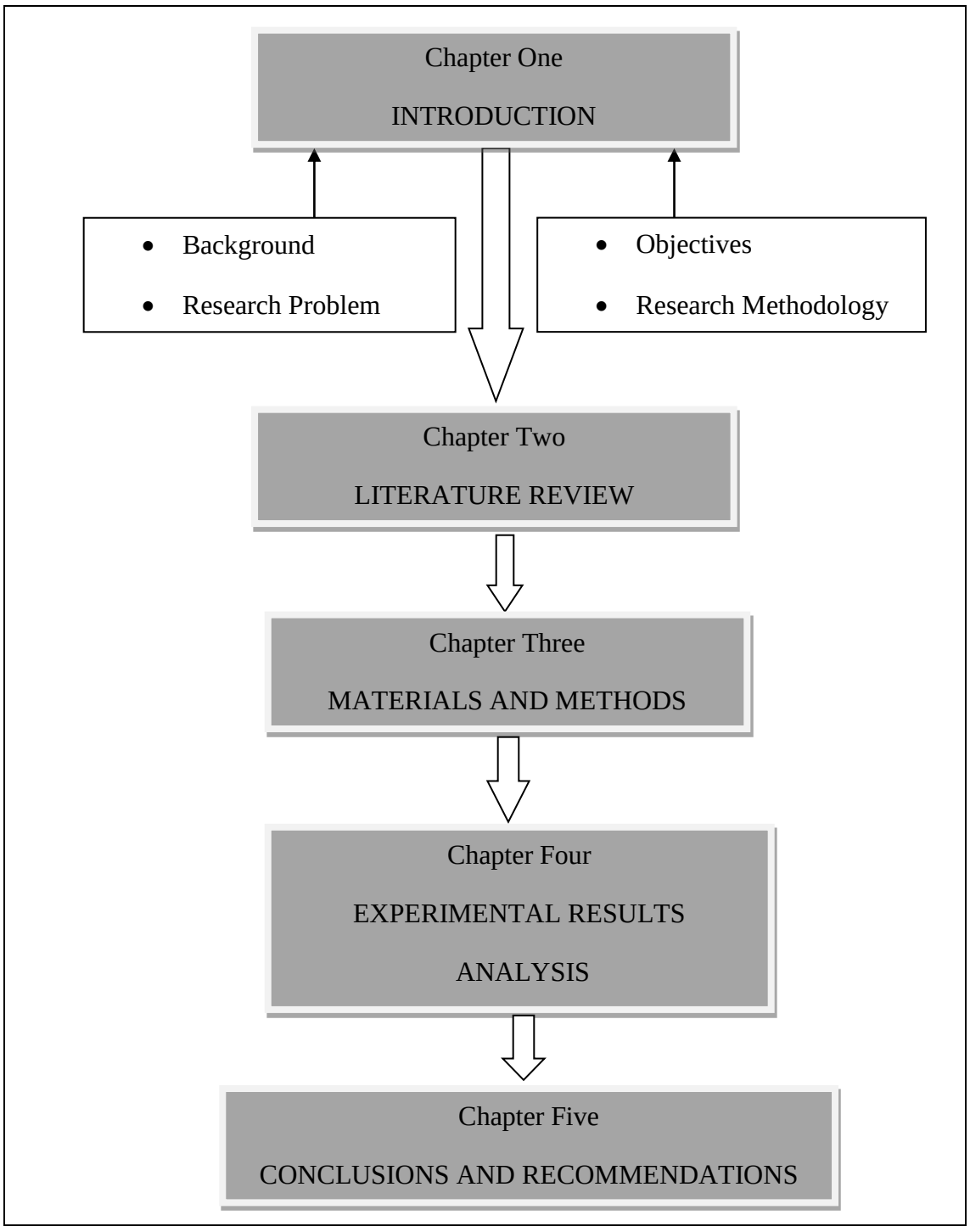


Figure 1.1: Dissertation Layout

CHAPTER 2

LITERATURE REVIEW

2.1 General introduction

This section outlines the background of the research. The formation and constituents of AMD are discussed first, followed by the impact of AMD on the environment and the available treatment options. The adsorption processes as well as the acid retardation process are also discussed in detail herein.

2.2 Formation and constituents of AMD

AMD is a low pH, sulphate and metal laden water resulting from the weathering of pyrite and/or other sulphide minerals. AMD can form in the underground workings of abandoned mines; mine waste dumps, tailings and ore stockpiles where pyrite is abundant (Evangelou, 1995). Pyrite is a common minor constituent in many mineral deposits and is normally associated with gold and coal deposits. When pyrite is exposed to oxygenated water due to mining, mineral processing or other earthmoving processes it is oxidized, initially forming sulphuric acid and ferrous iron (Singer and Stumm, 1970).

$$2FeS_2(s) + 7O_2(g) + 2H_2O(l) \rightarrow 2Fe^{2+}(aq) + 4SO_4^{2-}(aq) + 4H^+(aq) \quad (2.1)$$

In sufficiently oxidising environment (dependant on O_2 concentration, pH greater than 3.5 and bacterial activity) the ferrous iron released in Reaction 2.1 may be

oxidised to ferric iron, according to the following reaction (Blowes et al., 2003; Ackil and Koldas, 2006).

$$4\,Fe^{2+}(aq) + O_2(g) + 4H^+(aq) \rightarrow 4Fe^{3+}(aq) + 2H_2O(l) \quad (2.2)$$

At pH values between 2.3 and 3.5, ferric iron precipitates as $Fe(OH)_3$ as shown in Equation 2.3 (Ackil and Koldas, 2006). This causes a further drop in pH and leaves little ferric iron in solution. The remaining ferric iron reacts directly with pyrite to produce more ferrous iron and acidity as illustrated in Equation 2.4 (Ackil and Koldas, 2006; Jennings et al., 2008).

$$4Fe^{3+}(aq) + 12H_2O(l) \rightarrow 4Fe(OH)_3(s) + 12H^+(aq) \quad (2.3)$$

$$FeS_2(s) + 14Fe^{3+}(aq) + 8H_2O(l) \rightarrow 15Fe^{2+}(aq) + 2SO_4^{2-}(aq) + 16H^+(aq) \quad (2.4)$$

Upon consideration of the reaction scheme above (Equation 2.1 to 2.4), Reaction 2.2 has been found to be the slowest and consequently termed the rate limiting reaction of pyrite oxidation (Singer and Stumm, 1970). However, the presence of acidophilic bacteria such as Thiobacillus ferroxidans greatly accelerates the abiotic oxidation rate by a factor of hundreds to as much as millions. This maintains a high concentration of ferric iron in the system (Singer and Stumm, 1970, Blowes et al., 2003; Sanchez et al., 2008), thus resulting in highly oxidizing conditions. These acidic and oxidizing conditions provide a desirable environment for the leaching of other minerals such as galena, sphalerite, chalcopyrite, etc., (Equation 2.5 to 2.8) which are usually found in association with pyrite (Younger et al., 2002; Blowes et al., 2003).

Sphalerite: $ZnS\,(s) + 2\,O_2\,(aq) \rightarrow Zn^{2+}\,(aq) + SO_4^{2-}$ (2.5)

Galena: $PbS\,(s) + 2\,O_2\,(aq) \rightarrow Pb^{2+}\,(aq) + SO_4^{2-}\,(aq)$ (2.6)

Millerite: $NiS\ (s) + 2\ O_2\ (aq) \rightarrow Ni^{2+}\ (aq) + SO_4^{2-}\ (aq)$ (2.7)

Chalcopyrite: $CuFeS_2\ (s) + 4\ O_2\ (aq) \rightarrow Cu^{2+}\ (aq) + Fe^{2+}\ (aq) + SO_4^{2-}\ (aq)$ (2.8)

The result of the overall process is a water solution that is highly acidic and enriched with sulphate, iron, aluminium, zinc, nickel, lead and other toxic heavy metal ions. This solution is termed acid mine drainage (AMD).

This formation of AMD is quite complicated since factors like microbial activities, temperature (weather and seasonal conditions), availability of oxygen and type of mineral deposits vary from place to place, thus influencing the quality (pH and metals content) and amount of AMD produced (Lapakko, 2002; Jennings et al., 2008; McCarthy, 2011). It is therefore, highly probable that the constituents of AMD will vary from region to region. Hence, an effective solution to the problem of AMD will largely depend on the correct prediction of its characteristics. In South Africa, the Witwatersrand region has been identified as the most problematic area owing to the large number of abandoned mines which are gradually filling with AMD, with some eventually spilling out into the environment and contaminating water sources (Pratt, 2011). Table 2.1 shows a typical composition of AMD samples collected from two areas around the Witwatersrand region.

Table 2.1: Chemical characteristics of AMD collected in the Witwatersrand basin (Ekolu et al., 2014)

AMD Sample number	**pH**	**Electrical conductivity (mS m^{-1})**	**Ionic Concentration (mg/L)**							
			SO_4	Ca	Mg	Mn	Fe	K	Na	Cu
1	2.6	300	3080	910	245	117	78	2.5	179	0.6
2	2.7	340	3160	840	267	17	124	4.8	69	0.90

The samples shown in Table 2.1 have low pH and high conductivity values. They also contain a high concentration of toxic heavy metals such as iron, magnesium, manganese, copper etc. These characteristics confirm the findings of other similar studies (Naicker et al., 2003; Winde and Sandham, 2004). In addition, Tutu et al. (2008) also observed that relatively low pH values (typically below 3.5) were recorded close to mine tailings and also at locations near current tailings reprocessing activities. This was attributed to tailings footprints, rapid oxidation of freshly exposed tailings, and release of polluted groundwater from within the dumps during reclamation. Other areas showing high pollution levels included streams near active slimes dams and tailings spillages where tailings were exposed for reprocessing. The samples also contain elevated levels of sulphate ions which normally coincides with low pH although, exceptions do occur particularly where acidic water has been treated with lime, a practice commonly used to treat water pumped from underground mining activities (Tutu et al., 2008). As a result of these characteristics AMD is a great challenge in this region and South Africa as a whole. The environmental and ecological risks associated with such water characteristics are discussed in detail in the following section.

2.3 Environmental and ecological impact of AMD

The overall impact of AMD is very much dependent on local conditions and varies widely depending on the geomorphology, climate, the extent and distribution of the AMD generating deposits as well as post mining management of the affected landscapes (McCarthy, 2011; Swer and Singh, 2004). As discussed earlier, AMD introduces sulphuric acid and toxic heavy metals into the environment. In normal weathering processes, the AMD is produced at such a slow rate that the natural neutralizing processes are able to remove the acidity. However, in the case of the Witwatersrand deposits these processes are overwhelmed hence, the release of the acidic water and toxic heavy metals into the environment is inevitable (McCarthy,

2011). These toxic heavy metals are non-biodegradable and may contaminate drinking water which is ingested by humans causing severe health problems (Ochieng et al., 2010). Water pollution, deterioration of the ecosystem and degradation of agricultural lands are some of the conspicuous environmental consequences of AMD. This section gives a detailed discussion of the impacts of AMD constituents on plant, aquatic life and animal life.

2.3.1 Impact of low pH

Aquatic life

A Study by Tutu et al. (2006) revealed that most of the AMD samples collected from different areas within the Witwatersrand basin had pH values less than 3.5. The low pH is an indication of the presence of sulphuric acid in the water. The acidic water is a matter of prime concern since it is directly harmful to aquatic life. Most organisms have a very well defined range of pH tolerance (Morris et al., 1989; Elle and Callaghan, 1998). If the pH falls below the tolerance levels, it causes a disturbance in the balance of sodium and chloride ions in the blood of aquatic organisms. Hydrogen ions may be taken in and sodium ions expelled. This leads to death due to osmoregulatory or respiratory failure (Morris et al., 1989; Jennings et al., 2008). Several reports have also indicated that low pH levels alter gill membranes or gill mucus resulting in death due to hypoxia (Fromm, 1980; Swer and Singh, 2004; Jennings et al., 2008). Aquatic species like hatchery raised salmonids can tolerate pH 5.0, but below this level homeostatic electrolyte and osmotic mechanisms become impaired (Fromm, 1980).

Plants

Plants need a proper balance of macro and micronutrients in the soil and the soil pH has an important influence on the availability of nutrients and on the growth of different kinds of plants (Halcomb et al., 2009). If the pH of the soil is less than 5;

nitrogen, phosphorus and potassium are tied up in the soil and not available to plants (Halcomb et al., 2009). Calcium and magnesium, which are essential plant nutrients, may be absent or deficient in low pH soils. Low pH increases the toxicity of aluminium, iron and manganese. However, in soils with proper pH, they are non-toxic and elements like sulfur, calcium, magnesium, and molybdate will be available for plant uptake (Halcomb et al., 2009). Furthermore, low pH values reduce the activity of soil organisms that break down organic matter, and this in turn leads to the degradation of the soil structure.

Man-made structures

The aggressive nature of AMD may also result in corrosion and scaling problems with respect to man-made structures such as pipes, pumps etc. This can in turn lead to equipment failure and higher maintenance cost (Hodge, 1937; West et al., 2011).

2.3.2 Effect of high sulphate levels

As already discussed, most waters affected by AMD also contain elevated levels of the sulphate ion. The high sulphate ion content is a serious challenge that persists even after AMD has been treated by neutralization using limestone or dolomite. Table 2.2 shows the recommended maximum discharge levels for the sulphate ion.

Table 2:2: Recommended maximum sulphate levels (DWAF, 1993; WHO, 1996, US EPA, 1999)

Organization	Maximum sulphate level (mg/L)
US EPA	250
WHO	500
EU guide limit	1000
DWAF (South Africa)	600
Australia	1000

Comparing the sulphate levels of AMD found in the Witwatersrand area (Table 2.1) with the maximum recommended levels (Table 2.2), it is evident that the sulphate level in the AMD is substantial above the standard discharge levels. The sulphate ion had initially not received stringent discharge regulation owing to its lesser toxicity compared to other AMD constituents such as the acidity and heavy metals. However, high sulphate concentrations have been found to alter the taste of water causing laxative effects in animals and human beings (Morris and Levy, 1983). Water rich in sulphate also has a high scaling potential. In South Africa, for example, it is estimated that 75% of gold mines have scaling problems essentially related to saturation of water with respect to calcium sulphate (Juby, 1989). Macky et al. (1991) also estimated that poor mine service water can cost the gold mining industry in the region of R300 million annually based on its scaling and fouling potential. In addition, sulphate ions are some of the main contributors to water "mineralization'', which increases the conductivity and corrosion potential of receptor bodies (Bowell, 2000). These anions promote the following, among other things: corrosion of pipes, structures and equipment; fouling and deposition in boilers; and acidification of soils and blockage of soil pores, retarding irrigation or water drainage. As a result, sulphate is now being considered to be one of the more significant long term water quality issues for mining operations and process plants, particularly in countries with problems of fresh water supply such as South Africa and Australia (Du Plessis and Swartz, 1992; Bowell, 2000; Younger et al., 2002).

2.3.3 Impact of dissolved metals

The Witwatersrand gold and coal conglomerates contain traces of iron, manganese, aluminium, nickel and other heavy metals. The heavy metals are a result of the action of acid runoff and can be washed into water streams (Swer and Singh, 2004; Tutu et al., 2006; McCarthy, 2011). The impacts of these toxic heavy metals on aquatic, plant and animal life are detailed herein.

Aquatic life

Heavy metals increase the toxicity of AMD and also act as metabolic poisons (Earle and Callaghan, 1998). Iron, aluminium and manganese are the most common heavy metals which can compound the adverse effects of AMD. Heavy metals are generally less toxic at circumneutral pH. Some aquatic organisms such as brook trout are tolerant of low pH, but the addition of metals decreases that tolerance (Jennings et al., 2008). In addition to dissolved metals, precipitated iron or aluminium hydroxides decrease oxygen availability as they form. The precipitate may coat gills and body surfaces, smoother eggs, and cover the stream bottom, filling in crevices in rocks and making the substrate unstable and unfit for habitation by benthic organisms (Hoehn and Sizemore, 1977; Jennings et al., 2008).

Aluminium rarely occurs naturally in water at concentrations above a few tenths of a milligram per litre (Earle and Callaghan, 1998). However, higher concentrations do occur in AMD. Of the three major heavy metals present in AMD, aluminium has the most adverse effect on aquatic life (Earle and Callaghan, 1998). Its presence in water compounds the effect of low pH by interacting with hydrogen ions, further decreasing sodium uptake which may result in death of aquatic organisms. Stream studies by Ellen and Callaghan (1998) indicated that a combination of pH values less than 5.5 and dissolved aluminium concentration greater than 0.5mg/L will generally eliminate all fish species and many macroinvertebrates. This confirms the findings of Baker and Schofield (1982) in which pH levels between 5.2 and 5.4 were found to be most toxic to aquatic organisms due to aluminium intake. The aluminium precipitate also eliminates most of the filter feeders, such as Hydropsychid caddisflies, which normally comprise a major portion of total stream macroinvertebrates. Precipitated aluminium can accumulate on fish gills and interfere with their breathing (Brown and Sadler, 1989; Backer and Schorr, 2006)

Iron is a common major component of water affected by AMD and has a harmful effect on aquatic life. Very few aquatic organisms are found in streams with pH

values less than 3.5 and elevated dissolved iron concentrations (Earle and Callaghan, 1998). At pH values above 3.5 precipitation of iron as ferric hydroxide occurs. This may result in complete blanketing of the stream bottom, adversely affecting both macroinvertebrates and fish (Hoehn and Sizemore, 1977). Furthermore, Koryat et al. (1972) found that ferric hydroxide diminished total biomass of benthic organisms and limited fish populations in streams with survivable pH levels.

Manganese is also another metal found in AMD. It can be present in various forms, compounds and complexes with organic compounds. Manganese is difficult to remove from effluents because the pH has to be raised above 10 before manganese can precipitate (Earle and Callaghan, 1998). Manganese is therefore persistent and can be carried for long distances downstream of an AMD source. Reduction in calcium uptake, disruption of body ion levels, osmoregulatory imbalance and reduced fecundity in aquatic organisms are some of the adverse effects of manganese (Earle and Callaghan, 1998; Grippo, 2005).

Nickel is one of the minor constituents of AMD. Nickel is considered a hazardous substance and possesses carcinogenic and mutagenic properties. These properties occur along with acute and chronic effects which can cause several disorders and diseases such as nausea, vomiting, skin dermatitis, infertility, chronic headache, lung, kidney, liver, intestine and heart failure (Beliles, 1978).

Other heavy metals present in AMD such as cadmium, copper, lead and zinc can also result in either mortality or non-lethal effects such as stunted growth, reduced reproduction, deformities, or lesions (Lewis and Clark, 1997)

Impact on plant and animal life

Contamination of agricultural soil by heavy metals has become a critical environmental concern due to their potential adverse ecological effects (Yadav,

2010). Plants exposed to high level of heavy metals such as zinc, cadmium, nickel and copper show reduction in photosynthesis, water uptake and nutrient uptake (Yadav, 2010). Chlorosis, retarded growth and browning of root tips are some of the visible marks of plant exposure to heavy metals.

Pollution of the food chain may also result due to the consumption of heavy metal laden plants (Yadav, 2010). Moreover, direct exposure to heavy metals from AMD can cause disruption of metabolic functions of animal life (Ochieng et al., 2010). Heavy metals disrupt the metabolic functions in two ways; (1) they accumulate in vital organs and glands such as the heart, brain, kidneys, bone and liver where they disrupt their important functions, and (2) they inhibit the absorption, interfere with or displace the vital nutritional minerals from their original place, thereby, hindering their biological function (Singh et al., 2011).

2.3.4 Impact of solid precipitate from AMD

AMD can be neutralized by naturally occurring systems forming an orange-brown precipitate known as ochre (a mixture of ferric hydroxide and iron oxide). The ochre precipitate is very toxic to aquatic life. It reduces the area available for fish to lay their eggs on by smothering the seabed near the estuary, hence, reducing fish breeding (Hoehn and Sizemore, 1977; Ochieng et al., 2010). The smothering causes a loss of bottom dwelling organisms on the seabed, having domino effects up the food chain by reducing the food sources available for animals at the top of the marine food chain, e.g. fish and sharks (Jennings et al., 2008). Ochre also contains toxic elements such as copper, cadmium and zinc whose precipitate may coat the surface of the steam sediments destroying habitat, diminishing availability of clean gravels used for spawning, and reducing fish food items such as benthic macroinvertebrates.

Figure 2.1 shows a picture of water affected by AMD, taken from the West Rand, a part of the Witwatersrand region in South Africa.



Figure 2.1: A picture of water affected by AMD in the West Rand (IMC, 2010)

It can be seen that the water is orange-brown in colour. This could be attributed to the possible presence of dissolved iron and other metals in the water. Ochre, the orange brown precipitate can also be seen settling at the bottom of the water due to its large density in relation to water. Apart from the toxic effects mentioned earlier, deterioration of the ecosystem is the conspicuous impact of AMD observed in this picture. It is therefore, imperative to deal with the AMD issue in order to lessen its harmful impact on the receiving environment.

2.4 Source control of AMD

Source control is the most preferred method for dealing with the AMD issue, although this is not practically feasible in most locations. This section discusses some

of the methods that have been employed in an effort to prevent or reduce the rate of formation of AMD.

2.4.1 Flooding/sealing of underground mines

Oxygen and water are the essential ingredients in the formation of AMD hence, it follows that excluding either (or both) of these, it is possible to prevent or lessen AMD formation. Flooding and sealing underground deep mines can be used to achieve this purpose (Johnson and Hallberg, 2005). The dissolved oxygen (DO_2) present in the flooding waters (ca. 8 to 9mg/L) is consumed by mineral oxidizing (and other) micro-organisms present and replenishment of DO_2 by mass transfer and diffusion is impeded by sealing of the mine (Johnson and Hallberg, 2005). However, this method is only effective where all shafts and adits location are known and where inflow of water containing oxygen does not occur.

2.4.2 Underground storage of mine tailings

This method has been used for disposing and storing mine tailings that are potentially acid generating (Li et al., 1997). The objective is to prevent contact between acid producing minerals and dissolved oxygen. Shallow water covers may be used, and their effectiveness may be enhanced by covering the tailings with a layer of sediment or organic material, which has the dual benefit of limiting oxygen ingress and affording some protection against re-suspension of the tailings due to the actions of wind and waves (Johnson and Hallberg, 2005). Dry covers used for surface storage of reactive mineral spoils may also incorporate an organic layer. The ‘sealing layer’ that covers the spoil is usually constructed from clay. However, in areas of the world that experience acute wet and dry seasons, drying and cracking of the cover can render it less effective than in temperate zones.

In other places of the world such as in Canada, paste backfilling is also practiced as a protocol for mine reclamation (Benzaazoua and Bussiere, 2002). This is done to minimize acid formation by backfilling mine workings using a mixture of mine tailings. Portland cement and other binders are added to mine tailings to create a waste disposal option that is both geotechnically stable and geochemically non-reactive since sufficient neutralizing potential can be added to neutralize future acidity (Benzaazoua and Bussiere, 2002).

2.4.3 Depyritization

Depyritization of tailings is another technique used to prevent the formation of AMD. It involves the removal of sulfide minerals from mine tailings to create a benign sand fraction suitable to use as a general backfill and a companion low-volume sulfide concentrate requiring careful disposal. Most mine tailings contain small amounts of sulfide minerals that can be readily separated from non-acid forming silicate minerals using conventional mineral processing equipment to create a cleaned material with sufficient neutralizing potential to ameliorate any future acidity (Benzaazoua et al., 2000). The attractiveness of depyritization is that it is simple and economic (Sahoo et al., 2013). However, the main drawback to this method is that it may not be readily applicable to major sources of AMD such as underground mine workings.

2.4.4 Mine Capping

Mine capping can also be used to prevent rainfall from reaching acid-forming units in a backfilled mine (Chermak and Runnells, 1997; Fripp et al., 2000). It is generally used for surface mines. The cap is typically fly ash covered with top soil and seeded (Fripp et al., 2000). However, capping is only effective where the horizontal components of groundwater are negligible.

2.4.5 Blending of mineral wastes

Mixing acid generating and acid consuming materials to produce environmentally benign aggregates is an appealing and possibly low cost alternative for minimizing formation of AMD in waste piles of some mines (Day, 1994). An alternative to this theme is to add solid-phase phosphates such as apatite to pyritic mine waste in order to precipitate iron (III) as ferric phosphate thereby, reducing its potential to act as an oxidant of sulphide minerals (Johnson and Hallberg, 2005). However, the inhibition of pyrite oxidation using this approach may only be temporary, due to the process of 'armouring' of the added phosphate minerals (Evangelou, 1998).

2.4.6 Application of anion surfactants

Acidophilic bacteria are known for greatly accelerating the rate of formation of AMD as already discussed in section 2.1. Therefore, the inhibition of the activity of these lithotrophic (rock eating) iron and sulphur oxidizing bacteria found in mineral tailings is another technique used for reducing AMD formation. This generally involves the application of anionic surfactants such as sodium dodecyl sulfate (SDS), which are highly toxic to this group of microorganisms (Johnson and Hallberg, 2005). However, the effectiveness of biocide applications has been found to be highly variable affording at best, only short-term control of the problem and requiring repeated applications of the chemicals. In addition, bactericides may be toxic to aquatic organisms (Sahoo, 2013).

Given the practically constraints associated with the prevention of AMD at source level, the only other alternative is to minimize the toxicity of the released AMD on the receiving environment. This is achieved through various treatment options. The next section gives a detailed discussion on the treatment options available for AMD.

2.5 Treatment options for AMD

This section discusses the details of various treatment methods. Processes are broadly categorized as either active or passive treatments.

2.5.1 Active treatment methods

Active treatment methods are those methods that require continuous inputs of resources to sustain the process (Ochieng et al., 2010). Active treatment technologies include aeration, neutralization, which often include metal precipitation, membrane processes, ion exchange, and biological sulphate removal (EPA, 2008). Active treatment is characterized by on-going high intensity flow of chemicals into and out of a continuous treatment plant (Fripp et al., 2000; Johnson and Hallberg, 2005). It may include the installation of a water treatment plant, with a variety of reactor systems, such as agitated reactors, precipitators, clarifiers and thickeners. In the plant, the acid is first neutralized by dosing the AMD with lime or limestone and then passing it through settling tanks to remove sediments and particulate material. The effluent produced by such neutralization systems often contains more sulphate than is acceptable for either discharge to the environment or many other uses (Fields, 2010; West et al., 2011). Active treatment systems can also be a very expensive option due to the cost of lime (Johnson and Hallberg, 2005). Weather, equipment failure, and budget restrictions can result in lapses in treatment, which in turn can result in massive death of aquatic life (Fripp et al., 2000; Ochieng et al., 2010). Other active treatment technologies such as membranes and ion exchange can also produce water of acceptable standards. However, limitations such as membrane fouling and high cost of resin regeneration limit the use of these technologies. Below is a brief outline of some of the active treatment methods.

Lime Neutralization

This involves dispersing lime into a tank containing AMD and recycled sludge to increase water pH to about 9 (INAP, 2003). At this pH, most toxic metals become insoluble and precipitate, aided by the presence of recycled sludge that is generated from the same process. Optionally, air may be introduced in a tank to oxidize iron and manganese and assist in their precipitation (INAP, 2003). The resulting slurry is directed to a sludge-settling vessel, such as a clarifier. Clean water will overflow from the vessel for release, whereas settled metal precipitates will be recycled to the AMD treatment tank, with a sludge-wasting side stream. The only drawback to this method is the discharge of water saturated in gypsum ($CaSO_4$) and containing residual metal concentrations which may sometimes exceed drinking and irrigation water standards which according to EPA (1994) must not exceed 500mg/L of sulphate. In addition, the scaling nature of this water also makes it unsuitable for industrial use, and makes further processing difficult and costly (Robertson and Rohrs, 1995)

Ion exchange

Cation exchange processes have previously been investigated as a potential treatment for AMD (INAP, 2003). The principle is that an ion exchange resin can remove potentially toxic metals (cationic resins), or chlorides, sulphates and uranyl sulphate complexes (anionic resins) from mine water. Once the contaminants are adsorbed, the exchange sites on resins must be regenerated, which typically requires acidic and basic reagents and generates a brine solution that contains the pollutants in a concentrated form (Brown et al., 1987).

Adsorption

Most active treatment methods discussed earlier are ineffective due to low metal removal efficiency and high treatment cost for low contaminant concentrations (Kurniawan et al., 2011). Hence, adsorption has emerged as an alternative method for treating solution streams containing low metal ion concentrations which are still above the permissible discharge levels such as AMD. This is a result of the high

selectivity, low operational cost and minimal toxic sludge associated with the adsorption process (Kurniawan et al., 2011). Adsorbents such as activated carbon, silica gels and molecular sieves have been successfully used (Richardson et al., 2002). However, the financial constraints associated with these adsorbents have limited their use. Hence, much research in the recent years has focused on finding alternative low cost adsorbents. According to Bailey et al. (1999), an adsorbent can be considered as cheap or low cost if it is abundant in nature, requires little processing and is a by-product of waste material from industry.

Due to the challenges (mostly financial constraints and the failure to address high sulphate issue) encountered in active treatment technologies; an alternative will be to apply 'passive treatment' technologies which use natural ameliorative processes.

2.5.2 Passive treatment technologies

Passive treatment technologies are those systems that require little or no input of energy or reactive materials after initial installation, but only infrequent monitoring (Johnson and Hallberg, 2005; EPA, 2008). Passive treatment is the deliberate improvement of water quality using only naturally available energy sources such as gravity, microbial metabolic energy, photosynthesis etc., in systems which require only regular maintenance in order to operate effectively over the entire system design life (PIRAMID Consortium, 2003).

Many passive systems, especially those treating acidic waters, utilize one or more materials that would normally be classified as 'waste products'. These include materials from industrial processing and farming practices that, in most cases, can be locally sourced, thereby reducing transport costs (Bailey et al., 1999; INAP, 2003). The passive treatment methods use treatment systems such as constructed wetlands, diversion wells containing crushed limestone, or open ditches filled with limestone

and bioreactors that employ naturally occurring chemical and biological reactions to remediate AMD with little maintenance (EPA, 2008; Novhe, 2012). These can provide a potentially long-term solution to the AMD problem although, their success has been limited in cases where excessive volumes, high iron loadings and excessively low pH values are encountered **(**INAP, 2003; Novhe, 2012). Passive treatment on its own is, therefore, unlikely to offer a sustainable solution to the large volumes of AMD **(**Johnson and Hallberg, 2005). The widely used passive treatment methods include constructed wetlands, anoxic lime drains, alkalinity producing systems, in-situ treatment etc. Figure 2.2 is an illustration of some of the passive methods, showing various dimensions normally used for each method.

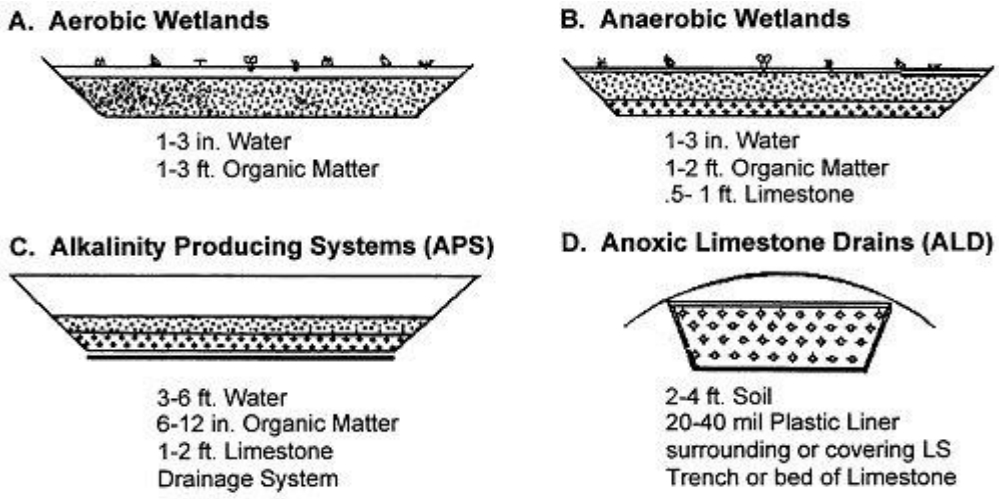


Figure 2.2: Passive treatment technologies (Skousen, 1999)

Constructed wetlands are generally divided into anaerobic and aerobic systems as shown in the figure. Both systems receive water that has been neutralized by limestone-based treatment processes. However, anaerobic wetlands generate alkalinity through bacterial activity and the use of Fe^{3+} as a terminal electron acceptor while aerobic wetlands are typically designed to promote precipitation of iron hydroxide (Fripp et al., 2000). The sediment-borne bacteria found in anaerobic systems are capable of reducing sulphate to sulphide ions. The sulphide ions then

bind with heavy metals, precipitating them out of solution, resulting in a water product with sulphate and metal levels within recommended standards. The attractiveness of constructed wetland treatment is in its low cost and the production of a near-neutral water product which can be readily discharged (Johnson and Hallberg, 2005; IMC, 2010). However, constructed wetlands are limited by the metal loads they deal with; hence adequate pre-treatment is required especially when dealing with high volumes and/or highly acidic water. Furthermore, some of the metal precipitates retained in sediments are unstable when exposed to oxygen (e.g., copper sulphide or elemental selenium) hence, it is crucial that the wetland sediments remain largely or permanently submerged (Johnson and Hallberg, 2005).

The use of anoxic lime drains (ALDs) is also a well-known passive technique. In ALDs, mine water is constrained to flow through a bed of limestone gravel held within a drain that is impermeable to both air and water (Johnson and Hallberg, 2005). This creates an environment rich in carbon dioxide and lacking in oxygen (INAP, 2005). This increases the dissolution of limestone and prevents the precipitation of iron hydroxide, which inhibits limestone dissolution and clogs the drain. Although, anoxic limestone drains produce alkalinity at a lower cost than constructed wetlands, they are not suitable for treating all AMD waters. In situations where the AMD contains significant concentrations of ferric iron or aluminium, the short-term performance of anoxic limestone drains may be good. However, the build-up of iron hydroxide precipitates gradually decreases drain permeability. This may, in turn cause failure of the drain within 6 months of construction (Johnson and Hallberg, 2005). Moreover, problems also occur where ALDs are used to treat aerated mine waters due to iron oxidation. Hence, passage of AMD through an anoxic pond prior to the anoxic limestone drain may be necessary to lower dissolved oxygen concentrations to prevent this oxidation. Another potential drawback is the formation of ferrous carbonate and manganous carbonate gels within ALDs which may cause the incongruent dissolution (Evangelou, 1995).

In-situ treatment is also one of the recognized passive treatment methods. It involves the introduction of alkaline material into the mine water body and impacted mine land (IMC, 2010). Permeable reactive barriers (PRBs) offer an approach for the passive interception and in-situ treatment of AMD-impacted groundwater. The reactive materials, which incorporate various forms of organic carbon, promote microbial mediated sulphate reduction, the generation of hydrogen sulphide, and the subsequent precipitation of sparingly soluble iron and other metals, such as Cd, Ni, Co, Cu, Zn (IMC, 2010). In-situ technologies are well suited for the management of localized seepage plumes from mine residues that contaminate shallow groundwater. However, the main drawback of these technologies is that they require a system with good mixing characteristics and sufficient access to the void water which may not be available in most polluted areas (IMC, 2010). In addition, problems such as inefficient mixing lead to usage of large quantities of the reagents which in turn increase operational cost.

2.6 Recently developed methods

This section looks at some of the recently developed methods for remediating AMD. Each technology is briefly discussed and evaluated. Most of the technologies are based on the active treatment technique.

2.6.1 CSIR Alkali-Barium-Calcium (ABC) Process

This is a precipitation process, involving the use of barium carbonate to precipitate dissolved sulphate from mine water. It consists of 3 stages which are pre-treatment, treatment with barium carbonate and the waste processing stage as shown in Figure 2.3. (De Beer et al., 2012).

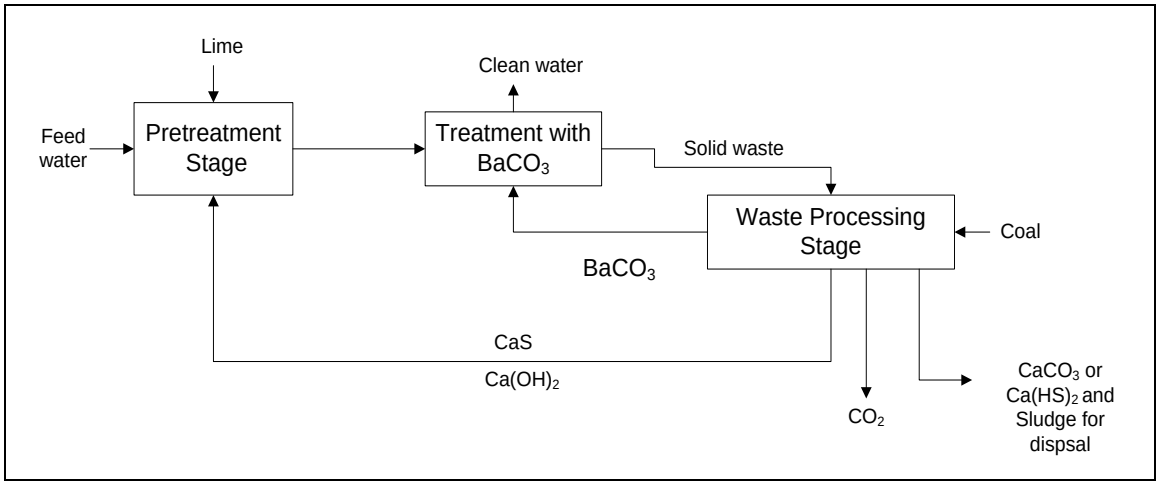


Figure 2.3: Process flow diagram for the CSIR-ABC process (De Beer et al., 2012)

In the pre-treatment stage, the feed water is treated with lime and CaS to remove free acid and metals. Tests conducted have also shown that during this stage, sulphate is lowered from 4 500 mg/L to 1250 mg/L (De Beer et al., 2012). In the water treatment stage, $BaCO_3$ is added into the water producing barium sulphate as the solid waste and clean water as shown in Figure 2.3. The water treatment stage is integrated with a sludge processing stage to recover the alkali, barium and calcium (ABC) from the sludge through reduction in a coal-fired kiln. Good quality water containing less than 100mg/L of sulphate is obtained in a cost effective way from polluted mine water through the recovery of by-products (De Beer et al., 2012). The major limitation of this technology is the amount of sludge produced which is expensive to dispose. High capital and operating costs associated with the thermal reduction of waste to produce CaS, gypsum and other solids for disposal also make the technology less cost-effective.

2.6.2 SAVMIN Process

This process was developed by Mintek to treat polluted mine water (AMD). Figure 2.4 shows the process flow diagram. The main process stages are as follows (Smith, 1999; Sibiliski, 2001).

Stage 1: Precipitation of dissolved metals and magnesium- Using lime, the pH of the feed water is raised to 12.0-12.3 to precipitate (trace) metals and magnesium.
Stage 2: Gypsum "de-supersaturation"- Using gypsum seed crystals, gypsum is precipitated from the supersaturated solution and removed.
Stage 3: Ettringite precipitation- Using aluminium hydroxide, dissolved calcium and sulphate are removed from the solution by the precipitation of ettringite (a calcium-aluminium sulphate mineral).
Stage 4 and 5: Recycling of aluminium hydroxide-Using sulphuric acid, the ettringite slurry from stage 3 is decomposed at pH 6.5 in a solution supersaturated with gypsum (no precipitation). The resulting aluminium hydroxide is recycled to the third stage and the solution supersaturated with gypsum is contacted with seed crystals (stage 2) to precipitate and remove gypsum. The remaining solution saturated with gypsum is recycled.
Stage 6: Carbonation and calcite precipitation-Using carbon dioxide, the pH of the solution from the third process stage (pH 11.2-12.4) is lowered to precipitate and remove calcite.

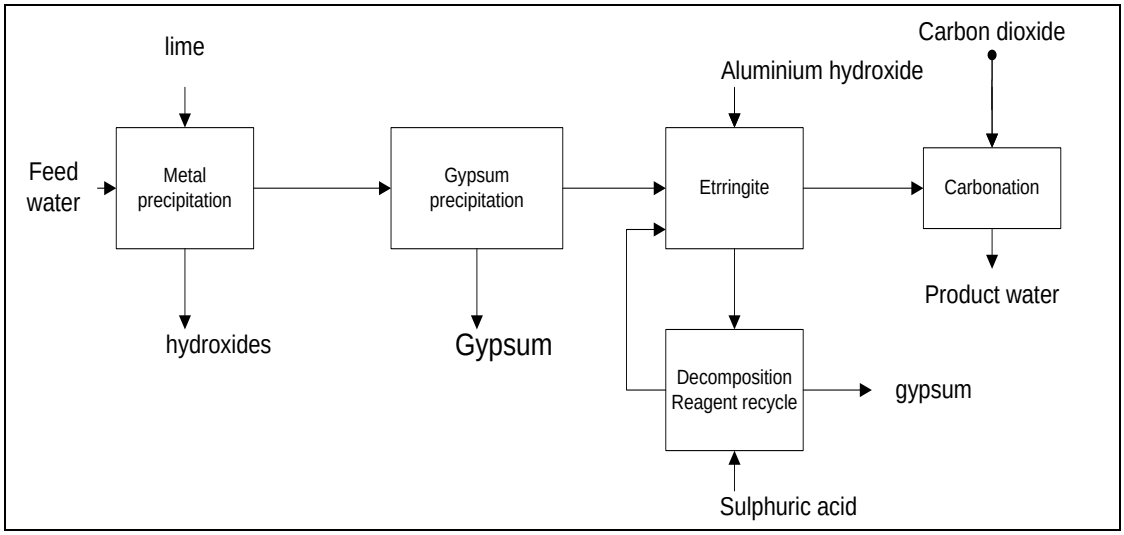


Figure 2.4: SAVMIN Process flow diagram

The end products of the SAVMIN process are potable water and a number of potentially saleable by-products such as metal hydroxides and calcite. One of the major advantages of the SAVMIN process is that high quality products can be obtained (Smith, 1999). A major disadvantage is the amount of the sludge produced by the process which presents disposal challenges.

2.6.3 SPARRO process

It is a membrane desalination process designed to treat calcium sulphate scaling mine water. The process was developed in the late 1970s by Resources Conservation Company in Seattle, USA (O`Neail et al., 1981). After the pre-treatment stage involving pH adjustment, removal of suspended solids through coagulation, settling and filtration, the feed water is pumped into a storage tank (INAP, 2003). From the tank, it is pumped to the reverse osmosis membrane module bank. Before reaching the module bank, the feed water is mixed with recycled gypsum seeds from the reactor. The treated water from the module is stored. The flow concentrate from the hydro-cyclone is further subdivided. Using a programmable controller, one part is further returned to the reactor and the other is blown up as brine (overflow) and seeds

(underflow). The SPARRO technology can treat most waste waters and produces good quality water at variable water recoveries (Pulles et al., 1992). However, the disadvantage is that the life of membranes is greatly reduced (due to fouling) by the quality of the feed water (INAP, 2003). Compared to the conventional reverse osmosis technology, the membrane life in the SPARRO process has been improved by introducing the use of a pump system, independent gypsum seed control and other design configurations (Pulles et al., 1992; Juby et al., 1996) but still it is not ideal. Improvements in the membrane performance will increase the economic viability of the SPARRO treatment process.

2.6.4 GYP-CIX Process

It is a continuous fluidized bed ion-exchange process that effectively removes calcium and sulphate from water that is saturated with gypsum (Everett et al., 1993; Robinson et al., 1998). It uses low cost chemicals such as lime and sulphuric acid for acid regeneration. The only waste product is gypsum and the treated water meets standards for re-use. The process consists of two stages of operation (Robertson and Rohrs, 1995; Robinson et al., 1998). The first involves the removal of cations in a multi stage continuous loading train, using cation exchange resin. The second operation entails the removal of the anion again in a multistage loading train using anion exchange resin. Sulphuric acid is used to regenerate the cation exchange resin while the lime slurry is used for anion resin regeneration. In both cases the waste produced is brine slurry containing precipitated calcium sulphate and water of re-usable quality (Robertson and Rohrs, 1995). The advantages of this process as stated above are the use of low cost chemicals and high water recoveries (Robinson et al, 1998). However, the main disadvantage of the process is the production of large volumes of gypsum sludge in the regeneration of the ion-exchange resins which presents disposal challenges.

2.6.5 THIOPAQ Process

It is a biotechnological process which uses two distinct microbiological populations and stages (Boonstra et al., 1999): (i) conversion of sulphate to sulphide by using hydrogen gas (from the conversion of ethanol/butanol to acetate and hydrogen) as the electron donor and precipitation of metal sulphides and (ii) conversion of any excess hydrogen sulphide produced to elemental sulphur, using sulphide-oxidising bacteria. In this way sulphate is removed from AMD to produce water of re-usable quality. This process has lost attractiveness over the years due to an increase in the price of ethanol and butanol which are energy sources for the process (Boonstra et al., 1999).

2.6.6 The Rhodes BioSURE Process

This is a locally invented biological treatment that has been used at Grootvlei East Rand Water Care Company. It was developed by the Environmental Biotechnology Group (EBRU) of Rhodes University (Neba, 2007). The process removes acidic sulphate using free waste stock, such as sewage sludge, instead of expensive carbon and electron donor sources such as ethanol and hydrogen. This makes it significantly cheaper than other similar alternatives (Neba, 2007). This technology is restricted by the availability of sewage sludge or other organic wastes used as carbon and energy sources; however, it has the advantage of providing an option for the co-disposal of sewage sludge, reducing the costs of landfill solid waste.

2.6.7 Tshwane University of technology Magnesium-Barium-Alkali (MBA) Process

This is an improvement on the CSIR-ABC Process. This is a more feasible option than the ABC Process as $Ba(OH)_2$ is used for two functions simultaneously: (i) sulphate removal by means of $BaSO_4$-precipitation, and (ii) magnesium removal by

$Mg(OH)_2$-precipitation based on an assessment performed by the Tshwane University of Technology (Fields, 2010). The same challenge of sludge disposal as in CSIR ABC process is also encountered in this method.

2.6.8 HiPRO (High Pressure Reverse Osmosis) Process

This process has been successfully used for water treatment at Emalahleni water reclamation plant, since September 2007 (Blueprint, 2009). It was developed by Key plan (Pvt) Ltd. Ultra-high water recoveries (greater than 97%) are consistently achieved (Blueprint, 2009). The final products from this process are portable water which is sold to the local municipality, a liquid brine solution(less than 3% of the total feed) and solid waste. The solid waste products are calcium sulphate of saleable grade as well as a calcium and metal sulphates product. However, the process produces waste brine and water sludge which is expensive to dispose.

2.6.9 EARTH (Environmental and Remedial Technology Holdings) Ion Exchange Process

This process uses ion exchange columns to recover uranium and sulphate ions from AMD (Howard et al., 2009). The uranium bearing solutions could be sold to uranium processors. The sulphate ions recovered are reacted with ammonia gas to form 20% ammonium sulphate solution (Howard et al., 2009). Metal cations are also recovered by use of cationic exchange resins, which are later eluted with nitric acid to form a mixed metal nitrate solution which can be sold. However, the overall cost of chemicals amounts to R11.00/m^3 and the value of the by-product (ammonium nitrate and sulphate) amounts to R10.00/m^3 (Fields, 2010), although these figures vary depending on the quality and composition of the feed water. The feasibility of this technology is dependent on there being a market for the products and stable prices.

Seasonal fluctuations and droughts may influence the financial viability of the technology (Fields, 2010).

Consequently, it can be seen that most of the current technologies developed to deal with the AMD problem, are not sustainable. In addition to producing water of acceptable standard, they also generate another waste stream which is not normally considered for by-products or useful application. This adds to the cost of disposal and creates more negative impact on the environment. As such, a solution that can deal with these technical challenges while providing financial returns is highly preferred. Hence, increasing research has been directed towards the possible recovery of valuable materials from AMD. The success of such research could provide financial benefits, which may be used to offset the treatment cost. In addition, the recovery of valuable materials significantly reduces the quantity of solid waste products, which in turn not only reduces the cost of disposal but also the deleterious effect of the waste on the environment.

Several potentially valuable products have been recovered from AMD, some of which have already been commercially applied in successful ventures (Hedin, 2002). Listed below are some the products which can be obtained from AMD (Hedin, 2002; Buzzi et al., 2013; Martí-Calatayud et al., 2013; Chen et al., 2014):

- Iron oxides
- Water
- Sulphuric acid

Of growing interest is the recovery of heavy metals and sulphuric acid, which could be due to their appreciable market value as well as the environmental benefits derived from their recovery, considering that these are the most toxic components of AMD. Conventional methods such as solvent extraction, electrochemical methods, adsorption, acid retardation, ion exchange etc., have been used to achieve this purpose. However, adsorption using low cost adsorbents has emerged as one of the

promising technologies for metal recovery. Likewise, the acid retardation process has become popular for acid recovery in the metal finishing industry owing to its simplicity and high acid recoveries. Hence, the present investigation aimed at testing the feasibility of using a combination of these processes for AMD remediation. A two stage approach was proposed, the first being metal removal using low cost adsorbent followed by acid recovery using the acid retardation process. Figure 2.5 shows the proposed flow sheet:

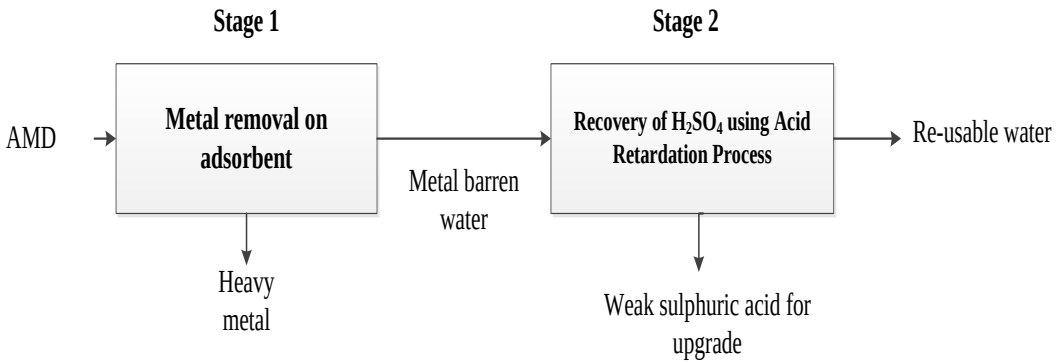


Figure 2.5: Proposal flow sheet for remediation of AMD

According to the flow sheet, a water product of acceptable quality together with a dilute sulphuric acid product could be expected. The full details of the applied processes follow in the next sections.

2.7 Adsorption of AMD

Several traditional methods exist for heavy metal removal from AMD and these include chemical precipitation, ion exchange, reverse osmosis, electrochemical treatment, membrane filtration and adsorption processes (Fu and Wang, 2011). However, methods such as ion exchange, reverse osmosis, electrochemical methods etc., have been found to exhibit low removal efficiencies and high treatment cost for low metal concentrations, which are nevertheless still above recommended maximum discharge levels such as those found in AMD solutions. Hence, adsorption has emerged as a promising alternative technique for the treatment of low metal effluents

due to its high selectivity, low operational cost and production of minimal toxic sludge (Kurniawan et al., 2011). Adsorbents such as activated carbon, silica gels and molecular sieves have been used successfully to remove metal contaminants from waste water (Richardson et al., 2002). However, the financial constraints associated with these adsorbents have limited their use. In addition, developing countries such as South Africa do not have the financial ability to invest in expensive adsorbents or any other costly treatment method. Therefore, much research in the recent years has been directed towards the search for potentially low cost adsorbents. According to Bailey et al. (1999), an adsorbent can be considered as cheap or low cost if it is abundant in nature, requires little processing and is a by-product of waste material from industry.

Amongst the adsorbents under investigation, much is being written about the use of natural materials such as biomass and clays. Dead biomass such as the cassava peel, tree bark etc., natural clays such as bentonite, attapulgite etc., and alumino-silicates such as zeolites have been identified as potential alternatives to the existing adsorbents (Wan Ngah and Hanafiah, 2008; Motsi, 2009; Enslin et al., 2010; Kosasih et al., 2010; Falayi and Ntuli, 2014). The utilization of low cost adsorbents is an attractive option since they can be used to remove toxic heavy metals from AMD and produce water with significantly less harmful impact on the receiving environment at a reasonable cost. Furthermore, the adsorbents can be regenerated and the metals recovered from them. This in turn increases the financial viability of the adsorption process, since valuable heavy metals can be recovered and the income generated used to compensate for the treatment cost.

Hence, in the present study bentonite clay, zeolite and cassava peel biomass were selected for feasibility tests on a real AMD sample. Some of the advantages of these adsorbents include:

- Low cost
- Relative abundance and availability
- High metal removal capacity

- Can be easily generated at a reasonable cost
- Cassava peel is an agricultural waste which has no economic value

The details of the adsorption process with respect to the structures of the adsorbents, the mechanisms involved, factors affecting the process and equilibrium isotherms are discussed in the next subsections. Bentonite clay and zeolite are presented first since both are crystalline materials, and cassava peel is discussed last because it is a biological material and undergoes a special type adsorption known as biosorption.

2.7.1 Adsorption process

Adsorption can be simply defined as a surface-based phenomenon which involves the adhesion of atoms, ions or molecules from a gas, liquid, or dissolved solid to a surface (Richardson et al., 2002). The phase that is being adsorbed is referred to as the adsorbate, and the material on which it adheres to is called the adsorbent. In cases, where the adsorbent is a biological material, the process is generally referred to as biosorption.

Structure of bentonite clay and zeolite adsorbents

The structure of the material plays a critical role in its performance as an adsorbent, as the crystalline framework contains exchangeable ions which may be responsible for metal adsorption. Figure 2.6 shows the crystalline structures of zeolite and bentonite clay.

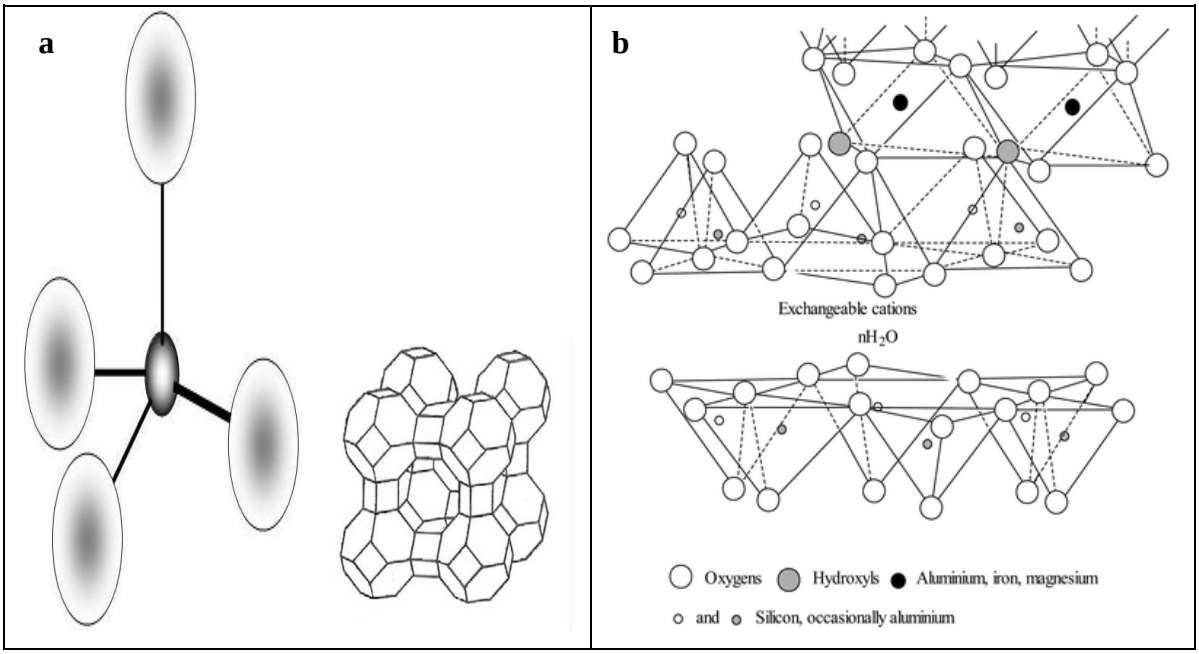


Figure 2.6: Structure of (a) zeolite and (b) bentonite clay (Xu et al., 2007)

The structure of both zeolite and bentonite clay are both crystalline in nature (Xu et al., 2005). However, on comparing Figure 2.6 (a) and (b), it can be seen that zeolite has a tetrahedral structure whereas bentonite clay has a layered structure. The difference in the structure, affects the properties of these adsorbents, which are discussed fully herein.

Figure 2.6 (a) shows that the crystalline structure of the zeolite adsorbent used in the present research. The zeolite has a general unit cell composition of $[Na_{12}(Al_{12}Si_{12}O_{48}).27H2O]$, and its Si/Al ratio is always close to 1.0 (Mumpton, 1999). It crystallizes into cubic forms as shown in the figure. Generally, zeolites are naturally hydrated aluminosilicates, which belong to the class of minerals known as 'tectosilicates'. Most common natural zeolites are formed by alteration of glass rich volcanic rocks (tuff) with fresh water in playa lakes or by seawater (Erdem et al., 2004). The structure of zeolites consists of three-dimensional frameworks of SiO_4 and AlO_4 tetrahedra. The aluminium ion is small enough to occupy the position in the center of the tetrahedron of four oxygen atoms, and the isomorphous replacement of

Si^{4+} by Al^{3+} produces a negative charge in the lattice (Erdem et al., 2004). The net negative charge is balanced by an exchangeable cation (sodium, potassium, or calcium). These cations can be exchanged with noxious cations such as manganese, lead, cobalt, copper and zinc found in waste water solutions (Álvarez-Ayuso et al., 2003; Perić et al., 2004). Zeolites are able to lose and gain water reversibly and to exchange extra framework cations, both without change of crystal structure (Mumpton, 1999). In addition, zeolites can also be modified by introducing functional groups on its surface to improve its selectivity for the substance to be removed (Ćurkovic et al., 1997). This is usually done by exposing the zeolite surface to high temperatures as well as surface modification with organic compounds and yeasts (Daković, 1986; Ćurkovic et al., 1997; Nsimba, 2012).

The selectivity of zeolites depends on various factors, but mainly on the cation exchange capacity (CEC) which is sometimes known as the Si/Al ratio. This is basically the amount of Al^{3+} ions that substitute the Si^{4+} ions in the tetrahedral zeolite framework (Mumpton, 1999). The greater the aluminium content, the more incoming ions are needed to balance the charge, thus the higher the exchange capacity. Other factors influencing the adsorption capacity of zeolites include:

- The hydration diameters; of ions sitting in the framework and those incoming into the zeolite.
- Hydration enthalpies
- Solubility of cations

Bentonite is alumina silicate clay made up of sodium and calcium montmorillonites. It belongs to a group of minerals known as ‘smectictes’. In bentonite (Figure 2.6 (b)), tetrahedral layers consisting of [SiO4] - tetrahedrons enclose the [$Me(O_5)$,OH)]-octahedron layer (Me is mainly Al, Mg, but Fe is also often found). The silicate layers have a slight negative charge that is compensated by exchangeable ions in the inter-crystallite region (Nsimba, 2012). It is these ions, which can be easily exchanged for noxious heavy metals found in waste water. The cation exchange

process is reversible and stoichiometric, which varies depending on the concentration of the metal ions, pH of the solution and the nature of the metal ion (Kaya and Oren, 2005).

As a result of its crystalline structure, bentonite has a high specific surface area, high plasticity, and can expand several times its original volume when placed in water forming viscous suspensions (Enslin et al., 2010). The ability to expand is a result of the incorporation of water molecules between the (tetrahedraloctahedral- tetrahedral) sheets in association with the interlayer cations (Na^+ and Ca^{2+}), which are driven off when the bentonite is heated in air. Most industrial applications involve the swelling property of bentonite to form suspensions. This is due to the fact that bentonite can disperse into colloidal particles and accordingly provide large surface areas per unit weight of clay. However, this property has been found to present operational challenges in waste water treatment. Although, bentonite can adsorb heavy metals, its use as an adsorbent in the filtration mode is limited due to the formation of a colloidal solution which is difficult to separate after the adsorption process. In addition, the use of bentonite adsorbent in the column mode is limited by the low permeability of the compacted bentonite bed (Kapoor and Viraraghavan, 1998). Hence, immobilization of the clay powder has been suggested to improve its performance and facilitate its removal from the treated solution.

Immobilization involves the incorporation of the biomass in a granular or polymeric matrix normally with the intention of improving the biomass performance and to facilitate its separation from the solution (Summers et al., 1996). Immobilization in a polysulfone matrix is a common practice (Kapoor and Viraraghavan, 1998). However, this necessitates the use of dimethylformamide (DMF) as a solvent, but DMF is considered a hazardous substance and its use must be avoided (Summers et al., 1996). In addition, the process is known to produce non-spheroidal beads which tend to pack asymmetrically, causing water to flow in certain channels rather than uniformly over all the beads. Therefore, the search for other supports has been

prompted. The use of sodium silicate as a binder is one of the promising ways for immobilizing bentonite. It has shown success as a substitute for polysulfone in other related work (Summers et al., 1996).

Possible Mechanisms involved in adsorption

The investigation of the mechanisms involved in the adsorption of heavy metals is crucial in environmental chemistry, especially in the development of tertiary wastewater systems with extreme pH values and salts loads, such as AMD. Several interactions involving toxic heavy metals and crystalline adsorbents such as bentonite and zeolites have been reported. These interactions range from weak, physical, Van der Waals forces and electrostatic outer-sphere complexes (such as ion exchange or surface precipitation/complexation) to chemical interactions. Chemical interactions can include inner-sphere complexation that involves a ligand exchange mechanism, covalent bonding, hydrogen bridges, and steric or orientation effects (Doula and Ioannou, 2003). These interactions are very strong, and regeneration might be a problem particularly in processes where they are dominant. On the contrary, outer-sphere interactions involve weak forces, and hence, these are usually rapid and can be easily reversed.

Generally, when the adsorption process begins, outer surface complexes are formed on external surface sites (Doula and Ioannou, 2003). The outer-surface complexation involves ion exchange reactions between heavy metal ions and surface counterbalance cations. As the metal concentration on the outer surface increases, metal ions are forced into internal surface sites and also form inner-sphere complexes. This type of complexation leads to more stable surface groups due to the formation of covalent bonds. Hydrogen cations are released as products and the process causes a total decrease in solution pH (Stumm, 1991). Scheidegger and Sparks (1996) also confirmed this phenomenon. According to their study, a continuum exists between

surface complexation (physical adsorption) and surface precipitation. Surface complexation was reported to be the dominant mechanism at low surface coverage. However, as the surface coverage increases nucleation occurs, and results in the formation of distinct entities or aggregates on the surface. Hence, it follows that at higher surface loading; surface precipitation becomes the dominant mechanism.

In addition to ion exchange, surface precipitation/complexation and sorption, dissolution of the crystalline structure has also been reported in heavy metal adsorption processes (Alvarez-Ayuso et al., 2003; Kaya and Oren, 2005). Heavy metal ions and ligands can affect surface sites and provoke dissolution of Al^{3+} and/or Si^{4+}. Generally, the reactivity of a surface, i.e., its tendency to dissolve, depends on the type of surface species present, e.g., an inner-sphere complex with a ligand such as Cl- facilitates the detachment of a central metal ion and enhances dissolution (Doula and Ioannou, 2003). The explanation of the above behavior is based on an electron density shift from ligands toward the central metal ion at the surface. This excess of electron density brings the negative charge into the coordination sphere of the Lewis acid center and simultaneously enhances surface protonation and can labilize the critical S-O (S: central metal, Si^{4+}, Al^{3+}) lattice bonds, thus enabling the detachment of the central metal ion solution (Doula and Ioannou, 2003). Similarly, surface protonation (low pH values) tends to increase the dissolution, because it leads to highly polarized interatomic bonds in the immediate proximity of the surface central ions and thus facilitates the detachment of a cationic surface group into the solution. The dissolution of most aluminosilicates increases with both increasing protonation and decreasing surface protonation, equivalent to the binding of OH^- ligands (Rivera et al., 2000); thus under alkaline conditions dissolution increases with increasing pH (Doula and Ioannou, 2003).

In seldom cases, the ion pairing mechanism has also been reported. This is a mechanism by which the presence of one ion can possibly facilitate adsorption of the other (Davis and Burgoa, 1995). Anionic ligands can be adsorbed to solids by

specific (inner-sphere complexation) and nonspecific (outer-sphere complexation), mechanisms. Outer-sphere complexation, in this case is the coordination of an anion to a protonated hydroxyl or surface metal cation; anions complexed in the outer-sphere of a solid are readily exchangeable and are free to move in solution because there is no complex formed with surface functional groups, but only a neutralization of surface charge (Doula and Ioannou, 2003). Amongst the anionic ligands, sulfate has been reported to form inner-sphere complexes with surface active sites (Davis and Burgoa, 1995); this increases the net negative charge, which in turn increases metal adsorption. However, ligands such as the chloride and nitrate ion form outer-sphere complexes and also enhance metal uptake indirectly.

Factors affecting adsorption

The removal of heavy metals by adsorption depends on the following factors:

Solution pH

The pH value of the solution plays a critical role in the amount of heavy metals adsorbed by clays and alumino-silicates. It not only influences the quantity of metals adsorbed, but also the characteristics of the retained metals as well as the structure of the adsorbent. In general, the amount of heavy metals adsorbed from solution is known to increase with an increase in pH (Ali and El-Bishtawi, 1997; Kaya and Oren, 2005; Motsi et al, 2009). At low pH values typically below 4, heavy metal adsorption has been found to be very low. Motsi et al. (2009) reported that less than 40% of Mn^{2+}, Zn^{2+} and Cu^{2+} ions in an AMD sample were adsorbed by the zeolite at pH values between 2.5 to 3.5. Kaya and Oren (2005) also found that the lowest Zn^{2+} sorption by bentonite took place at pH 3. Similar findings were reported in other work (Alvarez-Ayuso, 2003; Argun, 2008). The low metal adsorption has been attributed to the fact that zeolite or bentonite adsorbents preferentially adsorb H^{+} ions to heavy metals (Ali and El-Bishtawi, 1997; Kaya and Oren, 2005). This adsorption

of the H^+ ions also causes the active sites on the surface of the adsorbent to be protonated, resulting in increased electrostatic repulsions between the heavy metals and the protonated surface. In addition to the low metal uptake, low pH values are known to have a detrimental effect on the structure of the adsorbent. Hydrogen ions may exchange with the Al^{3+} ions in the alumino-silicate layers resulting in the dissolution and eventually the collapse of the adsorbent framework (Kaya and Oren, 2005).

As pH values progress above 4, heavy metal uptake has been reported to increase as the ion exchange and precipitation mechanisms come into play. Generally, at higher pH values, fewer H^+ ions are present in solution, and this reduces competition with metal ions for active sites resulting in higher metal retention (Ali and El-Bishtawi, 1997; Kaya and Oren, 2005). A combination of adsorption and ion exchange mechanisms has been reported as the dominant metal removal mechanism in the range 4 to 6 (Alvarez-Ayuso et al., 2003; Kaya and Oren, 2005). This is a result of the replacement exchangeable cation, i.e. Na^+, K^+, Ca^{2+}, Mg^{2+} with heavy metal cations in the aqueous solution. As the pH increases beyond 6, precipitation has been reported as the dominant mechanism for heavy metal retention. However, the presence of precipitates in solution at higher pH values has also been reported to clog the adsorbent and hence, hinder metal ion accessibility to active sites (Alvarez-Ayuso et al., 2003).

Contact time

Adequate contact time to interact with the active sites is required for effective heavy metal removal from solution. Generally, the amount of adsorbed heavy metals is known to increase with an increase in contact time, normally remaining nearly constant after equilibrium has been attained (Ghomri et al, 2013). This is because the active sites are initially unoccupied, however, as time passes they become filled with heavy metals. Hence, it follows that metal adsorption reaches a saturation stage when

all the possible available sites have been occupied and further adsorption could only take place at new surfaces (Erdem et al., 2004). Ghomri et al, 2013 reported equilibrium times of about 60 minutes for Cu^{2+} and 150 minutes for Zn^{2+}, Ni^{2+} and Co^{2+} ions, when a metal solution was contacted with zeolite adsorbent. This difference in heavy metal uptake at the same contact time was attributed to the difference in their chemical affinity and ion exchange capacity with respect to the active sites. Over 90% of nickel, zinc, chromium and cadmium metal removal from solution was attained after one hour on interaction in other related work (Alvarez-Ayuso, 2003). Similar results were also observed in other work with bentonite adsorbent (Triantafyllou et al., 1999; Al-Shahrani, 2012). However, other related research has reported longer equilibrium times in the range of 6 to 48 hours for the same adsorbent (Kaya and Oren, 2005; Summers, 1996). This difference could be a result of the origin of the bentonite, since this though to a lesser extent, influences the performance of the adsorbent.

Temperature

Generally, adsorption of metal ions has been found to increase with an increase in temperature (Meena et al., 2005). This indicates that the adsorption of heavy metals is an endothermic process. The increase in metal adsorption with temperature may be attributed (1) the increase in the number of active sites available for adsorption (2) desolvation of the adsorbing species and (3) the reduction in the boundary layer thickness, which in turn also reduces the mass transfer resistance (Meena et al., 2005). Since adsorption is an endothermic process, the external mass transfer rate of ions to the adsorbent surface is expected to increase at higher temperature, leading to greater adsorption being observed.

Competition between ions

In practice, most heavy metal solutions contain a mixture of different heavy metal ions which may influence the quantity of specific heavy metals adsorbed as well as the surface properties of the adsorbents. Several studies have been conducted in order to investigate the influence of competing ions on the adsorption process (Erdem et al., 2004; Motsi et al., 2009; Ghomri et al., 2013). Motsi et al. (2009) compared the adsorption of target heavy metals from an AMD solution containing Cu^{2+}, Fe^{3+}, Zn^{2+} and Mn^{2+}, to their single component systems. The results showed that the adsorption Fe^{3+} ions were not significantly affected by the presence of competing ions. This is because the main mechanism for Fe^{3+} adsorption was believed to be precipitation. The adsorption of the other three cations was significantly affected, with the amount adsorbed from the mixture decreasing by 33%, 41% and 39% for Cu^{2+}, Zn^{2+} and Mn^{2+} respectively, compared to their respective single component solutions. This observation indicated that different adsorption mechanisms may be involved in the adsorption of different heavy metals from solution. Similar findings were also reported in related work (Erdem et al., 2004; Ghomri et al., 2013). In addition, Erdem et al. (2004) also found out that ions with smaller ionic diameter had easier access to active sites compared to their bigger counterparts. This resulted, in the higher adsorption of these metals from the solution.

Adsorbent dosage

The rate of metal uptake has been found to generally increase with an increase in adsorbent dosage (Erdem et al, 2004; Motsi et al., 2009). This increase can be attributed to the introduction of more adsorption sites which adsorb more cations from the solution.

Agitation speed

In general, increasing the agitation speed reduces the external boundary layer thickness and increases the mass transfer rate of the metal ion to the adsorbent surface (Richardson et al., 2002). Optimizing the agitation speed is important since high speeds lead to the breakage of the weak bonds between the metal ion and the adsorbent, resulting in the metal ion being desorbed from the active sites.

2.7.2 Biosorption

Biosorption is a physicochemical process that occurs naturally in certain biomass which allows it to passively concentrate and bind contaminants onto its cellular wall (Volesky, 1990). Biosorption can be divided into metabolic dependent and non-metabolic dependent systems. Metabolic dependent biosorption involves the transportation of metal ions across a cell membrane resulting in intracellular accumulation. This is dependent on the metabolism of the cell, hence, this type of biosorption only takes place in living cells (Gadd et al., 1988). In non-metabolism dependent biosorption, heavy metal uptake occurs by means of physicochemical interactions between the metal and the functional groups present on the microbial cell surface (Kuyucak and Volesky, 1988). This is based on physical adsorption, ion exchange and chemical sorption, which is not dependent on cell metabolism. Cell walls of microbial biomass, which consist mostly of polysaccharides, proteins and lipids, have abundant metal binding groups such as carboxyl, sulphate, phosphate and amino groups (Gardea-Torresdey et al., 1990; Abia et al., 2003). This type of biosorption, i.e., non-metabolism dependent, is relatively rapid and can be easily reversed (Kuyucak and Volesky, 1988).

The later type of biosorption is of particular interest in the present study, since the biomass of interest i.e. cassava peel is dead biomass. Numerous studies have

established that cassava peel biomass contains carboxylic, hydroxyl and other cellulosic compounds which provide active sites for metal sequestration (Abia et al., 2003; Kosasin et al., 2010; Kurniawan et al., 2011; Ndlovu et al., 2012; Simate and Ndlovu, 2014). In these studies, cassava peel biomass has shown remarkable success in the removal of heavy metals such as copper, cadmium, zinc, nickel, cobalt, vanadium and chromium from various waste water solutions. Some of these studies have also revealed that modifying the biomass by treatment with alkalis and acids such as thioglycollic acid introduces new functional groups responsible for enhanced metal uptake (Abia et al., 2003; Ndlovu et al., 2012). In addition, literature reports that immobilizing cassava into pellets significantly improves heavy metal uptake (Simate and Ndlovu, 2014). Immobilization has also been reported to improve the mechanical strength, porosity and the life of the biosorbent. The supports normally used in biosorbent immobilization include polysulfone, polyurethane, alginate, polyacrylamide and polyethyleneimine (Rangsayatorn et al., 2004).

Possible mechanisms involved in biosorption

Due to the complex nature of biomass various mechanisms have been suggested to explain the heavy metal uptake. These mechanisms include physical adsorption, precipitation, chelation, co-ordination, complexation and ion exchange (Gadd, 2009). Although, one of the mechanisms may be dominant in each case, it is possible that it can occur concurrently with one or more of other mechanisms, in degrees that depend on the biosorbent and environmental conditions (Volesky, 2001). The uptake of metallic ions starts with the ion diffusion to surface of the evaluated biomasses. Once the ion has diffused though the cellular surface, it interacts with the sites that display some affinity with the metallic species. Some of these interactions are described below. These various biosorption mechanisms can take place simultaneously (Ahalya et al., 2003).

Physical adsorption: This is a process whereby the metal ions in solution bind onto polyelectrolytes in microbial cell wall through the help of weak Van der Waals

forces. Kuyucak and Volesky (1988) suggested that uranium, cadmium, zinc, copper and cobalt biosorption by some dead biomasses such as algae, fungi and yeasts takes place through electrostatic interactions between the metal ions in solutions and cell walls of microbial cells. The work of Kosasih et al. (2010) also reports the uptake of copper ions by electrostatic interactions.

Ion exchange: Cell walls of microorganisms contain polysaccharides and bivalent metal ions exchange with the counter ions of the polysaccharides. For example, the alginates of marine algae occur as salts of K^+, Na^+, Ca^{2+}, and Mg^{2+}. These ions can exchange with noxious counter ions such as Co^{2+}, Cu^{2+}, Cd^{2+} and Zn^{2+} resulting in the biosorptive uptake of heavy metals (Kuyucak and Volesky, 1988). Abia et al. (2003) also attributed the uptake of Cd^{2+}, Cu^{2+} and Zn^{2+} ions by cassava peel to the ion exchange mechanism.

Complexation/Co-ordination: This is a metal removal mechanism involving the combination of cations with molecules or anions containing free electron pairs often called ligands (Wang and Chen, 2006). Aksu et al. 1992 hypothesized that biosorption of copper by C. *vulgaris* and Z. *ramigera* takes place through both adsorption and formation of coordination bonds between metals and amino and carboxyl groups of cell wall polysaccharides. Complexation was found to be the only mechanism responsible for calcium, magnesium, cadmium, zinc, copper and mercury accumulation by Pseudomonas syringae. Micro-organisms may also produce organic acids (e.g., citric, oxalic, gluconic, fumaric, lactic and malic acids), which may chelate toxic metals, thus resulting in the formation of metallo-organic molecules. These organic acids help in the solubilization of metal compounds and leaching from their surfaces. In addition, metals may also be biosorbed or complexed by carboxyl groups found in microbial polysaccharides and other polymers (Ahalya et al., 2003). However, it does not necessarily mean that the presence of some functional group guarantees biosorption, perhaps due to steric, conformational or other barriers.

Precipitation: This mechanism may be either dependent on the cellular metabolism or independent of it. In the former case, the metal removal from solution is often associated with active defence system of the microorganisms. They react in the presence of a toxic metal producing compound, which favour the precipitation process. In the case of precipitation not dependent on the cellular metabolism, it may be a consequence of the chemical interaction between the metal and the cell surface.

Factors affection biosorption

The biosorption of heavy metals has been found to depend on the following factors:

Solution pH

The pH of the solution plays an influential role not only in the site solution chemistry of the biomass surface, but also on the solution chemistry of the heavy metals, hydrolysis, complexation by organic and/or inorganic ligands, redox reactions, precipitation, the speciation and the biosorption availability of the heavy metals (Esposito et al., 2002). The biosorptive capacity of metal cations increases with increasing pH of the sorption system, but not in a liner relationship. On the other hand, too high pH value can cause precipitation of metal complexes, so it should be avoided during experiments (Wang and Chen, 2006). For different biosorption system of metal ions, the optimal pH is different. Abia et al. (2003) reported an optimal pH value between 4 and 5 for the sorption of Cd^{2+}, Cu^{2+} and Zn^{2+} ions on cassava peel biomass. It was observed that as the pH decreased the adsorption capacity of the three metal ions also decreased. This observation suggested that the adsorption mechanism for the metals investigated might be an ion-exchange type process. Kosasih et al. (2010) and Kurniawan et al. (2011) also proved the pH dependency of biosorption of heavy metals on to cassava peels, with an optimal pH value of 4.5 reported for Cu^{2+}

and Ni^{2+} sorption respectively. Related work also reported an optimal pH value of 3 for V^{3+} and Co^{2+} (Ndlovu et al., 2012). In addition, the results on the work on cassava peel have shown little adsorption of metal ions as the pH decreases below 3.0 (Abia et al., 2003). This feature of low adsorption at low pH values has been used to study the regeneration of the loaded biosorbent using dilute acids, and this demonstrates the potential of recycling the metals.

Temperature

The effect of temperature varies and seems to depend largely on the type of biomass system. In some systems, temperature has been found to have no influence on the biosorption performances in the range of 20 to 35°C (Aksu et al. 1992). In other systems, adsorption has been reported to be exothermic, implying that biosorption capacity increases with a decrease in temperature (Kapoor and Viraraghavan, 1997). In the range of 15 to 40 °C, the maximum equilibrium biosorption capacity for heavy metal ions by some biomass such as yeast was reached at 25 °C (Wang and Chen, 2006). However, the metal sorption of cassava peel biomass has been reported to be endothermic. Optimal temperatures between 40 and 60 °C have been reported for various heavy metals uptake (Kosasih et al. 2011; Ndlovu et al., 2012). The adsorption capacity was found to decrease at higher temperatures, which could be attributed to the deactivation of active binding sites in the biomass.

Contact time

The biosorption of heavy metals is generally rapid ranging from a few minutes to about two hours. The biosorption of metals such as copper and nickel by cassava peel biomass has been found to be a rapid process, with equilibrium being attained within the first 30 minutes (Kosasih et al., 2010; Kurniawan et al., 2011). These results were attributed to metal-adsorbent interactions involving cation exchange reactions, surface complexation and/or chelation. Similar results were also observed in the work

of Ndlovu et al. (2012), where optimal contact times of 25 minutes and 30 minutes were recorded for cobalt and vanadium uptake, respectively. Although, the biosorption of heavy metals normally increases with an increase in contact time, it is advisable to optimize the contact time, considering the efficacy of desorption and regeneration of the biomass.

Competing ions/co-ions

The binding of metallic species by biomass is influenced by the presence of co-ions and anions which may be present in the solution (Oliveira et al., 2011). These ions compete with the metal ion of interest for active sites, resulting in a decrease in the metal uptake. The extent of inhibition depends on the binding strength of the metal ion of interest to biomass. Light metals such as alkaline and alkaline earth metals bind less strongly to the active sites than heavy metals; hence, their presence does not strongly interfere with the binding of the latter (Gadd, 2009). In some studies, alkali and alkaline earth metals were not adsorbed by biomass, possibly due to their inability to form complexes with the various ligand groups present on the biomass surface (Kapoor and Viraraghavan, 1997). Anions such as the CO_3^{2-}, SO_4^{2-} and PO_4^{2-} may clearly affect biosorption through the formation of soluble metal precipitates (Gadd, 2009). Chloride may influence biosorption though the formation of complexes such as $CdCl_3$.

Biomass dosage

The extent of biosorption is also influenced by the dosage of the adsorbent. An increase in the biomass mass dosage generally increases the quantity of metal ions taken up by the adsorbent (Gadd, 2009). This is due to the increased surface area of the biosorbent which in turn increases the number of binding sites (Gadd, 2009). However, the quantity of biosorbed solute per unit weight of biosorbent decreases with increasing biosorbent dosage which may be due to a complex interaction of

several factors. An important factor at high sorbent dosage is that the available solute is insufficient to completely cover the available exchangeable sites on the biosorbent, usually resulting in low solute uptake per given weight (Oliveira et al., 2011). In addition, Gadd et al. (1988) also hypothesized that the low solute uptake per unit weight was a result of the interference between the binding sites.

Agitation speed

The rate of agitation plays an influential role in the formation of the external boundary film and optimizing it is crucial in order to minimize the mass transfer resistance. When the agitation speed is increased, the mass transfer rate of the solute from the bulk solution to the liquid boundary layer is increased owing to the enhanced turbulence and the decrease in boundary layer thickness (Shen and Duvnjak, 2005).

2.7.3 Adsorption isotherms

The adsorption isotherms provide information on the amount of adsorbent required for removing a unit mass of pollutant under the operating conditions (Pandey et al, 2010). Adsorption isotherm models can be regarded as a benchmark for evaluating the performance of an adsorbent. Analysis of the isotherms is important in order to develop an equation that accurately represents the results and which could be used for design purpose (Ahmarruzzaman and Sharma, 2005). Several isotherm models describing the process of adsorption exist in literature, namely Freundlich, Langmuir, BET, Dubinin-Kaganer-Radushkevich (DKR) isotherm etc. Amongst all these isotherms, the Freundlich and Langmuir isotherms are the commonly used in adsorption, hence, these are dealt with in more detail.

Freundlich isotherm

The Freundlich sorption isotherm is one of the widely used mathematical description and usually fits the experimental data over a wide range of concentrations (Erdem et al., 2004). It describes adsorption in which the number of adsorption sites is large relative to the number of contaminant molecules. It was originally of an empirical nature, but was later interpreted as sorption on heterogeneous surfaces or surfaces supporting sites of varied affinities. It assumes equilibrium on heterogeneous surfaces (Gunay et al., 2007). This means that the energy of adsorption is not the same for all adsorption sites. According to this model the adsorbed mass per mass of adsorbent can be expressed by a power law function of the solute concentration, C_e, as (Freundlich, 1906):

$$q_e = K_F\, C_e^{\frac{1}{n}} \tag{2.9}$$

Where K_F is the Freundlich constant related to adsorption capacity, q_e (mg/g), $1/n$ is a measure of the surface heterogeneity, ranging between 0 and 1 for good adsorption. For linearization of the data, the Freundlich equation is written in logarithmic form:

$$log q_e = log K_F + \frac{1}{n} \log C_e \tag{2.10}$$

One of the drawbacks of this isotherm model is that it cannot predict any saturation of the sorbent by the sorbate; thus infinite surface coverage is predicted mathematically, implying multilayer adsorption on the surface (Hasany et al., 2002).

Langmuir adsorption isotherm

This isotherm is often used for the adsorption of a solute from a liquid solution. In the Langmuir model, adsorption increases linearly with increasing solute concentration at low concentration values and approaches a constant value at higher concentrations because there are limited numbers of adsorption sites per unit mass of adsorbent. The

Langmuir isotherm is also called the ideal localized monolayer model and was originally developed to represent chemisorption (Wang et al., 2009). Langmuir (1918) theoretically examined the adsorption of gases on solid surfaces, and considered sorption as a chemical phenomenon. The isotherm equation further assumes that adsorption takes place at specific homogeneous sites within the adsorbent (Pérez et al., 2007), that is, all the adsorption sites are equivalent and the ability of a molecule to be adsorbed on a given site is independent of its neighboring sites occupancy (Sarkar and Acharya, 2006; Febrianto et al., 2009). For linearization of the data, the Langmuir equation can be expressed as:

$$\frac{1}{q_e} = \left(\frac{1}{K_L q_{max}}\right)\frac{1}{C_E} + \frac{1}{q_{max}} \quad (2.11)$$

Where q_e is the adsorption capacity at equilibrium (mg/g), q_{max} is the theoretical maximum adsorption capacity of the adsorbent (mg/g), K_L is the Langmuir affinity constant (L/mg) and C_E is the supernatant equilibrium concentration of the system (mg/L). The essential characteristic of the Langmuir isotherm can be described by a separation factor which is called the equilibrium constant, R_L. The equilibrium factor is thus defined as:

$$R_L = \frac{1}{1+ K_L}.\frac{1}{C_o} \quad (2.12)$$

Where K_L is the affinity constant (l/mg), C_o is the initial concentration of the adsorbate (mg/L). An R_L value that is between 0 and 1 indicates a favorable adsorption process.

The Freundlich and Langmuir isotherm models can also be evaluated for lack of fit using the error function. The error function measures the difference in the amount of

adsorbate taken up by the adsorbent using the models to the actual uptake measured experimentally (Arenas et al., 2007; Simate, 2012)

$$F_{error} = \sqrt{\frac{\sum_i^p \left(\left(q_{i\,model} - q_{i\,experimental} \right) / q_{i\,experimental} \right)^2 \right)}{p}} \quad (2.13)$$

Where $q_{i\ \text{model}}$ is the amount of adsorbate predicted by the fitted model and $q_{i\ \text{experimental}}$ is the amount measured experimentally, and p is the number of experiments performed.

2.7.4 Mathematical models for fixed bed columns

Mathematical modelling of fixed bed columns depends on the mechanism responsible for metal uptake and includes mass balances between the solid and the fluid, the rate of the process, etc., (Chowdhury et al., 2013). Various mathematical models have been developed to describe metal uptake by different adsorbents. Amongst these models, the Adam-Bohart, Thomas, Yoon-Nelson, etc., models have been widely used in waste water treatment to predict the dynamic behavior of the fixed bed column and allow some kinetic coefficients to be estimated (Ahmad and Hameed, 2013; Chowdhury et al., 2013).

Thomas model

Since its development in 1944, the Thomas model has been widely used in various applications including modelling the dynamic behavior of biosorption processes in fixed bed columns (Thomas, 1944). The model is based on the assumption that the process follows Langmuir kinetics of adsorption-desorption with no axial dispersion. However, its main limitation is that its derivation is based on second order reaction

kinetics and considers that sorption is not limited by the chemical reaction but controlled by the mass transfer at the interface. This may lead to errors when the method is used to model biosorption processes in specific conditions (Calero et al., 2009). The linearized form of the equation is given as:

$$In\left[\left(\frac{C_0}{C_t}\right)-1\right]=\left(\frac{k_{Th}q_0m}{Q}\right)-\left(\frac{k_{Th}q_0V_{eff}}{Q}\right) \quad (2.14)$$

Where k_{Th}(mL/mg min) is the Thomas rate constant, q_o (mg/g) is the equilibrium adsorbate uptake, C_o and C_t (mg/L) are the inlet and outlet adsorbate concentrations and m (g) is the mass of adsorbent in the column.

Adams-Bohart Model

This model was established based on the surface reaction theory and it assumes that equilibrium is not instantaneous (Chowdhury et al., 2013). This means that the rate of adsorption is proportional to both the residual capacity of the adsorbent and the concentration of sorbing species. Although, the model was initial developed for application to solid-gas systems, its use has been extended to other types systems including biosorption. The mathematical equation of the model can be written as:

$$In\left(\frac{C_t}{C_0}\right)=K_{AB}C_{0t}-K_{AB}N_0\left(\frac{z}{U_0}\right) \quad (2.15)$$

Where K_{AB} (l/min.mg) is rate constant of Adam-Bohart model, Z (cm) is the bed depth, C_o and C_t are the inlet and outlet adsorbate concentrations, N_o (mg/l) is maximum ion adsorption capacity per unit volume of adsorbent column, and U_o (cm/min) is the linear velocity of influent solutions

Yoon-nelson model

This model is based on the assumption that the rate of decrease in the probability of adsorption for each adsorbate molecule is proportional to the probability of adsorbate adsorption and the probability of adsorbate breakthrough on the adsorbent (Yoon and Nelson, 1984; Ahmad and Hameed, 2010). The linearized model for a single component system is expressed as:

$$In\left[\frac{C_t}{C_O - C_t}\right] = k_{YN}t - \tau k_{YN} \quad (2.16)$$

Where K_{YN} (l/min) is the rate constant and τ is the time required for 50% adsorbate breakthrough.

2.8 Sulphuric acid recovery from AMD

After the AMD solution has been stripped of the noxious heavy metal ions, it still remains with some acidity, which if disposed to the environment causes serious challenges. Hence, the second aspect of this study involved testing the feasibility of using a process known as acid retardation to recover the sulphuric acid from AMD. Although, various technologies such as solvent extraction, crystallization, electrochemical methods, ion exchange etc., exist for acid recovery, the acid retardation process has emerged as the most popular method particularly in the metal finishing industry where huge amounts of waste acids are produced. This popularity emanates from the simplicity, low cost as well as high acid recoveries associated with the process (Gulbas et al., 1987; Sheedy, 1998). Therefore, in the present study feasibility tests were conducted to investigate the potential applicability of this process to AMD. The process is discussed in detail in the next subsections.

2.8.1 Acid retardation process

Acid retardation was initially introduced by Hatch and Dillon (1963). Acid retardation can be defined as a process which employs ion exchange resins to selectively adsorb acids from solution while dissolved metal salts are rejected. The term retardation emanates from the fact that the preferential adsorption of the acid causes the movement of the acid on the resin bed to be retarded (slowed down), relative to the movement of the salts, resulting in the separation of the two entities (Sheedy, 1998; Sheedy and Parujen, 2012). The process is reversible and the acid can be recovered by water elution.

Although, the process was introduced in 1963, it was not successfully commercialized at that time due to the limitations of conventional ion exchange equipment design. However, in 1978, acid retardation was successfully commercialized and applied as the RECOFLO Acid Purification System (Brown et al., 1979; Brown et al., 1987; Brown, 1996). The design comprised the use of fine mesh resin beads to increase surface area and improve reaction kinetics, short resin bed to reduce pressure drop and equipment size, full packing to minimize intermixing and dilution of feed and regenerant streams, and finally counter current flow to maximize chemical efficiency (Brown et al., 1987).

During process operation, the feed solution is normally passed over a bed of strong base anion exchange resin to separate the components. The resin has a greater affinity for the acid than for the salts resulting in chromatographic separation of salts from the acid whose movement is "retarded" by the greater affinity (Sheedy, 1998). When backwashed with water, the adsorbed acid is released. Typically, more than 90% of the sulphuric acid is recovered in the product stream and can be recycled if desired (Brown et al., 1987; Sheedy, 1998). By adjusting the volumes and flow rates of these various process steps, it is possible to optimize the process performance depending on the process objectives. As a result, hundreds of APU units have since been installed

worldwide for recovery of hydrochloric, sulphuric and nitric acid from metal finishing waste. The reason for the wide application of the acid retardation process in metal finishing industry is its low cost, simplicity and superior performance (Gulbas et al., 1987; Brown et al., 1996).

Acid retardation resins

While the use of specific ion exchange resins is required, the process is strictly not ion exchange (Sheedy, 1998). The acid is not exchanged onto specific sites and the process in not limited by the resins ion exchange capacity. In addition, unlike conventional ion exchange resins which are either cationic or anionic, some of the acid retardation resins are known to be amphoteric (Brown et al., 1987). This means that each resin bead has both cation and anion exchange groups. Although the mechanism is not fully understood these resins are considered to be in "self-neutralised" form (R^+R^-), that is, the positive charge associated with anion exchanger is neutralized by the negative charge associated with the cation exchanger. During the service or uptake cycle the cation and anion associated with the acid impurity (for example M^+N^-) are taken up by the resin together. This is shown in Equation 2.17.

$$R^+R^- + M^+N^- \rightarrow R^+R^-M^+N^- \quad (2.17)$$

When the resin is contacted with water, the resin becomes less selective for all the acid impurity and the resin self-neutralizes again, liberating the acid impurity (see Equation 2.18)

$$R^+R^-M^+N^- \rightarrow R^+R^- + M^+N^- \quad (2.18)$$

The resins used in the process are normally chosen to have high affinity for the acid to be removed and low affinity for the salt to be left behind (Brown et al., 1987). The

resins applied in acid retardation process are usually 20% smaller than conventional ion exchange resins (Sheedy and Parujen, 2012). This allows operation at higher flow rate and reduces the length of the mass transfer zone. In addition, work by Price and Hedbditch (1988) indicated that the exchange rate is inversely proportional to the square of the particle diameter, hence; reducing the size by 20% increases the exchange rate by 160%. Further, the resulting higher flow rates have been reported to reduce the volume of the resin required (Sheedy and Parujen, 2012). Finer particles also aid in fluid displacement which allows a reduction in rinse volume requirements. Examples of resins include Retardion 550WQ2 and Dowex 1 resins both supplied by the Dowex Chemical Company. These have been used successfully to recover acids from stainless steel liquors with close to 76% recovery (Hatch and Dillon, 1963). Related work also reported acid recovery by acid retardation resins (Dejak and Munns, 1987; Gulbas et al., 1987; Tan, 1996).

However, despite being effective in reducing ionic contaminants to acceptable levels, the resins used in the acid retardation process were normally found to suffer from lack of selectivity. Therefore, over the years, research has been directed towards improving the selectivity and efficiency of the resins. For example, Nenov et al. (1997) separated arsenic and sulphuric acid from aqueous solution containing arsenic using strong acid cation exchanger in the Na-form. Kraus et al. (1953) and Shamritska et al. (1972) extracted sulphuric acid from metal sulfate solutions using Dowex 1 anion exchange resin. Brown et al. (1979), Hatch and Dillon (1963), and Petkova et al. (1981) studied the separation and recovery of sulphuric acid from metal cations coexisting in the waste plating solution using Wofatit SBW anion exchanger and showed that the process is effective until the relative acid concentration in the effluents reaches C/Co = 0.55 (where C is the concentration at a given moment and Co is the initial concentration of the solution). Recent studies have also reported the high selectivity of Dowex MSA-1 and LEWATIT-K 6362 for sulphuric acid in waste acid solutions (Dowex, 2002; Ghare et al., 2014).

Mechanism

Despite its wide application, the mechanism of the acid retardation process is still not very well understood, thus various postulations and ideas have been suggested to explain the phenomenon. Gulbas et al. (1987) suggested that the reason for acid retardation is the different rates of diffusion of metal ions, dissociated acids and acid molecules, respectively. Neumann (2009) attributed the acid retardation to the effect of charge (Donnan effect). The process has also been reported to be driven by the acid concentration difference between the interior of the resin phase and the surrounding fluid (Sheedy and Parujen, 2012). Agrawal and Sahu (2009) suggested that the release of the acid from the resins by water is a result of the difference in osmotic pressure.

Parameters affecting acid retardation process

Information on process parameters is the key to achieving expected recovery in any process. The same process parameters affecting conventional ion exchange process also affect acid retardation process. The effects of different parameters on acid retardation process are summarized herein.

Contact time

Generally increasing the contact time increases the percentage amount of ions adsorbed at equilibrium which subsequently increases percentage recovery (Pehlivan and Altun, 2005). Neumann (2009) reported that the breakthrough of acid occurred after only one resin bed volume, with a breakthrough time of less than an hour for the recovery of sulphuric acid from an aluminium pickling solution. Similar results were also reported by Ghare et al. (2014) where sulphuric acid recovery increased with time from 5 to 10 minutes.

Resin bed height/Resin amount

The resin amount is also an important parameter in obtaining a quantitative uptake of ions. Increasing the resin amount increases the number of available sorption sites which in turn increases the amount of ions adsorbed per unit mass of solution (Pehlivan and Altun, 2005). An increase in the sorbet amount also results in a decrease in the contact time required to reach equilibrium as well as the equipment size. Ghare et al. (2014) reported an increase in acid recovery with an increase in bed height.

Temperature

The working capacity of an ion exchange depends on temperature. Generally, most ion exchange reactions are endothermic (Pehlivan and Altun, 2005). This implies that an increase in solution temperature will result in an increase in acid recovery. However, temperature above 149˚C has been found to have a deleterious effect on acid retardation resins (Hatch and Dillon, 1963).

Flow rate

The flow rate of the mobile phase is determined by the resin bead size, coarser resin beads have larger inter-bead spaces through which the fluid can move and capillary effects are smaller, so that coarser resins have faster fluid flow (Pehlivan and Altun, 2005). Faster flow usually leads to poor separations. In most applications fluid flow is controlled by gravity. The mobile phase moves as fast as gravity allows. At fine resin bead sizes, gravity is insufficient to induce flow (capillary forces and surface tension exceeds gravity) and pressurized columns must be used.

Bed packing

The resins must be packed in such a way that the resin is maintained in a state of compression even when the resin has shrunk. This patented technique is called "over packing" (Brown et al., 1987). Over packing reduces bed porosity and flow channeling improving the recovery of the acid. The bed must also have little or no free board to avoid dilution (Brown et al., 1987).

The primary appeal of the acid retardation process unlike the conventional ion exchange is that no chemicals are required for the regeneration of the resins, but only water is used (Brown et al., 1987). Regenerant chemicals not only represent an economic cost, but since they report to the waste in the form of neutral salts along with the original contaminants, an additional load of salt are discharged to the environment. This new development in AMD remediation technologies is therefore expected not only to reduce the amount of sludge produced but to significantly reduce the cost of the remediation process by producing a sale-able product, namely sulphuric acid.

2.9 Summary

In the chapter presented the background of the research. In particular the following were discussed in detail:

- The formation and constituents of AMD
- The impact of AMD on the environment
- Available treatment options
- Adsorption and acid retardation processes

CHAPTER THREE

MATERIALS AND METHODS

3.1 General introduction

This section provides details on the materials and sample preparations, experimental methods and analytical techniques used in this study.

3.2 Materials and sample preparations

3.2.1 Materials

The AMD solution with a pH value of 2.16 and chemical composition shown in Table 3.1 was sourced from Randfontein Gold Mine located west of the Witwatersrand region.

Table 3.1: AMD chemical composition

Component	Concentration(mg/L)	DWAF/ US EPA Discharge Limits
TS	5835	n/a
TDS	1303	0-1600
TSS	4532	0-25
Acidity	906.5	n/a
SO_4^{2-}	3730	0-500
Al^{3+}	0.28	0.03
Ca^{2+}	485	n/a
Co^{2+}	0.40	0.04
Fe^{3+}	193	10
Mg^{2+}	135	n/a
Mn^{2+}	45.3	0-10
Ni^{2+}	0.43	0.15

n/a- not available

In addition, to the high metal ion levels in the AMD sample, Table 3.1 shows that the solution has a high salt load as indicated by the high values of the sulphate ion, TS,TDS and TSS.

Bentonite powder was supplied by Ecca Holdings Corporation and ion exchange resins were obtained from Dow Chemical Company. Sodium silicate, nitric acid, thioglycollic acid reagent grade, zeolite powder, sodium hydroxide, sodium alginate, calcium chloride and brewer's yeast were all supplied by Sigma-Aldrich. Cassava tubers were obtained from a local vendor in South Africa.

3.2.2 Adsorbent preparation

Prior to experimental work, the adsorbents were prepared as follows:

Bentonite

When clay is in contact with water, it becomes viscous making its separation after adsorption very difficult. Therefore, in addition to bentonite powder, the use of bentonite beads was also evaluated for metal uptake in this study. Apart from minimising viscosity, bentonite beads are mechanically stable and can be easily separated from the solution after metal loading. The bead preparation was based on a method used by Summers et al. (1996). In this study, however, sodium silicate binder was used to immobilize bentonite powder instead of peat. Approximately 15 mL of sodium silicate (reagent grade) solution was added to 100 mL of distilled water in order to make the binder. The binder was mixed with the powder until a dough-like mixture was formed. Small spherical beads of approximately 1 mm in diameter were moulded from the mixture and then dried in an oven at 95˚C for 6 hours. Only beads without cracks were selected for the experiment while the rest were discarded. The cracks on the beads could be attributed to drying without rotation. Summers et al. (1996) reported that beads with an enhanced spheroidal shape were formed when a turbo-dyer was used, since it rolls the beads when drying.

Cassava

The biomass preparation was based on a method used by Abia et al. (2003). The cassava tubers obtained from the vendor were washed in deionized water and air-dried for 24 hours. The tubers were then cut into 5 cm pieces and carefully peeled to obtain the cassava peel waste. The peels were dried in an oven at 90˚C for approximately 12 hours until a constant weight was obtained. The dried samples were subsequently ground with a blender and sieved to less than 100 μm sizes using a standard sieve.

The cassava waste biomass powder was subsequently activated by soaking in 0.3M nitric acid for 24 hours. It was then washed in distilled water, air dried for 24 hours and divided into three portions. The first portion was left untreated and used in the control experiment. The other 2 portions were acid treated in a beaker with excess 0.50M and 1.00M thioglycollic acid solutions, respectively, for 24 hours at 30˚C. This acid treatment process leads to the thiolation of the hydroxyl groups of the cellulosic biomass by the following reaction (Horsfall and Abia, 2003):

$$biomass - OH + HSCH_2CO_2H \rightarrow biomass - SH + H_3CO_2^- + H^+ \quad (3.1)$$

The samples were then washed with deionized water, centrifuged and the supernatants discarded. The solid samples were air dried and used in the adsorption tests.

It is known that dead biomass is mechanically unstable and tends to float with the solution being treated (Gadd, 2009). However, literature reports that immobilization improves the mechanical strength, rigidity, porosity and the overall metal ion removal capacity as well as the life time of the biosorbent (Goksungur et al., 2003). Hence, in addition to cassava peel biomass powder, immobilized biomass was also evaluated for metal uptake in this study. The batch adsorption test results showed that 1M treated cassava biomass gave the highest metal adsorption efficiencies. Therefore, the immobilization process was carried out by hydrating about 100g of 1M treated cassava peel biomass in 250 mL of distilled water for 10 minutes at room temperature. The resulting slurry was mixed with an equal volume of 3% (w/v) sterile sodium alginate. Spherical beads with a diameter size ranging between 3 to 4 mm were made and added to 0.2M calcium chloride solution to allow them to harden. After a period of approximately 30 minutes, they were removed from the solution and washed with 0.9% sodium chloride solution to remove excess calcium ions. The same procedure was repeated to form beads with a diameter size of approximately 1.5 mm. The beads were subsequently air dried for 72 hours and used in the column tests.

Zeolite

The zeolite powder was divided into two portions. The first portion was left untreated and used in the control experiment. Approximately 20 g of the second portion was immobilized by suspending it in excess 6 g/L yeast solution for 24 hours. The suspension was then filtered using a vacuum filter. The solids obtained were washed in distilled water and dried at 80˚C for 6 hours, and used in the adsorption tests.

3.3 Experimentation

3.3.1 Batch adsorption tests

Batch adsorption experiments were conducted by contacting a known amount of adsorbent with 500 mL of AMD solution. No pH adjustments were made to the solution prior to the experiments. The purpose of doing this was to identify an adsorbent with the ability to remove metal ions from AMD with no loss in the solution acidity; which could subsequently be recovered. Flasks were sealed and shaken in a Labcon platform shaker (Model-50824) for a period of 1 hour. The changes in pH were monitored at predetermined time intervals using the pH meter (Metrohm-827), whilst simultaneously collecting a sample. Immediately after withdrawal, the samples were centrifuged at 3000 rpm for 6 minutes to separate solids from the liquid. A liquid sample was collected and analysed for metal, sulphate and acid content. All tests were replicated twice. In addition, polypropylene (PP) containers were used throughout this study and the containers were cleaned with metal free non-ionic detergent solution, rinsed with tap water, soaked in 3% nitric acid for 24 hours and then rinsed with de-ionised water as recommended by Arienzo et al. (2001).

The percentage removal (θ) of metal ions from AMD solution and mass of metal ions adsorbed by the biomass (q) in mg/g was determined using Equation 3.2 and 3.3, respectively:

$$\theta = \frac{(C_i - C_f)100}{C_i} \tag{3.2}$$

$$q = \frac{(C_i - C_f)V}{m} \tag{3.3}$$

where C_i and C_f, are the initial and final metal ion concentrations in solution (mg/L) respectively, V is the volume of the test solution (L) and m is the amount of biosorbent used (g).

3.3.2 Column adsorption tests

A column with an inside diameter of 1.5 cm and 60 cm in height was used in this study. Sufficient cassava waste beads were placed into the column to the height required in each test. Glass beads and cotton wool were placed at the bottom and top of the cassava beads, respectively, to prevent them from floating and flowing out of the column, during the experiment. The AMD solution was fed in an up flow direction using the Heidolph (Model-5001) peristaltic pump with an adjustable speed. Upward flow was preferred because it ensures that there is total coverage of the adsorbent by the solution and it also prevents the formation of channels during the operation of the column (Harland, 1994). The samples were collected from the effluent coming out from the top of the column at various time intervals. The experimental set up for the column tests is shown in Figure 3.1.

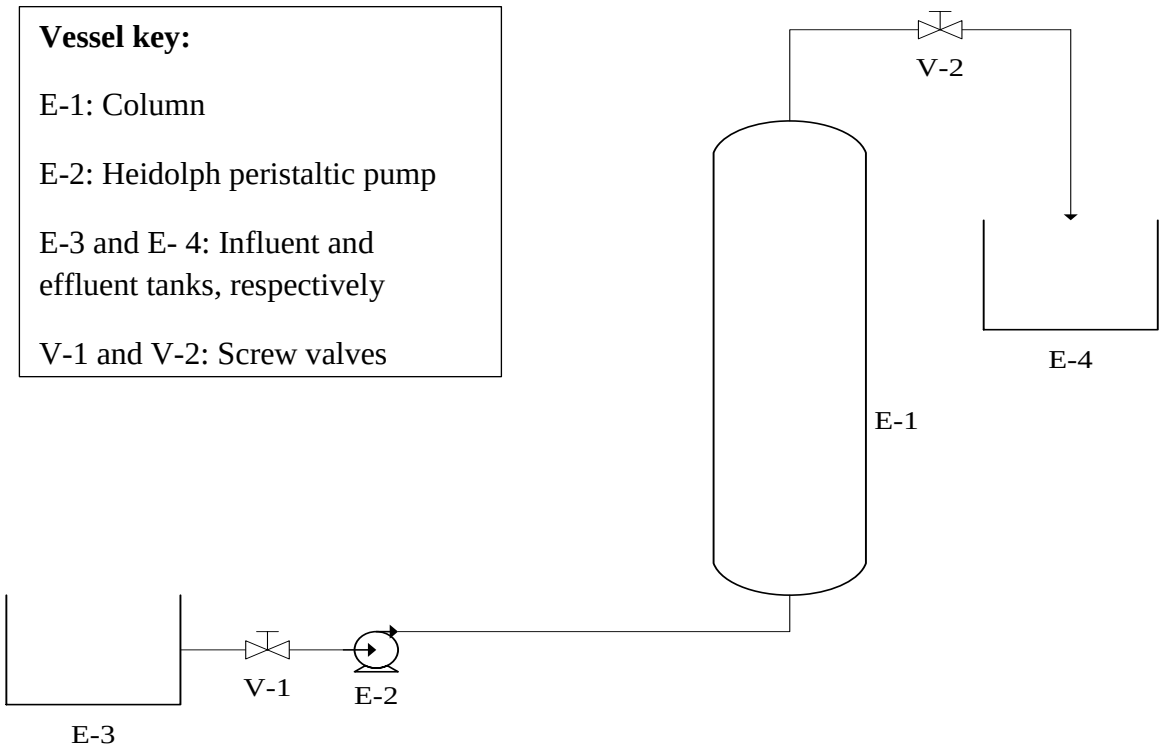


Figure 3.1: Experimental set up for column tests

The effect of bed depth, flow rate and bead size were investigated in the study. The parameters used in these tests were chosen based on those reported in literature (Goksungur et al., 2003; Seepe, 2015) and are shown in Table 3.2.

Table 3.2: Experimental conditions for column adsorption studies

Operating Parameter	Levels
Flow Rate	0.89 mL/s, 1.50 mL/s, 2.10 mL/s
Bed Height	15 cm, 30 cm, 45 cm
Bead Size	3 to 4 mm, 1.4 to 1.5mm
Running Time	180 minutes

Solution samples were collected at different time intervals and analysed for metal, sulphate and acid content.

3.3.3 Ion exchange column tests

The ion exchange tests were conducted using the effluent from the metal adsorption. After the metal adsorption stage, as shown in the proposal flow sheet (Figure 2.5), the metal barren solution still remains with acidity, which poses serious threats if discharged into the environment. Therefore, the second aspect of the study focused on the recovery of this acid using ion exchange column studies. An experimental set up similar to the one shown in Figure 3.1 was also used in the ion exchange tests. However, a column with inside diameter of 1.0 cm and 30 cm height was used in these tests. Sufficient resins were placed into the column to the required height. The AMD solution was fed in an upward flow direction and samples collected from the top of the column at different time intervals. These were analysed for metal, sulphate and acid content. The column dimensions as well as some parameters such as the bed height were based on information recommended by the resin manufacturer for laboratory tests (Dowex, 2001). A summary of the conditions used in the ion exchange tests is shown in Table 3.3.

Table 3.3: Experimental conditions for ion exchange column adsorption studies

Operating Parameter	Levels
Flow Rate	0.83 mL/s, 1.10 mL/s, 1.50 mL/s
Bed Depth	10 cm, 20 cm, 30 cm
Running Time	60 minutes

The acid was recovered from the loaded resins by subjecting the column to various cycles of de-ionized water. The eluate was subsequently upgraded in a rotary evaporator (Heidolph Laborata 4000) to obtain a concentrated acid solution and a water product.

3.4 Analytical techniques

The details of the various analytical techniques used in the present study are discussed in this section.

3.4.1 Determination of surface morphology, area and pore structure

The Carl-Zeiss Field Emission scanning electron microscope (SEM) was used to study the surface morphology of the adsorbents. The surface area, pore size and pore volume were determined using nitrogen adsorption fitted to the Brunauer Emmett Teller (BET) equation. Prior to the BET analysis, 0.2 g of each adsorbent was degassed in nitrogen at 400 ˚C for four hours using a Micrometrics Flow Prep 060 sample degas system. The BET surface area and pore structural parameters of the adsorbents were obtained at -196 ˚C using a Micrometrics (Tristar 3000) surface area and porosity analyser.

3.4.2 Determination of functional groups

Fourier Transform Infrared Spectroscopy (FTIR) was performed in order to identify the different functional groups present on zeolite, bentonite and cassava peel biomass surfaces before and after modification. FTIR spectra were measured directly using a Bruker Tensor device in the range 500 cm^{-1} to 4000 cm^{-1}.

3.4.3 Determination of chemical composition of adsorbents

Elemental compositions of bentonite and zeolite adsorbents were analysed using PANalytical Axios X-Ray Fluorescence (XRF) spectrometer. Phase analysis was further confirmed using the X-Ray Diffractometer (XRD-Bruker D2 phaser).

3.4.4 Sulphate and pH measurements

The sulphate ion concentration was analysed using the Merck Spectroquant Pharo 300 spectrophotometer and Merck reagent kit No. 14791. Metrohm 827 lab pH meter was used for all pH measurements.

3.4.5 Determination of total solids (TS), total suspended solids (TSS) and total dissolved solids (TDS)

Total solids (TS)

A dry 250 mL beaker which was kept at 105˚C in an oven for 1 hour was weighed. Approximately, 100 mL of a thoroughly mixed sample solution was measured into the beaker, and the beaker was placed in an oven with a constant temperature of 105˚C for 24 hours. After 24 hours, the beaker was allowed to cool and then reweighed. The total solids were calculated as follows:

$$Total\ solids\ (mg/L) = \frac{mg\ of\ solids\ in\ the\ beaker}{Volume\ of\ sample\ (mL)} \times 1000 \qquad (3.4)$$

Total suspended solids (TSS)

A dry filter paper which was kept at 105˚C in an oven for 1 hour was cooled in a desiccator, and then weighed. Approximately 100 mL of a thoroughly mixed sample solution was filtered and the filter paper dried at 105˚C in an oven for 24 hours. After 24 hours, the filter paper was cooled and reweighed. The total suspended solids were calculated as follows:

$$Total\ suspended\ solids\ (mg/L) = \frac{mg\ of\ solids\ in\ the\ filter\ paper}{Volume\ of\ sample(mL)} \times\ 1000 \qquad (3.5)$$

Total dissolved solids (TDS)

The total dissolved solids in the sample were calculated as follows:

$$Total\ dissolved\ solids\left(\frac{mg}{L}\right) = Total\ solids\left(\frac{mg}{L}\right) - Total\ suspended\ solids\left(\frac{mg}{L}\right) \quad (3.6)$$

3.4.6 Determination of the metal ion concentration

The concentration of Al^{3+}, Ca^{2+}, Co^{2+}, Fe^{3+}, Mg^{2+}, Mn^{2+} and Ni^{2+} ions in the solution was determined using the Spectro ARCOS FHS12 inductively coupled plasma-optical emission spectrometer (ICP-OES). The spectrometer automatically measures each sample three times and processes the outputs using the Smart Analyser Vision software.

3.4.7 Determination of the acid content

The acid content of the solution was determined by titrating 10 mL of the sample with 0.1M sodium hydroxide solution in the presence of bromothymol blue indicator.

3.4.8 Determination of the point of zero charge (pH_{PZC})

The point of zero charge was determined using a mass titration procedure described by Noh and Schwarz (1990). Three containers of 0.1M $NaNO_3$ solutions were prepared and their pH values adjusted to 3, 6, and 11 using 0.1M HNO_3 and 0.1M NaOH. For each initial pH, six containers were filled with 100mL of the solution and different amounts of each adsorbent (0.05%, 0.1%, 0.5%, 1%, 5% and 10% by weight/volume of solution). The solutions were then agitated at 150 rpm and the equilibrium pH measured after 24 hrs.

3.5 Summary

In this chapter the materials and methods used in the research were presented and discussed. The materials and equipment, preparation of samples for laboratory work, experimental methods for batch and column studies and analytical techniques were discussed in detail.

CHAPTER FOUR

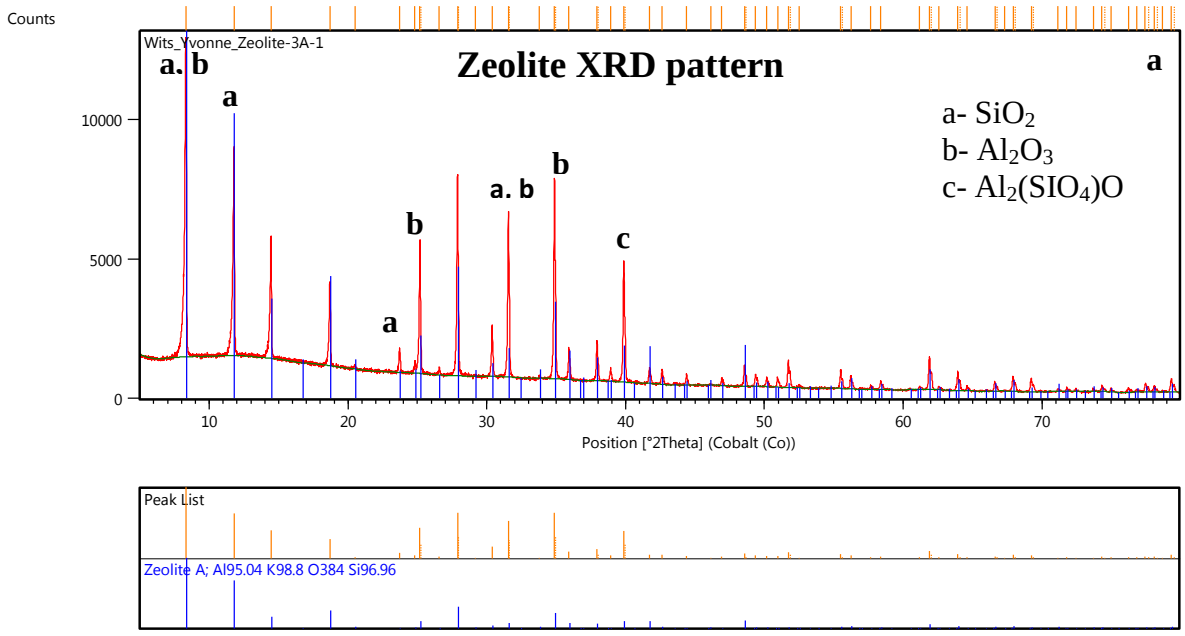
RESULTS AND DISCUSSIONS

4.1 Characterization results

This section presents and discusses the results for characterization of the adsorbents. Results on physicochemical properties, surface morphology, functional group identity, surface charge, qualitative and quantitative phase analysis are discussed in detail.

4.1.1 XRD analysis

XRD analysis is used to investigate the mineralogical structure of crystalline substances (Motsi, 2010). When X-rays interact with a crystalline substance, a diffraction pattern is produced. Each substance gives a unique pattern which is like the finger print of that substance. Therefore, XRD analysis was performed to investigate the mineralogical structure of cassava peel biomass, bentonite clay and zeolite adsorbents. Although, a diffraction pattern for the cassava peel biomass could be obtained, it was found to be complex and difficult to interpret since there were no distinct peaks formed. This was mainly due to the non-crystalline nature of the biomass. Therefore, the XRD results of the cassava peel biomass and consequently the XRF results are not presented in this report. The XRD results of zeolite and bentonite are shown in Figure 4.1.



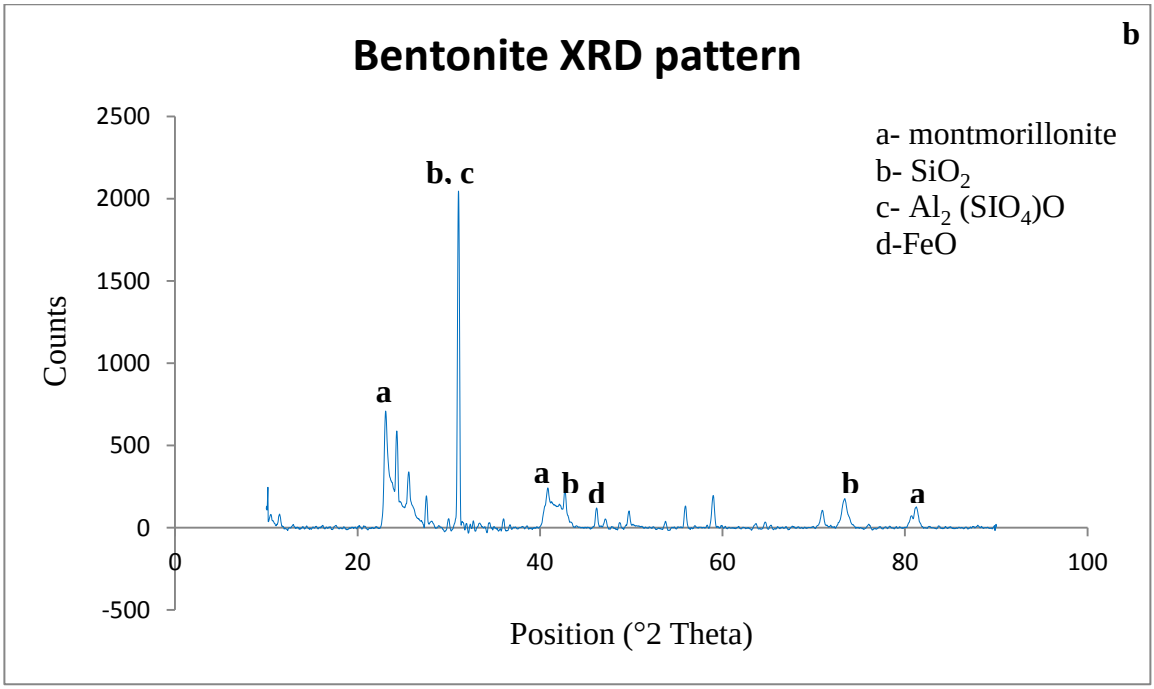


Figure 4.1: X-Ray Diffraction chart for (a) zeolite and (b) bentonite powder

The results indicate that the highest peaks occurred at a ˚2 Theta position of 8.5 for zeolite and 32 for bentonite clay. Both peaks correspond to silica and some small

amounts of sillimanite ($Al_2(SiO_4)O$) for bentonite clay. The sharp peaks seen in both diffraction patterns indicate the crystalline nature of the materials. The major phases found in zeolite were silica and alumina. Apart from silica and alumina, the bentonite clay adsorbent used in the present study also consisted of montmorillonite [$(Na,Ca)_{0.33}(Al,Mg)_2Si_4O_{10}(OH)_2\cdot(H_2O)_n$]. Small amounts of other phases such as iron oxide (FeO) and magnesium calcite (MgO 0.06, CaO, 0.94) and hedenbergite ($CaFeSi_2O_2$) were also found in the bentonite clay sample. This peak assignment is in agreement with the work of Nsimba (2012), where montmorillonite was also identified as the major phase in the bentonite sample used to treat waste mine water. The type and quantity of phases found in an adsorbent determines the number of cationic exchange sites and consequently the adsorption efficiency. This is explained in detail in section 4.1.2.

4.1.2 Chemical composition of adsorbents

Quantitative analysis of the major phases previously identified by XRD was obtained using X-Ray Fluorescence (XRF) and the results are presented in Table 4.1.

Table 4.1: Chemical composition of zeolite and bentonite

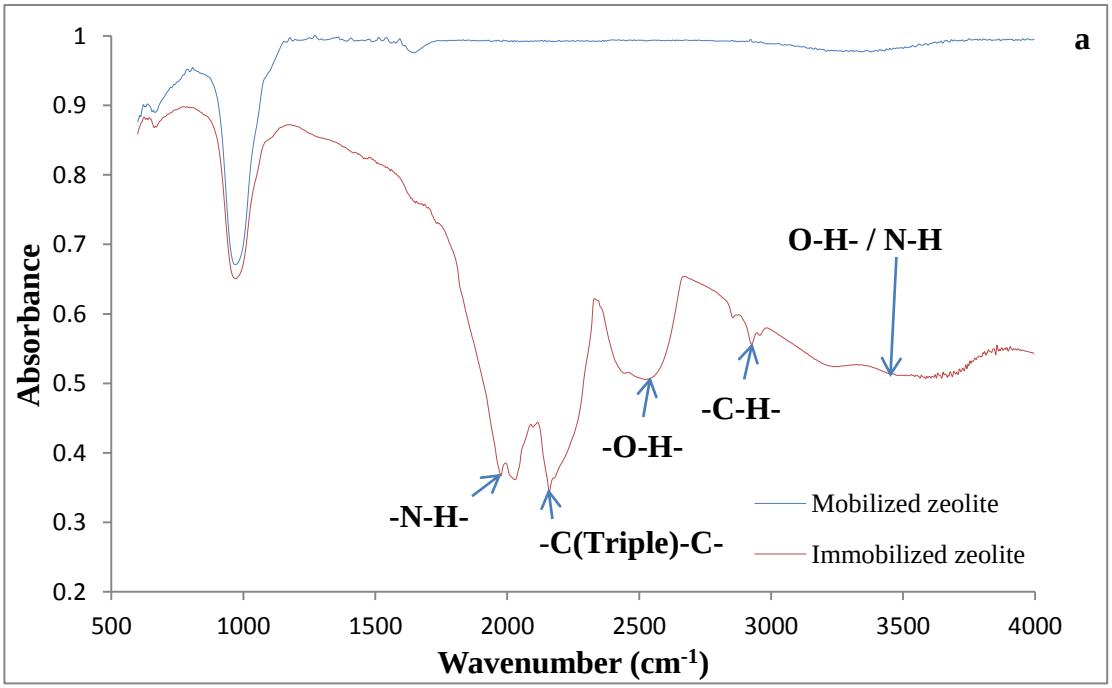
Major element (% w/w)	Zeolite	Bentonite clay
Al_2O_3	29.88	17.32
SiO_2	38.57	70.58
Fe_2O_3	0.02	0.35
CaO	0.03	1.45
Na_2O	18.16	2.28
FeO	≤ 0.01	2.81
MnO	0.01	0.07
MgO	≤ 0.01	3.43
K_2O	≤ 0.01	0.91
Loss of ignition(LOI)	9.25	16.45
Si/Al ratio	1.14	3.59

The results show that Al_2O_3 and SiO_2 are the major phases in both lattices, which concur well with the XRD results (Figure 4.1). The Si/Al molar ratio of the samples was calculated and found to be 1.14 for zeolite and 3.59 for bentonite clay. Ribeiro et al. (1984) classified zeolites into three groups according to their Si/Al ratio namely low silica (Si/Al≈1), intermediate silica (Si/Al from 2-5) and high silica zeolites (Si/Al > 10). Therefore, the zeolite used in this study falls under ‘‘low silica or aluminium rich zeolite A”, the most common commercial adsorbent, which is considered as having high aluminium content possible in tetrahedral aluminosilicate frameworks (Ribeiro et al., 1984; Erdem et al., 2004; Xu et al., 2007). Consequently, the zeolite adsorbent contains the maximum number of cationic exchange sites balancing the aluminium framework, and thus the highest cationic content and exchange capacities. Motsi (2010) further stated that, a low Si/Al ratio means that the zeolite surface area has a large negative charge and hence, more capacity for cations. The Si/Al ratio of the bentonite sample (in the intermediate range) may also suggest

the presence of a moderate negative charge, which also shows its high surface affinity for metal ions.

4.1.3 Fourier transform infrared spectroscopy (FTIR)

Adsorption is a complex phenomenon often involving the interaction of metal ions with various functional groups on the surface of the adsorbent. In biosorption, these functional groups are responsible for attracting and sequestering metal ions (Gadd, 2009). Hence, in the present study FTIR was carried out in the wavenumber range 500 to 4000 cm^{-1} to identify the type of functional groups found on the surface of each adsorbent. Figure 4.2 shows the FTIR spectra of zeolite, bentonite clay and cassava peel biomass adsorbents before and after modification. For comparison purposes, only the additional functional groups introduced by modification are indicated in the Figure.



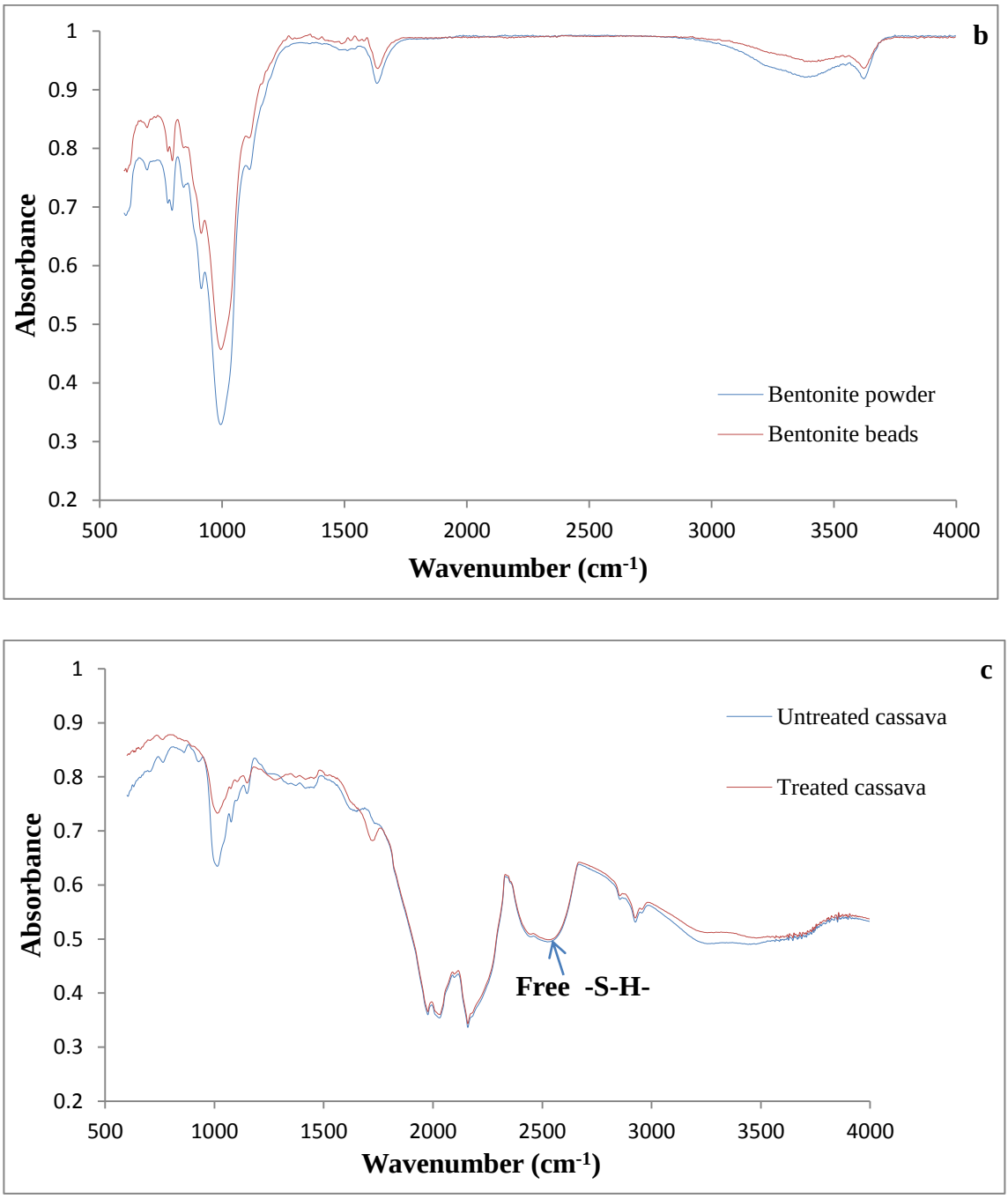


Figure 4.2: FTIR spectra of (a) zeolite (b) bentonite clay (c) cassava peel biomass before and after modification

Figure 4.2 (a) shows the FTIR spectra for the mobilized and immobilized zeolite adsorbents. Absorbance peaks were observed at 664.97 and 969.363 cm^{-1} for both

zeolite adsorbents. These correspond to C-O-Si and C (triple)-C which could be attributed to the presence of silanol groups and alkynes. Kalayci et al. (2013) reported the same functional group assignment in their work, where a similar zeolite adsorbent was used to remove organic pollutants from a waste solution. Additional absorbance peaks were also observed at 1633.67, 1978.87, 2183.31, 2577.49, 2933.59 and 3265.83 cm^{-1} for immobilized zeolite, due to the introduction of new functional group by yeast. The broad strong band at 3265.84 cm^{-1} represents O-H/N-H stretching and H-bonded stretch which can be attributed to the presence of amine, carboxylic, alcohol and phenol groups. The strong peak at 2933.59 cm^{-1} corresponds to O-H and C-H bond stretch which indicates the presence of carboxylic and alkanes groups. The broad weak band at 2577.49 cm^{-1} corresponds to O-H stretch which represents carboxylic groups. The peaks at 2183.31 cm^{-1} and 1633.67 cm^{-1} correspond to C(triple)-C stretch (alkynes) and N-H stretch (amines), respectively. In summary, immobilizing the zeolite using yeast introduced additional functional groups such amino, carboxylic, hydroxyl and nitro groups onto the zeolite surface.

Figure 4.2 (b) shows the spectra for bentonite clay powder and beads. It is evident that the functional groups found in both adsorbents are similar due to the close similarity of the patterns. This is because bentonite contains silicates (Table 4.1) which are also present in the sodium silicate binder. Therefore, it is expected that both adsorbents have similar peaks due to the similarity in composition. However, the bentonite beads appear to have a stronger absorbance for the same peaks, as shown by the higher height of the peaks. This could be attributed to the strong interactions between some functional groups in the sodium silicate binder with the groups on the bentonite clay surface. Peaks were observed at 693.66, 795.59, 914.89, 993.91, 1632.38, 3380.11 and 3621.85 cm^{-1}. These peaks mostly correspond to Si-O-Si, C-H, C (triple)-C and N-H, which could be attributed to the presence of alkynes, amines and silanol. Moreover, a closer study of the beads spectrum also revealed extra absorbance peaks at 778.39, 1488.72 which, however, also correspond to C-C and C-

H stretch. Therefore, in general, both bentonite adsorbents have similar functional groups such as alkynes, alkanes and silanol.

Figure 4.2 (c) presents the FTIR spectra of untreated and thioglycollic acid treated cassava. Although, it is known that –COO, C=O and other functional groups present in cassava biomass adsorb metal ions, previous studies have indicated that the thiolation process improves metal ion sorption (Abia et al., 2003; Ndlovu et al., 2013; Simate and Ndlovu, 2014). On comparing the two patterns, it is evident that the shapes are closely similar indicating the presence of similar functional groups in both adsorbents. Absorbance peaks were noted at 999.07, 1976.94, 2160.17, 2528.56, 2927.80 and 3687.72. These correspond to C-O stretch, C=O, C (triple)-C and O-H groups are associated with carboxylic, alkynes, esters and alcohol groups. The spectra for the thioglycollic acid treated cassava peel shows the addition of the sulfhydryl group (-SH) which proves that thiolation has taken place.

4.1.4 Point of zero charge (pH_{PZC})

The point of zero charge (pH_{PZC}) is a fundamental property of an adsorbent surface, and is described as the point where the total number of surface anionic sites is equal to the total number of surface cationic sites (Noh and Schwarz, 1990). It is used to evaluate the surface charge of an adsorbent qualitatively (Simate, 2012). At pH values above the pH_{PZC}, the surface has a negative charge, and would participate in cation attraction and cation exchange reactions. At pH values below the pH_{PZC}, the surface has a positive charge and will attract anions and participate in anionic exchange reactions. A mass titration analysis was used to determine the values of the pH_{PZC} and the results are summarized in Table 4.2.

Table 4.2: Mass titration results of bentonite, cassava peel and bentonite adsorbents.

Adsorbent	**pH_{PZC}**
Untreated cassava waste	4.92
0.5M treated cassava waste	3.40
1M treated cassava	2.74
Mobilized zeolite	9.60
Immobilized zeolite	9.24
Bentonite powder	9.10
Bentonite beads	9.18

From the pH_{pzc} of the cassava waste biomass, it can be seen that acid treatment resulted in a decrease in pH_{pzc} values. Previous research reports that a decrease in the pH_{pzc} of an adsorbent is a result of the addition of acidic groups on the surface of the adsorbent (Noh and Schwarz, 1990). Hence, it can be concluded that acid treatment introduced acidic functional groups which resulted in the observed decrease in the pH_{PZC} values. This concurs well with FTIR results which showed introduction of an acidic sulfhydryl group after thiolation. A slight decrease in pH_{PZC} value is also observed with the immobilized zeolite powder owing to the introduction of slightly acidic groups such as the nitro and carboxylic groups through treatment with yeast as already shown in Figure 4.2. The pH_{PZC} values of bentonite powder and beads are almost identical owing to the similar functional groups at both adsorbents' surfaces.

4.1.5 Physicochemical properties

The physicochemical properties were determined using nitrogen adsorption fitted to the BET equation (Brunauer, 1943). The results for bentonite, cassava and zeolite adsorbents are summarized in Table 4.3.

Table 4.3: Physicochemical properties of bentonite, cassava peel biomass and zeolite adsorbents

Adsorbent	BET surface area (m^2/g)	Pore size (nm)
Untreated cassava	0.30	42.49
0.5M treated cassava	1.21	13.84
1M treated cassava	1.34	8.86
Mobilized zeolite	0.94	164.99
Immobilized zeolite	0.52	15.47
Bentonite powder	39.58	9.99
Bentonite beads	29.65	11.38

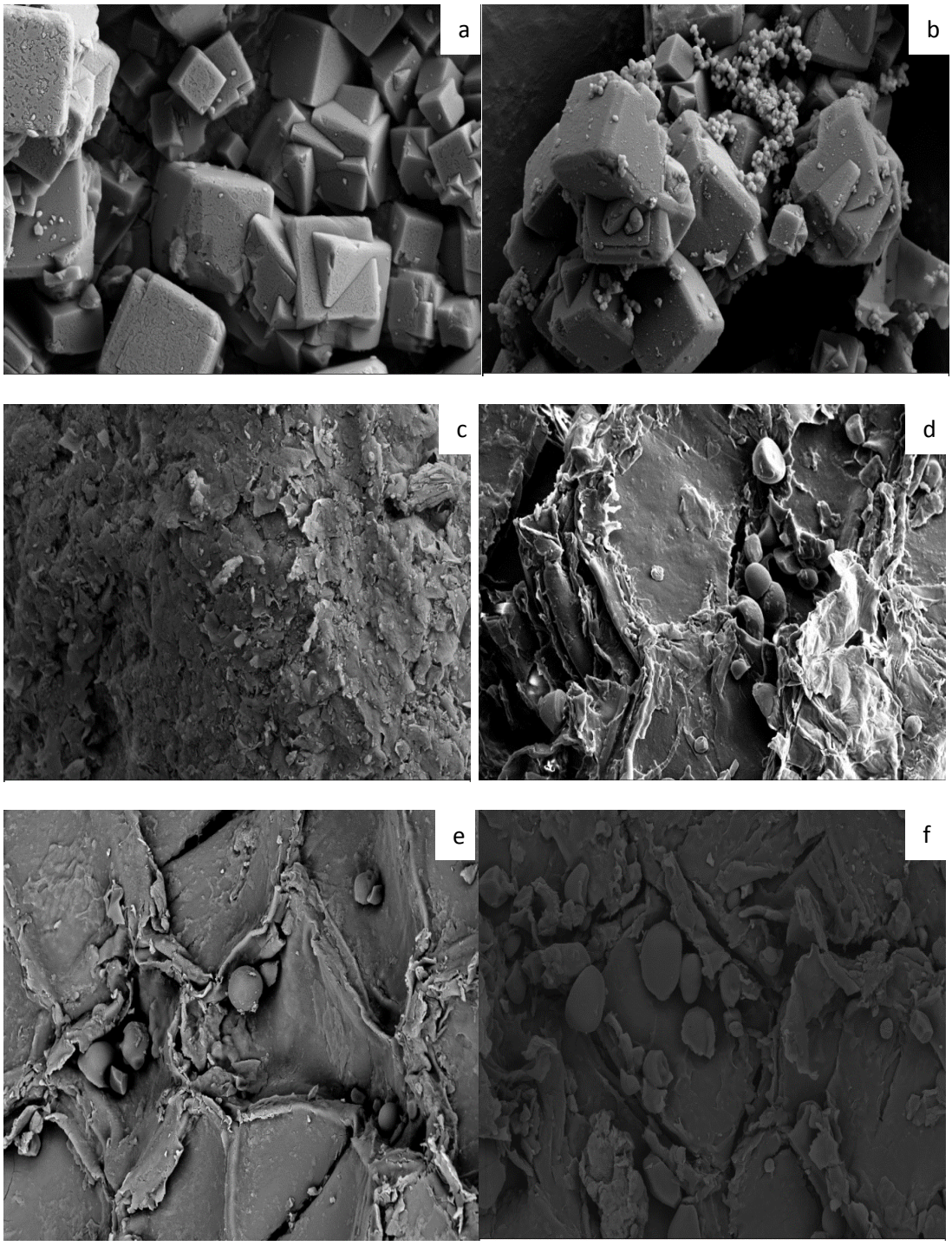
From the Table, it can be seen that acid treatment of the cassava waste biomass led to an increase in its surface area. Horsfall and Abia (2003) reported that acid treatment provides the adsorbent with a larger surface area and smaller porosity so that binding of metal ions may occur on the surface of the adsorbent. This generally implies that physical adsorption does not play a substantial role on metal adsorption onto cassava peel biomass. Mechanisms such as ion exchange, coordination, chelation, complexation and other surface mechanisms may be expected to be the dominant mechanisms of metal uptake by the cassava waste biomass (Kosasih et al., 2010). The same characteristic trends were reported in other related work (Horsfall and Abia, 2003; Fiol et al., 2006; Ndlovu et al., 2012; Seepe, 2015).

A decrease in surface area for the bentonite and zeolite adsorbents after immobilization was noted. The type and binding orientation of some functional groups onto an adsorbent has been reported to alter its surface geometry (Jal et al., 2004). Therefore, the occupation of the surface area and pore space by some functional groups in the silicate binder and yeast could have resulted in the reduced surface area and pore volume observed in this study. The decrease in surface area suggests a decrease in the number of active sites available for metal adsorption. However, because the mobilized zeolite surface was unoccupied by external functional groups, it had a higher pore size compared to all the adsorbents. This may indicate that the adsorbent surface has a larger pathway for metal ions to move during ion exchange and access the exchangeable cations inside the zeolite mass (Erdem et al., 2004).

4.1.6 Surface morphology

Surface morphology before metal adsorption

The surface morphology of the adsorbents prior to metal adsorption was observed using the Carl-Zeiss Field Emission SEM. The samples were coated with gold and palladium before the investigation to enhance electron conductivity. Figures 4.3 (a to g) show the surface morphology images of the different adsorbents.


a
b
c
d
e
f

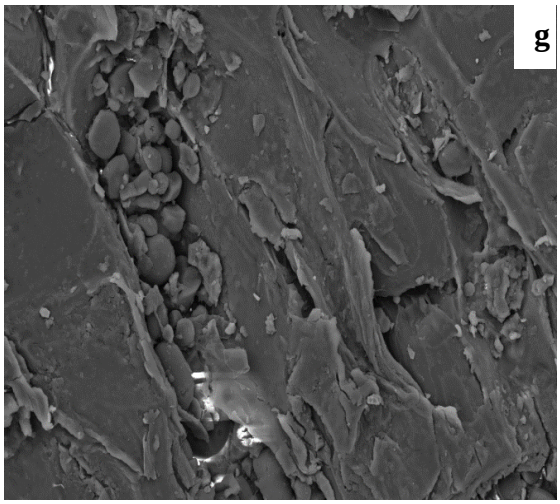


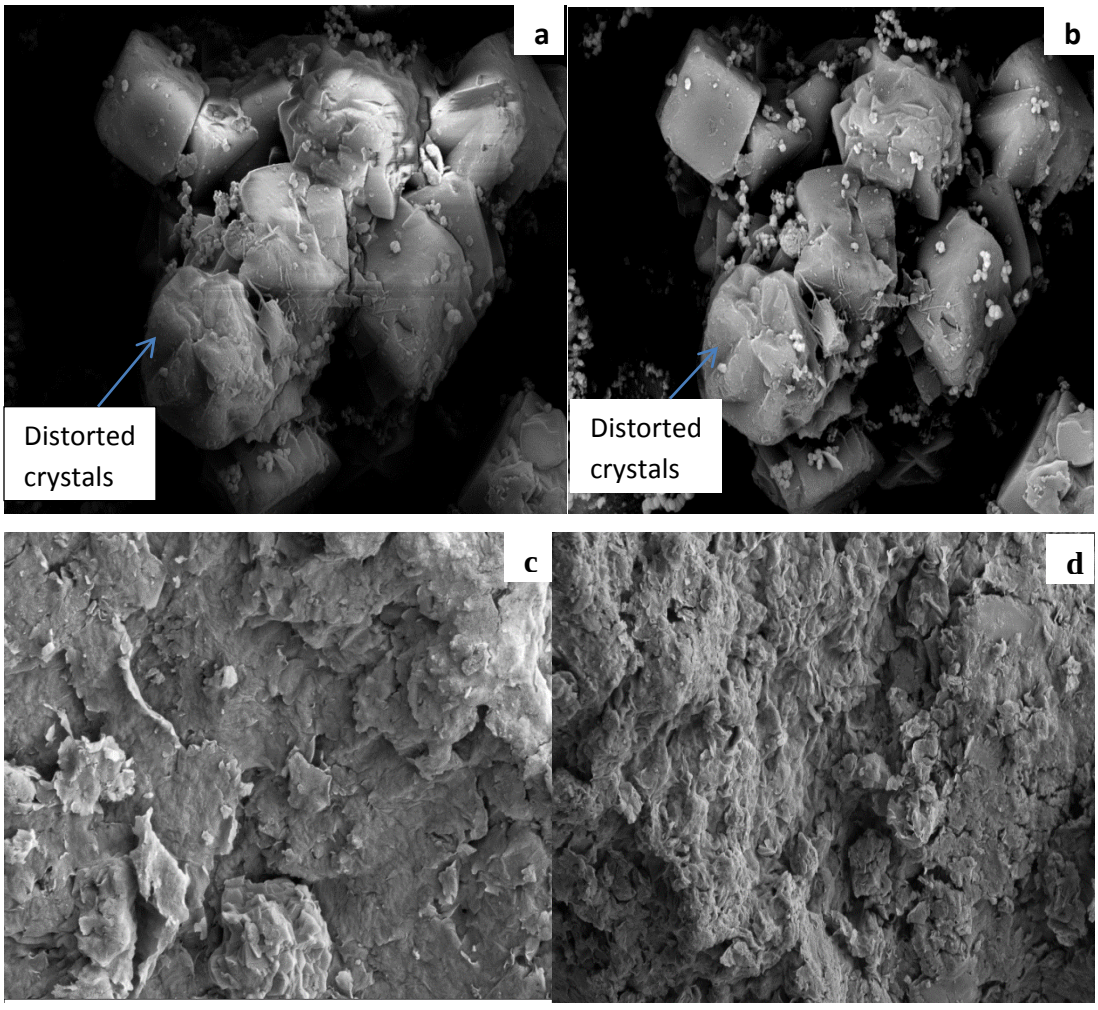
Figure 4.3: SEM images of (a) mobilized zeolite (b) immobilized zeolite (c) bentonite powder (d) bentonite beads (e) untreated cassava (f) acid treated cassava (g) immobilized cassava waste biomass before metal adsorption, all at 3000 times magnification.

Figure 4.3 (a) and Figure 4.3 (b) compares the surface morphologies of the mobilized and immobilized zeolite, respectively. Cubic forms of the crystalline material can be seen in Figure 4.3 (a). It can also be seen that, immobilization did not change the surface morphology of the zeolite adsorbent, since the cubic structure still remained intact (Figure 4.3 (b)). This finding is consistent with the SEM images of the same material used in the work of Kalayci et al. (2013). Foliated crystal morphologies can be seen with the bentonite adsorbents (Figure 4.3 (c) and Figure 4.3 (d)). The more foliated morphology of the bentonite beads (Figure 4.3 (d)) compared to the powder (Figure 4.3 (c)) may be due to the interaction of the surface with the sodium silicate binder. The foliated morphology may suggest the availability of a larger surface area for active adsorption. The heterogeneous nature of the bentonite surface can also be seen in the images. The images of the cassava peel adsorbents (Figure 4.3 (e) and Figure 4.3 (f)) confirm the low porosity, heterogeneous and complex nature of the cassava peel surface morphology that was reported in other research (Kosasin et al., 2010; Kurniawan et al., 2011). Acid treatment did not alter the surface morphology,

as can be seen from the SEM images (Figure 4.3 (e) and Figure 4.3 (f)). Comparing the surface morphology of the acid treated cassava waste biomass powder (Figure 4.3 (f)) with the immobilized waste biomass (Figure 4.3 (g)), it can be seen that both surface morphologies are closely similar. This suggests that immobilizing the waste biomass using sodium alginate did not alter the surface morphology.

Surface morphology after metal adsorption

The SEM images of the adsorbents after metal adsorption were also observed to investigate any changes in the surface morphology. Figure 4.4 presents the surface morphology images of the different adsorbents after metal adsorption.



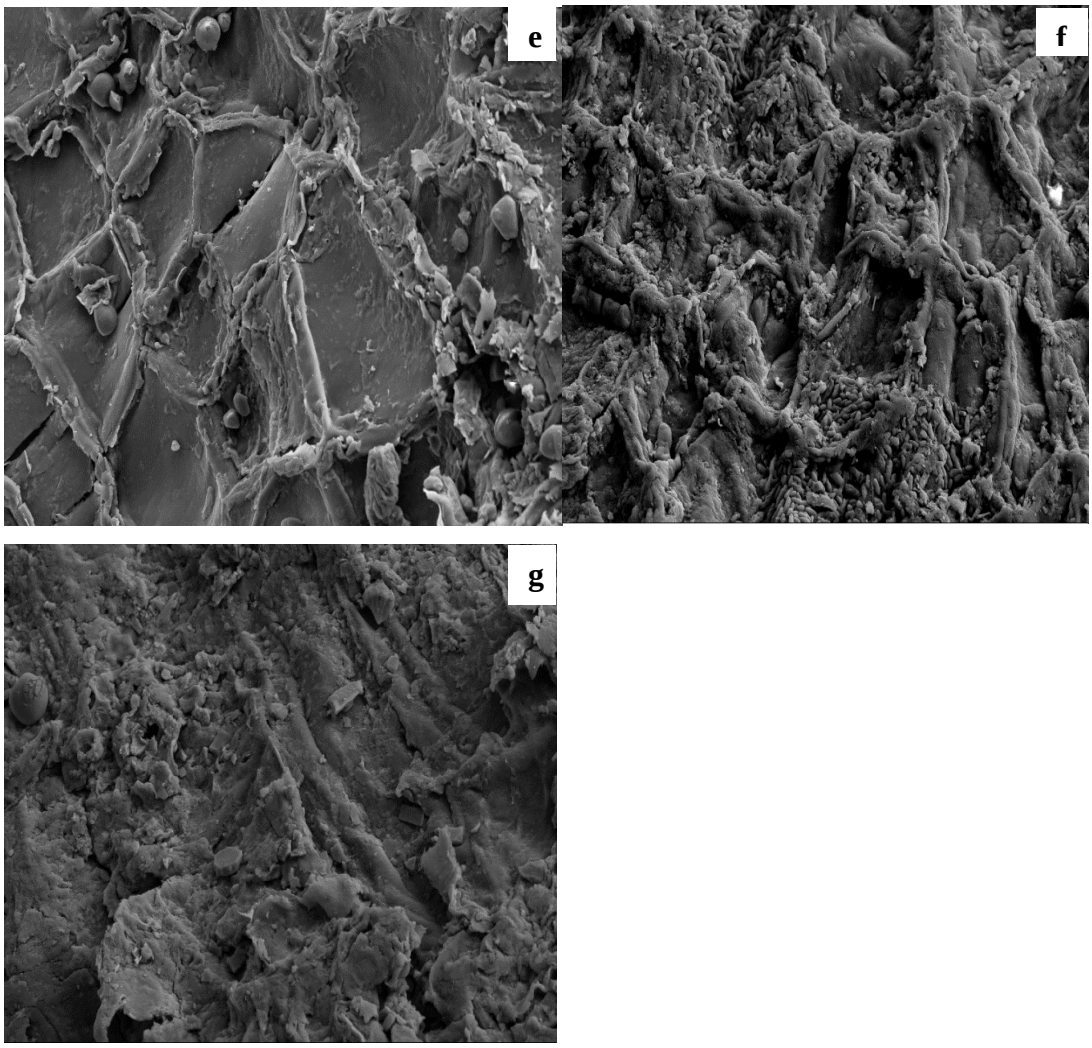


Figure 4.4: SEM images of (a) mobilized zeolite (b) immobilized zeolite (c) bentonite powder (d) bentonite beads (e) untreated cassava (f) acid treated cassava (g) immobilized cassava waste biomass after metal adsorption all at 3000 times magnification

Comparing Figure 4.4 (a) and Figure 4.4 (b) with Figure 4.3(a) and Figure 4.3 (b), respectively, it is clear that metal adsorption caused distortion of the cubic morphologies of the zeolite adsorbents. This can be attributed to dissolution and eventually the collapse of the zeolite structure as a result of the acidic solution, as will be discussed in detail in section 4.2.1. Comparison of Figure 4.3 (c) and Figure 4.3 (d) with Figure 4.4 (c) and Figure 4.4 (d) shows that the bentonite surface became

less foliated after metal adsorption as result of the interaction of the surface with the metal ions and the acidic solution. Comparing the surface of the untreated cassava adsorbent before metal adsorption (Figures 4.3 e) and after metal adsorption (Figures 4.4 e), it can be seen that metal adsorption did not cause much changes to the morphology of the adsorbent possibly due to reduced metal ion-surface interactions. However, comparison of the surface morphologies of the acid treated and immobilized cassava waste biomass, before (Figure 4.3 (f) and Figure 4.3 (g)) and after metal loading (Figure 4.4 (f) and Figure 4.4 (g)), respectively, shows that the surfaces became rougher after metal adsorption possibly due to the various interactions of the metal ions with the ligands on the biomass surface. However, the change in surface roughness was lesser in the immobilized cassava waste. This may be attributed to reduced metal-surface interactions which may have resulted from the diffusion limitations of some metal ions onto the immobilized biomass surface (Al-Anber, 2011).

4.2 Batch adsorption studies

The first aspect of this study involved assessing the suitability of using zeolite; bentonite clay and cassava peel biomass to remove harmful ions from a real AMD solution. Batch studies are normally used to access the capability of an adsorbent to take up metal ions. Therefore, batch studies were conducted in the present study in order to identify a low cost adsorbent with the highest ability to remove toxic heavy metals from real AMD with no loss in solution acidity, which could be recovered in the subsequent process stage. Screening tests were conducted in the batch mode to determine the best adsorbent from three low-cost adsorbents namely bentonite, zeolite and cassava peel biomass. The stability of the adsorbent in the acidic solution, the amount of acid in the solution, as well as its ability to remove most metal ions were used as a criterion in choosing the best adsorbent. Therefore, the effect of agitation time, adsorbent loading, temperature and agitation speed on the quantity of metals

and acidity remaining in solution was investigated. The quantity of the sulphate ions removed by the adsorbents was also examined because of its toxicity as already discussed in Chapter 2.

4.2.1 Metal removal results

Effect of agitation time

Adequate contact time is critical for metal accessibility to active adsorption sites; therefore, its effect on heavy metal uptake was investigated experimentally. Approximately 5g of each adsorbent was added to 500 mL of AMD solution. Unless stated otherwise, all agitation times, adsorbent dosages, temperatures and agitation speeds used in this study were chosen based on reported literature (Triantafyllou, 1999; Erdem et al., 2004; Kaya and Oren, 2005; Motsi, 2010; Aljil et al., 2014; Seepe, 2015). There were no initial pH adjustments made in all the tests so as to avoid losing solution acidity, which could be recovered in the subsequent process stage. The solutions containing zeolite and cassava adsorbents were then agitated in a Labcon platform shaker for 1 hour and samples collected at 10 minutes intervals. For bentonite adsorbent, the agitation time was longer, the mixture was agitated for 24 hours. This time was chosen based on preliminary adsorption tests, which indicated that times between 40 minutes and 4 hours as reported by previous researchers were not adequate to bring about any significant metal uptake. This could be attributed to the higher quantity of silica (Table 4.1) in the bentonite sample used in this study in comparison to those used in previous studies (Triantafyllou, 1999; Aljil et al., 2014). Samples of the solution treated with bentonite adsorbents were withdrawn at 20 minute time intervals for the first hour, then after 2, 6, 12, 18 and 24 hours. The pH levels were monitored and recorded at each time interval. The samples were stored and analysed for metal ion content. Since the agitation times were different, the adsorbents were compared based on the quantity of metals removed at equilibrium

time. Figure 4.5 to Figure 4.7 show the variation in percentage metal ions removed from AMD with contact time, using the unmodified and modified adsorbents.

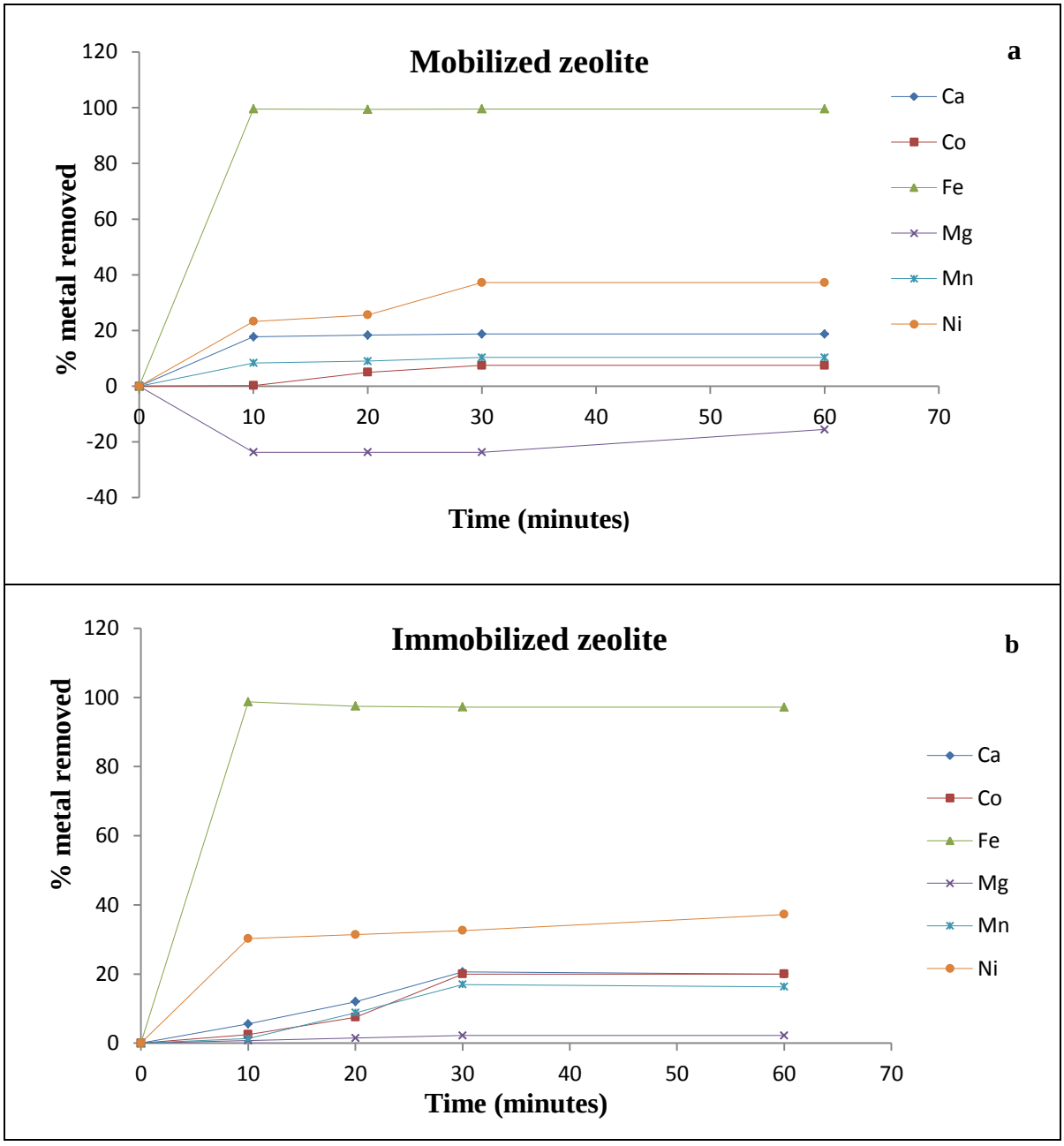


Figure 4.5: Effect of contact time on metal ion adsorption using (a) Mobilized and (b) Immobilized zeolite [Adsorbent dosage: 5g, Agitation speed= 150rpm, Temperature = 30 ˚C, Contact time = 1h].

The time-dependent behavior of metal adsorption on mobilized zeolite powder is illustrated in Figure 4.5 (a). The results show that the adsorption of all metals was rapid in the first 10 minutes (with up to 99.6% of Fe metal being removed at this time), and then slowed down considerably as the reaction approached equilibrium. The metal uptake occurred in the following order: $Fe^{3+} > Ni^{2+} > Ca^{2+} > Mn^{2+} > Co^{2+} > Mg^{2+}$. The initial fast rate could be attributed to the availability of unoccupied active sites on the newly exposed surface area of the adsorbent. However, despite the increase in metal uptake the adsorption efficiencies of most metal ions remained low. Approximately 31.0%, 10.35%, 7.50% and 18.76% of Ni, Mn, Co and Ca ions respectively, were removed at an equilibrium time of 30 minutes. The differences in the adsorption of Fe and the other metal can be attributed to the different mechanisms involved in their uptake by the zeolite adsorbent. However, the concentration of Mg ions was found to increase in the solution as shown by the negative metal uptake isotherm (Figure 4.5 (a)). This was attributed to dissolution of the zeolite structure during the adsorption process, as the zeolite structure is composed of some MgO phase (Table 4.1).

Since the AMD solution used in this study is highly acidic (initial pH= 2.16), competition between the H^+ ion and the metal ions present in the solution is anticipated. Erdem et al. (2004) reported that in a mixed ion solution, adsorption depends on the diameter of the hydrate cations. Cations with smaller hydrated diameters have higher affinity for reactive sites on an adsorbent compared to those with larger diameters, and consequently higher adsorption. In the present study, the diameters of the hydrate ions present in the AMD are of the order $H^+ < Ni^{2+} < Ca^{2+} < Co^{2+} < Mg^{2+} < Mn^{2+} < Fe^{3+}$ (Nightingale, 1959). Therefore, it is expected that the H^+ ion will have the maximum adsorption, since it has the least diameter. In other words, the ion can easily diffuse through the pores of zeolite mass and exchange with exchangeable cations in the framework. However, this exchange is very deleterious to the framework, since it causes the dissolution and eventually the collapse of the zeolite framework. In this study, the quantity of Al ions in the solution was observed

to increase from 0.28 mg/L to as much as 1.90 mg/L in 30 minutes. This observation provides compelling evidence of the dissolution of the zeolite structure, since Al is the major phase in the zeolite structure as already illustrated by the XRD and XRF results. In addition, the distortion of the cubic morphology of the zeolite (Figure 4.4 (a)) as well the presence of some additional magnesium ions in the effluent (Figure 4.5 (a)), may further support this suggestion since the zeolite structure is composed of some MgO phase (Table 4.1). The dissolution of the zeolite structure in acidic solutions has also been reported in other related work (Alvarez-Ayuso, 2003; Argun, 2008).

The solution pH was also observed to increase from 2.16 and reaching a maximum of 5.49 in 10 minutes (Table 4.4). This change in pH proves that ion exchange is taking place **(**Erdem et al., 2004) and this accounts for the initial metal ion uptake.

Table 4.4: Solution pH changes with time for mobilized and immobilized zeolite adsorbents

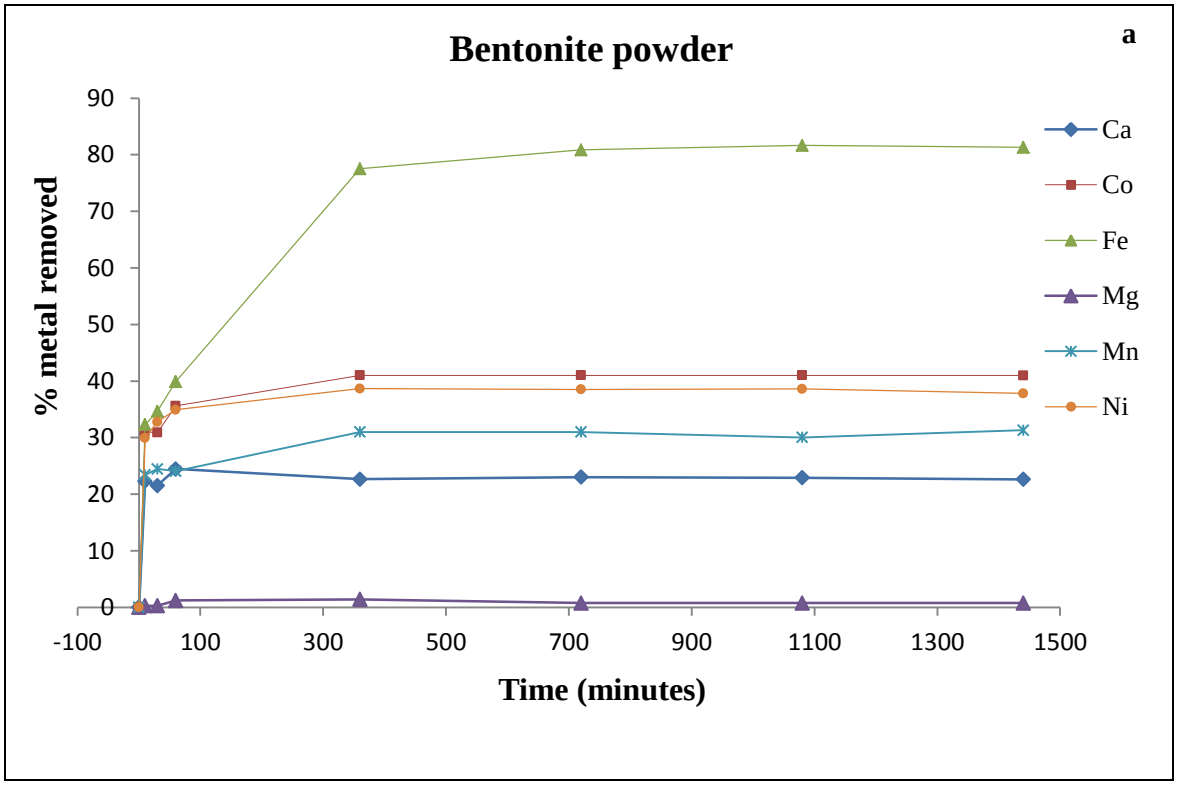
Time (min)	Mobilized zeolite	Immobilized zeolite
0	2.16	2.16
10	5.49	5.89
20	5.24	5.77
30	4.66	5.88
40	4.68	5.93
50	4.69	6.09
60	4.76	6.21

Since the solution is acidic the competition for exchange sites with the H^+ ion resulted in lower metal retention. Other metals such as Ni^{2+} and Ca^{2+} had a slightly higher adsorption efficiency compared to metals such as Mg^{2+} likely due to their smaller hydrated diameter. Although, the hydrated diameter of Fe^{3+} was one of the largest, its adsorption was not affected by the competition for reactive sites because its mechanism of removal is different from that of the other noxious heavy metal

present in the AMD solution (Ackil and Koldas, 2006). The removal of Fe^{3+} ions from this solution may be attributed to a combination of physical adsorption and precipitation mechanisms. Iron metal is known to precipitate as iron hydroxide ($Fe(OH)_3$) at pH levels above 3.5 (Evangelou, 1995; Ackil and Koldas, 2006). As already mentioned, pH levels reached values of 5.49 in 10 minutes in this study. Therefore, the precipitation of iron is expected to have occurred. Furthermore, an orange-brown precipitate obtained after the adsorption tests suggests the presence of the iron precipitate in the used adsorbent. The precipitation mechanism explains why Fe is the only metal ion that was significantly removed at equilibrium. The removal of other metals in the solution via the precipitation mechanism was highly unlikely since metal ions such Ca, Mg, Mn, and Ni precipitate at pH levels ranging between 10 and 14 (Maryland, 1994).

Comparing Figure 4.5 (a) and Figure 4.5 (b) shows that immobilizing the zeolite powder with yeast did not significantly improve the metal adsorption efficiency. The quantity of Fe^{3+} adsorbed remained substantially high (with approximately 96% removed at equilibrium), due to its removal via the precipitation mechanism. There was a slight increase in metal adsorption to 31%, 20%, 17% and 2% for Ni, Ca/Co, Mn and Mg respectively. The increase could be attributed to the presence of functional groups such as C-O (carboxyl) and O-H introduced by the yeast, which are known to be responsible for metal binding (Gardea-Torresdey et al., 1990). However, the reduction in surface area after immobilizing with yeast (Table 4.3) implies that they are fewer active sites for adsorption which, in this case, may have counteracted the effect of the functional groups, resulting in no significant change in metal uptake being observed. The differences in the quantity of metal ions adsorbed by the immobilized zeolite adsorbent could be related to the nature and amount of functional groups responsible for the interaction with the different metal ions. Although, the dissolution of the MgO phase was not present (Figure 4.5 (b)), the extent of dissolution of the zeolite structure via the Al_2O_3 phase increased in the immobilized zeolite. The quantity of Al ions in the effluent was found to increase from 0.28 mg/L

to 52.4 mg/L at equilibrium time, which was greater than the increase to 1.90 mg/L in the mobilized zeolite. The interaction of metal ions with the functional groups introduced by yeast in the immobilized zeolite may have greatly exacerbated the dissolution of the adsorbent structure.



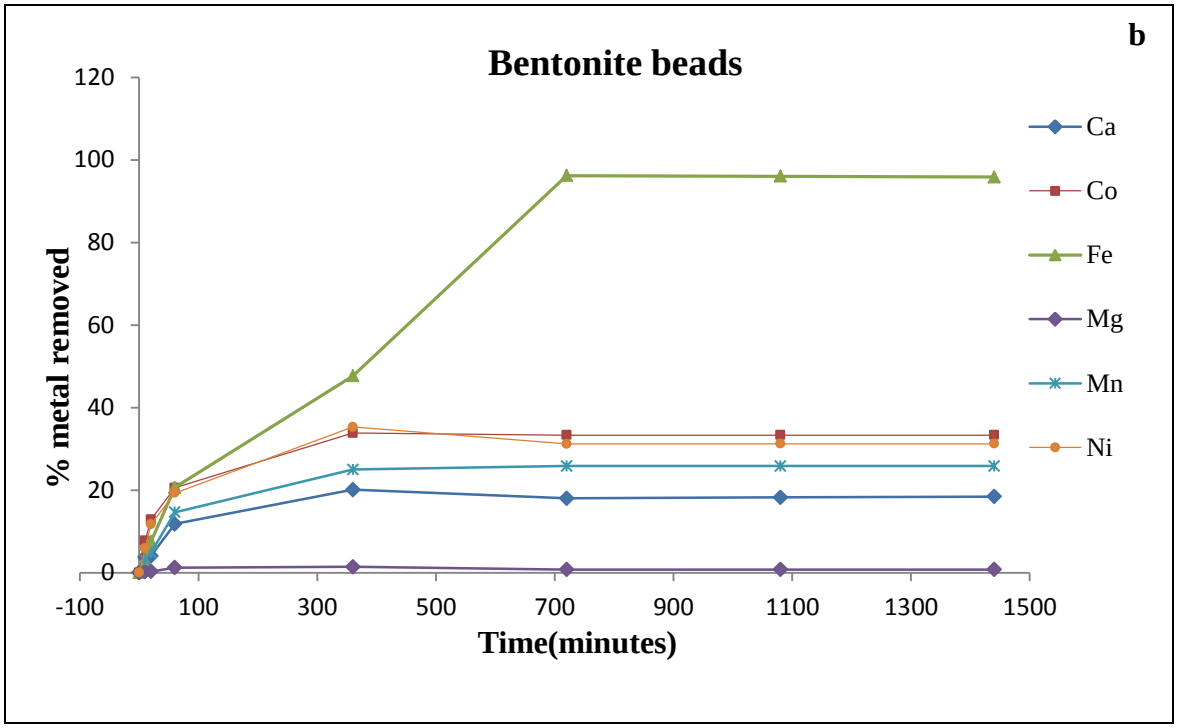
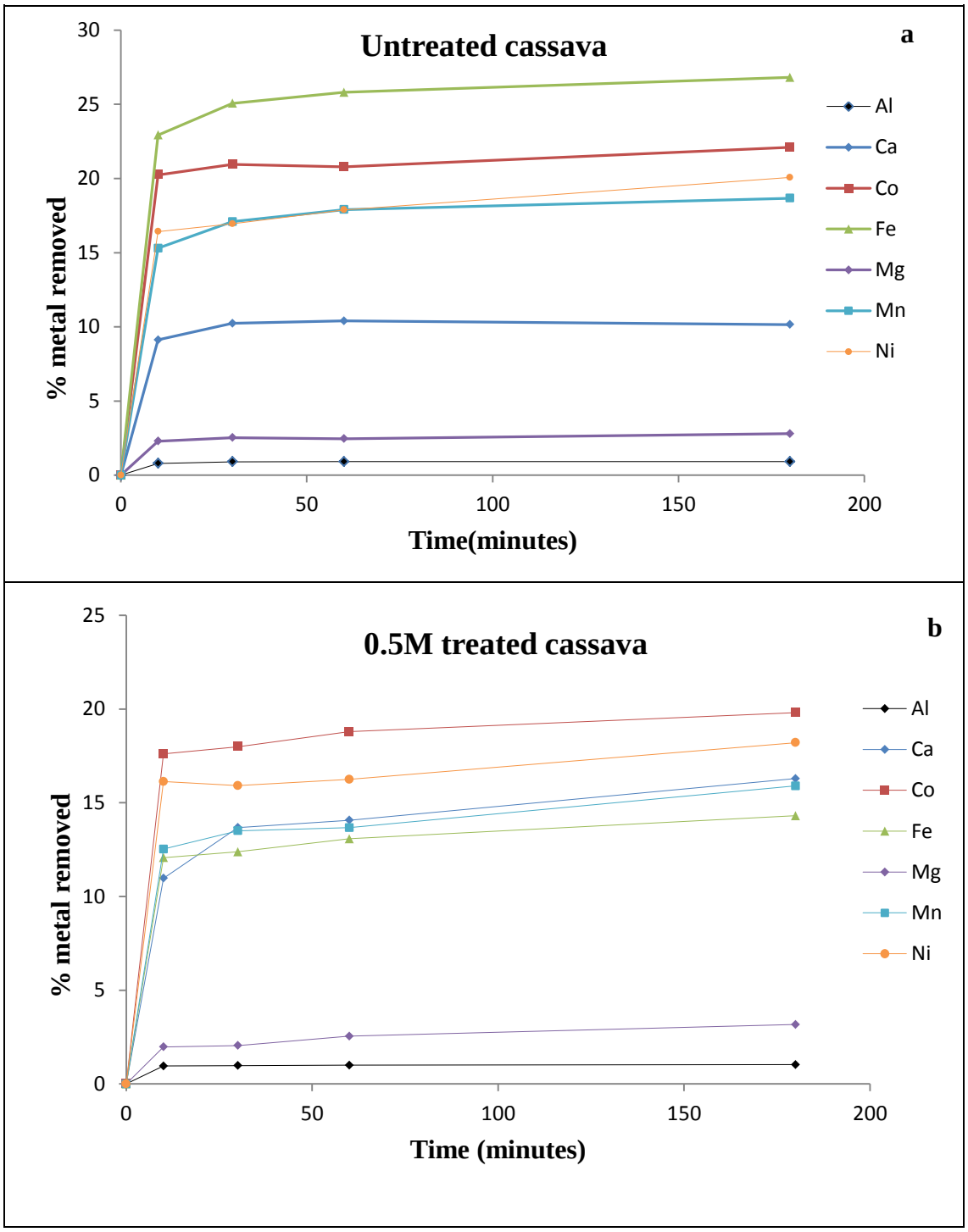


Figure 4.6: Effect of contact time on metal ion adsorption using (a) Bentonite powder and (b) Bentonite beads [Adsorbent dosage: 5 g, Agitation speed= 150 rpm, Temperature = 30 ˚C, Contact time = 24 hrs].

Figure 4.6(a) shows the results of metal uptake by bentonite clay powder. It can be deduced from the Figure that adsorption increased rapidly in the first 300 minutes (5 hours) and then slowed down as the process approached equilibrium at 360 minutes. Approximately 77.5% Fe metal ions were adsorbed onto bentonite powder in the 360 minutes equilibrium time. The removal of other metals using bentonite powder also increased but the values remained low with up to 40.9% Co, 22.2% Ca, 30% Mn, 38% Ni and less than 1% Mg removed at equilibrium time. This difference in the uptake of Fe and other heavy metals can also be attributed to the difference in the mechanisms involved in their adsorption by bentonite. An increase in the solution pH to 3.97 observed in the present work provided a desirable environment for iron to precipitate. Therefore, it is expected that the iron removal was through the precipitation mechanism. Since the pH was changing, it implies that ion exchange was taking place (Erdem et al., 2004) hence; the removal of the other metals can be

attributed to the ion exchange mechanism. However, the overall metal removal was low due to the competition with the H^+ ion for active sites.

As already discussed bentonite powder forms a colloidal solution when in contact with water. This makes separation of the adsorbent from the solution difficult after adsorption. Therefore, immobilization of the powder into beads was also carried out. The results of the metal adsorption efficiency with time using bentonite beads are shown in Figure 4.6 (b). The results indicate that bentonite beads took a longer agitation time, i.e., 12 hours, to achieve the same iron removal as that of the bentonite powder possibly due limited active surface area compared to that of the powder (Table 4.3). The removal efficiencies of the other metal ions remained low as well, with only 20%, 35%, 1,4%, and 24% of Ca^{2+}, Co^{2+}, Mg^{2+} and Ni^{2+}, respectively, adsorbed at equilibrium. In general, the poor results of the other metal ions observed in this study with both bentonite adsorbents (powder and beads), may be attributed to the low pH associated with the AMD solution treated (initially pH value= 2.16). Firstly, at low pH values the hydrogen ions (H^+) compete with the metal ions for adsorption sites and hence, decrease the chances of metal adsorption from solution. Secondly, pH values less than 3 are known to cause dissolution of bentonite (Thomas et al., 1950; Altin et al., 1999). The less foliated bentonite surface morphology after metal adsorption (Figure 4.4 (c) and Figure 4.4 (d)) may be evidence of the dissolution of the surface resulting from its interaction with the acidic AMD solution. In addition, metal ions with a larger hydrated radii such as Mg^{2+} etc., had lower adsorption efficiencies possibly due to reduced affinity for reactive sites of the bentonite adsorbent.


a
Untreated cassava
% metal removed
Time(minutes)
Al
Ca
Co
Fe
Mg
Mn
Ni
b
0.5M treated cassava
% metal removed
Time (minutes)
Al
Ca
Co
Fe
Mg
Mn
Ni

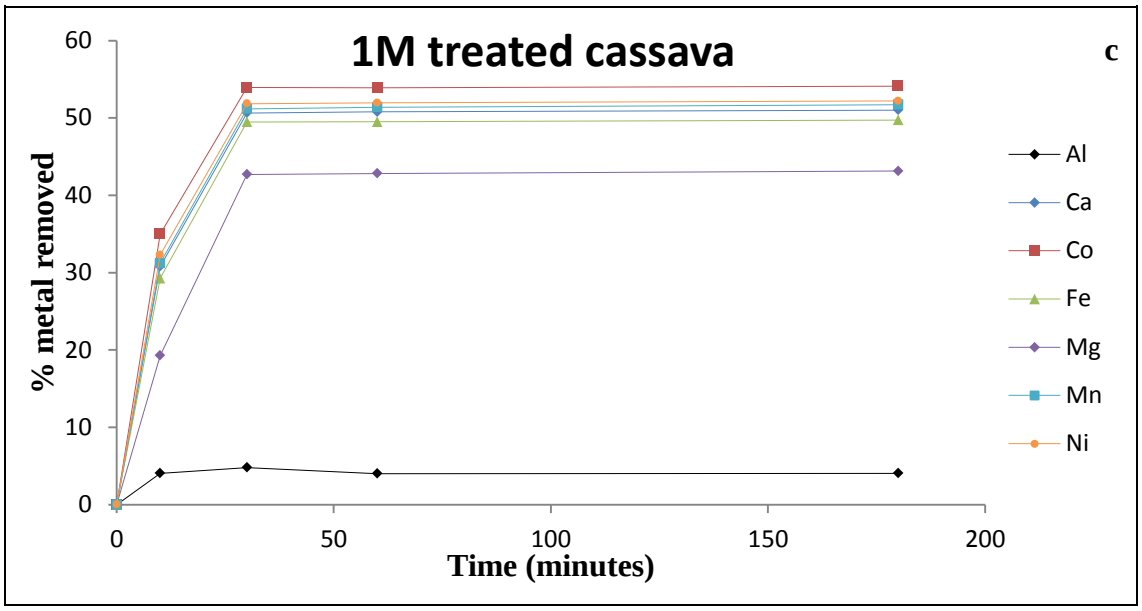


Figure 4.7: Effect of contact time on metal ion adsorption using (a) Untreated cassava (b) 0.5M treated cassava and (c) 1M treated cassava [Adsorbent dosage= 5g, Agitation speed= 150rpm, Temperature = 30 ˚C, Contact time = 1h].

Figures 4.7 (a to c) show the variation in percentage metal ions removed with time for untreated, 0.5M and 1M thioglycollic acid treated cassava peel biomass, respectively. A rapid increase in metal ion removal is observed in the first 10 minutes of the experiment, which is attributed to the availability of unoccupied active sites. The Co^{2+} and Ni^{2+} ions were the mostly adsorbed metal ions by the cassava waste adsorbents. This could be attributed to their smaller hydrated ionic diameter compared to their counterpart ions, which makes it easier to access active sites. Horsfall et al. (2003) indicated that the smaller the ionic size, the greater its affinity to reactive sites, of the hydroxyl and sulfhydryl ligands in the untreated and acid treated biomass. Comparison of the three figures (Figures 4.7 (a) to (c)), showed that acid treatment led to an increase in metal uptake. This can be attributed to the introduction of the sulfhydryl group which enhances metal adsorption (Abia et al., 2003). The differences in the results of metal uptake by 0.5M and 1M treated cassava peel biomass may be due to the increase in the quantity of the sulfhydryl groups with acid treatment. However, the overall metal removal values by the cassava peel adsorbents

in this study of 20 to 55% remained lower than those reported in literature. Seepe (2015) reported that close to 70% of Co^{2+}, Cr^{3+} and V^{3+} ions were removed in 30 minutes using 1M treated cassava waste biomass. The lower metal retention observed in the present work could be attributed to the competition of H^{+} ions with the metal ions for active sites. In previous studies, the pH value was adjusted to alkaline values before the tests (Kosasih et al., 2010; Kurniawan et al., 2011, Seepe, 2015). Therefore, even though chemical modification improved adsorption in these studies due to the increase in the number of active sites, better ion exchange and formation of new functional groups which favor metal uptake (Abia et al., 2003; Horsfall et al., 2003; Seepe, 2015); it did not yield the same results in the present investigation probably due to the slightly lower initial pH of the AMD solution.

Behavior of aluminium in zeolite and bentonite adsorbents

As already seen, the adsorption of aluminium ions is not shown in the results for zeolite (Figure 4.5) and bentonite adsorbents (Figure 4.6). This is because Al ions are not adsorbed from acidic solutions by these adsorbents. In fact, the quantity of these ions in the effluent increases with time as shown in Table 4.5. This implies that Al ions were added into the solution (instead of being removed).

Table 4.5: Concentration of Al ions in the effluent with time

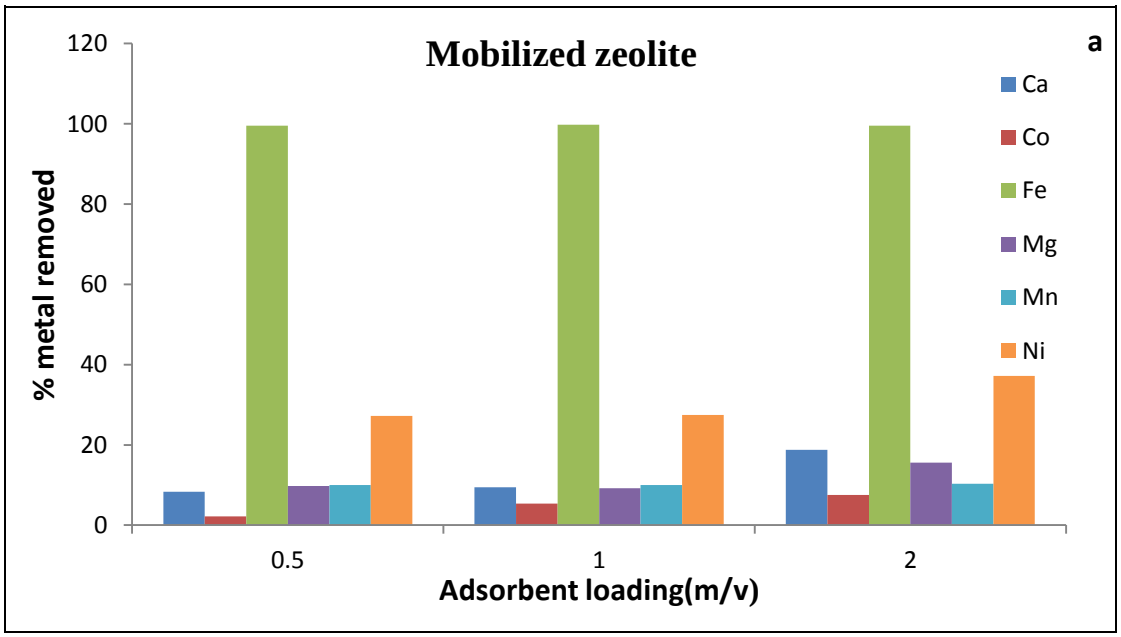
Time (min)	Mobilized Zeolite(mg/L)	Immobilized Zeolite(mg/L)	Bentonite Powder(mg/L)	Bentonite Beads(mg/L)
0	0.28	0.28	0.28	0.28
10	0.41	38.50	0.84	0.86
20	0.80	47.60	-	-
30	0.81	52.10	0.91	2.38
60	-	52.40	1.33	2.31
360	-	-	2.84	2.51
720	-	-	3.24	4.11
1080	-	-	3.23	4.76
1440	-	-	3.24	5.38

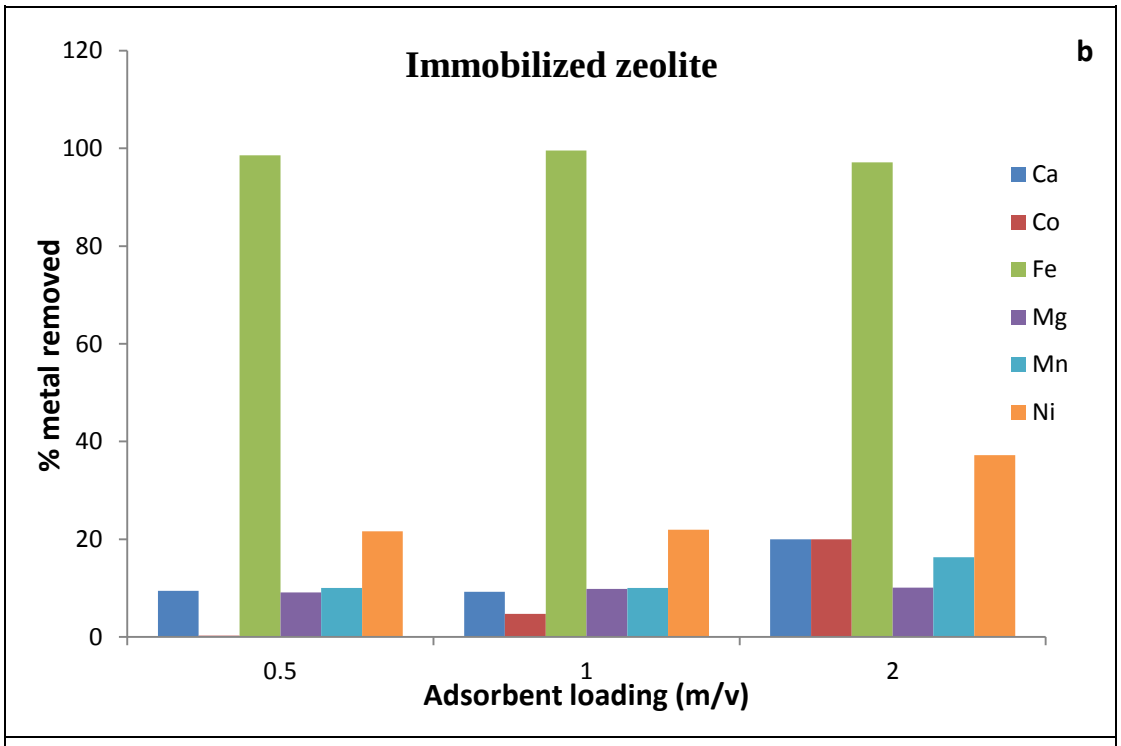
This observation may be attributed to the dissolution of the zeolite and bentonite crystalline structures during the adsorption process (Altin et al., 1999; Alvarez-Ayuso, 2003). The H^+ ions in the AMD solution exchange with the Al ions in the adsorbents, and this leads to the dissolution and eventually the collapse of the crystalline framework, as previously discussed. This observation implies that zeolite and bentonite adsorbents are not good adsorbents for the removal of Al ions from acidic waste solutions. As a result of the nature of Al isotherms obtained (negative adsorption instead of positive), the adsorption efficiency results for Al ions are not shown in all the Figures for metal adsorption using zeolite and bentonite adsorbents.

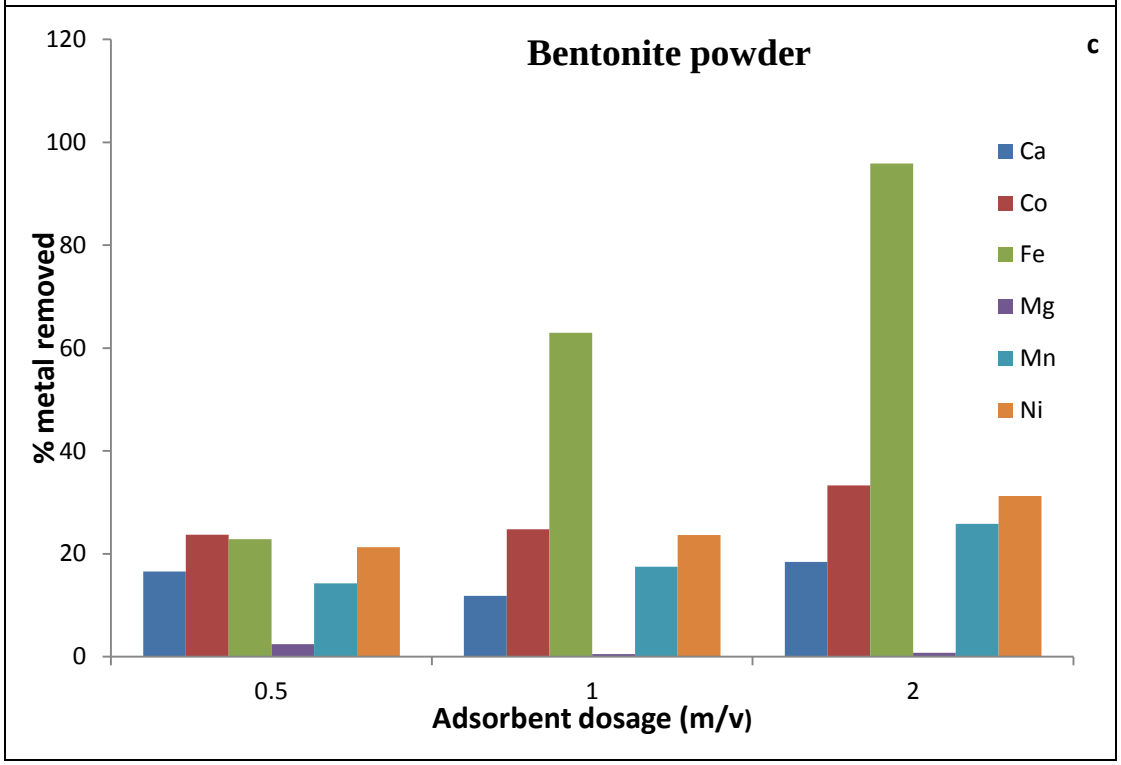
Effect of adsorbent dosage

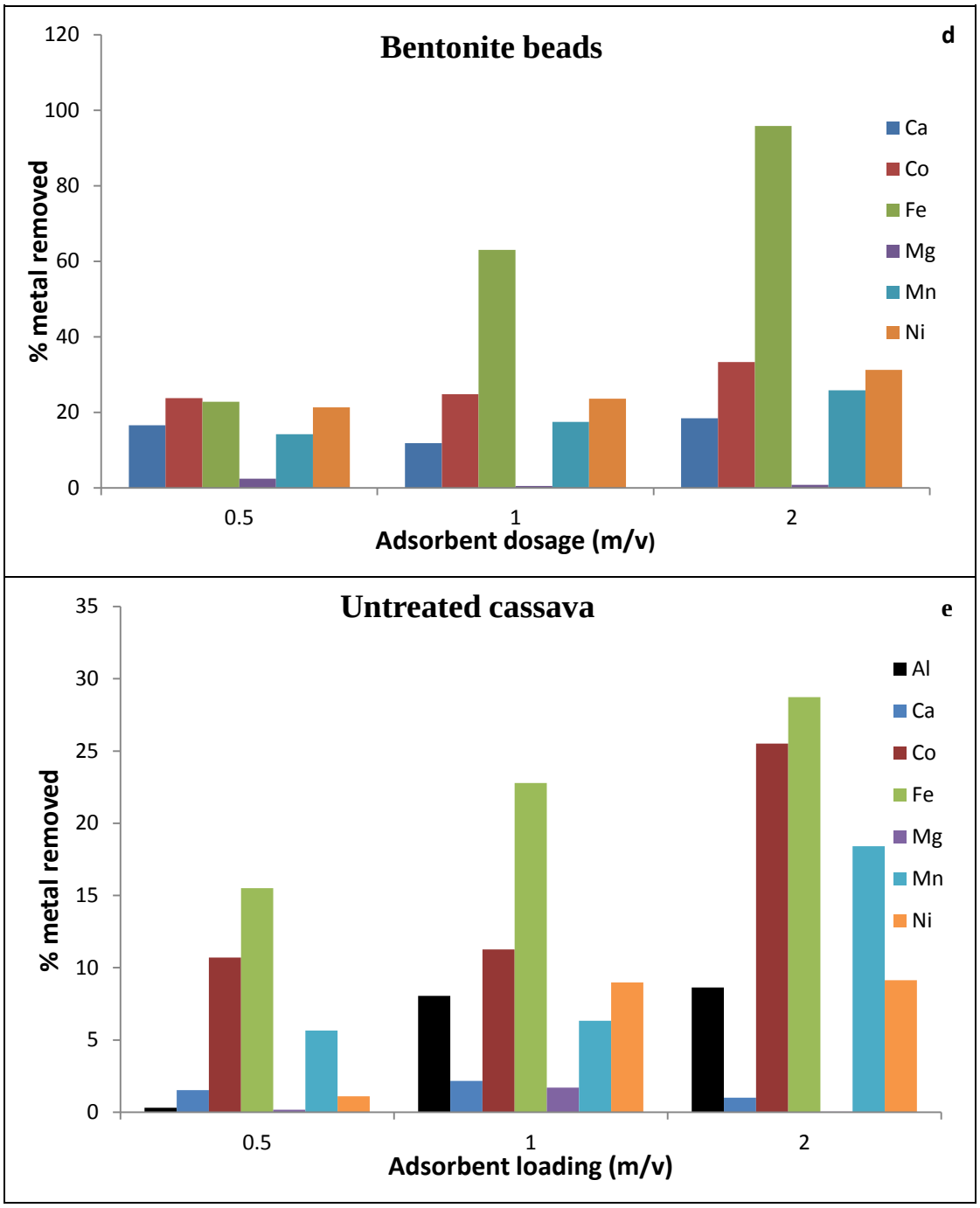
The quantity of the adsorbent in a solution affects the amount of metal ions adsorbed; therefore, the effect of the adsorbent dosage on metal uptake was investigated. Approximately 2.5g, 5g and 10g of each adsorbent was mixed with 500 mL of real

AMD solution and shaken at 150 rpm for an hour for cassava and zeolite; and 24hours for bentonite adsorbents to achieve equilibrium. The adsorption times were based on preliminary test work and the dosages were based on previous studies found in literature, as stated previously. The solution samples were collected at the end of the contact time and analysed for metal ion content. Figure 4.8 shows the variation in the percentage of metal ions removed versus adsorbent loading. It is evident that the adsorption of Al (only by cassava adsorbents), Ca, Co, Fe, Mg, Mn and Ni ions from AMD using the different adsorbents increased with increasing adsorbent loading. This may be attributed to the increase in surface area which in turn increases the number of active sites available for adsorption per unit space. However, the removal values of metals such as Co, Ni and Mn remained quite low when compared to those reported in literature (Motsi, 2010; Nsimba, 2012; Seepe, 2012). This may be due to the competitive adsorption effect which is associated with mixed ion solutions such as the real AMD solution in this study. It is expected that a further increase in the adsorbent loading could reduce this effect and significantly improve the uptake of these metals, though this may necessitate the use of larger volumes of adsorbent, which increases the treatment cost.




Immobilized zeolite
b
120
100
80
60
40
20
0
% metal removed
0.5
1
2
Adsorbent loading (m/v)
Ca
Co
Fe
Mg
Mn
Ni


Bentonite powder
c
120
100
80
60
40
20
0
% metal removed
0.5
1
2
Adsorbent dosage (m/v)
Ca
Co
Fe
Mg
Mn
Ni


Bentonite beads
d
% metal removed
120
100
80
60
40
20
0
0.5
1
2
Adsorbent dosage (m/v)
Ca
Co
Fe
Mg
Mn
Ni
Untreated cassava
e
% metal removed
35
30
25
20
15
10
5
0
0.5
1
2
Adsorbent loading (m/v)
Al
Ca
Co
Fe
Mg
Mn
Ni

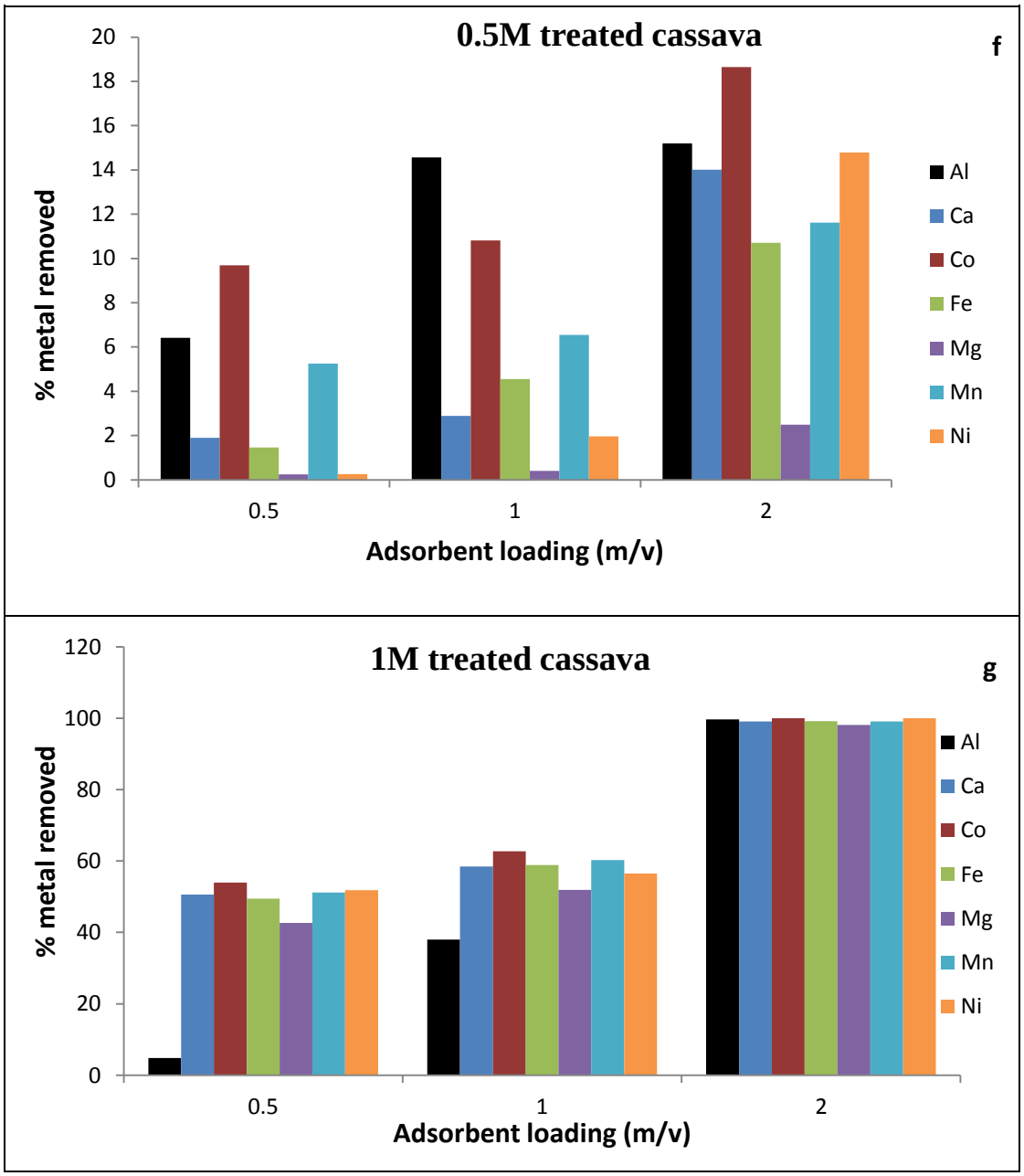


Fig 4.8: Effect of adsorbent loading on metal ion adsorption using (a) Mobilized and (b) Immobilized zeolite (c) Bentonite powder and, (d) beads (e) Untreated (f) 0.5M treated and (g) 1M treated cassava [Agitation speed= 150 rpm, temperature = 30 ˚C, contact time = 1h for zeolite and cassava peel; 24 hrs for bentonite].

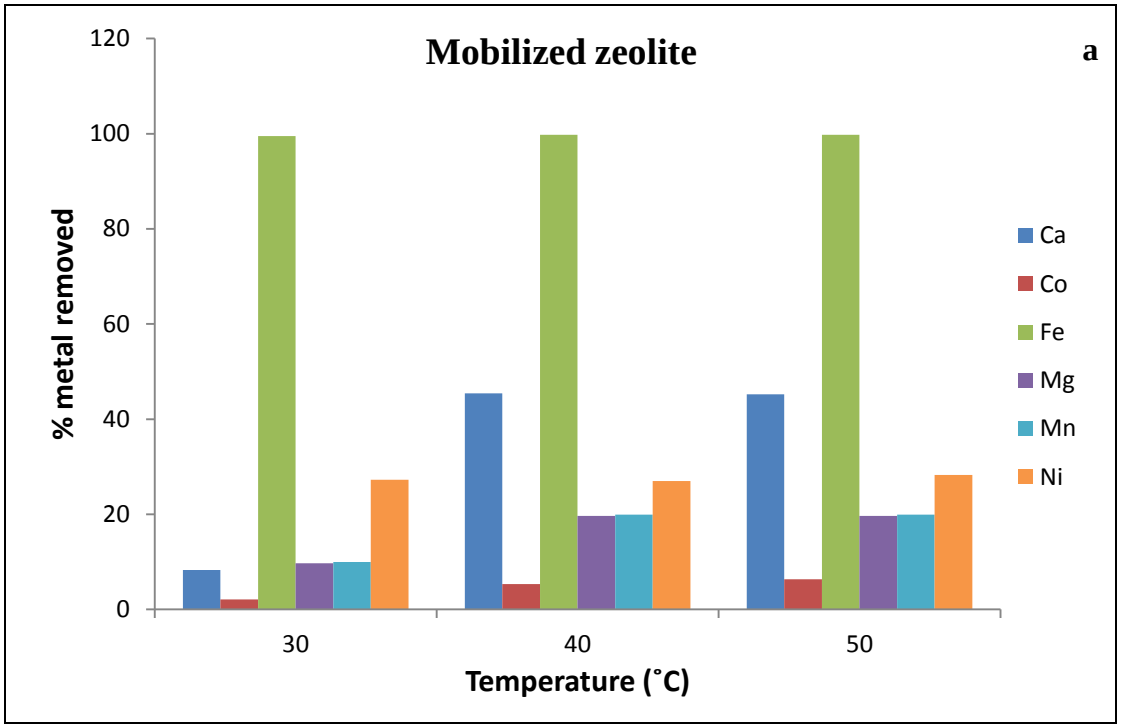
Comparing the metal uptake at different adsorbent loading by the mobilized and immobilized zeolite (Figure 4.8 (a) and Figure 4.8 (b)), it can be seen that immobilized zeolite had slightly larger metal adsorption efficiencies possibly due to the presence of the functional groups added by the yeast. The metal adsorption efficiencies for the bentonite adsorbents were closely similar at different adsorbent loadings (Figure 4.8 (c) and (d)). This may be attributed to similar surface functional groups on both bentonite surfaces as already seen in Figure 4.2 (b).

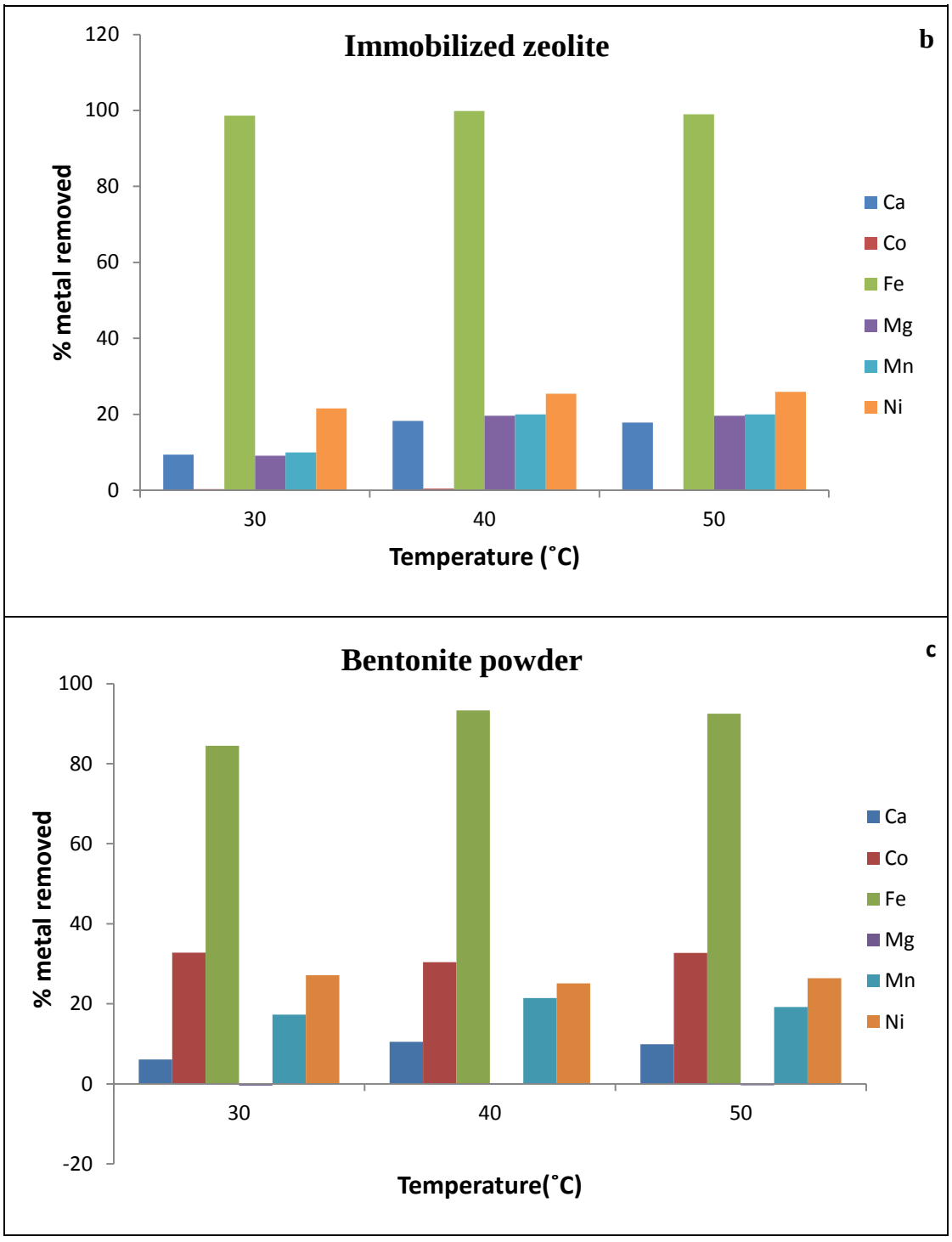
The results also revealed that cassava peel biomass was the only adsorbent that remained stable in the acidic solution, and an increase in metal adsorption was also noted with adsorbent loading. The results further indicated that the quantity of metal ions removed increased with acid modification, which may be attributed to the larger number of sulfhydryl groups which attract and sequester the metal ions. Despite, a small difference in metal uptake between untreated and 0.5M treated cassava peel biomass; significant improvement in results was obtained with 1M treated cassava peel biomass. Over 90% of most metals were removed when the adsorbent loading was increased to 2%. This may be attributed to increase in the number of binding sites resulting from the increase in adsorbent loading and the higher degree of acid treatment. The same trend in results was also reported in other related work (Abia et al., 2003; Horsfall et al., 2004; Seepe, 2015).

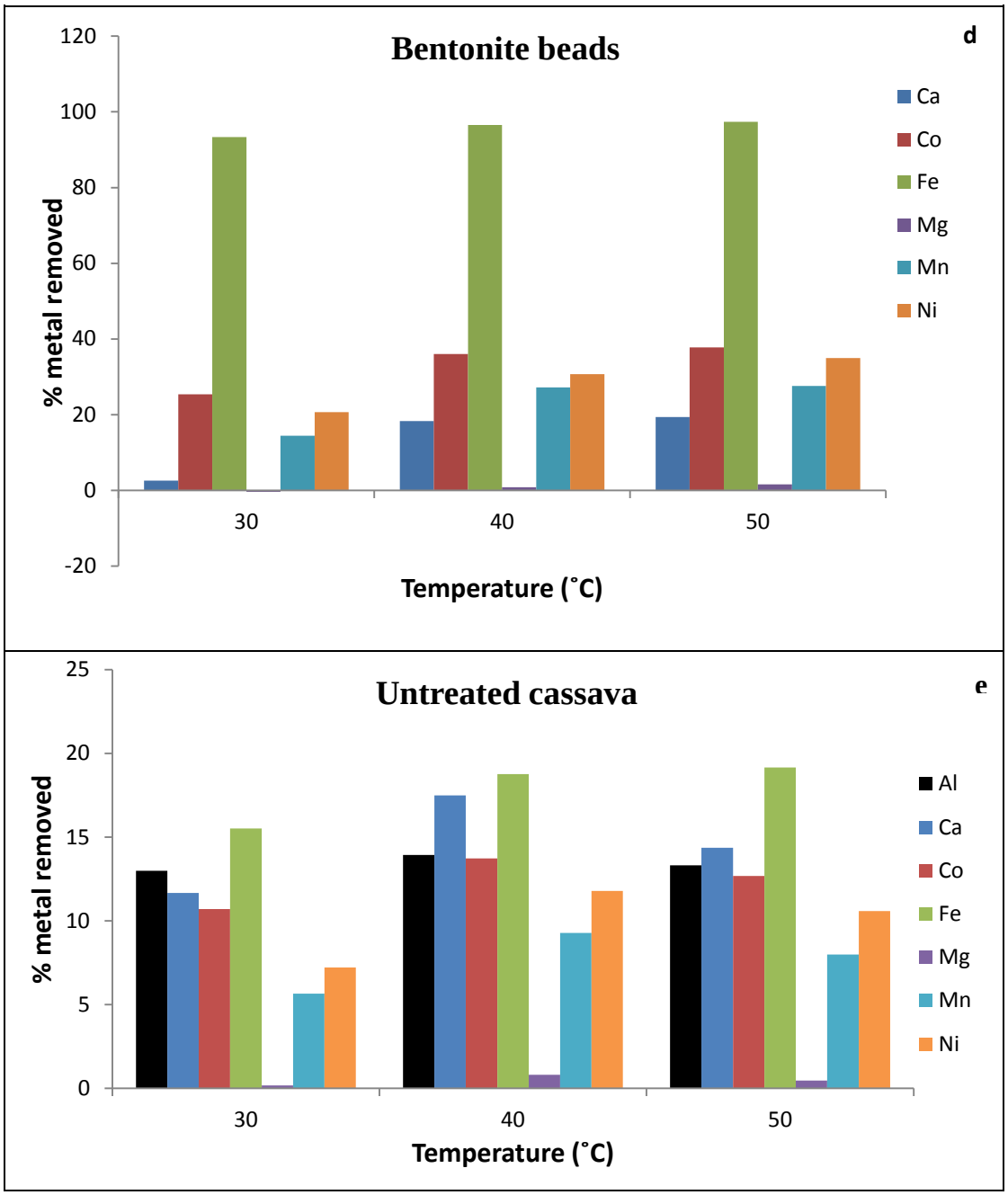
Effect of temperature

The investigation of the effect of temperature is crucial in adsorption processes, since temperature gives a measure of the kinetic energy of reacting species. High temperatures have been reported to increase metal adsorption through increasing the number of active sites, desolvation of the adsorbing species, and reduction in the mass transfer resistance (Meena et al., 2005). Therefore, in the present investigation, the AMD solution temperature was varied between 30 ˚C and 50 ˚C. Approximately, 5g of each adsorbent was mixed with 500 mL of AMD solution and then agitated at

150 rpm. The zeolite and cassava peel mixtures were agitated for 1 hr and bentonite mixture for 24 hrs. Solution samples were collected at the end of the contact time and analysed for metal ion content. Figure 4.9 shows the percentage of metal ions removed at different temperatures.




b
Immobilized zeolite
% metal removed
120
100
80
60
40
20
0
30
40
50
Temperature (˚C)
Ca
Co
Fe
Mg
Mn
Ni
c
Bentonite powder
% metal removed
100
80
60
40
20
0
-20
30
40
50
Temperature(˚C)
Ca
Co
Fe
Mg
Mn
Ni


Bentonite beads
d
% metal removed
Temperature (˚C)
Ca
Co
Fe
Mg
Mn
Ni
Untreated cassava
e
% metal removed
Temperature (˚C)
Al
Ca
Co
Fe
Mg
Mn
Ni

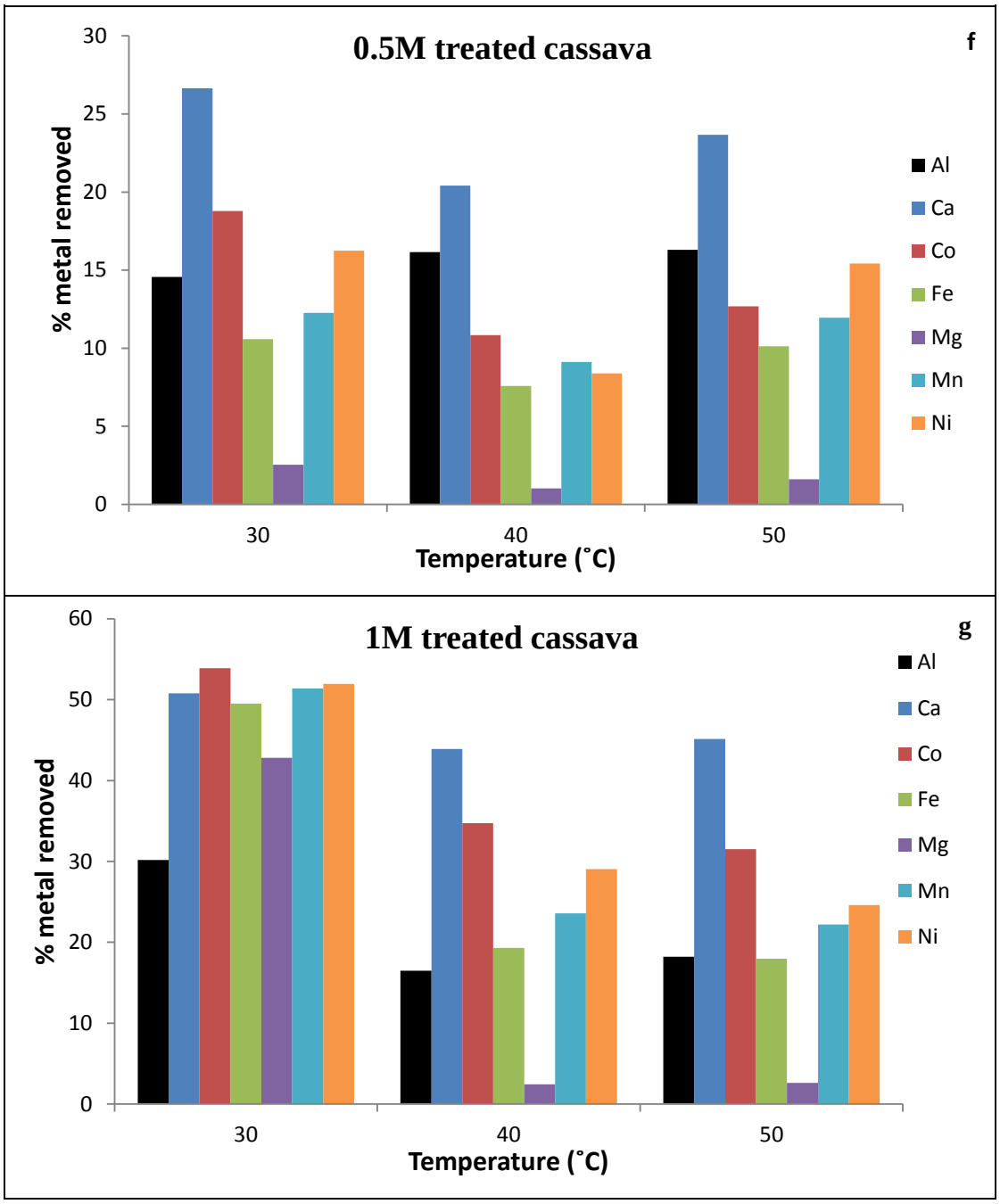


Figure 4.9: Effect of temperature on metal ion adsorption using (a) Mobilized and (b) Immobilized zeolite (c) Bentonite powder and, (d) beads (e) Untreated (f) 0.5M treated and (g) 1M treated cassava waste [Adsorbent dosage: 5g, Agitation speed= 150rpm, Contact time = 1h for zeolite and cassava peel; 24 hrs for bentonite].

Comparing the results for the two zeolite adsorbents (Figure 4.9 (a) and 4.9 (b)), it can be seen that as the temperature increased from 30˚C to 50˚C there was an increase in the adsorption of most heavy metal ions. The increase in adsorption capacity of the zeolite adsorbents with temperature indicates an endothermic process. The increase in adsorption with temperature may be attributed to a decrease in the boundary layer thickness, which in turn reduces the mass transfer resistance (Meena et al., 2005). Since adsorption is an endothermic process, the external mass transfer rate of ions to the adsorbent surface increases at higher temperature, leading to greater adsorption being observed. The adsorption efficiency was slightly lower for the immobilized zeolite (in comparison to the mobilized zeolite) at higher temperatures possibly due to the destruction of some functional groups responsible for metal uptake at these temperatures.

A similar adsorption trend was observed with the bentonite adsorbents (Figure 4.9 (c) and (d)). The removal of Fe metal using bentonite powder increased from 82% to 93% with an increase in temperature from 30˚C to 50˚C (Figure 4.9 (c)) and 93% to 97% for the beads (Figure 4.9 (d)). This observation can also be attributed to the reduction in boundary layer thickness, which reduces the mass transfer resistance and increases the transport rate to the adsorbent surface, resulting in higher metal uptake. In addition, at higher temperatures, ions have been reported to become smaller owing to their reduced hydration radii and thus their movement becomes faster (Inglezakis et al., 2004), resulting in higher adsorption efficiencies. Moreover, it is reported that cations move faster at high temperatures because the retarding electrostatic interactions become weaker and the ions become smaller because solvation is reduced (Inglezakis et al., 2004). However, despite the increase in the adsorption of the other metals (other than Fe), the values remained quite low likely due to the competitive ion effect associated with mixed ion solutions, such as AMD. Comparison of the metal uptake efficiencies using the bentonite powder with that of the beads (Figure 4.9 (c) and (d)), it can be seen that temperature changes did not result in any

significant difference between the two adsorbents. This may be due to similarity in the type of functional groups on both surfaces.

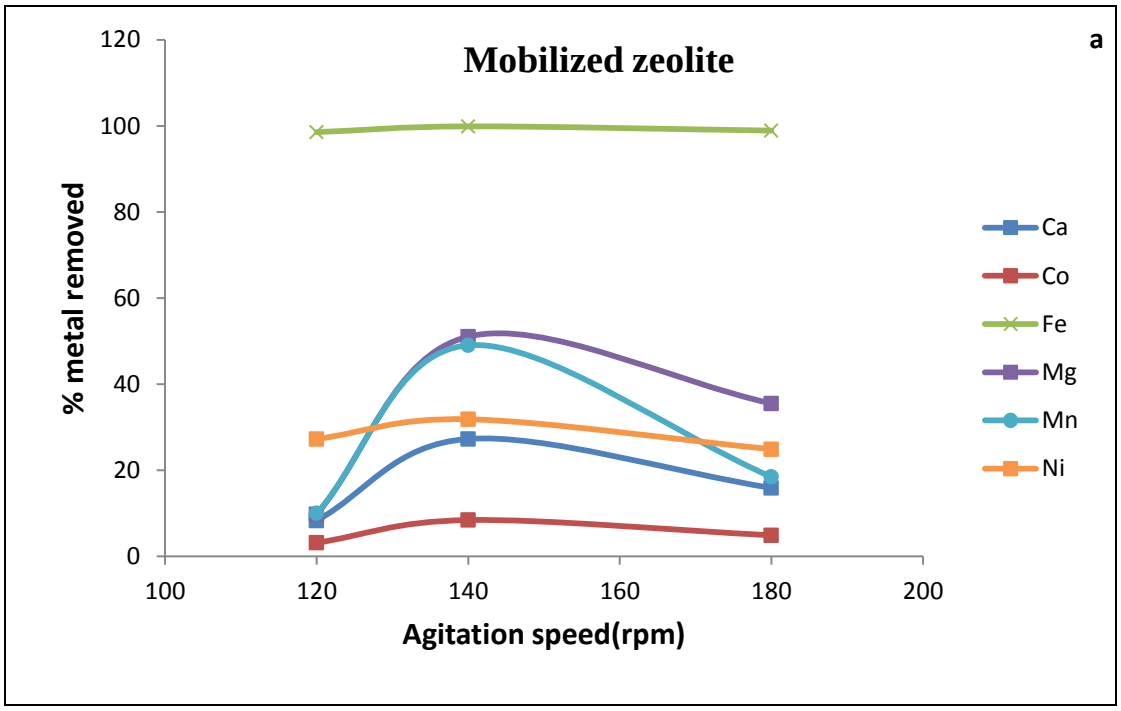
The results of the variation in metal uptake with time using cassava adsorbents were different as can be seen in Figures 4.9 (e) to (f). The results indicate that the quantity of most heavy metal ions removed generally decreased as the temperature increased from 30 ˚C to 50 ˚C. The highest metal removed was observed at 30 ˚C for all three cassava peel adsorbents. This decrease could be attributed to the destruction of active sites in the biomass at higher temperatures. These results confirm the findings of other work where adsorption has been reported to be exothermic, indicating that biosorption capacity increases with a decrease in temperature (Kapoor and Viraraghavan, 1997). Seepe (2015) also reported a decrease in the uptake of Co^{2+}, Cr^{3+} and V^{3+} metal as the temperature increased from 40 to 50 °C. However, Kosasih et al. (2011) reported an endothermic uptake of copper metal with an increase in temperature from 30 to 60 °C using cassava peel biomass. The differences in the results of Kosasih et al. (2011) with those observed in the present study, could be attributed to the combined effect of the acidic nature of AMD solutions and high temperature which may have negatively affected the active sites of the biomass.

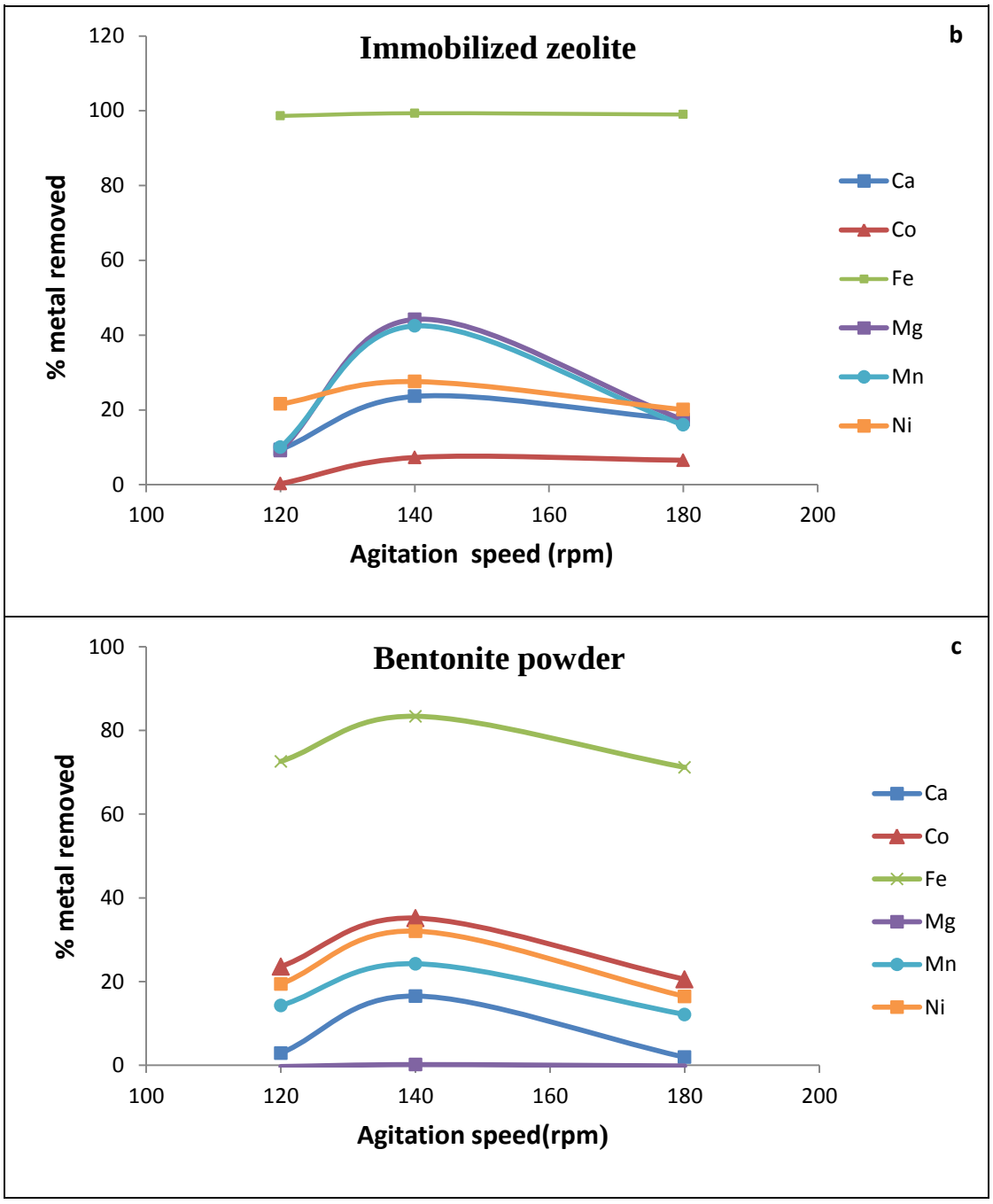
Effect of agitation speed

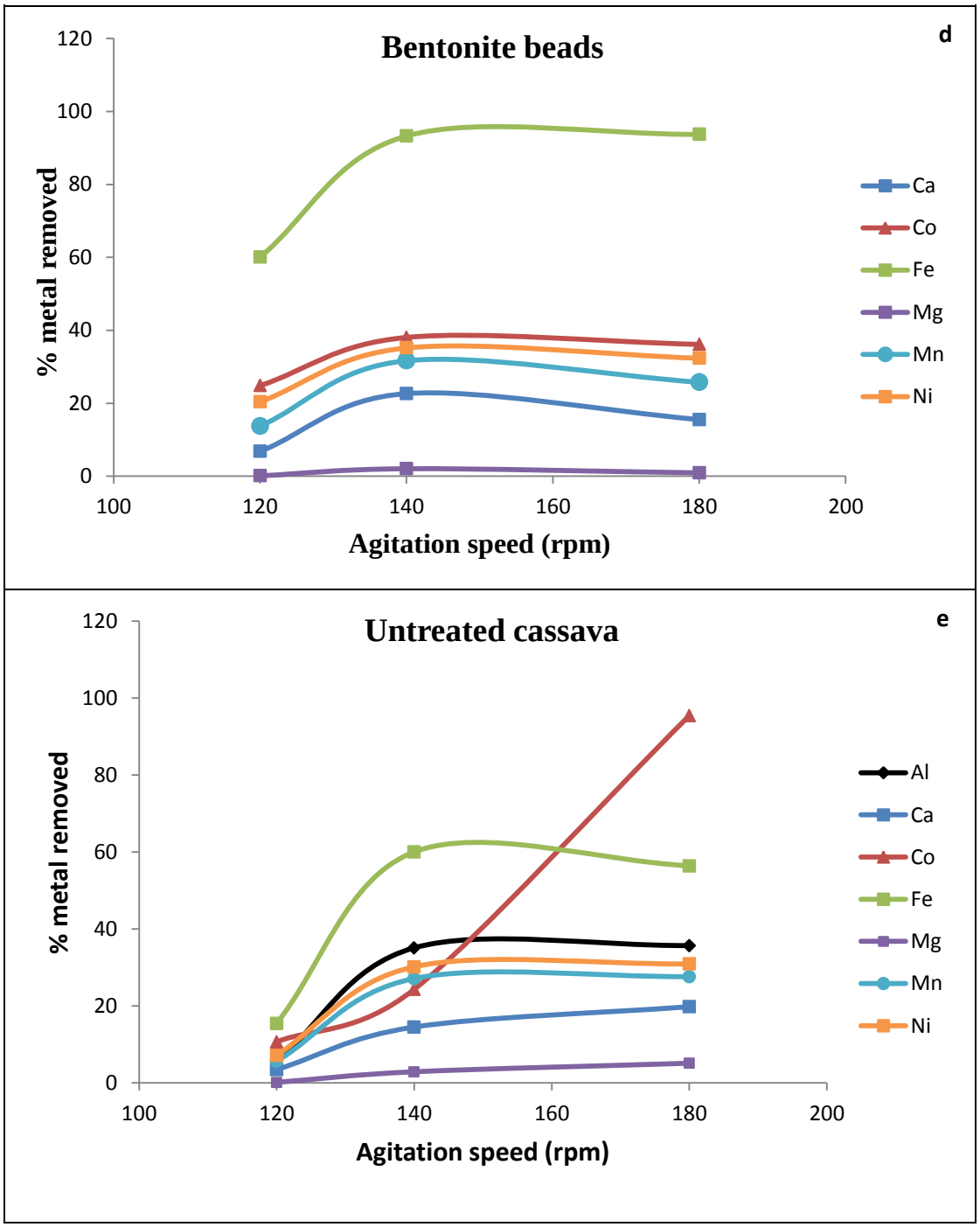
The rate of agitation plays an influential role in the formation of the external boundary film and its optimization is crucial in order to minimize the mass transfer resistance. At higher agitation speeds, the mass transfer rate of the solute from the bulk solution to the liquid boundary layer is increased owing to the enhanced turbulence and decrease in boundary layer thickness (Shen and Duvnjak, 2005). In addition to the decrease in boundary layer thickness, agitation also results in the abrasion of adsorbent grains, producing freshly broken and highly reactive locations on the surface. Hence, this mechanical effect increases the number of possible adsorption locations, which in turn increases the rate of adsorption (Trgo and Peric,

2003). However, the production of fine adsorbent particles due to abrasion makes the separation of the solids from the liquid difficult (Inglezakis et al., 1999).

The effect of agitation speed in the present study was investigated by mixing 5g of each adsorbent with 500 mL of AMD solution. The mixture was shaken between 120 rpm and 180 rpm. The agitation speeds were chosen based on previous studies available in literature (Motsi, 2010; Nsimba, 2010; Ndlovu et al., 2012; Seepe, 2015). The zeolite and cassava peel mixtures were agitated for 1 hr and bentonite mixture for 24 hrs. Solution samples were collected at the end of the contact time and analysed for metal ion content. Figure 4.10 shows the variation in metal adsorption efficiency with agitation speed.




b
Immobilized zeolite
% metal removed
120
100
80
60
40
20
0
100
120
140
160
180
200
Agitation speed (rpm)
Ca
Co
Fe
Mg
Mn
Ni
c
Bentonite powder
% metal removed
100
80
60
40
20
0
100
120
140
160
180
200
Agitation speed(rpm)
Ca
Co
Fe
Mg
Mn
Ni


d
Bentonite beads
% metal removed
Agitation speed (rpm)
Ca
Co
Fe
Mg
Mn
Ni
e
Untreated cassava
% metal removed
Agitation speed (rpm)
Al
Ca
Co
Fe
Mg
Mn
Ni

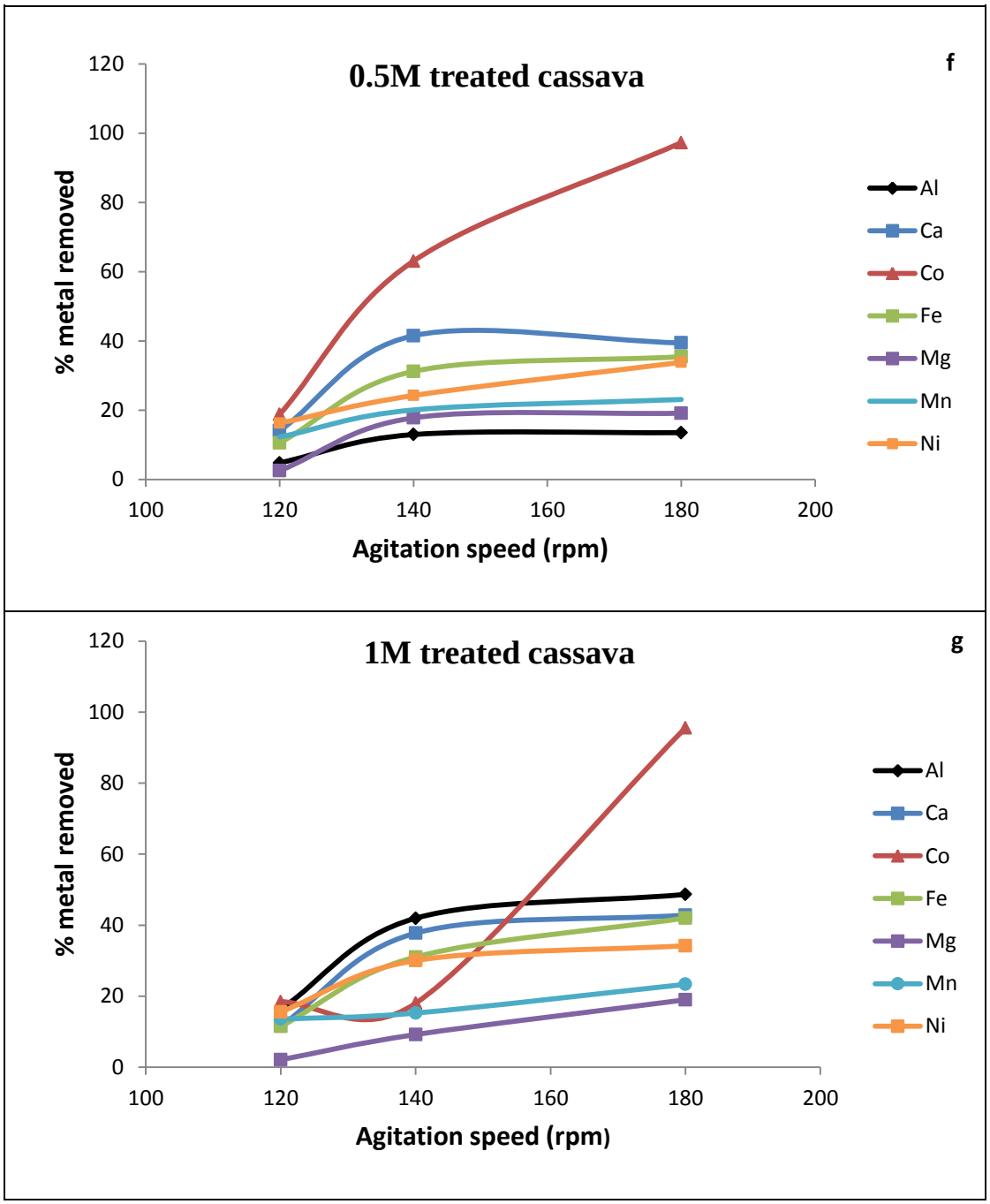
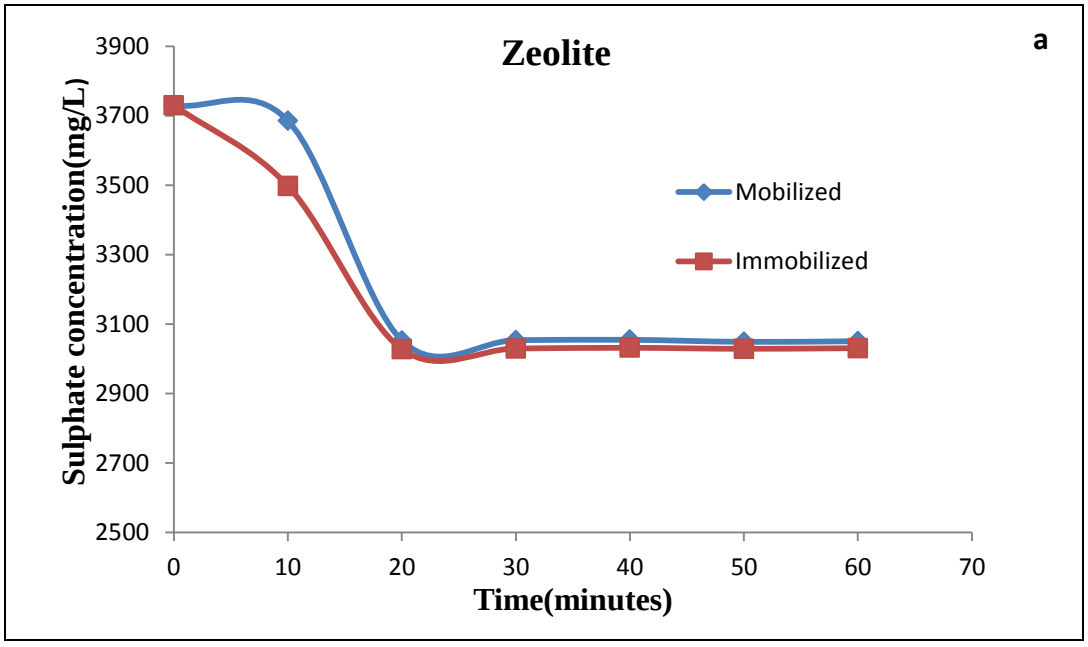


Figure 4.10: Effect of agitation speed on metal ion adsorption using (a) mobilized and, (b) immobilized zeolite beads (c) bentonite powder and, (d) beads (e) Untreated, (f) 0.5M treated and (g) 1M treated cassava peel [Adsorbent dosage: 5g ; Temperature = 30˚C, Contact time = 1h for zeolite and cassava peel; 24 hrs. for bentonite].

The results indicate that the quantity of metal ions removed generally increased as the agitation speed increased from 120 rpm to 140 rpm for all the adsorbents. This is because high agitation speeds generally maximize the mass transfer rate of the metal ions to the adsorbent surface, resulting in higher metal adsorption. For the zeolite and bentonite adsorbents (Figure 4.10 (a-d)), a decrease in metal uptake was noted as the speed increased from 140 rpm to 180 rpm. This is because severe turbulence results in the breakage of the bond formed between the metal ions and the adsorbent, resulting in desorption of the metal ions from the surface sites (Ndlovu et al., 2012). This observation also suggests that physical adsorption rather than chemical adsorption is taking place. For the cassava adsorbents (Figure 4.10 (e-g)), adsorption of most heavy metals increased and reached a maximum at 140 rpm, and remained constant as the speed increased to 180 rpm. These results can be attributed to the fact that the increase in agitation speed, improves diffusion of the metal ions towards the surface of the adsorbent. The same trend was also reported in the removal of Co^{2+}, Cr^{3+} and V^{3+} from a waste water solution using cassava waste (Seepe, 2015). This also suggests that an agitation speed in the range 120-140 rpm is sufficient to ensure that all the surface binding sites are made available for the metal adsorption. As the speed increased to 140 rpm, the adsorption process reaches a rate-limit over which there was no significant change. Hence, 140 rpm can said to be the optimum agitation speed for removal of the most heavy metals from a real AMD using cassava peel biomass. However, the Co isotherm trend suggests that an agitation speed of 180 rpm may be sufficient for its optimum removal from AMD. Therefore, to remove all the metals in the AMD solution a speed of 180 rpm is recommended.

4.2.2 Solution acidity and sulphate content

The AMD is characterized by low pH values. This implies high acidity which translates to high sulphate levels as already shown in Table 3.1. Therefore, the quantity of acid and sulphate ions in this effluent was also examined in the study, due to the toxicity of the components as well as need for recovery of the acid in the acid retardation process. Figure 4.11 shows the levels of sulphate ions in the effluent with time using the different adsorbents.



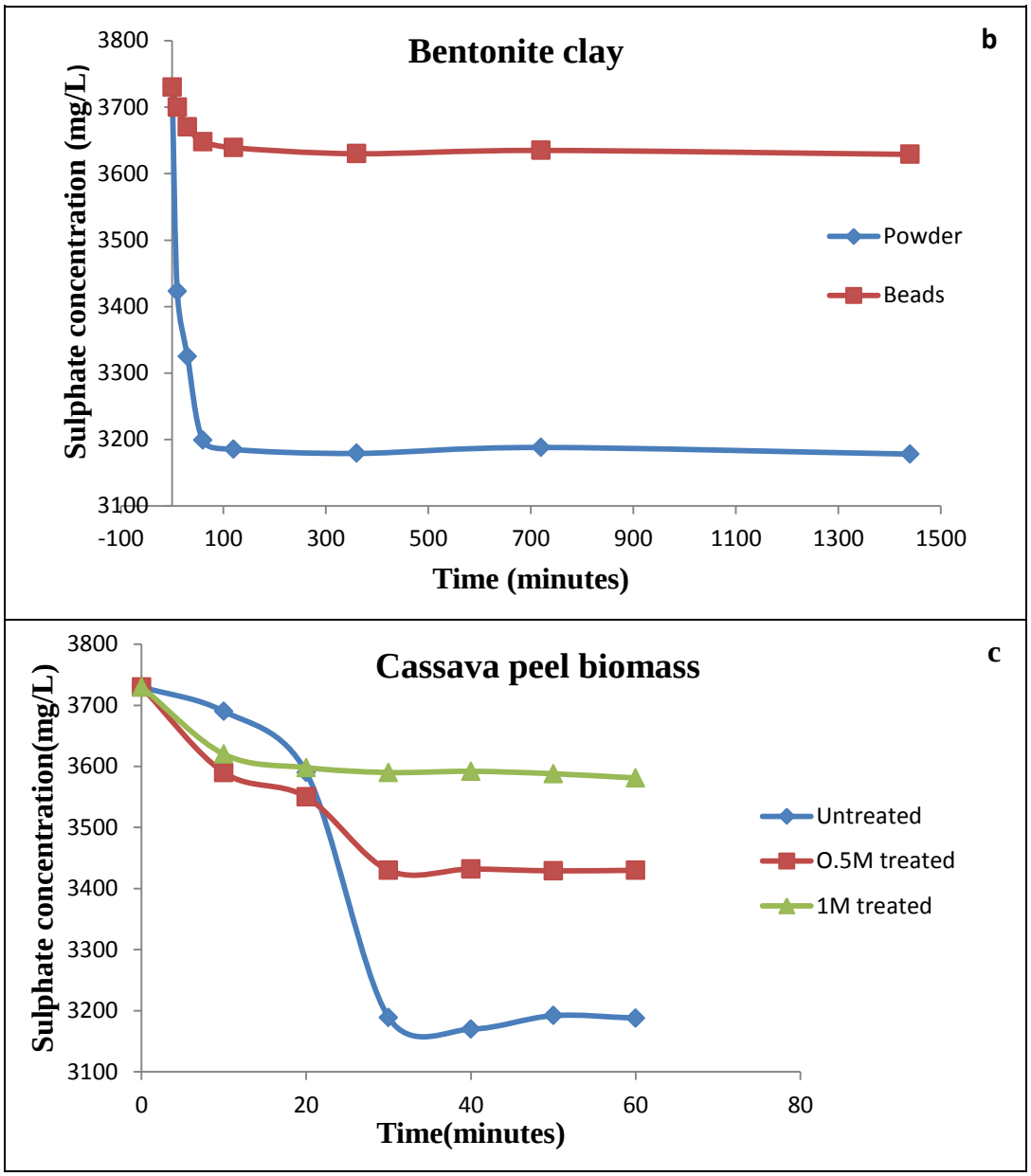


Figure 4.11: Sulphate ion trends in the effluent with time for (a) zeolite (b) bentonite clay (c) cassava peel biomass adsorbents [Adsorbent dosage: 5g, Agitation speed= 150rpm, Temperature = 30 ˚C, Contact time = 1h for zeolite and cassava peel; 24 hrs for bentonite].

The results indicate that the sulphate levels in the effluent decreased initially, and then remained virtually constant as the process approached equilibrium. The highest sulphate removal was obtained using the zeolite adsorbents; a decrease from 3780

mg/L to about 3200 mg/L at an equilibrium time of 20 minutes was noted. This translates to approximately 18.8% sulphate removal. Bentonite adsorbents had the second highest removal with approximately 14.8% of sulphate ions being removed by the bentonite powder at equilibrium. The sulphate removal from the crystalline adsorbents could be due to the interactions of the ion with the various surface active groups. Davis and Burgua (1995) reported that among the anion ligands, sulphate is believed to form inner-sphere complexes with surface sites in an adsorbent. These complexes are said to increase the net negative charge, which in turn also increases metal adsorption. However, the sulphate removal was slightly lower for the bentonite beads possibly due to the lower surface area available for adsorption compared to the powder.

The lowest sulphate removal was observed in the use of cassava adsorbents. The quantity of the sulphate ions removed followed the trend: Untreated cassava> 0.5M treated cassava> 1M treated cassava adsorbents. A decrease from approximately 14 to 4% removal when using untreated to 1M treated cassava peel adsorbents was noted. It is reported that ligands such amino, carboxyl, hydroxyl etc., provide the cell wall of a biomass with an overall negative charge (Gardea-Torresday et al., 1990; Gadd, 2009). It is therefore, expected that an increase in the quantity of the negative functional groups with acid treatment as already indicated by the FTIR analysis (Figure 4.2c) could have led to an increase in repulsions with the negatively charged sulphate ion resulting in its lower uptake.

However, despite the removal of some sulphate ions by the adsorbents, Figure 4.11 indicates that the sulphate levels were still substantially above the maximum discharge levels of 250mg/L and 500 mg/L recommended by the USEPA and DWAF, respectively. Hence, it can be concluded that the three adsorbents failed to reduce the sulphate levels to the permissible discharge levels.

In terms of acid content, the quantity of acid in the solution with time could not be determined due to the amount of sample being insufficient for the acid-base titration

analysis. However, analysis of the effect of temperature, adsorbent loading and agitation speed revealed that the acid remaining in solution followed the sequence: zeolite < bentonite < cassava peel biomass adsorbent. The zeolite and bentonite adsorbents gave the highest acid loss of approximately 90 to 96% from the solution. This is because these adsorbents contain CaO, Na_2O and MgO which are basic in nature, and hence, have a buffering effect on the acidic solution. The rapid rise in solution pH levels from 2.16 up to around 5 in the zeolite mixture suggests the buffering effect of these constituents. The cassava peel adsorbents gave the least acid removal. In fact, results suggested that the amount of acid in the solution increased with acid treatment. The acid content was increased by approximately 88% when the loading of 1M acid treated cassava was increased to 2%. The presence of additional acid in the solution may be due to the contribution of the thioglycollic acid used for pretreating the cassava biomass. Investigation of the other parameters on acid removal indicated that temperature and agitation speed had no significant effect on acid levels. The results indicated that the acid content remained virtually constant at different temperatures and agitation speeds. The acid removal in this study was highly undesirable, since the ultimate aim is for acidity to be recovered and converted into a saleable product. The financial benefits could be used to offset the treatment cost.

4.2.3 Selection of a low cost adsorbent

The main purpose of the batch studies was to screen three adsorbents (i.e., bentonite, zeolite and cassava peel biomass) with the objective of selecting the best adsorbent in terms of heavy metal removal and least acid loss in AMD. The factors affecting the metal removal such as agitation time, adsorbent dosage, temperature and agitation speed were investigated. The basis used in the evaluation included high metal removal, least acid loss from the solution and high structural stability of the adsorbent. The results indicated that low pH values are not favorable to natural clays and aluminosilicate minerals such as bentonite and zeolite adsorbent, respectively. As

already explained, low pH values cause dissolution and eventually the collapse of the structure of both crystalline adsorbents. The presence of additional aluminium ions in the effluent provided evidence of this dissolution, since it is known that these adsorbents contain substantial quantities of alumina in their structure. These two adsorbents are likely to perform well in solutions that are not acidic, where the primary objective is just the removal of the metals. However, in this study, they could not perform well without neutralizing the acid (i.e., increasing the pH). Neutralization results in the loss of solution acidity which could be otherwise recovered. Therefore, despite, some heavy metal removal, the two adsorbents did not perform satisfactory in real AMD solution treatment due to the instability of their structures in addition to the neutralization of acid.

According, to the results of the batch tests, cassava waste biomass performed better than the other two adsorbents. The results showed that the quantity of metals removed increased with acid treatment. This is because the acid treatment (thiolation) adds extra functional groups onto the cassava surface which enhance biosorption of the heavy metals. Amongst the factors affecting the removal by the cassava peel biomass, the dosage appeared to be the most influential. The results of the effect of adsorbent loading indicated that low cassava peel biomass loadings did not yield much significant metal uptake. However, as the loading was increased beyond 2%, the results showed that significant metal uptake was obtained. Over 90 % of most of the metals were removed at pH levels close to 3 using 1M acid treated cassava peel biomass. The results also showed that high adsorbent loading (> 2%) in combination with low temperature of 30 ˚C and agitation speed of 180 rpm produced the highest metal removal from AMD.

Generally, it can be seen that all the three low cost adsorbents have the potential to reduce the metal content in AMD to the required discharge levels. However, the instability of bentonite clay and zeolite in the acidic solutions as well as the acid loss due to neutralization of the solution eliminated the adsorbents for further test work. Consequently, cassava peel biomass was selected for subsequent adsorption tests.

4.3 Adsorption isotherms

Adsorption isotherm models can be regarded as a benchmark for evaluating the performance of an adsorbent. The analysis of the isotherms is important in order to develop an equation that accurately represents the experimental results and which could be used for design purpose (Ahmarruzzaman and Sharma, 2005). Amongst the known models, the Freundlich and Langmuir isotherms are the most commonly used in water and wastewater treatment. Therefore, batch equilibrium data for the cassava peel biomass was fitted into the linear forms of the isotherms to determine the adsorption capacity of the biomass for various heavy metals in AMD at 30 ˚C. The Langmuir sorption model was used to estimate the maximum theoretical metal uptake not reached in the experiments, and the Freundlich adsorption model estimated the adsorption intensity of metal ions onto the cassava waste biomass. The isotherm parameters for various metals in AMD are summarized in Table 4.6.

From the Langmuir isotherm, the adsorption affinity constant, b (L/mg), and the maximum adsorption capacity, q_{max} (mg/g) of Al^{3+}, Ca^{2+}, Co^{2+}, Fe^{3+}, Mg^{2+}, Mn^{2+} and Ni^{2+} forming a monolayer on the surface of the cassava peel biomass were estimated to be 0.001 L/mg, 0.366 L/mg, 13039 L/mg, 0.945 L/mg, 2.188 L/mg, 1.174 L/mg and 3089 L/mg, and 41.66 mg/g, 43.67 mg/g, 0.0348 mg/g, 17.98 mg/g, 8.51 mg/g, 4.484 mg/g and 0.077 mg/g, respectively. The small values of b *(*for Al^{3+}, Ca^{2+}, Fe^{3+}, Mg^{2+}, Mn^{2+}), which represent the affinity between the sorbent and sorbate, suggests a weaker binding between the ions and the biomass surface, indicating a physisorption process (Volesky, 2004). The higher values of b for Co^{2+} and Ni^{2+} suggest a stronger binding capacity between the adsorbent surface and the metals, thus indicating chemisorption of the metal ions at the surface of the cassava peel biomass. The higher affinity of the cassava peel for Co^{2+} and Ni^{2+} concurs well with the findings of other related studies (Kurniawan et al., 2010; Seepe, 2015).

Table 4.6: Linear Langmuir and Freundlich isotherm parameters for the adsorption of heavy metals from AMD by cassava peel biomass.

	Langmuir isotherm $1/q_e=(1/q_{max}.b).1/C_e+ 1/q_{max}x$				**Freundlich isotherm** $\log q_e= \log K_F +1/n \log C_e$		
Metal ion	q_{max}(mg/g)	R_L x10^{-4}	b (L/mg)	R^2	K_F(mg/g)	n	R^2
Al	41.66	3600	0.001	0.8000	0.21	4.71	0.2500
Ca	43.67	12.6	0.366	0.7368	23.46	8.51	0.4999
Co	0.0348	1.75	13039	0.8024	0.041	14.24	0.5537
Fe	17.98	21.3	0.945	0.6566	10.85	8.78	0.5245
Mg	8.51	24	2.188	0.8481	6.21	12.30	0.5245
Mn	4.484	80.5	1.174	0.9217	1.99	3.949	0.8478
Ni	0.077	8.63	3089	0.7703	0.722	2.53	0.3578

The Freundlich adsorption coefficient, K_F (mg/g) and intensity n for Al^{3+}, Ca^{2+}, Co^{2+}, Fe^{3+}, Mg^{2+}, Mn^{2+} and Ni^{2+} were estimated to be 0.21 mg/g, 23.46 mg/g, 0.041 mg/g, 10.85 mg/g, 10.85 mg/g, 1.99 mg/g and 0.722 mg/g, and 4.71, 8.51, 14.24, 8.78, 12.3, 3.949 and 2.53, respectively. The values of n (which are all greater than 1) show surface heterogeneity and favorable adsorption of heavy metals onto the surface of the cassava peel biomass. However, the experimental data generally fitted better into the Langmuir isotherm as indicated by the higher correlation coefficients of most metals compared to those obtained using the Freundlich isotherm.

Although the value of R^2 is a measure of how close the model fits the data, it cannot be used to judge model lack of fit because it does not take into account the number of degrees of freedom for model determination (Simate, 2012). In fact, a large value of R^2 does not necessarily mean that the model is a good one since addition of a variable

to the model will always increase R^2 regardless of whether the additional variable is statistically significant or not. Thus, it is possible for models that have large values of R^2 to yield poor predictions of new observations or estimates of the new response (Simate, 2012). Therefore, in addition to using R^2 values, the models were also evaluated for lack of fit using the error function (F_{error}) calculated using Equation 4.1. The error function measures the difference in the amount of adsorbate taken up by the adsorbent using the models to the actual uptake measured experimentally (Arenas et al., 2007; Simate, 2012).

$$F_{error} = \sqrt{\frac{\sum_i^p \left(\left(q_{i\ model} - q_{i\ experimental} \right) / q_{i\ experimental} \right)^2 \right)}{p}} \quad (4.1)$$

Where $q_{i\ model}$ is the amount of adsorbate predicted by the fitted model and $q_{i\ experimental}$ is the amount measured experimentally, and p is the number of experiments performed. A summary of the error functions for the different metals in AMD using the Langmuir and Freundlich models is presented in Table 4.7.

Table 4.7: Langmuir and Freundlich isotherm error function values of different metals

Metal ion	Langmuir	Freundlich
Al	0.71	1.49
Ca	0.18	9.46
Co	0.01	0.01
Fe	0.17	3.74
Mg	0.16	1.44
Mn	0.17	0.73
Ni	0.99	12.63

From Table 4.6, it can be seen that the error function values for the various heavy metals using the Langmuir isotherm model (all less than 1) are significantly lower than those obtained using the Freundlich model. The lower values indicate a better fit of the model to the experimental data, which confirm the results already shown using the correlation coefficient (R^2). In addition, the Langmuir model is widely used in representing biosorption of heavy metals (Gadd, 2009).

4.4 Column adsorption studies

4.4.1 Introduction

Although, batch studies give information on the ability of an adsorbent to remove heavy metals, they are neither economical in practice nor the data obtained adequate to give accurate scale up information required in the design of industrial adsorption columns (Motsi, 2009). Therefore, column adsorption studies have to be undertaken to obtain some information through the breakthrough curve, which determines the operating life span of a fixed adsorbent bed. For the successful operation of biosorption in the column mode, immobilization of the biomass is conducted to increase the adsorbent's mechanical strength, density, reusability and resistance to mechanical environments (Goksungur et al., 2003). In addition, literature also reports that immobilizing cassava peel biomass significantly improves heavy metal uptake (Simate and Ndlovu, 2014; Seepe, 2015). Therefore, immobilization of the cassava biomass using sodium alginate binder was also carried out in this study. Sodium alginate binder was chosen as it is non-toxic, and cheaply and abundantly available.

4.4.2 Surface chemistry structure of immobilized cassava waste biomass

As already discussed, cassava waste biomass consists of functional groups which are able to attract and sequester heavy metals. In addition, acid treatment with 1M

thioglycollic acid increased the quantity of these groups through the introduction of the thiol groups as already shown in Figure 4.2. Therefore, FTIR analysis was also conducted in the range 500 to 4000cm^{-1} in order to examine any changes in the quantity and type of functional groups after loading metal ions onto the immobilized cassava waste biomass. Figure 4.12 compares the FTIR spectra of the immobilized cassava peel biomass before and after metal loading.

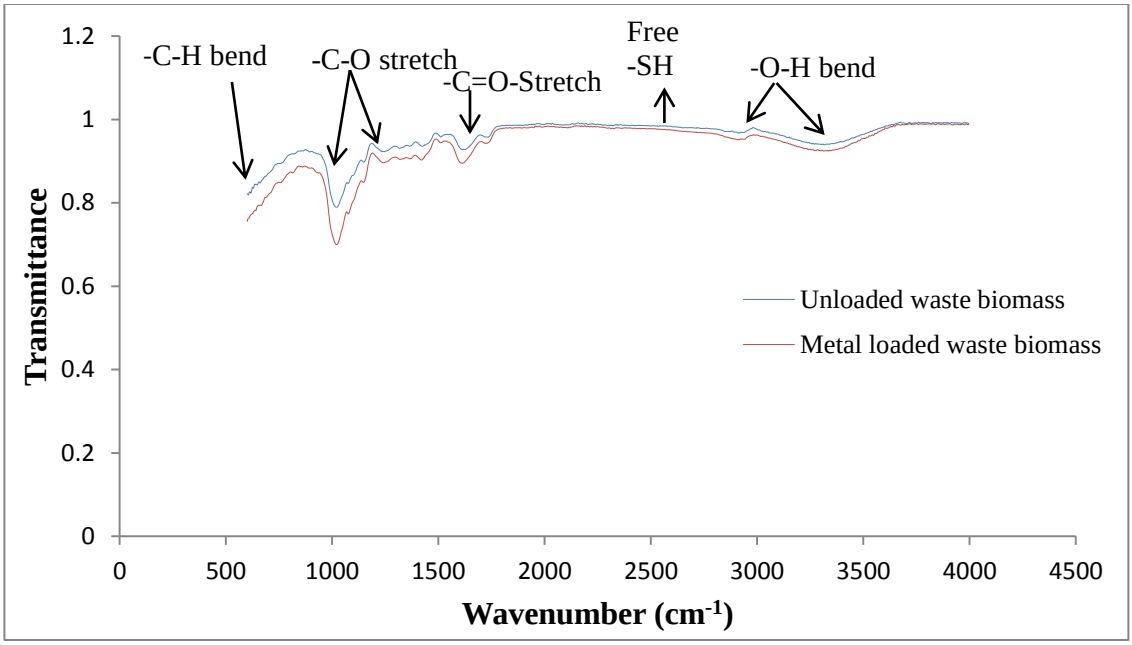


Figure 4.12: FTIR spectra of cassava peel biomass beads before and after metal loading

Comparing the two patterns in Figure 4.12, it can be seen that both patterns are closely similar, and this indicates the presence of identical functional groups in both unloaded and metal loaded waste biomass. However, a closer look at the patterns also reveals a slight shift as well as a decrease in the vibration of the peaks after metal adsorption. The peaks that were expected to be at 648, 979, 1168, 1473, 1656, 2962 and 3340 cm^{-1} had shifted to 644, 1026, 1155, 1427, 1606, 2937 and 3328 cm^{-1} owing to the adsorption of heavy metals such as Co^{2+}, Fe^{3+}, Mn^{2+} and Ni^{2+} from AMD. The decrease in the vibration of the OH bends seen at 2962 and 3340cm^{-1} could be

attributed to the interaction of metal ions with the functional groups on the surface of the biomass through a hydrogen bond (Kalayci et al., 2013). The changes observed in the other peaks indicate possible interactions of particular functional groups with the heavy metals found in AMD.

The surface morphology of the immobilized cassava before and after metal loading was also studied (Figure 4.3 (g) and Figure 4.4 (g)). As previously discussed in section 4.1.6 the biomass surface became slightly rougher after metal adsorption possible due the interaction of the acidic solution with the various ligands on the biomass surface.

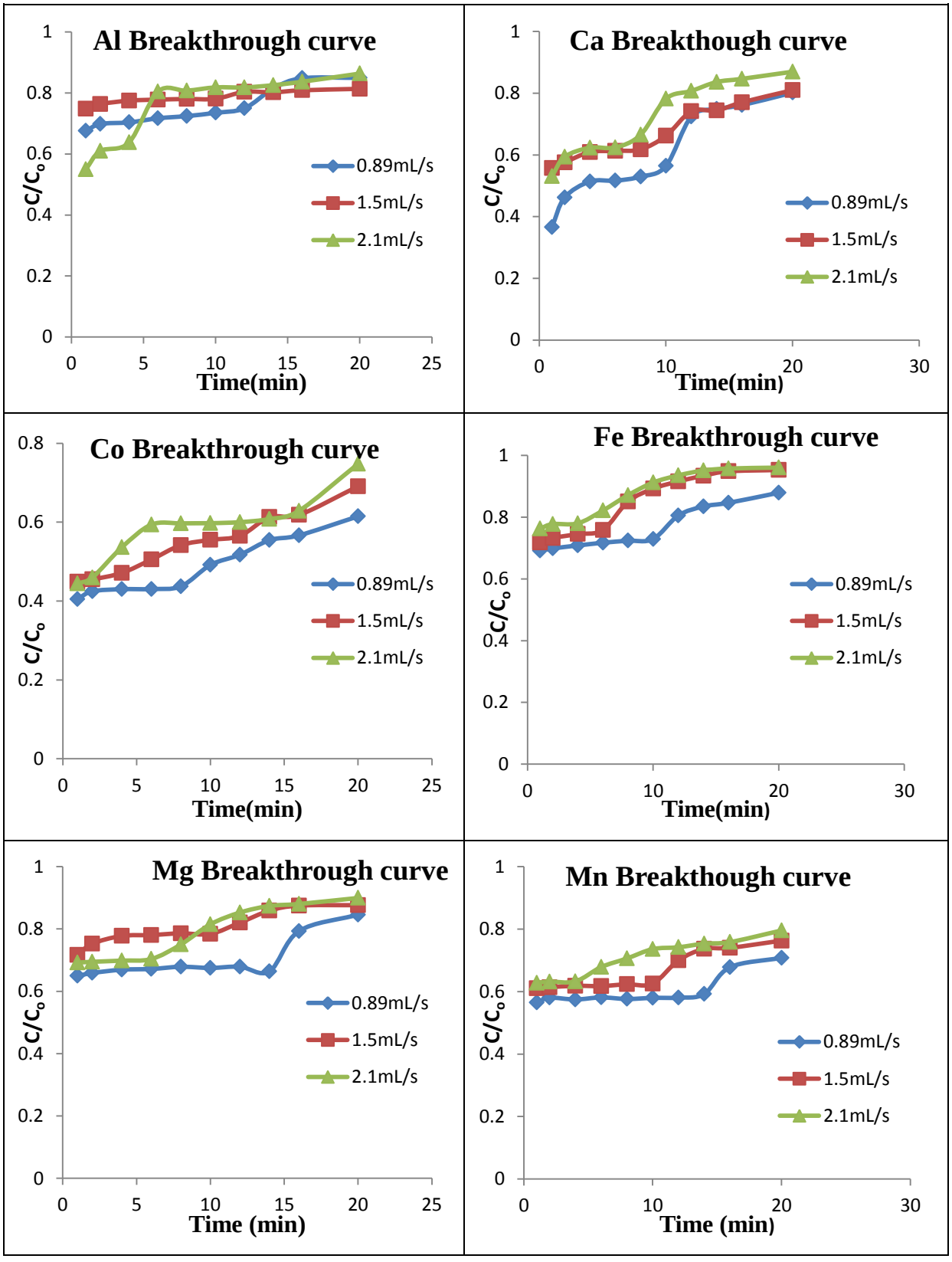
4.4.3 Fixed bed adsorption studies

To investigate the biosorption of heavy metals from the AMD solution in the column mode, continuous flow adsorption studies were conducted in an acrylic tube column. Cassava biomass beads were loaded into the fixed bed system. Glass beads and cotton wool were placed at the top and bottom of the bed to prevent loss of the adsorbent during operation. During the tests, the AMD solution was pumped in an up flow mode using a peristaltic pump (Heidolph pump drive 5001) to ensure total coverage of the adsorbent by the solution and prevent the formation of channels during column operation (Harland, 1994). The effects of parameters affecting the behaviour of breakthrough curves such as flow rate and adsorbent bed height, etc., were investigated in these column studies. The experimental data obtained was then fitted into models commonly used for evaluating column kinetics in waste water treatment namely Thomas and Adams-Bohart models. The results of the work are presented in detail in the following sub-sections.

Effect of flow rate

The effect of flow rate on the biosorption of heavy metals from AMD was investigated by varying the feed flow rate between 0.89 and 2.1 mL/s with constant adsorbent bed height of 30 cm. The values for the adsorbent size, bed height and flow rates used in this investigation were obtained from available literature (Goksungur et al., 2003; Seepe, 2015). The residence time was based on information obtained from preliminary column studies. Although, batch studies, revealed that equilibrium was attained in times ranging from 30 to 60 minutes, preliminary column adsorption studies indicated that the breakthrough of most metals in AMD was reached in less than 20 minutes contact time. Therefore, the present test work was run for 20 minutes and the solution samples were collected at various time intervals. The breakthrough curves were constructed using C/C_o (where C is the effluent concentration at time t and C_o is the initial concentration of the influent stream) versus time as shown in Figure 4.13.

It can be seen from Figure 4.13 that most of the curves do not follow the shape of an ideal breakthrough curve, which is an S-shape as described by Oliveira et al. (2011). This could be because a real industrial AMD solution was used for the column tests. Therefore, the presence of competing cations, anions and possibly organics etc., in the solution could have resulted in the abnormal breakthrough curves such as those shown in Figure 4.13. In the ideal S-shaped breakthrough curve, the breakthrough time is arbitrarily inferred for C/C_o at 0.05; while the saturation time is defined ideally when C/C_o values reach 1.0 (generally at 0.90-0.95). However, due to the complex nature of the AMD solution used in this study, breakthrough was considered to have taken place when there was a sharp increase in the effluent concentration. In addition, the shapes of the curves obtained at different flow rates as well as the C/C_o values indicate that saturation of the adsorbent was almost reached for most metal ions.


Al Breakthrough curve
C/Co
Time(min)
0.89mL/s
1.5mL/s
2.1mL/s
Ca Breakthough curve
C/Co
Time(min)
0.89mL/s
1.5mL/s
2.1mL/s
Co Breakthrough curve
C/Co
Time(min)
0.89mL/s
1.5mL/s
2.1mL/s
Fe Breakthrough curve
C/Co
Time(min)
0.89mL/s
1.5mL/s
2.1mL/s
Mg Breakthrough curve
C/Co
Time (min)
0.89mL/s
1.5mL/s
2.1mL/s
Mn Breakthough curve
C/Co
Time (min)
0.89mL/s
1.5mL/s
2.1mL/s

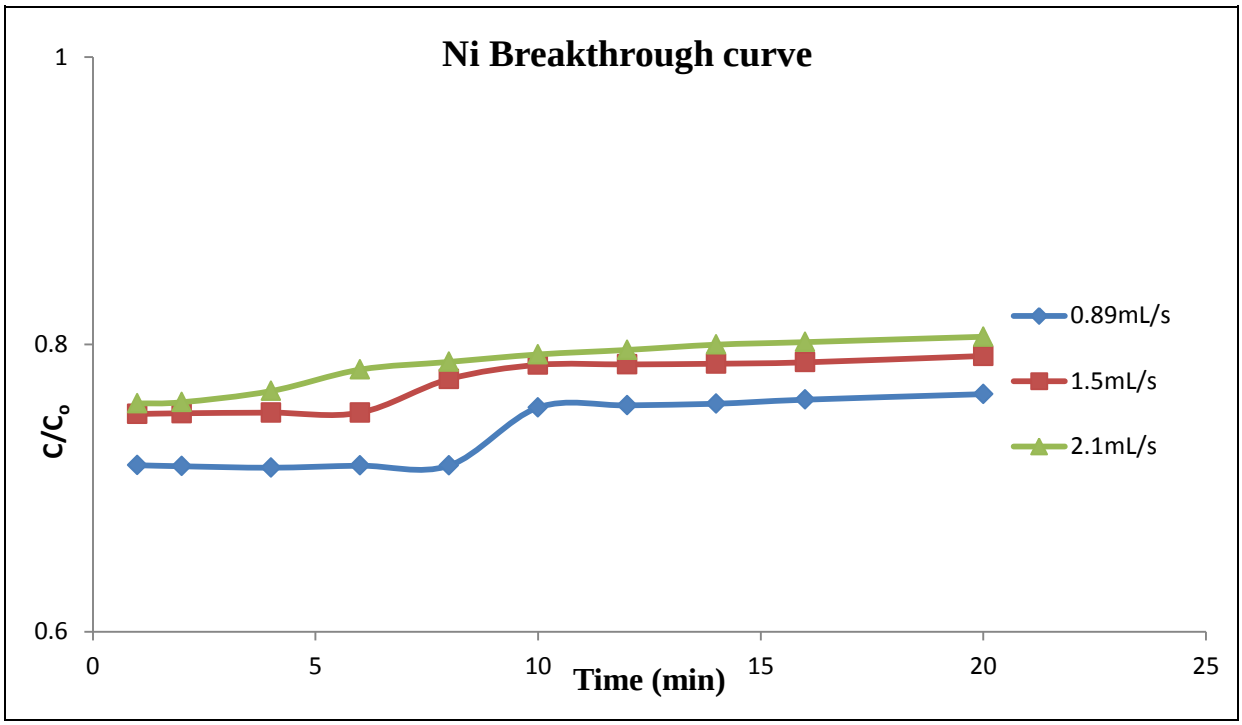


Figure 4.13: Breakthrough curves for heavy metals in AMD at different flow rates (Adsorbent size= 3mm, Bed height =30cm, Temp. = 25˚C).

From Figure 4.13, it can also be seen that metal uptake by the immobilized cassava waste biomass was favoured at the lowest flow rate of 0.89 mL/s used in this study. This was attributed to sufficient contact time (between the metal ions and the biomass surface), which allows metal ions to diffuse through the pores of the adsorbent and attain equilibrium. Furthermore, it can be seen that breakthrough as well as saturation occurred faster as the flow rate was increased from 0.89 mL/s to 2.1 mL/s. For instance, the breakthrough times decreased from 12 min to 4 min for Al^{3+}, 10 to 6 min for Ca^{2+}, 10 to 8 min for Co^{2+}, 10 to 4 min for Fe^{3+}, 14 to 6 min Mg^{2+}, 14 to 4 min for Mn^{2+} and 8 to 2 min for Ni^{2+} when the flow rate was increased from 0.89 mL/s to 2.1 mL/s. In addition, as the flow rate increased, the metal concentration in the effluent increased rapidly resulting in steeper breakthrough curves. This may be due to the residence time of the solution being inadequate for adsorption equilibrium to be attained at faster flow rates implying that the metal ions leave the column before reaching equilibrium (Chowdhury et al., 2013). Therefore, the contact time of heavy

metal ions with the cassava biomass beads is shorter at higher flow rate, which causes a reduction in the metal removal efficiency. Seepe (2015) also observed that the removal of Co^{2+}, Cr^{3+} and V^{3+} from a synthetic solution using cassava pellets decreased at higher flow rate due to insufficient residence time as well as the diffusion limitations of the solute into the pores of the sorbent at higher flow rates (Vijayaraghavan et al., 2005). These results are also consistent with those obtained in other related work (Goksungur et al., 2003; Abdel-Razek, 2011; Chowdhury et al., 2013; Anisuzzaman et al., 2014). Table 4.8 summarizes the parameters of the breakthrough curves for the various metals in the AMD solution.

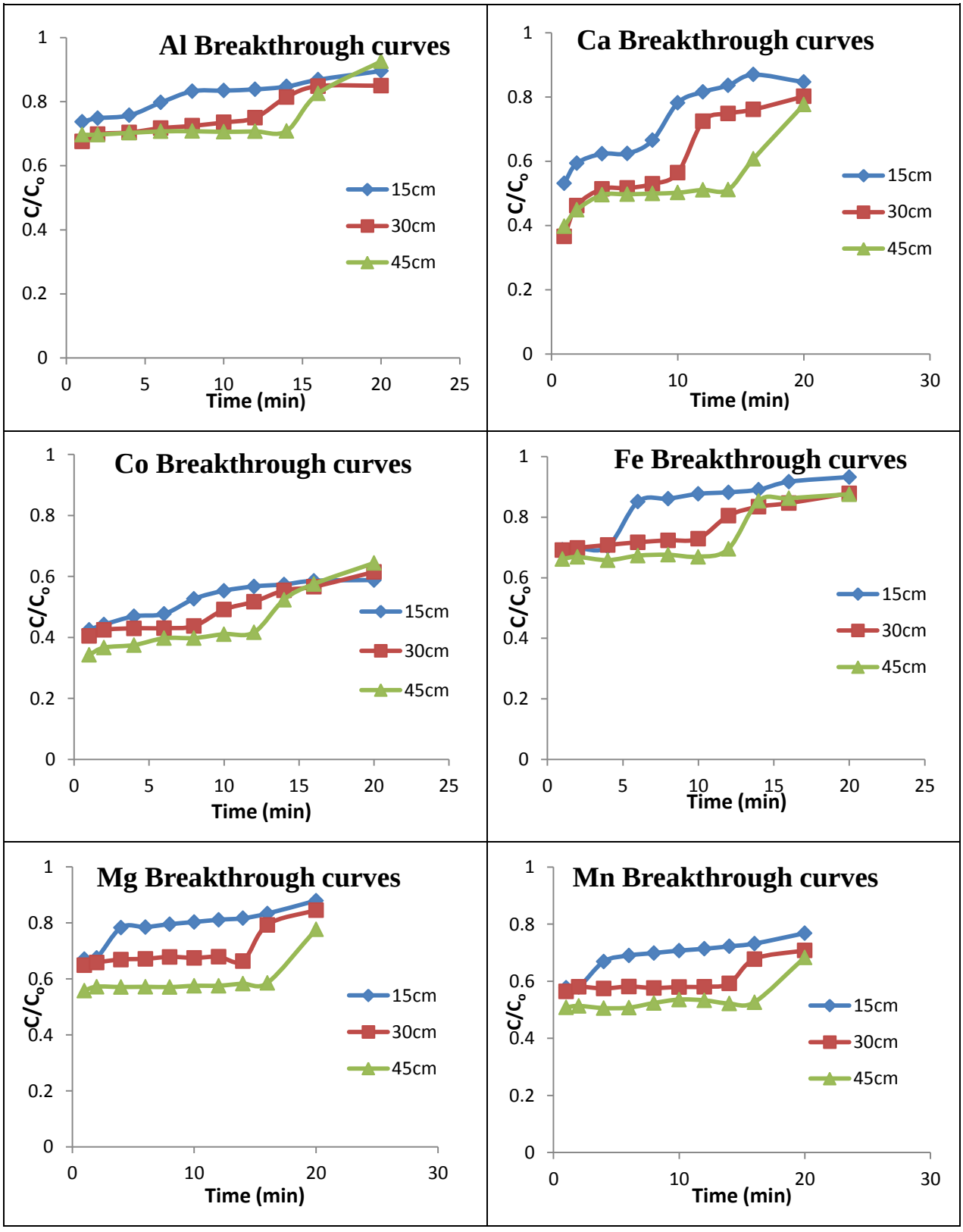
Table 4.8: Parameters of the breakthrough curves for metals in AMD at different flow rates (Adsorbent size= 3mm, Bed height =30cm, Temp. = 25˚C).

Metal ion	Flow rate(mL/s)	Breakthrough time(min)	Concentration at breakthrough(mg/L)	Required maximum discharge concentration(mg/L)
Al	0.89	12	0.18	0.03
	1.5	10	0.21	
	2.1	4	0.22	
Ca	0.89	10	272	n/a
	1.5	8	301	
	2.1	6	496	
Co	0.89	8	0.17	0.04
	1.5	4	0.19	
	2.1	3	0.20	
Fe	0.89	10	139	0-10
	1.5	6	145	
	2.1	4	151	
Mg	0.89	14	89	n/a
	1.5	10	109	
	2.1	6	95	
Mn	0.89	14	27	0-10
	1.5	10	28	
	2.1	4	29	
Ni	0.89	8	0.31	0.15
	1.5	6	0.32	
	2.1	2	0.33	

Besides, showing the concentration of metal ions at breakthrough, Table 4.8 also compares the concentration of various metals at breakthrough time with the recommended maximum discharge levels. The results indicate that despite a decrease in the quantity of metal at breakthrough with reduction in flow rate, the metal content in the effluent still remained significantly above the recommended maximum discharge levels. This may be attributed to the competitive nature of mixed ion solutions, such as the AMD used in this study. Ions with smaller diameters such as Co^{2+} and Ni^{2+} had the highest adsorption efficiency while larger ions such as Fe^{3+} and Mg^{2+} had the least adsorption owing to their lesser affinity to the reactive sites of the sulfhydryl and other ligands in the treated biomass. This order of adsorption concurs well with the results of the batch tests which indicated that the cassava waste surface had higher affinity for Co^{2+} and Ni^{2+} ions. This trend in ionic size dependency was also reported in other work involving the use cassava waste biomass (Horsfall et al., 2003; Seepe, 2015). As a result of the favourable adsorption of metals at the lowest flow rate, subsequent tests were run at 0.89 mL/s.

Effect of bed height

As already discussed, the quantity of the adsorbent affects the extent of biosorption. An increase in the biomass quantity generally increases the quantity of metal ions taken up by the adsorbent (Gadd, 2009). In this work, the effect of adsorbent bed height on metal adsorption from AMD was investigated by varying the bed height between 15 and 45 cm. These values were obtained from literature (Goksungur et al., 2003; Seepe, 2015). The AMD solution was pumped in an up flow mode at a constant flow rate of 0.89 mL/s. Due to the complex nature of the AMD solution, breakthrough was assumed to have occurred when there was a sharp increase in the effluent concentration. Figure 4.14 shows the breakthrough curves for the heavy metals in AMD at different adsorbent bed heights.


Al Breakthrough curves
Ca Breakthrough curves
Co Breakthrough curves
Fe Breakthrough curves
Mg Breakthrough curves
Mn Breakthrough curves
C/Co
Time (min)
15cm
30cm
45cm

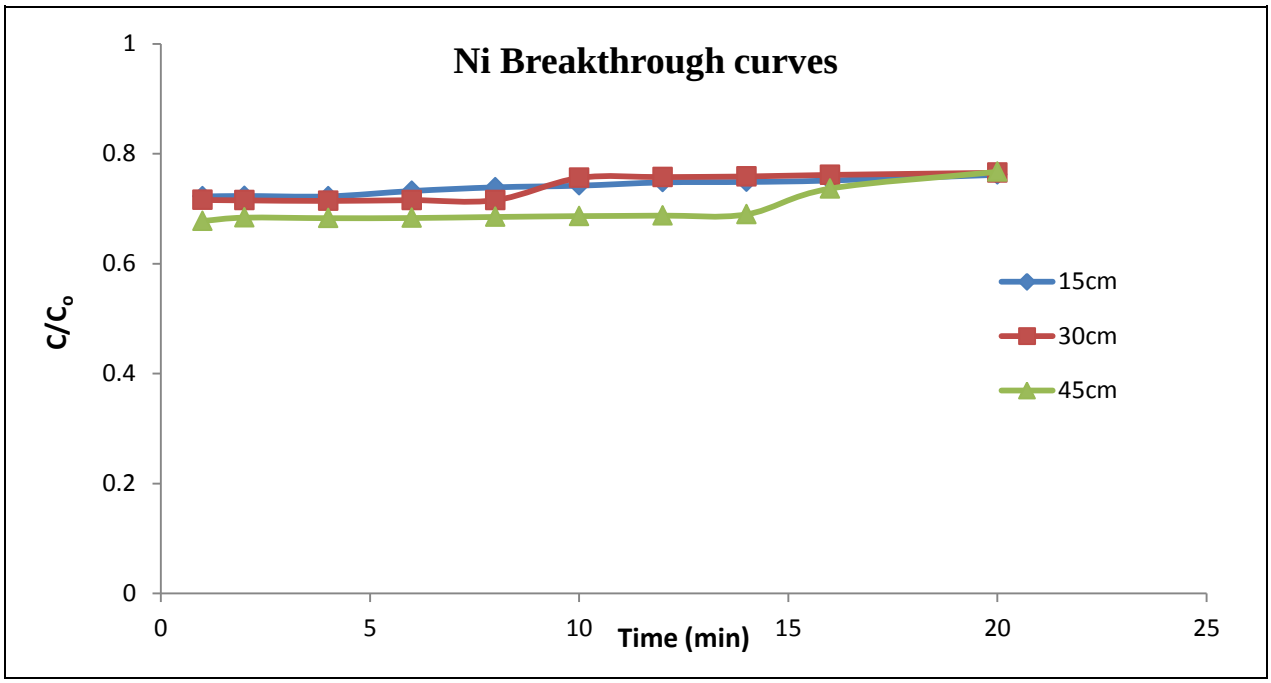


Figure 4.14: Breakthrough curves for heavy metals in AMD at different adsorbent bed height (Adsorbent size= 3 mm, Flow rate =0.89 mL/s, Temp. = 25˚C).

As can be seen from the plots of the breakthrough curves, the breakthrough and saturation times (for most metals) increased when the bed height was increased from 15 to 45 cm. For example, the breakthrough times were found to increase from 4 to 14 min for Al^{3+}, 6 to 14 min for Ca^{2+}, 6 to 12 min for Co^{2+}, 4 to 12 min for Fe^{3+}, 2 to 16 min for Mg^{2+}, 2 to 16 min for Mn^{2+} and 4 to 14 min for Ni^{2+} with an increase in bed height from 15 to 45 cm. The increase in metal adsorption with bed height may be attributed to the increase in the surface area and, therefore, active sites resulting from the increase in the amount of adsorbent in the bed. Furthermore, the increase in bed height increases the mass transfer zone (Goksungur et al., 2003; Chowhurry et al., 2013). The mass transfer zone in a column moves from the entrance of the bed and proceeds towards its exit. Hence, an increase in bed height would create a longer distance for the mass transfer zone to reach the exit (Chowhurry et al., 2013), and this leads to extended breakthrough and saturation times, which are observed in Figure 4.14. Similar trends were also reported in the use of other biomaterials for metal ion

adsorption (Goksungur et al., 2003; Taty-Costodes et al., 2005; Chowdhury et al., 2013; Anisuzzaman et al., 2014; Seepe, 2015).

Table 4.9 summarizes the parameters of the breakthrough curves of the various metals in AMD at different bed heights. Apart from the increase in breakthrough time, Table 4.8 also shows that the concentration of metals in the effluent at breakthrough decreased with bed height. However, it can also be seen that the concentrations of various heavy metals in the effluent are still substantially above the recommended maximum discharge levels even at the largest bed height. This may be a result of the complex nature associated with the constituents of the real AMD solution used in the study. In previous studies, single metal solutions and sometimes simulated mixed ion solutions were used (Goksungur et al., 2003; Taty-Costodes et al., 2005; Chowdhury et al., 2013; Seepe, 2015), therefore it can be expected that the values of metal adsorption efficiency would be lower in an actual solution due to the combined effect of competing cations and anions associated with actual AMD solutions.

Table 4.9: Breakthrough times for metals in AMD effluent at different bed height (Adsorbent size= 3 mm, Flow rate =0.89 mL/s, Temp. = 25˚C).

Metal ion	Bed height(cm)	Breakthrough time, t_b(minutes)	Concentration at breakthrough (mg/L)	Required maximum discharge concentration(mg/L)
Al	15	4	0.21	0.03
	30	12	0.20	
	45	14	0.19	
Ca	15	6	303	n/a
	30	10	274	
	45	14	248	
Co	15	6	0.19	0.04
	30	8	0.17	
	45	12	0.16	
Fe	15	4	141	0-10
	30	8	139	
	45	12	134	
Mg	15	2	91	n/a
	30	14	90	
	45	16	78	
Mn	15	2	30	0-10
	30	14	26	
	45	16	24	
Ni	15	6	0.31	0.15
	30	8	0.30	
	45	14	0.29	

Despite the use of the minimum flow rate and maximum bed height as reported in other related studies (Seepe, 2015), the results indicated that the metal ion

concentration in the effluent was still above the maximum recommended discharge levels. It can also be seen from Figure 4.11 and 4.12 that the adsorbent was saturated with most metal ions Therefore, this observation may suggest that additional quantities of the adsorbent are required for the metal ions in AMD to be reduced to permissible levels. However, increasing the bed height beyond 45cm could reduce the length of the effective mass transfer zone and also increase the pressure drop (Sheedy and Parujen, 2012). Thus, in a longer column most of the adsorbent is inactive, which reduces metal ion uptake.

In order to investigate any improvements in the metal adsorption in the column mode, an option of connecting a second column in series with the first column was explored. This is believed to increase the quantity of the adsorbent, while keeping the pressure drop at reasonable values. Furthermore, it is also known that reducing the size of the adsorbents increases the surface area of the exposed active sites, which in turn increases adsorption. Hence, the effect of the size of adsorbents on metal uptake in the column mode was also investigated by the reducing the size of the adsorbent from 3 mm to approximately 1.5 mm.

Effect of adsorbent size and additional column

To investigate the effect of size of immobilized adsorbents on adsorption of heavy metals from AMD, the column was loaded up to 45 cm with beads of approximately 1.5 mm in diameter. The AMD solution was pumped in an up flow mode at 0.89 mL/s. Preliminary results revealed improvement in metal uptake using the smaller sized adsorbent. However, the concentrations of most heavy metals in AMD were still above the maximum recommended discharge levels. Therefore, the effect of continuous flow through 2 columns connected in series was also investigated. The columns were each loaded up to 45 cm with cassava waste beads of approximately 1.5 mm in diameter. During the column tests, the effluent from the first column was fed continuously to the bottom of the second column using a silicon tube, and

solution samples which were later analysed for metal content were collected at various time intervals.

A plot of C/Co against time was made. Due to the nature of the AMD solution, breakthrough was assumed to have occurred when there was a sharp increase in effluent concentration. The results of single as well as double continuous flow columns each containing 1.5 mm cassava waste beads in comparison with those obtained using the 3 mm adsorbents are summarized in Table 4.10.

Table 4.10: Breakthrough parameters for heavy metals in AMD at different conditions (Adsorbent bed height (single column) = 45 cm, Flow rate = 0.89 mL/s, Temp. = 25˚C).

Metal ion	No. of columns	Bead size (mm)	Breakthrough time(min)	Concentration at Breakthrough(mg/L)	% Adsorption efficiency
Al	1	3.0	14	0.20	28.57
	1	1.5	16	0.16	42.86
	2	1.5	20	0.15	46.43
Ca	1	3.0	14	248	48.87
	1	1.5	16	160	67.01
	2	1.5	20	114	76.49
Co	1	3.0	12	0.16	60.00
	1	1.5	14	0.04	90.00
	2	1.5	16	0.03	92.50
Fe	1	3.0	12	134	30.57
	1	1.5	16	117	39.38
	2	1.5	20	102	47.15
Mg	1	3.0	16	78	42.22
	1	1.5	16	74	45.19
	2	1.5	20	61	54.81
Mn	1	3.0	16	24	47.02
	1	1.5	16	22	51.43
	2	1.5	20	17	62.47
Ni	1	3.0	14	0.29	32.56
	1	1.5	16	0.21	51.16
	2	1.5	20	0.19	55.81

The results indicate that the breakthrough time increased when the bead size was reduced from 3 to 1.5 mm. This may be due to the increased number of active

adsorption sites at reduced adsorbent sizes, which increases the bed capacity and consequently the breakthrough times (Crini and Badot, 2010). The results also indicate a substantial decrease in the concentration of metal ions in the effluent at smaller adsorbent bead size. This is because smaller adsorbent sizes reduce internal diffusion and mass transfer limitation of the adsorbate penetrating inside the adsorbent (Al-Anber, 2011). In other words, equilibrium is more easily attained and nearly full adsorption capability can be achieved. Therefore, the better adsorption efficiency results obtained for the 1.5 mm immobilized cassava waste biomass suggests that most of the internal surface of the particle might have been utilized for adsorption. This also indicates that adsorbents of smaller size have shorter diffusion paths in which metal ions transfer faster (Al-Anber, 2011). It can be seen that the concentration of Co^{2+} in the effluent was reduced to the permissible discharge levels by the 1.5 mm immobilized cassava waste biomass. This can be attributed to the smaller hydrated diameter of the metal ion (which allowed Co^{2+} ions easier access to active sites of the cassava waste biomass) in comparison to that of the other cations present in AMD, as previously discussed.

Comparison of a single column loaded with 1.5 mm immobilized cassava waste biomass with the double fixed bed column system revealed that the breakthrough and saturation times increased substantially when a double column system was used. This may be a result of the additional mass transfer zone offered by the second column, which lengthens the time for the effluent to move through it and, consequently, the breakthrough and saturation times. Table 4.10 also shows that the concentration of metal ions at breakthrough in a double column system was lower compared to the single column. This may be attributed to the availability of more active sites for adsorption which result in lower metal concentration in the effluent at breakthrough. However, comparison of the adsorption efficiencies shows that having a second column did not achieve significant reduction in the metal ions in the effluent. Although, the concentration of Co^{2+} was reduced to permissible discharge levels, the concentration of the other heavy metal ions in the effluent remained significantly

above the recommended discharge levels. This result may be attributed to the presence of some diffusion limitations associated with ions such as Al^{3+}, Mg^{2+}, Ca^{2+} etc., onto the cassava waste biomass. The size of the hydrated ion greatly affects these limitations, as already mentioned. Therefore, in a mixed ion solution, ions with a larger hydrated diameter are more likely to experience greater diffusion resistance onto the cassava waste biomass compared to those with a smaller hydrated diameter. Reducing the size of the adsorbent reduces this resistance, as previously discussed. However, it can be seen from the results that increasing the quantity of the adsorbent did not significantly reduce the diffusion resistance, which provides an explanation for the low adsorption efficiencies of most metal ions even with the addition of the second column.

4.4.4 Column dynamics studies

Evaluation of column dynamics is a useful tool for understanding the efficiency of a continuous adsorption system. Amongst the known column models, the Thomas and Adam-Bohart models are the mostly used in waste water treatment (Naja and Volesky, 2006; Ahmad and Hameed, 2010; Chowdhury et al., 2013). Therefore, the adsorption performance of heavy metals through the column was analysed using the Thomas and Adams-Bohart models by considering the operating limit of mass transfer zone of a column (Naja and Volesky, 2006).

Application of the Adam-Bohart model

The Adam-Bohart model was established on the surface reaction theory and is based on the assumption that equilibrium is not instantaneous (Chowdhury et al., 2013). The linearized form of the model is given as:

$$In\left(\frac{C_t}{C_0}\right) = K_{AB}C_0t - K_{AB}N_0\left(\frac{z}{U_0}\right) \quad (4.2)$$

where C_o and C_t are the inlet and outlet adsorbate concentrations, respectively, z (cm) is the bed height, U_o (cm/min) is the linear velocity calculated by dividing the flow rate by the column sectional area, N_o (mg/L) is the saturation concentration and K_{AB} (L/mg min) is the mass transfer coefficient. The experimental data was fitted onto the model to determine the mass transfer coefficient (K_{AB}) and the saturation concentration (N_o). The values of K_{AB} and N_o were then calculated from the slope and intercepts of a linear plot of In (C_t/C_o) against time. The mass transfer coefficients (K_{AB}) and other statistical parameters for various heavy metals in AMD at different conditions, obtained using regression analysis are summarized in Table 4.11.

Table 4.11: Adam-Bohart parameters for heavy metals in AMD at different conditions using regression analysis.

Metal ion	**C_o (mg/L)**	**Bead size (mm)**	**Bed height (cm)**	**Flow rate(mL/s)**	**K_{AB} (mL/min-mg) x10^{-4}**	**N_o(mg/g)**	**R^2**
Al	0.28	3.0	15	0.89	471.400	0.064441	0.9251
		3.0	30	0.89	25.0000	0.725485	0.9869
		3.0	30	1.50	146.428	0.155266	0.9093
		3.0	30	2.10	175.000	0.164026	0.9379
		3.0	45	0.89	257.140	0.07153	0.9869
		1.5	45	0.89	275.000	0.071802	0.4108
Ca	485	3.0	15	0.89	0.665979	90.48029	0.9503
		3.0	30	0.89	0.573196	68.76233	0.9055
		3.0	30	1.50	0.585567	94.24487	0.9080
		3.0	30	2.10	0.641237	109.9969	0.9416
		3.0	45	0.89	0.558763	53.03602	0.8292
		1.5	45	0.89	0.564948	82.78054	0.8951
Co	0.40	3.0	15	0.89	610.000	0.136475	0.9633
		3.0	30	0.89	562.5	0.079668	0.9787

		3.0	30	1.50	567.5	0.118428	0.9868
		3.0	30	2.10	627.5	0.139189	0.8729
		3.0	45	0.89	402.5	0.083821	0.9022
		1.5	45	0.89	1147.5	0.077649	0.9792
Fe	193	3.0	15	0.89	0.880829	38.24037	0.7936
		3.0	30	0.89	0.751295	25.3655	0.9792
		3.0	30	1.50	0.772021	36.914	0.9933
		3.0	30	2.10	0.88601	37.11736	0.9585
		3.0	45	0.89	0.673575	21.8788	0.7284
		1.5	45	0.89	0.953368	23.92093	0.7555
Mg	135	3.0	15	0.89	0.903704	38.23168	0.7831
		3.0	30	0.89	0.837037	26.92708	0.6436
		3.0	30	1.50	1.385185	24.92751	0.9712
		3.0	30	2.10	1.481481	32.30795	0.9712
		3.0	45	0.89	0.792593	25.3138	0.4745
		1.5	45	0.89	0.666667	35.77338	0.9779
Mn	45.3	3.0	15	0.89	2.980132	16.39636	0.7948
		3.0	30	0.89	2.229581	13.06401	0.6624
		3.0	30	1.50	2.781457	15.68248	0.8597
		3.0	30	2.10	2.958057	18.28596	0.9397
		3.0	45	0.89	2.251656	10.30654	0.5175
		1.5	45	0.89	2.339956	12.72084	0.9252
Ni	0.43	3.0	15	0.89	67.44186	0.470734	0.9686
		3.0	30	0.89	27.90698	0.504779	0.9848
		3.0	30	1.50	74.4186	0.312705	0.8624
		3.0	30	2.10	79.06977	0.392921	0.8989
		3.0	45	0.89	23.25581	0.533184	0.8314
		1.5	45	0.89	118.6047	0.20809	0.6248

From the Table 4.11, it can be seen that the mass transfer coefficient (K_{AB}) generally increased with increase in flow rate but decreased with adsorbent bed height. This trend in K_{AB} values indicates that the overall system kinetics was dominated by external mass transfer in the initial part of the adsorption column (Ahmad and Hameed, 2010). It can also be seen that metal ions such as Co^{2+} and Ni^{2+} had very large K_{AB} values compared to the other metal ions in AMD, and this may be due to their higher affinity for the cassava waste beads. In addition, the sorption capacity (N_o) also increased with increase in flow rate, but decreased with increase in bed height. This may be due to saturation occurring faster at higher flow rates and reduced bed height. The trends concur well with those reported in similar studies in literature (Ahmad and Hameed, 2010; Chowdhury et al., 2013 Anisuzzaman et al., 2014). Furthermore, the results showed that a reduction of the adsorbent size from 3 mm to approximately 1.5 mm led to an increase in K_{AB} and reduction in N_o. This is because smaller particles reduce internal diffusion paths and mass transfer limitation of the adsorbate penetrating inside the adsorbent (Al-Anber, 2011). In other words, equilibrium is more easily attained and nearly full adsorption capability may be attained. From the correlation coefficients (mostly > 0.75) and other parameters, it can be seen that the experimental data generally fitted well with the Adam-Bohart model.

Application of the Thomas model

This model is based on the assumption that the adsorption process follows the Langmuir kinetics of adsorption without axial dispersion (Thomas, 1944). The linearized form of the model is expressed as:

$$In\left[\left(\frac{C_o}{C_t}\right)-1\right] = \left(\frac{k_{Th}q_o m}{Q}\right) - k_{Th}C_o t \qquad (4.3)$$

where k_{Th} (mL/ mg min) is the Thomas rate constant, q_o (mg/g) is the equilibrium adsorbate uptake, C_o is the initial metal concentration (mg/L) and m (g) is the amount

of adsorbent in the column. The experimental data was fitted onto the Thomas model to determine the rate constant (k_{Th}) and the maximum sorption capacity ($q_{o)}$. The k_{Th} and q_o values were calculated from the slope and intercepts of linear graph of In[(Co/Ct) -1] versus time from the column experiments. The model parameters of the different metals at different conditions are summarized in Table 4.12.

Table 4.12: Thomas parameters for heavy metals in AMD at different conditions using regression analysis.

Metal ion	Bead size (mm)	Bed height (cm)	Flow rate(mL/s)	k_{Th}(mL/min-mg) x10^{-4}	q_o(mg/g)	R^2
Al	3.0	15	0.89	0.100000	-47.9745	0.4193
	3.0	30	0.89	0.103214	-23.7104	0.9613
	3.0	30	1.50	0.104286	-52.2434	0.9913
	3.0	30	2.10	0.104286	-89.0941	0.9131
	3.0	45	0.89	0.203929	-10.6679	0.9638
	1.5	45	0.89	0.014192	-24.0171	0.4193
Ca	3.0	15	0.89	2.020619	-3521.5	0.9018
	3.0	30	0.89	1.983505	7177.551	0.9112
	3.0	30	1.50	2.024742	5962.284	0.8554
	3.0	30	2.10	2.057732	-3263.47	0.9464
	3.0	45	0.89	1.381443	8699.808	0.7563
	1.5	45	0.89	0.284895	133177.2	0.9529
Co	3.0	15	0.89	1227.5	17.81911	0.9687
	3.0	30	0.89	1145.0	13.7269	0.9496
	3.0	30	1.50	1292.5	12.40771	0.9833
	3.0	30	2.10	1355.0	9.53953	0.8481
	3.0	45	0.89	1042.5	14.51459	0.7771
	1.5	45	0.89	140.0	494.0748	0.9640

Fe	3.0	15	0.89	6.637306	-3686.83	0.9883
	3.0	30	0.89	6.202073	364.4539	0.9132
	3.0	30	1.50	6.658031	-5841.76	0.9514
	3.0	30	2.10	7.440415	-8976.45	0.9716
	3.0	45	0.89	5.715026	516.3269	0.8008
	1.5	45	0.89	4.876208	3295.574	0.9829
Mg	3.0	15	0.89	4.185185	-12694.9	0.8613
	3.0	30	0.89	3.355556	-4336.86	0.6230
	3.0	30	1.50	3.518519	-15027.4	0.9301
	3.0	30	2.10	3.82963	-23655.3	0.9679
	3.0	45	0.89	3.340741	-327.045	0.6680
	1.5	45	0.89	1.594526	4187.761	0.7105
Mn	3.0	15	0.89	9.227373	-2876.46	0.8523
	3.0	30	0.89	6.092715	-864.576	0.6504
	3.0	30	1.50	9.448124	-1760.76	0.8532
	3.0	30	2.10	10.1766	-3535.89	0.9628
	3.0	45	0.89	5.518764	336.7149	0.4924
	1.5	45	0.89	4.871118	2754.987	0.6917
Ni	3.0	15	0.89	400.0	-146.702	0.9658
	3.0	30	0.89	390.6977	-72.6847	0.8787
	3.0	30	1.50	395.3488	-150.572	0.8527
	3.0	30	2.10	420.9302	-210.200	0.9424
	3.0	45	0.89	260.4651	-60.0482	0.4720
	1.5	45	0.89	78.68119	43.95617	0.6219

From Table 4.12, it can be seen that the coefficient (k_{Th}) increased with increase in flow rate and bead size, but decreased with increase in bed height. However, the maximum sorption capacity (q_o) decreased significantly with increase in flow rate but increased significantly with increase in bed depth and decrease in adsorbent bead

size. The lower q_o values observed at lower bed depth and higher flow rates were attributed to earlier saturation of the adsorbent at these conditions. The trend in the q_o and k_{Th} values obtained in this work are consistent with those reported in literature (Ahmad and Hameed, 2010; Chowdhury et al., 2013). However, it can be noted that reasonable results were only obtained at the reduced flow rate and bead size as well as at the highest bed depth. It was difficult to quantify the saturation concentration at the other conditions using this model, since it produced negative q_o values. This could be attributed to the presence of external diffusion limitations of associated with some metal ions onto the cassava waste biomass at these conditions. From the experimental data (Figure 4.13 and 4.14), it can be seen that most C/C_o values for the metal ions in AMD at different flow rates and bed heights were greater than 0.50. This implies that the natural logarithms of [(Co/C) -1] which give the vertical values for the Thomas model will be negative. As such, the intercept (from which q_o is calculated) will be negative resulting in negative q_o values. This shows that the model is not ideal for representing applications where the breakthrough occurs at values greater than or close to C/C_o= 0.5. For instance, it can be seen that the immobilized cassava waste biomass had a large affinity for Co^{2+}, and therefore, the values and trends in q_o and k_{Th} were good and in agreement with those in reported literature (Ahmad and Hameed, 2010; Chowdhury et al., 2013). The correlation coefficients (all > 0.75) also reflect that the trend for cobalt fits well into the Thomas model. However, the q_o values for the other metals at lower bed depths, larger adsorbent bead size and higher flow rates reflect that the Thomas model in not ideal for representing experimental data at these conditions. In addition, literature reports that the Thomas model is suitable for adsorption processes where the external and internal diffusions will not be the limiting step (Aksu and Gonen, 2004; Ahmad and Hameed, 2010). Therefore, it can be expected that possible external and internal diffusion limitations associated with various heavy metals (except Co^{2+}) in AMD at the stated conditions resulted in the lower metal uptake by the immobilized cassava waste biomass.

4.4.5 Summary of column studies

The aim of the column studies was to investigate the removal of toxic heavy metal ions from AMD using immobilized cassava waste biomass. The information obtained from the breakthrough curves of column studies can be used for scale-up purposes. A fixed bed loaded with the adsorbent at different conditions was used in these studies. The results indicated that adsorption of heavy metals by the immobilized sorbent was favored at the lowest flow rate (0.89 mL/s) and highest bed height i.e. 45 cm. However, it was also noted that despite improvement of results in these conditions, the concentration of metal ions remained substantially above the maximum required discharge levels. Therefore, to further investigate improvement in metal uptake, the bead size was reduced by approximately half the original size and a double continuous flow column system was used. The results of the reduced adsorbent size in single and double continuous columns indicated an increase in metal uptake due to reduced mass transfer limitations at smaller sizes, as well as increase in the quantity of active sites in two columns in series. The concentration of Co^{2+} was reduced to permissible values owing to its smaller ionic diameter, and consequently easier access to active sites of the cassava waste biomass.

To evaluate the kinetic behavior of the fixed bed column, the experimental data at different conditions was fitted into the Adam-Bohart and Thomas models. The results showed that all metal ions with C/Co values less than 0.5 at breakthrough fitted well with both models. However, comparison of the correlation coefficient of the two models indicated that the data generally fitted better with the Adam-Bohart model. In addition, the Thomas model produced negative maximum sorption (q_o) values as a result of the C/Co being greater than 0.5 at breakthrough for most metals, particularly, at reduced bed height and increased flow rate. This, therefore, implies that the Thomas model is not ideal for representing such experimental data. It is further assumed that this finding may indicate that despite the kinetic system being dominated by external mass transfer (Chowdhury et al, 2013), the possible presence of some external and internal diffusion limitations at lower bed depths and higher

flow rates may have resulted in lower metal uptake of metals such as Mg^{2+}, Mn^{2+}, Ca^{2+}, etc. These limitations could also be the reason behind the lower overall metal uptake by the immobilized cassava waste biomass compared to the cassava waste powder (see Figure 4.7 (c)).

4.5 Acid retardation

After the metals have been removed, the solution still remains with some acidity which poses serious risks when disposed into the environment. The conventional method of removing the acidity in mine water treatment is through neutralization using an alkaline agent (Johnson and Hallberg, 2005). However, neutralization results in loss of the acid value which could otherwise be recovered, and the financial benefits used to offset the treatment cost. Consequently, research interests have been spurred towards acid recovery from acid solutions due the environmental as well as economic benefits which could be derived from the approach. However, very little attention has been paid to acid recovery from AMD. Therefore, the present work evaluated the feasibility of using a technology namely, acid retardation process, which is widely used in the metal finishing industry, to recover sulphuric acid from AMD.

The acid retardation process employs ion exchange resins which have high affinity for the acid, and separates the acid from its salts by slowing down its movement relative to the metal salts. Although, the resins initially used for the process suffered from lack of selectivity, studies over the years have focused on improving this property (Shamritska et al., 1972; Brown et al., 1979, Petkova et al., 1981). Recent studies report the high selectivity of Dowex MSA-1 and LEWATIT-K 6362 for sulphuric acid from waste acid solutions (Dowex, 2002; Ghare et al., 2014). Therefore, Dowex MSA-1 was chosen for feasibility studies on AMD. In addition, to the reported high selectivity, ion exchange resins from the Dow Chemical Company

have long and reputable applications in the acid retardation process as reported in previous work (Kraus et al., 1953; Hatch and Dillon, 1963; Shamritska et al., 1972; Petkova et al., 1981; Dowex, 2002).

4.5.1 Properties of Dowex MSA-1 resins

The properties and recommended operating conditions of the resins as obtained from the manufacturer (Dowex, 2001) are shown in Table 4.13.

Table 4.13: Dowex MSA-1 properties

Property	Description/Value
Resin type	Type 1 strong base anion
Matrix	Styrene-DVB, macroporous
Functional group	Quaternary amine
Mesh size	20-50
Ionic form	Cl^-
% moisture	60
Maximum operation temperature (˚C)	100
Total exchange capacity (meq/g)	4.0
pH range	0-14
Total rinse requirements	3-6 bed volumes

4.5.2 Acid retardation test

To investigate the dynamic behavior of the ion exchange bed, the effect of bed height and flow rate on acid uptake was studied. An AMD solution with properties given in Table 3.1 and initial acidity of 906.5 mg/L was used in the acid retardation column studies. Prior to each test work, the ion exchange resins were backwashed with deionized water to ensure proper packing and classification of the bed.

Effect of flow rate

The effect of flow rate on acid uptake was studied by varying the flow rate between 0.83 and 1.5 mL/s, at a constant bed height of 20 cm. The column dimensions of 1.0 cm diameter and 30 cm height were based on values recommended by the resin manufacturer for laboratory evaluation tests (Dowex, 2001). Additional space of about 2 cm was allowed in the column for internal pressure caused by the expansion of the resins, during operation. The AMD solution was pumped in an up flow mode using a peristaltic pump (Heidolph pump drive 5001). Solution samples were collected from the top of the column at various time intervals and analyzed for acid content. The breakthrough curves for the acid uptake are presented in Figure 4.15.

It can be seen that the shapes of the breakthrough curves were closely related to the S-shaped breakthrough curve described by Oliviera et al. (2011). However, due to the low acid uptake (shown by high C/C_o values) obtained in this study; breakthrough was assumed to take place when there was a sharp increase in the concentration of the effluent.

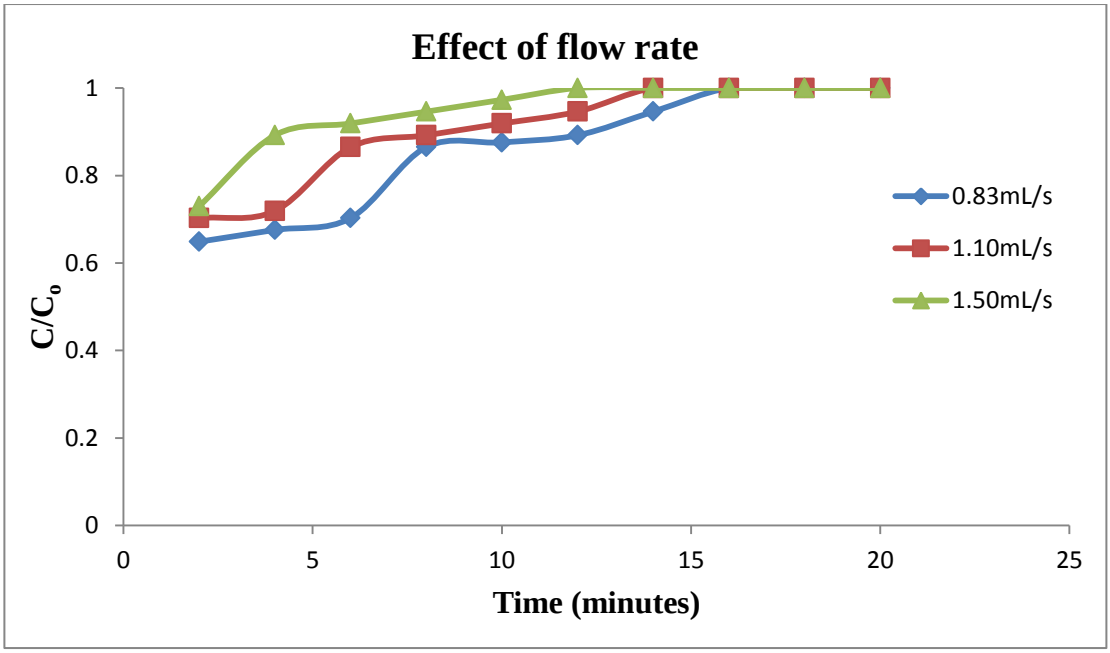


Figure 4.15: Breakthrough curves for acid uptake from AMD at different flow rates (Bed height =20cm, Temp. = 25˚C).

The changes in the quantity of acid at different flow rates shown in Figure 4.15 indicate that Dowex MSA-1 ion exchange resins have the ability to adsorb sulphuric acid from the AMD solution. This adsorption can be attributed to the acid retardation phenomenon, whereby, the ion exchange resins slow down the movement of the acid in relation to the metal salts, resulting in its separation. This form of acid uptake is believed to be caused by the Donnan effect, in which the resin selectively adsorbs the hydronium ion creating an uneven distribution of acid concentration between the resin and the external solution (Gulbas et al., 1987; Neumann, 2009). As a result, metal salts cannot diffuse into the resin phase and this leads to the separation of the acid from its salts.

From Figure 4.15, it can also be seen that the quantity of acid adsorbed at breakthrough increased with a decrease in flow rate. In addition, breakthrough and saturation were reached earlier at higher flow rates. For instance, the breakthrough time decreased from 6 to 2 minutes when the flow rate was increased from 0.83 to 1.50 mL/s. This is because at higher flow rates, the mass transfer zone reaches the top of the column faster resulting in earlier saturation times. Moreover, at higher flow rates, the contact time between the resins and the solution is lower, and some of the acid leaves the column before attaining equilibrium. This results in less acid uptake and more acid appearing in the effluent. In commercial applications of the acid retardation process short contact times typically ranging between 5 to 10 minutes are used for both the acid sorption and elution steps (Brown, 2002; Sheedy and Parujen, 2012). The optimized short-bed technology allows operation at these short contact times. However, available literature reports breakthrough times between 5 to 10 minutes for only acid uptake in laboratory tests (Ghare et al., 2014), which concurs well with the findings of this research. The shorter breakthrough times for the acid retardation process compared to conventional ion exchange systems is attributed to the use of much smaller resin beads (approximately 20% smaller diameter) compared to conventional ion exchange systems (Sheedy and Parujen, 2012). Reducing the size greatly improves the exchange kinetics as well as the length of the effective mass

transfer zone. Table 4.14 summarizes the breakthrough parameters of the acid uptake by Dowex MSA-1 at different flow rates.

Table 4.14: Breakthrough parameters for acid uptake by Dowex MSA-1 at different flow rates

Flow rate (mL/s)	Breakthrough time(min)	Saturation time(min)	Concentration at breakthrough (mg/L)
0.83	6	16	636.3
1.10	4	14	651.8
1.50	2	12	660.8

The Table indicates that the quantity of acid in the effluent remained high even after the acid sorption process. Although, the maximum quantity of acid in industrial effluent is not specified in mg/L, DWAF states that the pH of the effluent must be between 5 and 10 (DWAF, 1996). However, the pH of the solution was found to be in the range 2.25 to 3, indicating the presence of acid in the effluent. The lesser acid uptake in this study could be attributed to the lower residence time of the solution in the column. In literature lower flow rates, typically in the range 3 to 5 mL/min (0.05mL/s to 0.083 mL/s), were used for acid retardation laboratory tests (Hatch and Dillon, 1963). This allows adequate contact time between the solution and the resins to effect the acid adsorption from its salts. However, in this investigation the flow rates could not be reduced below 0.83 mL/s due to pump constraints.

Effect of bed height

The effect of bed height was investigated by varying the resin bed height between 10 and 30 cm. The AMD solution was pumped at a constant flow rate of 0.83 mL/s. The results are presented in Figure 4.16.

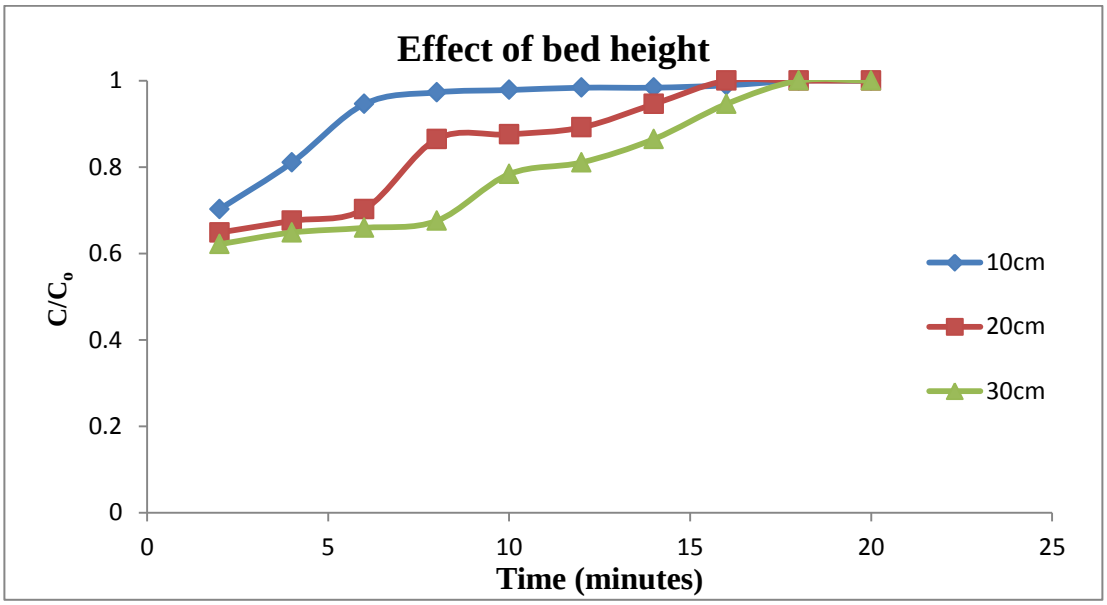


Figure 4.16: Breakthrough curves for acid uptake from AMD at different bed heights (Flow rate =0.89mL/s, Temp. = 25˚C).

The results indicate that the quantity of acid taken up by Dowex MSA-1 increased with increase in bed height. This is due to the increase in the availability of active sites for acid uptake at higher bed depths. In addition, breakthrough and saturation times increased with bed height. The increase in bed height increases the mass transfer zone (Ahmad and Hameed, 2010). The mass transfer zone in a column moves from the entrance of the bed and proceeds towards its exit. Therefore, a longer ion exchange bed creates a longer distance for the mass transfer zone to reach the exit, subsequently, resulting in increased breakthrough as well as saturation times (Ahmad and Hameed, 2010). The trend in acid uptake is in agreement with other related studies (Ghare et al., 2014). However, in commercial applications of the acid retardation process, the bed height can only be increased up to 61cm to maximize the effective mass transfer zone (Brown, 2002; Sheedy and Parujen, 2012). Scale up is achieved by increasing only the diameter of the column. Hence, in commercial practice, the process is sometimes referred to as the 'short bed ion exchange technology'. Table 4.15 summarizes the breakthrough parameters for the acid uptake by Dowex MSA-1 at different bed heights.

Table 4.15: Breakthrough parameters for acid uptake by Dowex MSA-1 at different bed heights

Bed height (cm)	Breakthrough time(min)	Saturation time(min)	Concentration at breakthrough (mg/L)
10	2	6	637.8
20	6	16	636.3
30	8	18	611.9

From Table 4.15, it can be seen that the concentration of sulphuric acid in the effluent remained high even at the maximum bed depth. In fact, the values indicate that only about 33% of the initial acid content was taken up by the resins. The low acid uptake can also be attributed to the insufficient contact time between the solution and the resin. It is believed that reducing the influent flow rate to approximately 1mL/min as reported in literature may improve the acid uptake (Hatch and Dillon, 1963; Dowex, 2001). In addition, increasing the quantity of the resins (through either adding a second column or using a bigger column) may also increase acid uptake. However, this may not be the most preferred option since it increases the operational costs.

4.5.3 Elution studies

The acid from the loaded ion exchange resins could be recovered by elution with water, as already discussed. Therefore, acid loaded ion exchange resins were subjected to a number of cycles of deionized water to establish the quantity of water required for complete elution of the acid from the resins. The volume of the eluent water used in each cycle was equivalent to one bed volume of the resins. Approximately, 15mL aliquots of the eluate were collected for the acid-base titration analysis, after each cycle. The acid concentration after each elution cycle is shown in Figure 4.17.

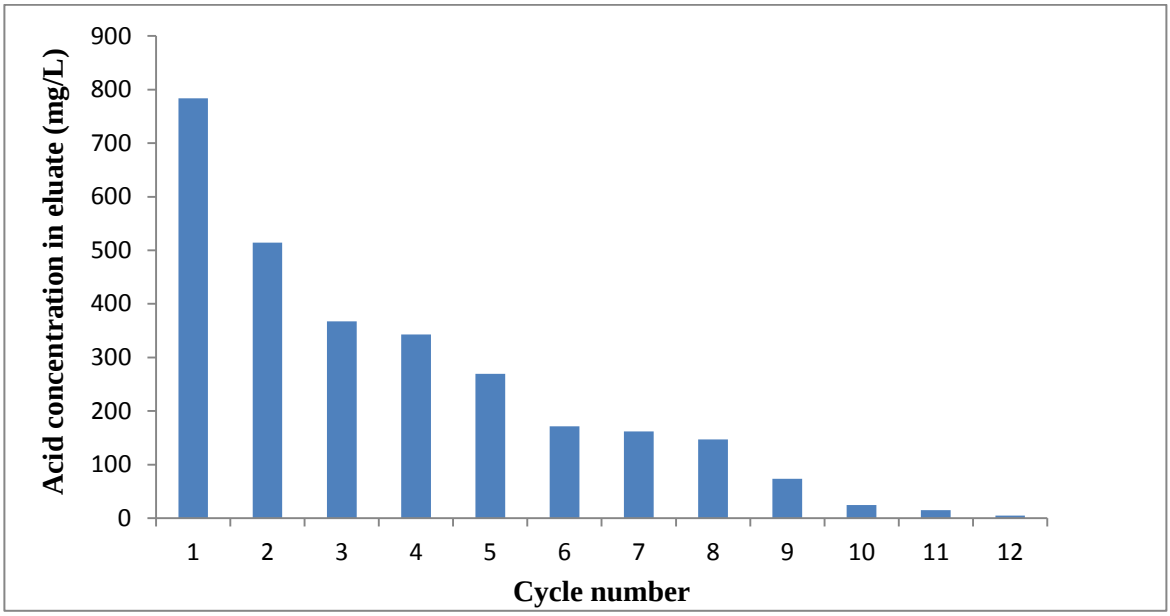


Figure 4.17: Elution cycles of sulphuric acid from Dowex MSA-1 resins (Bed height =30cm, Temp. = 25˚C).

The decrease in the quantity of acid after each water elution cycle as seen in Figure 4.17, indicate that the acid can be recovered from Dowex MSA-1 using water as the eluent. Approximately 11 to 12 cycles of water were required to completely recover all the acid from the loaded resin. The release of the acid from the resins by water may be attributed to the difference in osmotic pressure between the resins and the water eluent (Agrawal and Sahu, 2009). The number of cycles of water used for elution was found to be greatly dependent on the flow rate of the eluent. Preliminary elution results indicated that pumping at lower flow rates between 0.83 mL/s to 1.0 mL/s increased the number of cycles required for elution to around 15 to 20 cycles. However, increasing the flow rate to 1.5 mL/s reduced the number of cycles to the ones shown in Figure 4.17. This may be a result of the increase in turbulence which increases the difference in osmotic pressure allowing more acid to desorb from the resin surface.

4.5.4 Evaporation

The bulk eluate obtained during the elution studies was collected in a 5L container. Approximately 100 mL of the thoroughly mixed solution was heated using oil at 105 ˚C in a rotary evaporator (Heidolph Laborata-4000) for about 6 hours, to obtain a concentrated acid solution and water product. During the evaporation process, the color of the solution was observed to change from colorless to brown-orange and a precipitate was formed. Qualitative analysis of the precipitate using Energy-dispersive X-ray spectroscopy (EDS) revealed that the precipitate consisted mainly of iron oxide, and small amounts of sulphur (Figure 4.18). This result may be attributed to the precipitation of iron as a jarosite in acidic solutions, which has been reported to take place at temperatures between 50 and 105 ˚C (Verner et al., 1980). This also indicates that the acid from the elution process contained some iron impurities. After approximately 6 hours (when approximately 98% of the water had evaporated), the process was stopped and a solution sample of the concentrated acid and water vapor was collected and analyzed for acid content.

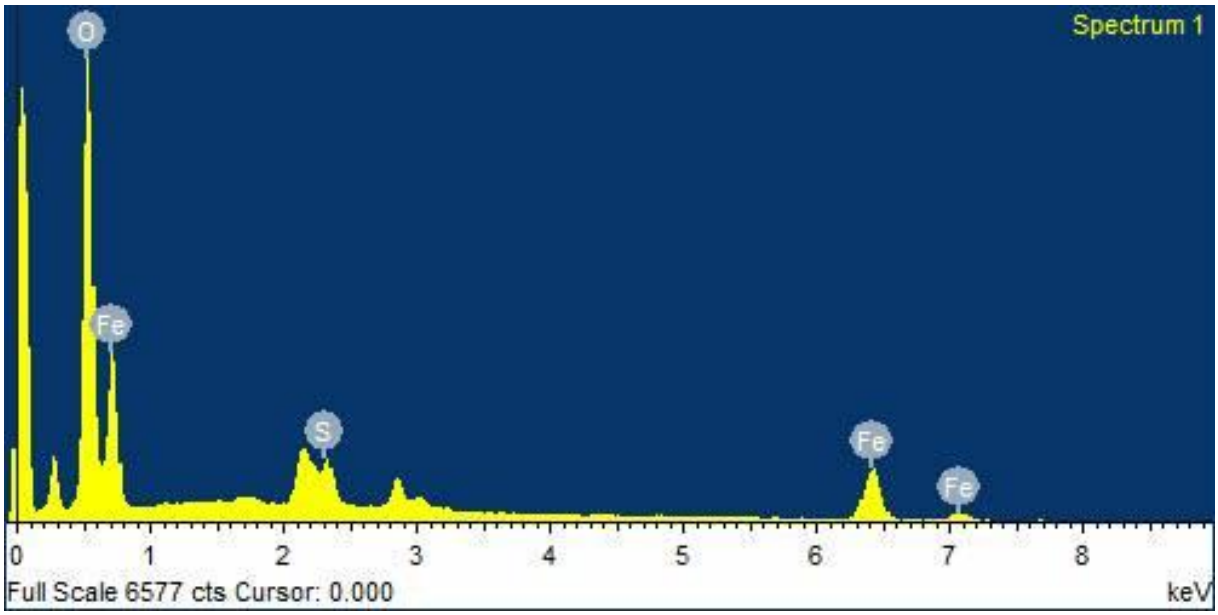


Figure 4.18: EDS spectra of precipitate formed during the evaporation process

The process was stopped at approximately 70% acid (when approximately 98% of the water was evaporated) concentration, because almost no sulphuric acid can be detected in the water vapour up to an acid concentration of 70% (Dietrich processing systems, 2013). The quantity of acid in the water vapour at various time intervals was monitored using the acid titration analysis of the samples of condensed vapor. It must be noted, however, that obtaining higher concentrations of the acid compromises the quality of both acid and product water. The evaporation procedure was repeated three times. A sample of the acid solution and the water product obtained in the evaporation process were then analyzed for acid content as well as impurity content in terms of metal content. The chemical composition of the acid solution and water product are presented in Table 4.16.

Table 4.16: Chemical composition of the acid and water product obtained in the evaporation process

Characteristics	Acid product	Water product
pH	1.80	7.03
Acidity (mg/L)	1372	n.d
Ca(mg/L)	15.05	10.02
Co (mg/L)	0.00353	0.000375
Fe (mg/L)	< 0.108923	< 0.061655
Mg (mg/L)	5.248	1.0496
Mn (mg/L)	< 0.329758	n.d
Ni (mg/L)	< 0.00277845	n.d

*n.d – not detected

The results indicate that the dilute acid from the elution process could be concentrated to higher values using an evaporator. In the present study, the dilute acid solution was upgraded up to 1372 mg/L. Minor metal ion impurities were found in both acid and water product. However, the metal contaminants concentrations in the water product are within permissible discharge levels (DWAF, 1996). Although, the water may not

be ideally suitable for human consumption, it can be recycled back to the elution process or used for other purposes such as fire quenching, dust suppression, etc.

4.6 Economic evaluation of the process

The economic evaluation of a process is important in establishing the financial viability of a project. Therefore a critical economic evaluation of the proposed process was also undertaken. Prior to the evaluation, a detailed mass balance of the proposed process was carried to determine the quantity of raw materials required as well as the quantity of products formed at a given feed flow rate. The assumptions used in the calculations are summarized in Table 4.17.

Table 4.17: Assumptions used in economic evaluation calculations

Description	Units	Value
Annual working hours	Hrs./yr.	8064
Plant estimated downtime	Hrs./yr.	384
Plant available time	Hrs./yr.	7680
Plant capacity	L/hr.	1500
Density of AMD water	Kg/m^3	1000
Density of 70% H_2SO_4	Kg/m^3	1615

Based on the assumptions in Table 4.17, a mass balance of the proposed process was carried out. The concentration of the feed and the products was based on the results obtained in the experimental work conducted in this study. The efficiencies of different process stages were based on reported literature (Sheedy and Parujen, 2012; APV, 2015). A summary of the mass balance of the proposed process is shown in Table 4.18.

Table 4.18: A summary of the mass balance of the proposed process

Description	Units/annum	Value
Feed		
Total volume of AMD treated	ML	11.52
Quantity of de-ionized water used	ML	19.20
Products		
Re-usable water	ML	30.58
Total sulphuric acid	Kg	8337
Iron oxide	Kg	3.33

It can be seen from Table 4.18 that for the 11.52 ML of AMD treated per year, approximately 8337 kg of 70% sulphuric acid and 3 kg of iron oxide can be produced. A conceptual energy balance calculation also showed that an estimated 14 000MWh of electricity is required annually to run the process. Approximately 90% of this energy will be used to vaporize the water from an initial temperature of 25 ˚C.

4.6.1 Estimation of the proposed process costs

The proposed process is composed of three stages which are metal adsorption, acid retardation and acid upgrade. Since information on commercial applications of the cassava waste biomass was not available, the capital cost of the equipment in the metal adsorption section was estimated based on similar biomass process (EPA, 1980). The cost of the acid retardation section was based on information on acid sorption plant from 1987 (Dejak and Munns, 1987) while that of the evaporation unit was based information available from a vendor website (APV, 2015). In all cost estimates, the six-tenth rule (Equation 4.4) was used to estimate the value of the proposed plant (Sinnott, 2005).

$$C_f = C_1 \left(\frac{S_2}{S_1}\right)^{0.6} \quad (4.4)$$

Where C_1 is the capital cost of the plant with capacity S_1 and C_f is the capital cost of the proposed plant with capacity S_2.

All inflationary adjustments were done using the 2015 Chemical Engineering Plant Cost Index (CEPCI) as well as indices published by Vatavuk (2002).

Cost of metal adsorption unit

$$\text{Cost of biomass unit in in 1980} = \$2816000 \left(\frac{1500\text{kg/hr}}{237\ 500\text{kg/hr}}\right)^{0.6} = \$\ 134\ 862$$

$$\text{Cost of biomass unit in 2015} = \text{Cost in 1980} \left(\frac{\text{Cost index in 2015}}{\text{Cost index in 1980}}\right)$$

$$\text{Estimated cost of biomass unit in 2015} = \$134\ 862 \left(\frac{573.4}{261.2}\right) = \$296\ 056$$

Cost of acid retardation unit

$$\text{Cost of acid recovery unit in 1987} = \$200000 \left(\frac{1500\text{kg/hr}}{1500\text{kg/hr}}\right)^{0.6} = \$200\ 000$$

$$\text{Cost of acid recovery unit in 2015} = \text{Cost in 1987} \left(\frac{\text{Cost index in 2015}}{\text{Cost index in 1987}}\right)$$

$$\text{Estimated cost of acid recovery unit in 2015} = \$200\ 000 \left(\frac{573.4}{323.8}\right) = \$354\ 169$$

Cost of evaporation unit

As already mentioned, the cost of the evaporation unit was based on information available on a vendor website (APV, 2015). The cost of the equipment was also estimated using the six-tenth rule.

$$\text{Estimated cost of evaporation unit} = \$2\ 700\ 000\left(\frac{1500\text{kg/hr}}{45\ 500\text{Kg/hr}}\right)^{0.6}$$

$$= \$348\ 508$$

Estimated total equipment cost = **US$998 733**

The cost for Engineering and services were also estimated based on factors of the total equipment cost obtained from Peter and Timmerhaus (1991). The total capital costs as well as the operating costs of the proposed process are shown in Table 4.19.

Table 4.19: Proposed AMD plant costing

Capital cost estimation

Description		**Cost US$**
Evaporating unit		348508
Biomass reactor		296056
Acid retardation & pre-filter unit		354 169
	Sub-total equipment	**998 733**
Purchased equipment installation		359543.88
Instrumentation		279645.24
Piping		319594.56
Electrical design and plant control systems		199746.6
Building (including services)		199746.6
Yard improvements		79898.64
Engineering and supervision		399493.2
Civils design and construction		479391.84
Contractor's fees		79898.64
Sub Total Engineering & Services		**2396959.2**
Total plant cost Installed		**3 395 692**
Sub-Total contingency		319594.56
Total capital cost requirement		**3 715 287**

Annual raw materials costs

Raw material	Annual requirements (t)	Price (US$/ t)	Total price (US$)
Nitric acid	8.5	300	3550.00
Sodium Alginate	16	500	8000.00
Thioglycollic acid	41	1500	61500.00
Dowex ion exchange resins	0.3816	8122	3099.36
De-ionized Water (for Elution)	19200	0.34	6528.00
Calcium chloride	1.99	130	258.70
Sodium chloride	4.05	48	194.40
Total			**82 130.46**

Operating cost estimation

	VARIABLE OPERATING COSTS	
Variable costs	**Typical value**	**Annual Cost($)**
Raw materials	Raw material Table	82 130.46
Miscellaneous	7.5% C_f	242 301.31
Electricity	14,000,000KWh@ $0.13/unit	1820000.00
Other Utilities	10% of maintenance costs	16153.42
Sub-Total variable operating cost		2160585.19
	FIXED OPERATING COSTS	
Fixed costs	**Typical value**	**Annual cost ($)**
Maintenance	5% C_f	161534.21
Operation Labor	6% C_f	193841.05
Laboratory Costs	20% OL	38768.21
Supervision	20% OL	38768.21
Plant Overheads	50% OL	96920.52
Capital Charges	10% C_f	323068.41
Insurance	1% C_f	32306.84
Local Taxes	2% C_f	32306.84
Sub-fixed operating cost		917514.30
Total operating cost		**3078099.49**

Revenue estimation

Product Name	Annual Production(t)	Price ($/t)	Annual Revenue ($)
70% Sulphuric acid	8.34	560	4670.40
Iron oxide	0.20	300	60.00
Total			**4730.40**

From Table 4.19, it can be seen that an estimated total capital expenditure of US$3.72 Million is required to set up the proposed process plant. In addition, approximately US$2.76 Million will be required annually for plant operation. The high energy requirements associated with the acid upgrade process which accounts for over 60% of the annual operating costs is a major concern in this process. Reducing the operating pressure, such as evaporating the solution in a vacuum is an option that can greatly reduce these costs. Other options including the use of cheaper alternative sources of energy such as solar or wind as well as energy optimization through pinch analysis technology can greatly reduce these costs.

The cost of raw materials is small (in comparison to other operational costs) and it accounts to only 2% of the annual operating expenditure. Of this amount more than 88% goes to biomass immobilization due to the high cost of thioglycollic acid. A cheaper alternative chemical for introducing new functional groups on the cassava waste biomass will significantly reduce the raw material costs. Apart from the cost of high volumes of de-ionized water required for resin elution, the annual cost of the acid retardation process is fairly reasonable amounting to only 10% of the annual raw material costs**.** This is because the resins used for the acid sorption process have been reported to have a life span of about 5 to 10 years (Cushnee, 2009). However, a 20% replacement rate per annum was assumed to allow for possible resin damage, fouling etc.

For a feed flow rate of 1500L/hr. AMD solution and 7680 hrs./year of plant operation, approximately 8.34 tons of sulphuric acid can be produced per annum

which translates to about US$4 670.40 in revenue. Although, the revenue from sulphuric acid is small, it can still be used to offset some of the operational costs such as the purchase of raw materials, etc. The quantity of the iron oxide product, though of suitable quality for marketing in the paint pigmentation industry, was found to be barely enough to have any significant impact on the economics of the proposed process.

If the overall process is considered in an economic sense (US$4 670.40 revenue versus US$2.76 Million annual operating cost), it may be seen that the process is not profitable. However, if one goes back to the main objective which is to treat the toxic AMD and produce water of acceptable quality, we can draw some advantages from this process. Presently, most treatment methods (which also have approximately similar or even higher operational expenditure) can treat waste AMD and produce portable water. However, as already discussed valuable sulphuric acid is lost in the processes. In addition, enormous quantities of solid sludge are produced which also add to the operational costs on its disposal. Furthermore, the sludge poses as a potential health hazard in the secured landfills in which they are disposed. Recovering the sulphuric acid from AMD significantly reduces the sludge burden, and this makes the proposed process environmentally attractive.

In addition, the concept of metal removal using a low cost biomass adsorbent and sulphuric acid recovery can be incorporated into existing AMD treatment technologies. One such technology is the HiPRO process (discussed in section 2.6) at Emalahleni, South Africa. As already discussed, this process is able to produce potable water from waste AMD. However, the main challenges in this process include the high cost of operation (mostly due to the high cost of membranes) as well as the production of waste brine and other solids which require disposal. Incorporating the acid retardation technology to the reverse osmosis process, will have several significant advantages. Firstly, the quantity of the solid waste requiring disposal will be substantially reduced owing to acid recovery. Secondly, the membranes will receive less contaminated water (due to acid removal) resulting in

less energy requirements. Thirdly, the water for resin elution (which is usually purchased) is produced from the process and can be recycled back into the process for elution. The overall effect of this is substantial reduction in operating costs. In addition, the health hazard associated with disposal of sludge in secured landfills is greatly reduced, and thus the process can be deemed eco-friendly. Use of cheaper energy alternatives and energy optimization in the acid upgrade process will further increase the financial viability of such a project.

Overall discussion

The acid retardation tests were conducted to test the feasibility of acid recovery from AMD. The Dowex MSA-1 ion exchange resins were chosen for the feasibility tests due to its reported high selectivity for acid (Dowex, 2002). The effect of flow rate and bed height on acid uptake was investigated. The results showed that Dowex MSA-1 has the ability to adsorb acid from an AMD solution. The acid uptake was attributed to the acid retardation process caused by the Donnan effect. The breakthrough times ranged from 2 to 8 minutes when the bed height was increased from 10 to 30 cm, while maintaining a constant flow rate of 0.83 mL/s. In addition, the breakthrough times increased from 2 to 6 minutes when the flow rate was reduced from 1.50 to 0.83 mL/s, at a constant bed height of 20 cm. The maximum acid uptake in this study was obtained at a bed height of 30 cm and a flow rate of 0.83 mL/s. A maximum acid uptake of about 33% of the initial acid content was observed. However, the acid content in the effluent still remained substantial high. The low acid uptake was attributed to insufficient residence time of the solution in the column, which was caused by the high influent flow rates used in the feasibility tests. Reducing the flow rate beyond 0.83 mL/s was not possible due to the limitations of the available pumps.

Elution tests were subsequently carried out in order to recover the acid from the loaded resins. The results showed that water can be used as an eluent for acid recovery. The release of the acid was attributed to the difference in osmotic pressure

between the eluent and the loaded resins. The release of the acid was found to be greatly dependent of the flow rate of the eluent. Higher flow rates were found to be favorable due to the increase in the osmotic pressure difference, hence, the release of more acid per cycle. At an eluent flow rate of 1.50 mL/s, approximately 11 to 12 cycles were required to completely desorb the acid from the loaded resin.

The eluate from the elution process was then evaporated in a rotary evaporator to upgrade the concentration of the acid. Some of the Fe impurities in the dilute acid solution were removed from the solution via precipitation at temperatures between 50 and 105 ˚C. However, the overall results showed that a concentrated acid product and water of re-usable quality could be obtained. The water product may be recycled back to the elution process, to minimize the volumes of water used.

In summary, the acid retardation process has the potential to address the acid problem associated with AMD. Although high volumes of water are used for the elution process, incorporating the acid retardation process with existing technologies can produce potable water which can be recycled back into the process.

4.7 Summary

This chapter presented and discussed the findings of this research. The study was composed of two main aspects, i.e., removal of toxic metals and recovery of acid from a real AMD solution. The metal removal aspect was evaluated using batch and column studies. Prior to the batch and column studies, three low cost adsorbents (bentonite, zeolite and cassava peel biomass) were characterized in terms of surface morphology, physicochemical properties, functional groups and, quantitative and qualitative phases. The results of the batch studies showed that the adsorption efficiencies of most metals at less than 50% for both zeolite and bentonite adsorbents, were lower compared to cassava peel biomass at approximately 90%. Subsequently, cassava peel biomass was chosen for further tests. The experimental data from the

batch experiments was fitted into the Langmuir and Freundlich isotherm models. The data was found to fit better into the Langmuir model.

The results of the column adsorption tests indicated that the immobilized cassava waste biomass has the ability to remove heavy metals. However, the metal adsorption was found to be lower than that reported in the batch experiments due to some diffusion limitations associated with adsorption onto the immobilized surface. The experimental data was fitted into the Thomas and Adam-Bohart models. The data fitted better into the Adam-Bohart model. This finding was attributed to the increased internal and external diffusion limitations of some metal ions at reduced bed depths and higher flow rates.

After the metals have been successfully removed from AMD, the solution remains with some acidity. Feasibility tests for acid recovery from AMD were conducted using a process known as acid retardation. The results indicated that sulphuric acid could be recovered from AMD using the Dowex MSA-1 ion exchange resins. Furthermore, the acid could be upgraded by evaporation and a water product obtained. The water was found to be of suitable quality for use in fire quenching, dust suppression etc. An economic evaluation of the proposed process showed that an estimated capital cost of US$3.7 million will be required to set up a plant with a capacity of 1 500L/hr. An additional cost of approximately US$3 million will be required to run the plant annually. Although, the revenue obtained from the sulphuric acid is small, it can be used to offset some of the operational costs. In addition coupling this process with existing technologies such as the HiPRO process and optimizing energy requirements will greatly reduce the operating costs.

CHAPTER FIVE

CONCLUSION AND RECOMMENDATIONS

5.1 Conclusion

5.1.1 Introduction

AMD presents serious challenges when discharged into the environment owing to the toxicity of its constituents. Traditional methods such as precipitation, neutralization, membrane separation etc., are able to remediate AMD. However, the financial constraints associated with these processes limit their use. In addition, valuable products such iron oxide, sulphuric acid and many other metals which could be recovered are lost in the process. These products could be used to offset the treatment costs, greatly reducing the overall operation cost. Therefore, the aim of the present research was to test the feasibility of using adsorption and acid retardation processes as alternative techniques for AMD remediation.

In order to achieve this aim, the objectives were defined as:

- To identify the best low cost adsorbent amongst zeolite, bentonite clay and cassava peel biomass based on metal adsorption efficiency and acid retention
- To obtain scale up information using the column adsorption studies
- To recover the remaining sulphuric acid using acid retardation process
- To recover water of re-usable quality through the acid upgrade process

5.1.2 Batch adsorption studies

Batch adsorption studies are normally used to assess the ability of an adsorbent to remove an undesirable pollutant from a solution. In this research, batch studies were conducted in order to evaluate the metal adsorption efficiency of three low cost adsorbents (bentonite, zeolite and cassava waste biomass) on a real AMD solution. The overall intention was to choose an adsorbent which could adsorb the highest quantity of metals from the AMD solution without resulting in a significant loss of solution acidity. The effects of contact time, adsorbent loading, temperature and agitation on metal adsorption efficiencies using the modified and unmodified adsorbents were investigated. Apart from the adsorption of Fe^{3+} which was above 90%, the metal adsorption efficiencies of the other metals remained less than 50% using bentonite and zeolite adsorbents compared to close to 90% with the 1M treated cassava waste biomass. In addition, the zeolite and bentonite adsorbents had a buffering effect on the solution, resulting in the loss of the acid value which could alternatively be recovered. Furthermore, the structural integrity of zeolite and bentonite adsorbents were compromised leading to the dissolution of the crystalline structures. Apart from the higher metal adsorption efficiency, the cassava waste biomass was able to maintain high solution acidity; thus showing potential for acid recovery after metal removal. Consequently, cassava waste biomass was chosen for further tests.

The batch equilibrium data for the biomass was fitted into the linear forms of the Freundlich and Langmuir isotherms to determine the adsorption capacity of the biomass for various heavy metals in AMD at 30 ˚C. The Langmuir sorption model was used to estimate the maximum theoretical metal uptake not reached in the experiments, and the Freundlich adsorption model estimated the adsorption intensity of metal ions onto the cassava waste biomass. The higher correlation (> 0.75) and lower error function values (all less than 1) obtained with the Langmuir model

compared to the Freundlich model, indicated that the data fitted well with the Langmuir model. From the Langmuir isotherm, the adsorption affinity constant, b (L/mg), and the maximum adsorption capacity, q_{max} (mg/g) of Ca^{2+}, Co^{2+}, Fe^{3+}, Mg^{2+}, Mn^{2+} and Ni^{2+} forming a monolayer on the surface of the cassava peel biomass were estimated to be 0.366 L/mg, 13039 L/mg, 0.945 L/mg, 2.188 L/mg, 1.174 L/mg and 3089 L/mg, and 43.67 mg/g, 0.0348 mg/g, 17.98 mg/g,8.51 mg/g, 4.484 mg/g and 0.077 mg/g, respectively. The small values of b (for Ca^{2+}, Fe^{3+}, Mg^{2+}, Mn^{2+}), which represent the affinity between the sorbent and sorbate, suggest a weaker binding between the ions and the biomass surface, indicating a physisorption process (Volesky, 2004). The higher values of b for Co^{2+} and Ni^{2+} were believed to suggest a stronger binding capacity between the adsorbent surface and the metals, thus indicating chemisorption of the metal ions at the surface of the cassava peel biomass. The higher affinity of the cassava peel biomass for Co^{2+} and Ni^{2+} were in agreement with the findings of other related studies (Kurniawan et al., 2010; Seepe, 2015).

The removal of sulphate ions by the three adsorbents was also evaluated in the batch studies. Although, the zeolite and bentonite adsorbents were able to remove more sulphate ions compared to cassava waste biomass, the quantity of the ions in the effluent remained significantly above the maximum discharge levels of 600mg/l recommended by DWAF (1996).Therefore, it can be concluded that all three adsorbents failed to reduce the sulphate levels to permissible discharge levels.

5.1.3 Column tests

The objective here was to obtain information through the breakthrough curves which could be used for scale-up purposes. For this purpose, continuous flow adsorption studies at different conditions using immobilized cassava waste biomass were conducted. In addition to increasing the adsorbent's mechanical strength, density, reusability and resistance to mechanical environments (Goksungur et al., 2003), literature also reported that immobilization improves metal adsorption (Simate and

Ndlovu, 2015; Seepe, 2015). The results showed that the immobilized cassava waste biomass could adsorb heavy metals and the adsorption was in the order Co^{2+}> Ni^{2+}> Ca^{2+}> Mn^{2+}> Fe^{3+}> Mg^{2+}. Ions with smaller hydrated diameter such as Co^{2+} and Ni^{2+} had higher adsorption efficiencies compared to the other cations due to easier access to active sites of the biomass (Horsfall et al., 2003). The adsorption of all metals by the immobilized sorbent was favoured at the lowest flow rate (0.89 mL/s) and highest bed height, i.e., 45 cm. However, it was also noted that despite improvement of results in these conditions, the concentration of metal ions remained substantially above the maximum required discharge levels. Therefore, to investigate any improvement in metal uptake, the adsorbent bead size was reduced by approximately half the original size and two columns in series were used. The results of reducing the size of the adsorbent in a single and two column system indicated an increase in metal uptake due to enhanced mass transfer at smaller sizes, as well as increase in the quantity of active sites, respectively. The concentration of Co^{2+} was reduced to permissible values owing to its smaller ionic diameter, and consequently easier access to active sites of the cassava waste biomass. The rest of the other metals ions were still above the permissible discharge limits. The addition of a second column did not significantly increase the metal adsorption efficiency. This was attributed to limitations of ions with a larger hydrated diameter such as Mg^{2+}, Mn^{2+}, Ca^{2+}, etc., to diffuse through the cassava waste biomass surface. As a result, the concentration of most metal ions (apart from Co^{2+}) remained substantially above the permissible limits. The trend in the results, however, generally indicated that using adsorbent of smaller size and multiple fixed bed system could reduce the metal ions to permissible levels recommend by DWAF (1996).

To evaluate the kinetic behavior of the fixed bed column, the experimental data at different conditions was fitted onto the Adam-Bohart and Thomas models. The results showed that all metal ions with C/Co values less than 0.5 (such as Co^{2+}) at breakthrough fitted well with both models. However, comparison of the correlation

coefficients of the two models indicated that the data generally fitted better with the Adam-Bohart model. In addition, the Thomas model produced negative maximum sorption values (q_o) as a result of the C/Co being greater than 0.5 at breakthrough for some metals, particularly, at reduced bed height and increased flow rate. It was then concluded that the Thomas model is not ideal for representing the experimental data for this study. It was further believed that this finding may suggest that despite the kinetic system being dominated by external mass transfer as indicated by the Thomas model parameters (Chowdhury et al, 2013), the possible presence of some external and internal diffusion limitations at lower bed depths and higher flow rates may have resulted in lower metal uptake of metal such as Mg^{2+}, Mn^{2+}, Ca^{2+}, etc. The lower overall metal adsorption efficiencies by the immobilized cassava waste biomass in comparison to that using cassava waste powder were also attributed to these limitations. The diffusion limitations of these metal ions, in addition, to the acidic nature of the solution used in this study may be the reason why the results contradict those of reported literature (Simate and Ndlovu, 2014; Seepe, 2015).

5.1.4 Acid retardation tests

The metal barren solution remains with some acidity, which poses serious environmental threats when discharged in the biosphere. However, the acid could be recovered and the financial gains used to offset the AMD treatment costs. Therefore, acid retardation tests were conducted to test the feasibility of acid recovery from AMD using Dowex MSA-1 ion exchange resins. The effect of flow rate (0.83 to 1.50 mL/s at 20 cm height) and bed height (10 to 30 cm at 0.83 mL/s) on acid uptake was investigated. The results showed that Dowex MSA-1 has the ability to adsorb acid from an AMD solution. The acid uptake was attributed to the acid retardation process caused by the Donnan effect. The breakthrough times ranged from 2 to 8 minutes when the bed height was increased from 10 to 20 cm, while maintaining a constant flow rate of 0.83 mL/s. In addition, the breakthrough times increased from 2 to 6 minutes when the flow rate was reduced from 1.50 to 0.83 mL/s, at a constant bed

height of 20 cm. The maximum acid uptake of approximately 33% was obtained at a bed height of 30 cm and 0.83 mL/s flow rate. However, the acid content in the effluent still remained substantial high possibly due to the insufficient residence time of the solution in the column, which was caused by the high influent flow rates. Reducing the flow rate below 0.83 mL/s was not possible in this study due to the limitations of the available pumps.

Elution tests were, subsequently, carried out in order to recover the acid from the loaded resins. The results showed that water can be used as an eluent for acid recovery. The release of the acid was attributed to the difference in osmotic pressure between the eluent and the loaded resins (Agrawal and Sahu, 2009). Higher flow rates were found to increase the rate of acid desorption due to the increase in turbulence which also increases the osmotic pressure difference, and consequently acid release. Approximately 11 to 12 cycles (1 cycle equivalent to 1 bed volume of resins) of water were required to completely desorb the acid from the loaded resin, using an eluent flow rate of 1.50 mL/s.

5.1.5 Acid upgrade

To upgrade the concentration of the acid, the eluate from the elution process was evaporated in a rotary evaporator. The results showed that a concentrated acid product and water of re-usable quality could be obtained. Although, the eluate had minor Fe and other metal ion contaminants, the results from the evaporation process showed that Fe could be precipitated out of the solution as a jarosite at temperatures between 50 and 105 ˚C (Verner et al., 1980). The trend in the results indicated that slower flow rates may be required to ensure adequate contact time required for higher acid uptake. The research also showed that a water product suitable for recycle or use in other processes such as dust suppression could be obtained from the acid upgrade process.

5.1.6 Economic evaluation

The economic evaluation of the proposed process showed that the revenue from the sulphuric acid can be used to offset some of the operational costs such as the purchase of raw materials etc. However, the high energy costs associated with the acid upgrade process was found to be a major concern on the economics of the process. Finding cheaper alternative energy sources and applying energy optimization will greatly increase the financial viability of the proposed process. Furthermore, incorporating the concept of toxic metal removal using low cost biomass and sulphuric acid recovery to existing technologies such the HiPRO process will substantially reduce the operational costs of these processes, since the process will treat less contaminated water.

5.2 Recommendations

Based on the findings of the present research the following recommendations are proposed for future work:

- Conduct continuous flow metal adsorption studies on multiple fixed bed columns containing cassava waste biomass, in order to reduce the metal concentration in the effluent to permissible values.
- The batch results indicated that zeolite and bentonite adsorbents were able to remove most heavy metals particularly at higher adsorbent loadings. However, the treatment processes resulted in acid loss from the solution, as well as dissolution of the crystalline structures. Therefore, future studies should look at removing the acid first using the acid retardation process followed by adsorption.

- Batch studies also showed that an agitation speed between 160-180rpm is required for the optimal removal of Co^{2+} ions from a real AMD solution. Hence, future work should investigate the removal of Co^{2+} ions in this range.
- Conduct the acid retardation process using flow rates in the range of 1mL/min to investigate any improvement in the acid uptake.
- Compare the acid uptake from AMD using two or more different recommended ion exchange resins such as Dowex MSA-1 and LEWATIT-K 6362, etc.
- Investigate the effect of incorporating sulphuric acid recovery to existing technologies such as the HiPRO, SPARRO, etc. In addition, the overall process design (including process optimization) should also be greatly considered to choose the best process route in terms of efficiency as well as financial benefits.

REFERENCES

Abdel-Razek, A.S., 2011. Removal of chromium ions from liquid waste solutions using immobilized cunninghamella elegans. Nature and Science 9(7), 211-219.

Abia, A.A., Horsfall, M., Didi, O., 2003. The use of chemically modified and unmodified cassava waste for the removal of Cd, Cu and Zn ions from aqueous solution. Bioresource Technology 90, 345–348.

Ackil, A., Koldas, S., 2006. Acid mine drainage (AMD): causes, treatment and case studies. Journal of Cleaner Production 14, 1139-1145.

Adler, R.A., Claassen, M., Godfrey, L., Turton, A.R., 2007. Water, mining and waste. An historical and economic perspective on conflict management in South Africa. The Economics of Peace and Security Journal 2(2), 33-41.

Ahalya, N., Ramachandra, T.V., Kanamadi, R.D., 2003. Biosorption of Heavy Metals. Research Journal of Chemistry and Environment 7(4), 71-79.

Ahmad, A.A., Hameed, B.H., 2010. Fixed bed adsorption of reactive azo dye onto granular activated carbon prepared from waste. Journal of Hazardous Materials 175 (1-3), 298-303.

Ahmaruzzaman, M., Sharma, D.K., 2005. Adsorption of phenols from wastewater. Journal of Colloid and Interface Science 287, 14-24.

Aksu, Z., 1992. The biosorption of copper (II) by C. vulgaris and Zramigera. Environmental Technology 13, 579-586.

Aksu, Z., Gonen, F., 2004. Biosorption of phenol by immobilized activated sludge in a continuous packed bed: prediction of breakthrough curves. Process Biochemistry 39, 599-613.

Al-Anber, A.M, 2011. Thermodynamics Approach in the Adsorption of Heavy Metals, Thermodynamics - Interaction Studies - Solids, Liquids and Gases. ISBN: 978-953-307-563. Available at http://www.intechopen.com/books/thermodynamics interaction-studies-solids-liquids-and-gases/thermodynamics-approach-in-the-adsorption-of-heavy-metals. [Accessed: August 2015].

Ali, A. A., El- Bishtawio, R., 1997. Removal of lead and nickel ions using zeolite tuff. Journal of Chemical Technology and Biotechnology 67, 27-34.

Alibaba, 2015. Product prices. Available on http://www.alibaba.com/trade/search ?fsb=y&IndexArea=product_en&CatId=&SearchText=70%25. [Accessed: September 2015].

Aljil, S.A., Alsewailem, F.D., 2014. Adsorption of copper and nickel on bentonite clay from waste water. Athens Journal of National and Formal Sciences 1(1), 21-30.

Altin, O., Ozbelge, O.H., Dogu, T., 1999. Effect of pH, flow rate and concentration on the sorption of Pb and Cd on montmorillonite-Experimental. Journal of Chemical Technology and Biotechnology 74, 1131-1138.

Al-Shahrani, S.S., 2012. Treatment of wastewater contaminated with nickel using Khulays activated bentonite. International Journal of Engineering and Technology 12, 14-18.

Álvarez-Ayuso, E., Garcìa-Sánchez, A., Querol, X., 2003. Purification of metal electroplating waste waters using zeolites. Water Research 37, 4855-4862.

Anisuzzaman, S.M., Bono, A., Krishnaiah, D., Tau, Y.T., 2014. A study on dynamic simulation of phenol adsorption in activated carbon packed bed column. Journal of King-Saud University-Engineering Sciences. Available at http://dx.doi.org/10.1016 /j.jksues.2014.01.001. [Accessed: June 2015].

APV, 2015. Evaporator handbook, Fouth Edition. Available at http://userpages. umbc.edu/~dfrey1/ench445/apv_evap.pdf. [Accessed: September 2015].

Arenas, L. T., Lima, E. C., dos Santos, A. A., Vaghetti, J. C. P., Costa, T. M. H., Benvenutti, E. V., 2007. Use of statistical design of experiments to evaluate the sorption capacity of 1,4-diazoniabicycle (2.2.2) octane/silica chloride for Cr (VI) adsorption. Colloids and Surfaces A: Physicochemical and Engineering Aspects 297, 240-248.

Argun, M.E., 2008. Use of clinoptilolite for the removal of nickel ions from water: Kinetics and thermodynamics. Journal of Hazardous Materials 150, 587-595.

Arienzo, M., Chiarenzelli, J., Scrudato, R., 2001. Remediation of metal-contaminated aqueous systems by electrochemical peroxidation: An experimental investigation. Journal of Hazardous Materials 87, 187-198.

Bailey, S.E., Trudy, J., Olin, T.J., Bricka, M.R., Adrian, D.D., 1999. A review of potentially low-cost sorbents for heavy metals. Water Research 33(11), 2469-2479.

Baker, J. P., Schofield, C. L., 1982. Aluminium toxicity to fish in acidic waters. Water, Air, and Soil Pollution 18, 289-309.

Beliles, R.P., 1978. Toxicity in Heavy Metals in the Environment. Part 2, Marcel Dekker, New York.

Benzaazoua, B., Bussiere, B., Kongolo, M., McLaughlin, J., Marion, P., 2000. Environmental desulphurization of four Canadian mine tailings using froth flotation. International Journal of Mineral Processing 60(1), 57-74.

Benzaazoua, B., Bussiere B., 2002. Chemical factors that influence the performance of mine sulphidic paste backfill. Cement and Concrete Research 32(7), 1133-1144.

Blanchard, G., Maunaye, M., Martin, G., 1984. Removal of heavy metals from waters by means of natural zeolites. Water Research 18(12), 1501-1507.

Blowes, D.W., Ptacek, C.J., Jambor, J.L., Weisener, C.J., 2003. The geochemistry of acid mine drainage. Treatise on Geochemistry 9, 149-204.

Blueprint, 2009. Emalahleni; Blueprint for treatment of acid mine drainage. Available at http://www.avengwater.co.za/news-room/press-releases/emalahleni-blueprint-treatment-amd. [Accessed: February 2014].

Bohart, G.S., Adams, E.Q., 1920. Some aspects of the behavior of charcoal with respect to chlorine. Journal of the American Chemical Society 42(3), 523-544.

Boonstra, J.V.L.R., Janssen, G., Buisann, C.J.N., 1999. Biological treatment of acid mine drainage. Bio Hydrometallurgy and the Environment toward the Mining of the 21st century, Elsevier, 559-567.

Bowell, R.J., 2000. Sulfate and salt minerals: the problem of treating mine waste. Mining and Environmental Management, 11-14.

Brown, D.J.A., Sadler, K., 1989. Fish survival in acid waters. In: Acid Toxicity and Aquatic Animals Society for Experimental Biology Seminar Series 34.Cambridge University Press, 31-44.

Brown, C.J., Davey, D., Simmons, P.J., 1979. Purification of sulphuric acid anodizing solutions. Plating and Surface Finishing 66, 54.

Brown, C.J., Russer, A., Sheedy, M., 1987. New ion exchange processes for brine purification. US patent 1564492.

Brown, C.J., 1990. Productivity improvements through recovery of pickle liquors with the APU. Iron and Steel Engineer, 55-60.

Brown, C.J., 1996. The Flourex process for regeneration of nitric/Hydrofluoric stainless steel pickle liquors. In: 2nd International Symposium on ion control in hydrometallurgy, Ottawa.

Brown, C.J., 2002. Recovery of stainless pickle liquors: Purification vs regeneration. Eco-tech Technical paper 158.

Brunauer, S., 1943. The adsorption of gases and vapours. Oxford University Press.

Calero, M., Hernainz, F., Blazquez, G., Tenorio, G., Martin-lara, M.A., 2009. Study of Cr (III) biosorption in a fixed bed column. Journal of hazardous material 171, 886-893.

Cağin, V., 2006. Use of clinoptilolite for copper and nickel removal from aqueous solutions. PhD thesis. Middle East Technical University.

Chen, T., Yan, B., Chan, L., Xiao, X., 2014. Pollution control and metal resource recovery for acid mine drainage. Hydrometallurgy 147–148, 112–119.

Chermak, J.A., Runnells, D.D., 1997. Development of Chemical Caps in Acid Rock Drainage Environments. Society for Mining, Metallurgy and exploration 49(6), 93-97.

Coetzee, H., Van Tonder., Wade, P., Esterhuyse, S., 2007. Acid mine drainage in the Witwatersrand. Council for Geoscience, 180.

Crini, G., Badot, P-M, 2010. Sorption processes and pollution: Conventional and non-conventional sorbent for pollutant removal from wastewaters. ISBN 978-2-84867-404-2.

Ćurkovic, L., Cerjan-Stefanović, Š. Filipan, T., 1997. Metal ion exchange by natural and modified zeolites. Water resource 31, 1379-1382.

Cushnie, G.C., 2009. Pollution Prevention and Control Technologies for Plating Operations (Second edition). Ann Arbor, Michigan: National Center for Manufacturing Sciences.

Dakovic, A., 1986. Surface modified zeolites-Adsorbents for mycotoxins and carriers of drugs. In: 3rd Croatian-Slovenian Symposium on Zeolites.

Davis, J.G., Burgoa, B., 1995. Interactive mechanisms of anion and adsorption with calcium leaching and exchange. Soil Science 160, 256-264.

De Deitrich processing systems, 2013. Concentration of sulphuric acid and its application. Available on http://www.qvf.com/qvf-process-systems/mineral-acids/concentrationing-of-sulfuric-acid.html. [Accessed on 08/01/15].

De Beer, M., Maree, J.P., Wilsenach, J., Motaung, S., Bologo, L., Radebe, V., 2012. Acid Mine Water Reclamation using the ABC Process. CSIR: Natural Resources and the Environment.

Dejak, M., Munns, K., 1987. Acid purification and recovery using resin sorption technology-A review. Environmental II (F), 1-20.

Dold, B., 2010. Basic concepts in environmental geochemistry of sulphide mine waste management. In: Kumar, E.S. (Editor), Waste management. In-tech, Rijeka, 173-198.

Doula, M., Ioanoou, A., Dimirkou, A., 2002. Copper adsorption and Si, Al, Ca, Mg and Si release from clinoptilolite. Journal of Colloid and Interface Science 245, 237-250.

Doula, M.K., Ioanoou, A., 2003. The effect of electrolyte anion on Cu adsorption desorption by clinoptilolite. Microporous and Mesoporous Materials 58, 115-130.

Dowex, 2001. Lab guide-Column separations using resins and adsorbents. Available at http://msdssearch.dow.com/PublishedLiteratureDOWCOM/dh_015a/0901b8038015ac4e.pdf?filepath=liquidseps/pdfs/noreg/016-00003.pdf&fromPage=GetDoc. [Accessed: June 2014].

Dowex, 2002. Ion Exchange resins: Powerful Chemical Processing Tools. The Dow Chemical Co, form number 177-01395-603QRP.

Du Pleiss, G.H., Swartz, J.A., 1992. Tubular Reverse Osmosis treatment of Secunda mine water: a pilot plant investigation. Water Science Technology 25, 193-201.

DWAF (Department of Water Affairs and Forestry), 1996. South African Water Quality Guidelines (second edition), Volume 3: Industrial Use.

Earle, J. and Callaghan, T., 1998. Impacts of mine drainage on aquatic life, water uses, and man-made structures. Department of Environmental Protection, Chapter 4, 4.1 – 4.10.

Ekolu, S., Diop, S.D., Azene, F., 2014. Analysis of corrosion characteristics of acid mine drainage on infrastructure materials. Available on http://reference.sabinet. co.za/webx/access/electronic_journals/civeng/civeng_v22_n7_a4.pdf. [Accessed: April 2016].

Englert, A. H., Rubio, J., 2005. Characterisation and environmental application of a Chilean natural zeolite, International Journal of Mineral Processing 75, 21-29.

Enslin, F., Mey, V., Waander, L.F., 2010. Acid leaching of heavy metals from bentonite clay, used in the cleaning of acid mine drainage. The Journal of the Southern African Institute of Mining and Metallurgy 110, 187-191.

EPA, 1980. Construction cost for municipal wastewater treatment plans: 1973-1978. Technical report EPA/430/9-80-003.

EPA, 2008. Report on the Environment-Final Report. Available on http://cfpub.epa. gov/ncea/cfm/recordisplay.cfm?deid=190806. [Accessed: February 2014].

Erdem, E., Karapinar, N., Donat, R., 2004. The removal of heavy metal cations by natural zeolites. Journal of Colloid and Interface Science 280, 309-314.

Esposito, A., Pagnanelli, F., Veglio, F., 2002. pH-related equilibria models for biosorption in single metal systems. Chemical Engineering Science 57, 307–13.

Evangelou, V. P., 1995. Pyrite oxidation and its control. New York: CRC press, 275.

Evangelou, V. P., 1998. Pyrite chemistry: the key for abatement of acid mine drainage. In: Geller A, Klapper H, Salomons W (editors). Acidic Mining Lakes: Acid Mine Drainage, Limnology and Reclamation. Berlin Springer, 197– 222.

Everett, D.J., Plessis, J.D., Gussman, H.W., 1999. The treatment of underground mine water for the removal of calcium and sulphates by a GYP-CIX, process. In: International Mine Water Association Symposium, Zambia.

Faghihian, H., Marageh, M.G., Kazemian, H., 1999. The use of clinoptilolite and its sodium form for removal of radioactive caesium, and strontium from nuclear wastewater and Cu^{2+}, Ni^{2+}, Co^{2+}, Ba^{2+} form municipal wastewater. Applied Radiation and Isotopes 50, 655-660.

Falayi, T., Ntuli, F., 2014. Removal of heavy metals and neutralisation of acid mine drainage with un-activated attapulgite. Journal of Industrial and Engineering Chemistry 20, 1285–1292.

Febrianto, J., Kosasih, A.N., Sunarso, J., Ju, Y., Indraswati, N., Ismadji S., 2009. Equilibrium and kinetic studies in adsorption of heavy metals using biosorbent: A summary of recent studies. Journal of Hazardous Materials 162, 616-645.

Fiol, N., Villaescusa, M., Martinez, N., Miralles, J., Poch, J., Serarol, S., 2006. Sorption of Pb(II), Ni(II), Cu(II) and Cd(II) from aqueous solution by olive stone waste. Separation and Purification Technology 50, 132–140.

Freundlich, H., 1906. Uber die adsorption in lusungen. Journal of Physical Chemistry 57, 385. (In German).

Fripp, J., Ziemkiewicz, P.F., Charkavork, H., 2000. Acid mine drainage treatment - Technical Notes Collection. Vicksburg: Army Engineer Research and Development Center. Report No. ERDC TN-EMRRPSR-14.

Fromm, P.O., 1980. A review of some physiological and toxicological responses of freshwater fish to acid stress. Environmental Biology of Fishes 5(1), 79-93.

Fu, F., Wang, Q., 2011. Removal of heavy metal ions from wastewaters: a review. Journal of Environmental Management 92, 407–418.

Gadd, G.M., White, C., DeRome, L., 1988. Heavy metal and radionuceotide uptake by fungi and yeasts. In: Norri, R.., Kelly, D.P., (Editors.), Biohydrometallurgy. Chippenham, Wilts, UK.

Gardea-Torresday, J.L., Becker-Hepak, M.K., Hosea, J.M., Darnall, D.W., 1990. Effects of Chemical Modification of Algae Carboxyl Groups on Metal Ion Binding. Environmental Science Technology 24, 1372-1378.

Ghomri, F., Lahsini, A., Laajeba, A., Addaaou, A., 2013. The removal of heavy metal ions (copper, zinc and cobalt) by natural zeolite. Larhyss Journal, ISSN 1112-3680, 37-54.

Goksungur, Y., Uren, S., Guvenc, U., 2003. Biosorption of Copper Ions by caustic treated waste baker's yeast biomass. Turkish Journal of Biology 27, 23-29.

Grippo, R., 2005. Manganese as an Aquatic Pollutant. In: Workshop on Manganese in Coal Mine Drainage US Department of the Interior Office of Surface Mining.

Gülbas, M., Kammel, R., Lieber, H.W., 1987. Improvements of hydrometallurgical processes by application of the acid retardation procedure-actual situation and developments. Institute for Metallurgy, Technical University of Berlin, Germany.

Gunay, A., Arslankaya, E., Tosun, I., 2007. Lead removal from aqueous solution by natural and pretreated clinoptilolite: Adsorption equilibrium and kinetics. Journal of Hazardous Material 146, 362-371

Harland, C.E., 1994. Ion Exchange: Theory and Practice, second edition. The Royal Society of Chemistry.

Halcomb, M., McMinnville, T., Fare, D., Witte, W.T., 2009. Soil pH explained. Agricultural Extension Service. The University of Tennesse. Availabe at http://www.utextension.utk.edu/mtnpi/handouts/Fertility/Soil_pH_Explained.pdf.[Accessed: June 2014].

Hatch, M., Dillon, J., 1963. Acid retardation: simple physical method for separation of strong acids from their salts. Industrial and Engineering Chemistry Process Design and Development 4, 253-263.

Hasany, S.M., Saeed, M.M., Ahmed, M., 2002. Journal of Radioanalytical and Nuclear Chemistry 252, 477.

Hedin R.S., 2003. Recovery of marketable iron oxide from acid mine drainage in the USA. 93-97.

Hodge, W.W., 1937. Pollution of Streams by Coal Mine Drainage. Industrial and Engineering Chemistry 29, 1048-1055.

Hoehn, R.C., Sizemore, D.R., 1977. Acid mine drainage (AMD) and its impact on a small Virginia stream. Water Resources Bulletin 13, 153-160.

Horsfall, Jr, M., Abia, A, A., 2003. Sorption of cadmium (II) and zinc (II) ions from aqueous solutions by cassava waste biomass (Manihot Sculenta Cranz). Water Research 37, 4913- 4923.

Howard, D., Gobler, C., Robinson, R.E.G., Cole, P.M., 2009. Sustainable purification of mine water using ion exchange technology. In: Abstracts of the International Mine Water Conference, 447-453.

Inglezakis, V.J., Diamandis, N.A.D., Loizidou, M.D., Grigoropoulou, H.P., 1999. Effect of pore clogging on kinetics of lead uptake by clinoptilolite. Journal of Colloid and Interface Science 215, 54 – 57.

Inglezakis, V.J, Hadjiandreou, M.D. Loizidou, M.D., Grigoropoulou, H.P., 2001. Pretreatment of natural clinoptilolite in a lab scale ion-exchanged packed bed. Water Research 35, 2161-2166.

Inglezakis, V.J, Loizidou, M.D., Grigoropoulou, H.P., 2004. Ion exchange studies on natural and modified zeolites and the concept of exchange site accessibility. Journal of Colloid and Interface Science 275, 570-576.

International Network for Acid Prevention (INAP), 2003. Treatment of sulphate in mine water effluent. Available at http://www.inap.com.au. [Accessed: October 2013].

Inter-ministerial Committee (IMC), 2010. Mine water managements in the Witwatersrand with special emphasis on acid mine drainage report to the inter-ministerial committee, December.

Jal, P.K., Patel, S., Mishra, B.K., 2004. Chemical modification of silica surface by immobilization of functional groups for extractive concentration of metal ions. Talanata 62, 1005-1028.

Jennings, S.R., Neuman, D.R., Blicker, P.S., 2008. Acid Mine Drainage and Effects on Fish Health and Ecology: A Review. Reclamation Research Group Publication, Bozeman, MT.

Johnson, D.B., Hallberg K.B., 2005. Acid mine drainage remediation options: a review. Science of the Total Environment 338, 3-14.

Juby, G.J.G., Schutte, C.F., Leeuwen, J., 1996. Desalination of calcium sulphate scaling mine water: Design and operation of the SPARRO process. Division of Water Utilisation Engineering, Department of Chemical Engineering- University of Pretoria, South Africa.

Juby, G.J.G., 1989. Membrane desalination of mine water. In: WISA Conference.

Kalayci, T., Bardakç, B., Kinaytürk, N.K., 2013. Removal of 2-Nitrophenol by Linde Type A (LTA) zeolites. International Journal of Physical Sciences 8(1), 1-5.

Kapanji, K.K., 2009. The removal of heavy metals from waste water using South Africa clinoptilolie. MSc Dissertation. University of the Witwatersrand, JHB.

Kapoor, A., Virarahgavan, T., 1998. Biosorption of heavy metals on Aspergillus niger: Effect of pretreatment. Bioresource Technology 63, 109-113.

Karathasis, A.D, Barton, C.D., 1999. Aerobic and Anaerobic metal attenuation processes in constructed wetland treating acid mine drainage. Environmental Geosciences 5(2), 43-56.

Kaya, A., Oren, H.A., 2005. Adsorption of zinc from aqueous solutions to bentonite. Journal of Hazardous Materials 125(1-3), 183-189.

Koryak, M., Shapiro, M.A., Sykora, J.L., 1972.Rifle zoobenthos in streams receiving acid mine drainage. Water Research 6, 1239-1247.

Kosasih, A.N., Febriantoa, J., Sunarsoc, J., Jua, Y-H., Indraswatib, N., Ismadjia S., 2010. Sequestering of Cu(II) from aqueous solution using cassava peel (Manihot esculenta). Journal of Hazardous Materials 180, 366–374.

Kurniawana, A., Kosasiha, N.A., Febriantoa, J., Jub, Y., Sunarsoc, J., Indraswatia, N., Ismadjia, S., 2011. Evaluation of cassava peel waste as low cost biosorbent for Ni-sorption: Equilibrium, kinetics, thermodynamics and mechanism. Chemical Engineering Journal 172, 158– 166.

Kuyucak N., Volesky, B., 1988. Biosorbents for recovery of metals from industrial solutions. Biotechnology Left 10 (2), 137-142.

Lapakko, K., 2012. Metal mine rock and waste characterisation tools: an overview. Mining. Minerals and Sustainable Development 67, 1-25.

Levenspiel, O., 1999. Chemical Reaction Engineering, 2nd Edition. Wiley Eastern Ltd, 41-92.

Lewis, M.E., Clark, M.L., 1997. How does streamflow affect metals in the upper Arkansas river. US Department of Interior Geological Survey.

Liu, Y., Liu, Y. J., 2008. Biosorption isotherms, kinetics and thermodynamics. Separation and Purification Technology 61 (3), 229-242.

Langmuir, I., 1916. The Constitution and fundamental properties of solids and liquids: Part 1. Journal of American Chemical Society 38(11), 2221-2295.

Luther I. G. W., 1987 Pyrite oxidation and reduction: molecular orbital theory considerations. Geochimica et Cosmochimica Acta 51, 3193–3199.

Mackay, J.G., Wiechers, H.N.S., Pulles, W., Howarth, D., Busby, R.W., Combrinck C., 1991.Water quality and associated cost implications for South Africa gold mining industry. In: 2nd Biennial Conference of the Water Institute of South Africa, Johannesburg, May.

Maryland, 1994. Removing heavy metals from wastewater. Engineering research center report. University of Maryland. United States of America.

McCarthy, T.S., 2011. The impact of acid mine drainage in South Africa. South African Journal of Science 107(5/6).

McKibben, M. A., Barnes, H. L., 1986. Oxidation of pyrite in low temperature acidic solutions: rate laws and surface textures. Geochimica et Cosmochimica Acta 50, 1509-1520.

Meena, K.A., Mishra, K.G., Rai, K.P., Rajagol, C., Nagar, P.N., 2005. Removal of heavy metal ions from aqueous solutions using carbon aerogel as an adsorbent. Journal of Hazardous Materials 122 (1-2), 161-170.

Morris, M.E., Levy, G., 1983. Absorption of sulphate from orally administered magnesium sulfate in man. Journal of Toxicology-Clinical Toxicology 20, 107.

Morris, R., Taylor, E.W., Brown, D.J.A., Brown, J.A., 1989. Acid toxicity and aquatic animals. Society for experimental Biology Seminar Series 34. Cambridge University Press, 282.

Moses, C.O., Nordstrom, D.K., Herman, J.S., Mills, A.L., 1987. Aqueous pyrite oxidation by dissolved oxygen and ferric iron. Geochimica et Cosmochimica Acta 51, 1561-1571.

Motsi, T., Rowson, N.A., Simmons, M.J.H., 2009. Adsorption of heavy metals from acid mine drainage by natural zeolite. International Journal of Minerals and Processing 92, 42-48.

Motsi, T., 2010. Remediation of acid mine drainage using natural zeolite. PhD Thesis. University of Birmingham. United Kingdom.

Mumpton, A.F., 1999. La roca magica; Uses of natural zeolites in agriculture and industry. In: National Academy of Sciences Colloquim, USA.

Naicker, K., Cukrowska, E., McCarthy, T.S., 2003. Acid mine drainage arising from gold mining activities in Johannesburg, South Africa and environs. Journal of Environmental Engineering 122, 29–40.

Naja, G., Volesky, B., 2006. Behaviour of the mass transfer zone in a biosorption column. Environmental Science and Technology 40(12), 3996-4003.

Ndlovu, S., Simate, G.S., Seepe, L., Shemi, A., Sibanda, V., Van Dyk, L., 2013. Removal of Co^{2+}, V^{3+} and Cr^{3+} from synthetic waste water using cassava waste. South African Journal of Chemical Engineering 18, 51-69.

Neba, A., 2007. The Rhodes BioSURE process and the use of sustainability indicators in the development of biological mine water treatment. PhD Thesis. Rhodes University, Grahamstown.

Nightingale, E.R., 1959. Phenomenological theory of ion solvation. Effective radii of hydrated ions. Journal of Physical Chemistry 63, 1381-1387.

Noh, J. S., Schwarz, S., 1990. Effect of HNO_3 treatment on the surface acidity of activated carbon. Carbon 28, 675-682.

Novhe, N.O., 2012. Evaluation of the applicability of the passive treatment for the management of polluted mine water in the Witwatersrand Goldfields, South Africa. International Mine Water Association annual conference, 417-424.

Nsimba, B.E., 2012. Development of biophysical system based on bentonite, zeolite and microorganisms for remediating gold mine waste waters and tailings ponds. PhD Thesis. University of the Witwatersrand .JHB.

Ochieng, M.G., Seanego, S.E., Nkwonta, O.I., 2010. Impacts of mining on water resources in South Africa: A review. Scientific Research and Essays 5(22), 3351-3357.

Oliveira, R. C., Jouannin, C., Guibal, E., Garcia Jr, O., 2011. Samarium (III) and praseodymium (III) biosorption on Sargassum sp: Batch study. Process Biochemistry 46(3), 736-744.

O'Neail, T. M., Kirchner, O.E., Day, W.J., 1981. Achieving high recovery from brackish water with seeded reverse osmosis systems. In: 42nd Annual Meeting, International Water Conference, Pittsburgh, Pennsylvania, October.

Pandey, P. K., Sharma, S. K., Sambi, S. S., 2010. Kinetics and equilibrium study of chromium adsorption on zeolite NaX. International Journal of Environmental Science and Technology 7 (2), 395-404.

Parujen, P., 1997. Anodizing acid purification using resin sorption technology at Pioneer metal finishing. Eco-Tec Technical paper 124.

Pehlivan, E., Altun, T., 2006. The study of various parameters affecting the ion exchange of Cu^{2+},Zn^{2+},Ni^{2+},Cd^{2+},and Pb^{2+} from aqueous solution on Dowex 50W synthetic resin. Journal of Hazardous Materials 134 (1-3), 149-156.

Pérez, N., Sánchez, M., Rincón, G., Delgado, L., 2007. Study of the behavior of metal adsorption in acid solutions on Lignin using a comparison of different adsorption isotherms. Lating American Applied Research 37, 157-162.

Perić, J., Trgo, M., Medvidović, N.V., 2004. Removal of zinc, copper and lead by natural zeolite- a comparison of adsorption isotherms. Water Research 38, 1893-1899.

Peter, M. S., Timmerhaus, K.D., 1991. Plant economics for chemical engineers. Fifth Edition. Clark , B.J., and Morris, J.M. (Editors).

PIRAMID-Consortium, 2003. Engineering guidelines for passive remediation of acidic and/or metalliferous mine drainage and similar wastewaters. University of Newcastle, Newcastle Upon Tyne, UK.

Pratt, S.E., 2011. All that glitters. Acid mine drainage: The toxic legacy of gold mining in South Africa, Earth magazine. 23 September. Available at http://www. earthmagazine .org/article/all-glitters-acid-mine-drainage-toxic-legacy-gold-mining-south-africa. [Accessed: October 2013].

Pulles, W., Juby, G.J.B., Busby, R.W., 1992. Development of slurry precipitation and recycle reverse osmosis (SPARRO) technology for desalinating scaling mine waters. Water Science and Technology 25(10), 177-192.

Rangasayatorn, N., Pokethitiyook, P., Upatham, E.S., Lanza, G.R., 2004. Cadmium biosorption by cells of Spirulina platensis TISTR 8217 immobilized in alginate and silica gel. Environmental International 30, 57-63.

Rengaraj, S., Joo, C.K., Kim, Y., Yi, J., 2003. Kinetics of removal of chromium from water and electronic process wastewater by ion exchange resins. Journal of Hazardous Materials 102 (2-3), 257-275.

Ribeiro, F.R., Rodrigues, A.E., Rollmann, L.D., Naccache, C., 1984. Zeolites: Science and Technology. Martinus Nijhoff Publishers, the Hague.

Richardson, J.F., Harker, J.H., Backhurst, J.R., 2002. Coulson and Richardson's Chemical Engineering Volume 2, Fifth edition, Butterworth Heinemann.

Rivera, A., Fuentes, G.R., Altschuler, E., 2000. Time evolution of a natural clinoptilolite in aqueous medium: conductivity and pH experiments. Microporous and Mesoporous Materials 40(1-3), 173-179.

Robertson, A. M., Rohrs, R.G., 1995. Sulphate removal of acid mine drainage water after lime treatment. In: Conference on Mining and the Environment, Sudbury, Ontario, 575-586.

Robinson, R.E., Barnard, R., Le Riche, J.J., 1998. The treatment of acid effluent from Grootvlei mine using novel IX techniques. Journal of the South African Institute of Mining and Metallurgy, 343-353.

Sahoo, K.P., Kim, K, Equeenuddin, M.S., Powell, M.A., 2013. Current approaches for mitigating acid mine drainage. Reviews of Environmental Contamination and Toxicology 1 (226), 1-32.

Sanchez, E., Lopez-Pamo, E., Santofimia, E., Aduvire, O., Reyes, J., Barettino, D., 2005. Acid mine drainage in the Iberian Pyrite Belt (Spain): Geochemistry, mineralogy and environmental implications. Applied Geochemistry 20(7), 1320-1356.

Sanchez, J., 2008. Acid mine drainage in the Iberian pyrite belt: an overview with special emphasis on generation mechanisms, aqueous composition and associated mineral phases. Conferencia invitada: Sánchez Espana Macla 10, 34-43.

Sarkar, M., Acharya, P.K., 2006. Use of fly ash for the removal of phenol and its analogues from contaminated water. Waste Management 26, 559–570.

Scheidegger, A.M., Sparks, D.L., 1996. A critical assessment of sorption-desorption mechanisms at the soil mineral/water interface. Soil Science 161(12), 813-831.

Schorr, M.S., Baker, C.J., 2006. Localised effects of coal mine drainage on fish assemblages in a Cumberland Plateau stream in Tennessee. Chattanooga, Tennessee.

Sheedy, M., 1998. Recoflo ion exchange technology. In: TMS annual meeting, San Antonio, Texas.

Sheedy, M., Parujen, P., 2012. Acid separation for impurity control and acid recycle using short bed ion exchange. The Minerals, Metal and Materials Society 2012.

Shen, J., Duvnjak, Z., 2005. Adsorption kinetics of cupric and cadmium ions on corncob particles. Process Biochemistry 40, 3446-3454.

Sibiliski, U., 2001. AngloGold desalination pilot plant project. In: Conference on environmental responsible mining in South Africa, September 2001. CSIR, Pretoria, South Africa.

Silva, R., Rubio, L., 2011. Sulphate ions removal from aqueous solution: Separation from coal effluents using aluminium-bearing salt. 2- 6.

Simate, G.S., 2012. The treatment of brewery wastewater using nanotubes synthesized from carbon dioxide carbon source. PhD Thesis. University of the Witwatersrand, Johannesburg.

Simate, S.G., Ndlovu, S., 2014. The removal of heavy metals in a packed bed column using immobilized cassava peel waste biomass. Journal of Industrial and Engineering Chemistry 21, 635-643.

Singer, P. C., Stumm, W., 1970. Acid mine drainage: The rate determining step. Science 167, 1121-1123.

Singh, G., 1987. Mine water quality deterioration due to acid mine drainage. International Journal of Mine water 6(1), 49-61.

Singh, R., Guatam, N., Mishra, A., Gupta, R., 2011. Heavy metals and living organisms: An overview. Indian Journal of Pharmacology 43(3), 246-253.

Sinnott, R.K., 2005. Coulson & Richardson's Chemical Engineering, Volume 6, Chemical Engineering Design (4th Edition), Elsevier

Smith, J.P., 1999. The purification of polluted mine water. In: International symposium on Mine, Water and Environment (IMWA) Congress, Seville, Spain.

Stumm, W., 1991. Chemistry of the Solid–Water Interface. J. Wiley and Sons Inc., New York.

Stumm, W., Morgan, J.J., 1996. Aquatic chemistry: equilibria and rates in natural waters. Willey-Interscience, New York.

Summers, Jr, B.L., Gress, L, B, Aero-Terra-Aqua Technology Corp., 1996. Bead for removing dissolved metal contaminants. US Patent 5578547.

Swart, E., 2003. The South African legislative framework for mine closure. Journal of South African Institute of Mining and Metallurgy, 489-492.

Tangaromsuk, J., Pokethitiyook, P., Kruatrachue, M., Upatham, E.S., 2002. Cadmium biosorption by Sphingomonas paucimobilis biomass. Bioresource Technology 85, 103-105.

Taty-Costodes, V.C., Fauduet, H., Porte, C., Ho, Y.S., 2005. Removal of lead (II) ions from synthetic and real effluents using immobilized Pinus sylvestris sawdust: Adsorption on a fixed-bed column. Journal of Hazardous Material 123, 135-144.

Thomas, H.C., 1944. Heterogeneous ion exchange in a flowing system. Journal of the American Chemical Society 66 (10), 1664–1666.

Thomas, C.L., Hickley, J., and Stecker, G., 1950. Chemistry of clay cracking catalysts. Industrial and Engineering Chemistry 42, 866-871.

Trgo, M., Peric, J., 2003. Interaction of the zeolitic tuff with Zn containing simulated pollutant solutions. Journal of Colloid and Interface Science 260, 1017-1021.

Triantafyllou, S., Christodoulou, E., Neou-Syngouna, P., 1999. Removal of nickel and cobalt from aqueous solutions by Na-activated bentonite. Clays and Clay Minerals 47 (5), 567–572.

USEPA, 2002. Edition of Drinking Water Standards and Health Advisories. EPA 822-R-02-038, Washington DC.

Valdes, H., Sanchez-Polo, M., Rivea-Utrilla, J., Zaroor, C.A., 2002. Effect of ozone treatment on surface properties of activated carbon. Langmuir 18, 2111-2116.

Vatavuk, 2002. Updating the CE plant cost index. Available at http://www. chemengonline.com/Assets/File/CEPCI_2002.pdf. Accessed [September 2015].

Verner, B., Sefton, E., Godefridus, M.S., Kirby, C.R., Genik-Sas-Berezowsky, E., 1980. Process for the precipitation of iron as jarosite. US Patent 4193970.

Vijayaraghavan, K., Jegan. J., Palanivelu. K., Velan. M., 2005. Batch and column removal of copper from aqueous solution using a brown marine alga Turbinaria ornata. Chemical Engineering Journal 106, 177-84.

Volesky, B., 1990. Biosorption and biosorbents. In: Biosorption of heavy metals. Volesky, B. (Editor), CRC press. Boca Rotan, Florida.

Volesky, B., 2001. Detoxification of metal-bearing effluents: biosorption for the next century. Hydrometallurgy 59, 203-216.

Volesky, B., 2004. Sorption and Biosorption. BV Sorbex, Lambert, Quebec, Canada.

Volesky, B., 2007. Biosorption and me. Water Research 41, 4017–29.

Wang, J., Chen, C., 2006. Biosorption of heavy metals by Saccharomyces cerevisiae: A review. Biotechnology Advances 24, 427-421.

Wang, J., Xu, F., Xie, W., Mei, Z., Zhang, Q., Cai, J., Cai, W., 2009. The enhanced adsorption of dibenzothiophene onto cerium/nickel-exchanged zeolite Y. Journal of Hazardous Materials 163, 538-543.

Wan Ngah, W. S., Hanafiah, M. A. K. M., 2008. Removal of heavy metal ions from wastewater by chemically modified plant wastes as adsorbents: A review. Bioresource Technology 99, 3935-3948.

West, A., Kratchvil, D., Fatula, P., 2011. Sulphate removal from acid mine drainage for potential water re-use. In: 72nd Annual International Water Conference, Orlando, Florida.

Winde, F., Sandham, L.A., 2004. Uranium pollution of South African streams - an overview of the situation in gold mining areas of the Witwatersrand. Geo Journal 61, 131–149.

WHO, 1996. Guidelines for drinking water quality. Geneva, 2nd edition.

Xu, R., Pang, W., Yu, J., Huo, Q., Chen, J., 2007. Chemistry of zeolites and related porous materials: Synthesis and structure. John Willey and sons (Asia) Pte. Ltd. ISBN 978-0-470-82233-3.

Yadav, S.K., 2010. Heavy metals toxicity in plants: An overview on the role of glutathione and phytochelatins in heavy metal stress tolerance of plants. South African Journal of Botany 76, 167–179.

Younger, P.L., Banwart, S. A., Hedin, R. S., 2002. Mine Water: Hydrology, Pollution, Remediation. The Netherlands: Kluwer Academic Press.

Appendix A

Point of zero charge (pH_{PZC}) results

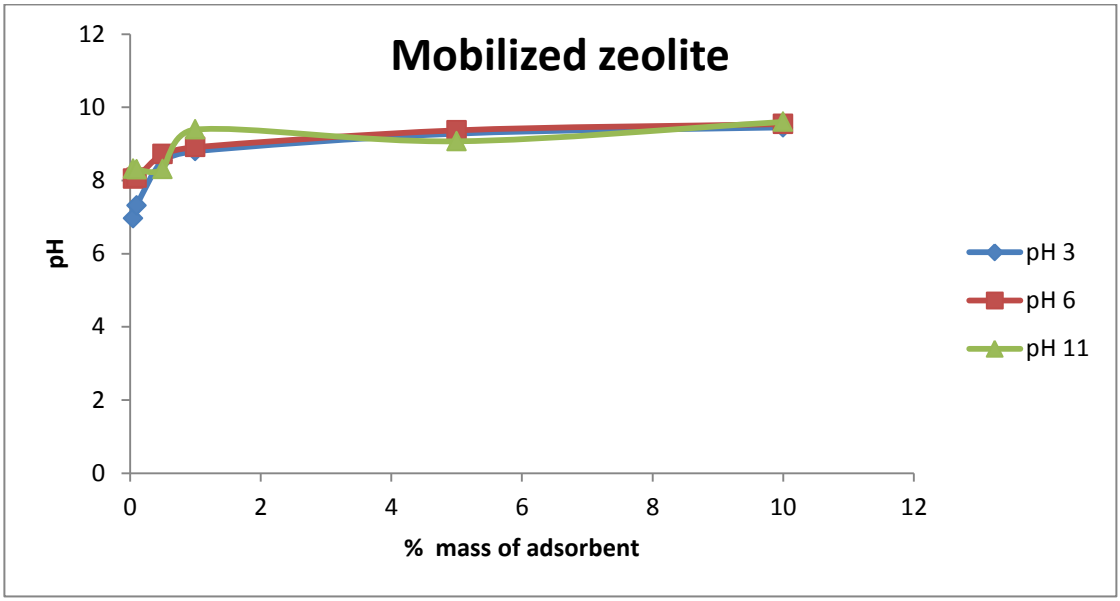


Figure A1: Mass titration results for mobilized zeolite

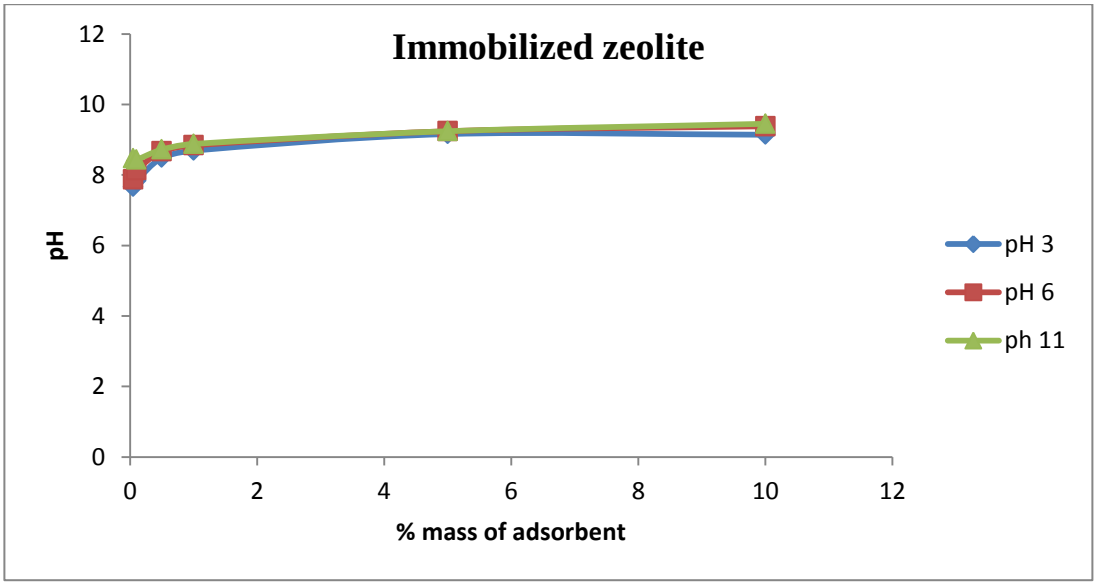


Figure A2: Mass titration results for immobilized zeolite

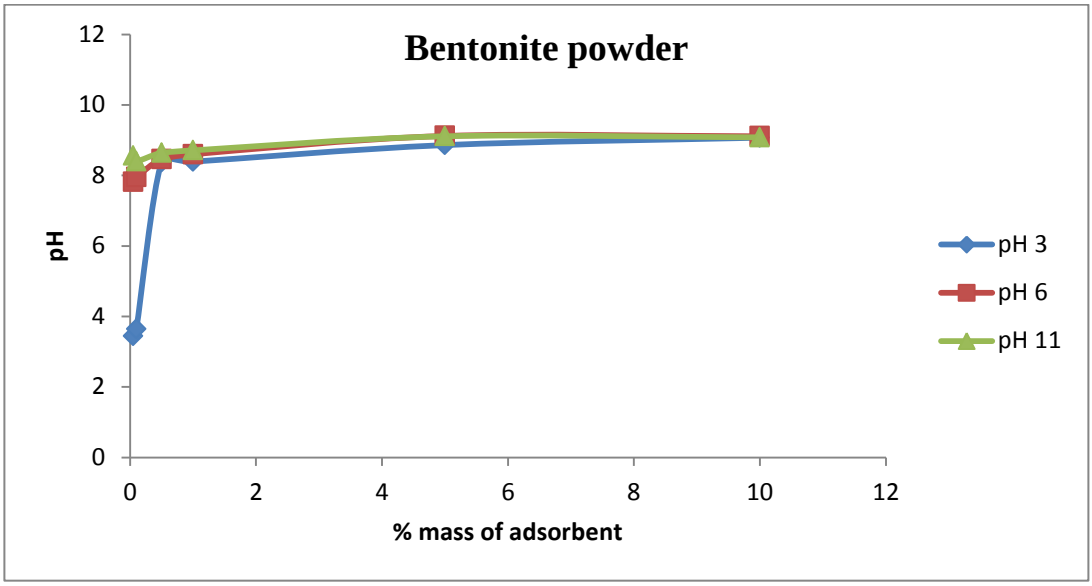


Figure A3: Mass titration results for bentonite powder

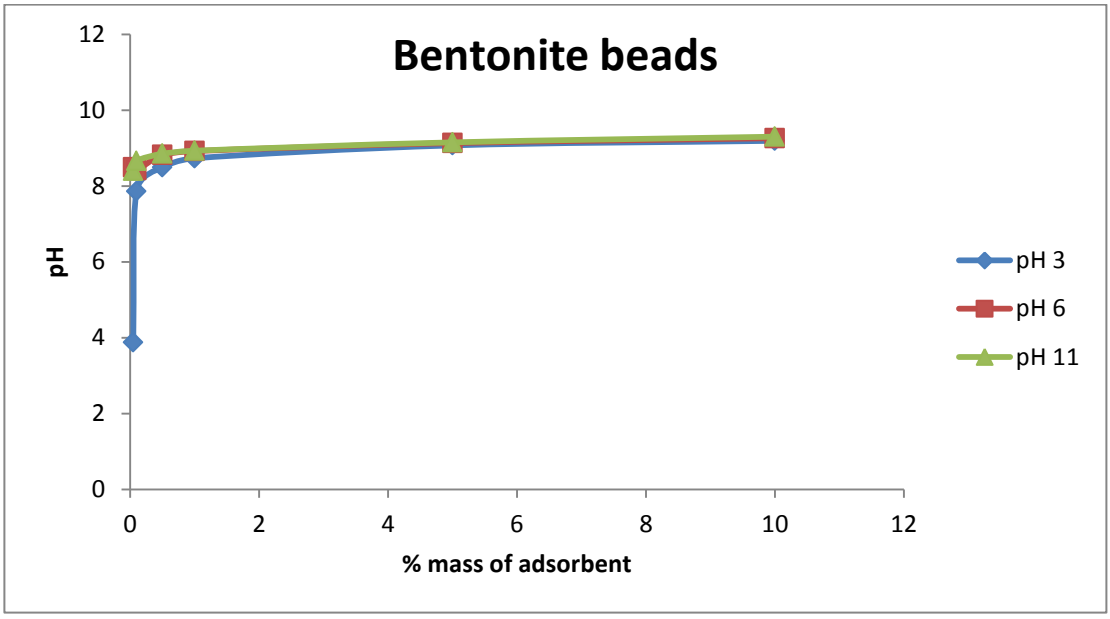


Figure A4: Mass titration results for bentonite beads

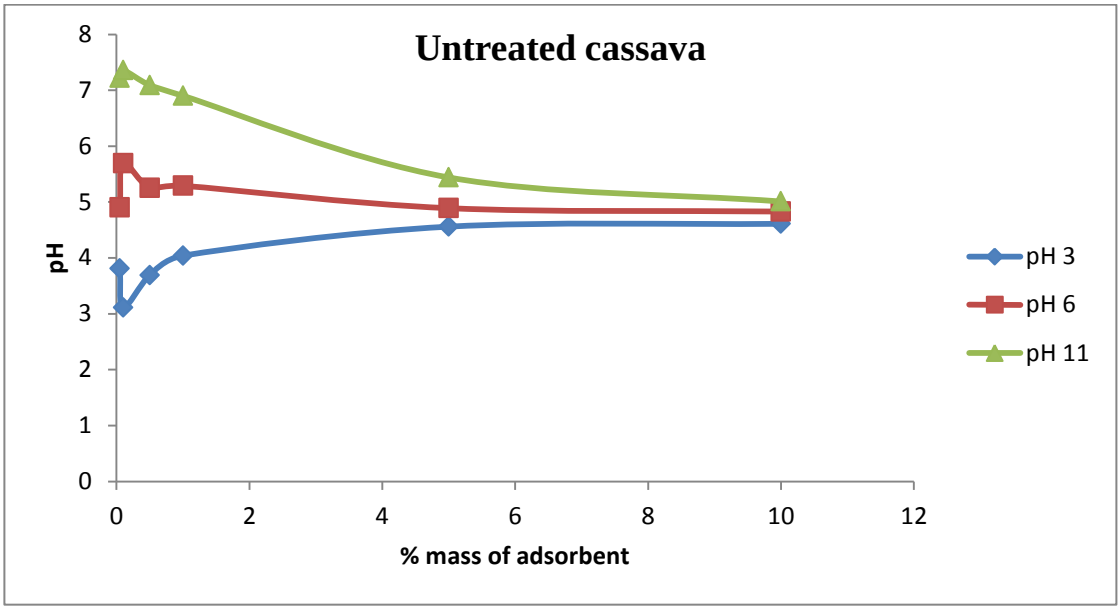


Figure A5: Mass titration results for untreated cassava waste biomass

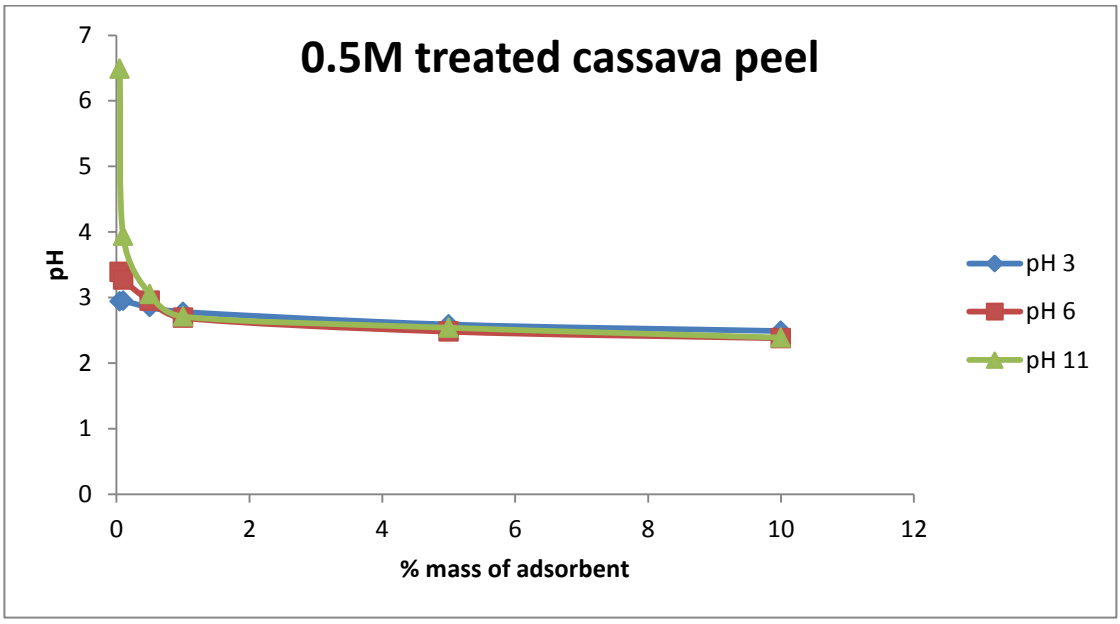


Figure A6: Mass titration results for 0.5M cassava waste biomass

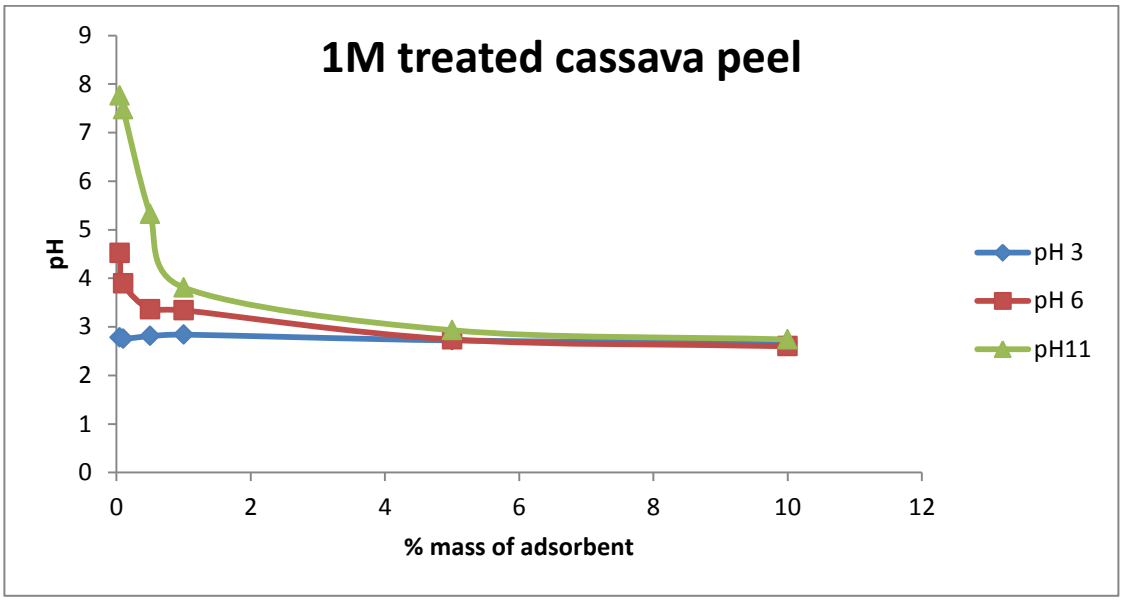


Figure A7: Mass titration results for 1M cassava waste biomass

Data for solution pH changes with time

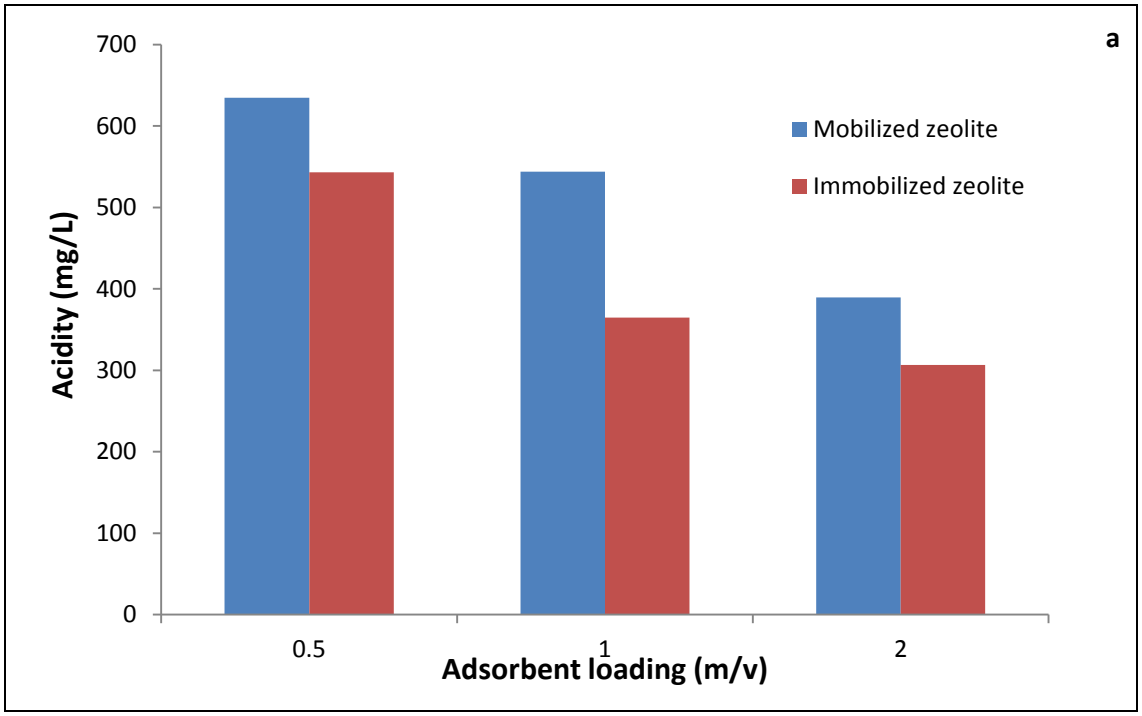
Table A1: Data for solution pH changes with time for bentonite powder and beads

Time (min)	Bentonite powder	Bentonite beads
0	2.16	2.16
10	2.35	2.60
30	2.45	2.69
60	2.40	2.27
120	2.53	2.82
360	3.97	2.87
720	3.83	3.60
1440	3.87	3.87

Table A2: Data for solution pH changes with time for untreated and acid treated cassava waste biomass

Time (min)	Untreated cassava waste	Acid treated cassava waste
0	2.16	2.16
10	2.18	1.88
20	1.93	2.00
30	2.13	2.05
40	2.36	1.95
50	2.29	1.90
60	1.96	1.96
180	2.31	2.10

Solution Acidity



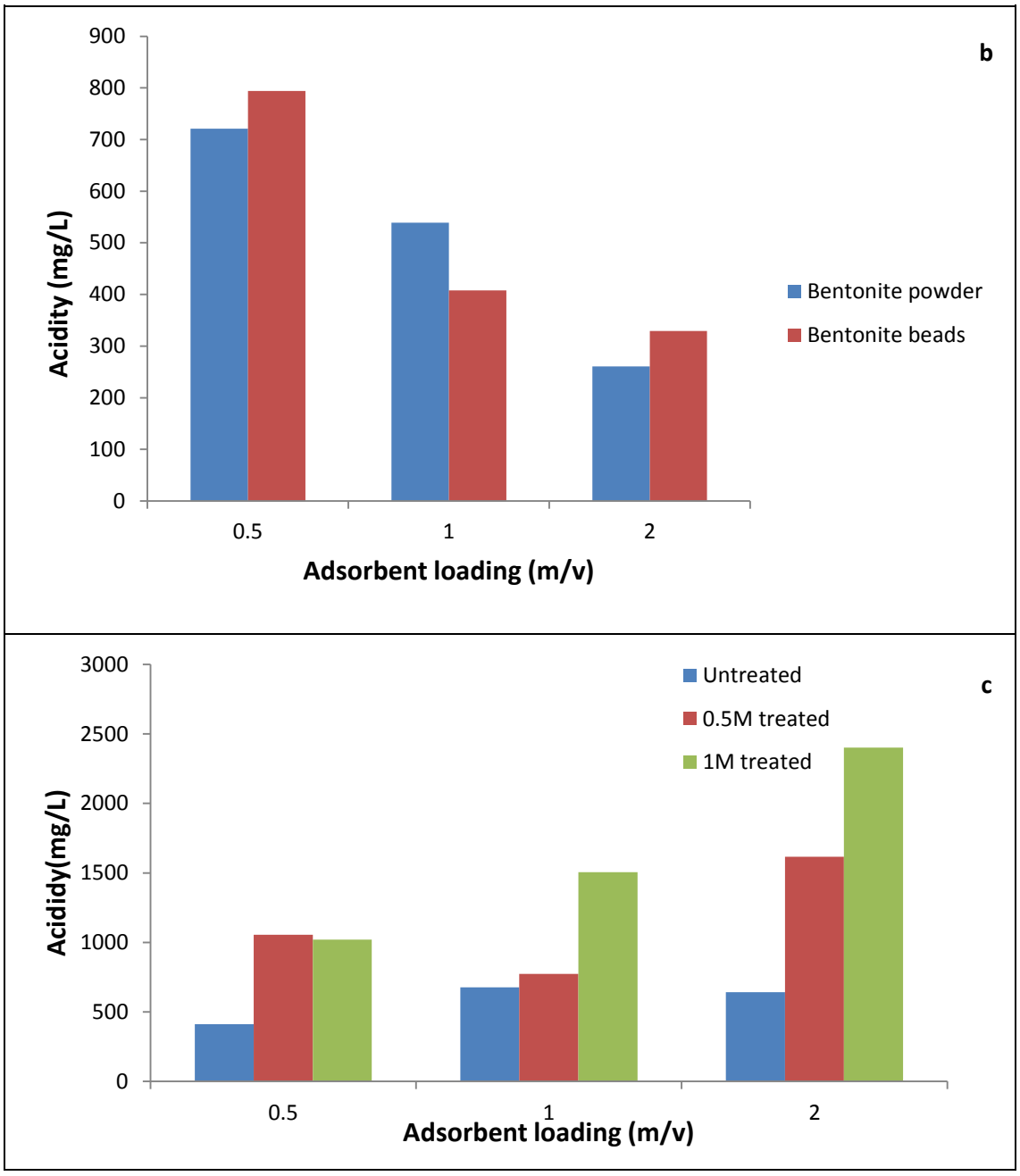
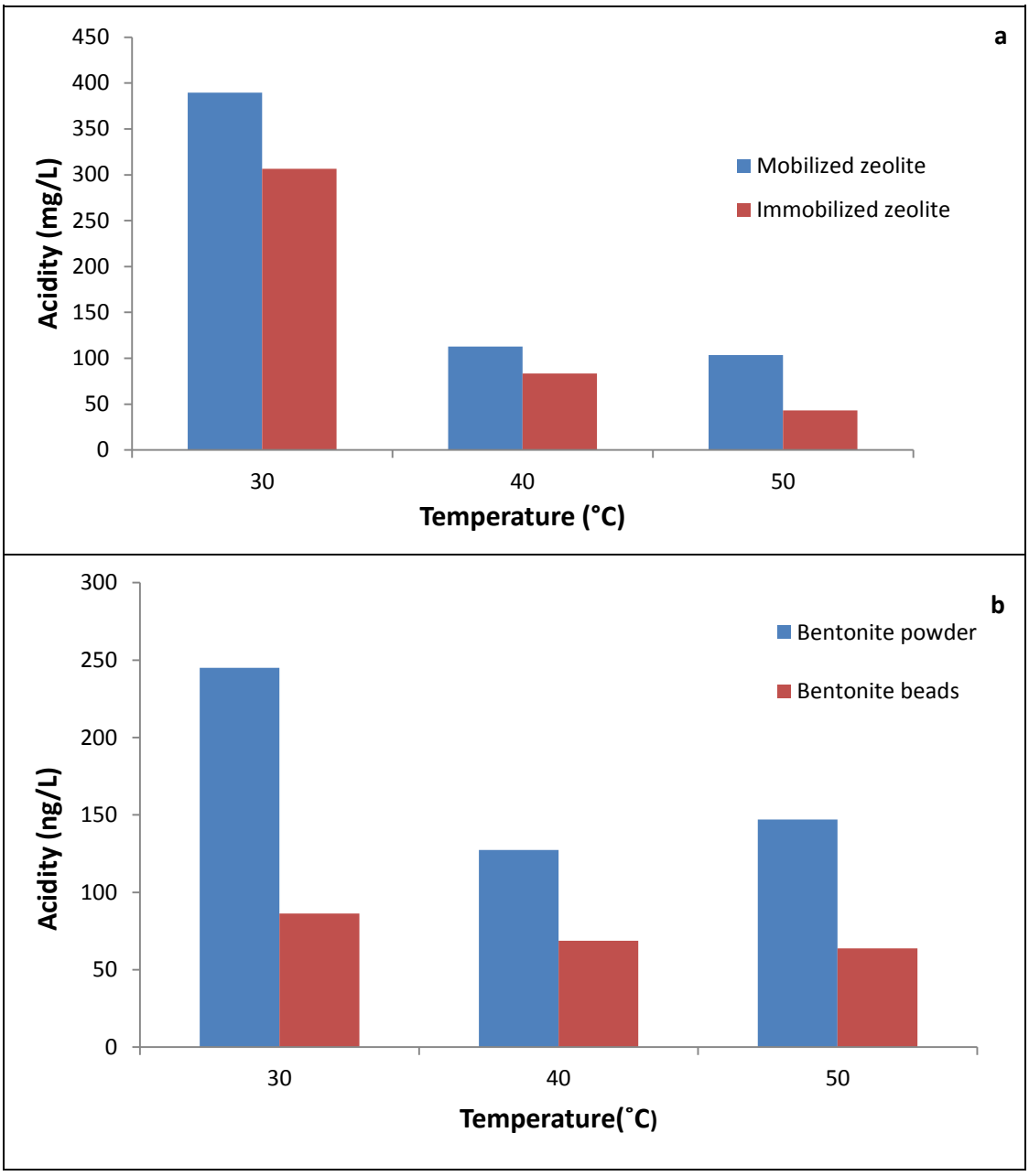


Figure A8: Effect of adsorbent loading on solution acidity using (a) zeolite (b) bentonite (c) cassava peel biomass adsorbents


a
Acidity (mg/L)
450
400
350
300
250
200
150
100
50
0
30
40
50
Temperature (°C)
Mobilized zeolite
Immobilized zeolite
b
Acidity (ng/L)
300
250
200
150
100
50
0
30
40
50
Temperature(˚C)
Bentonite powder
Bentonite beads

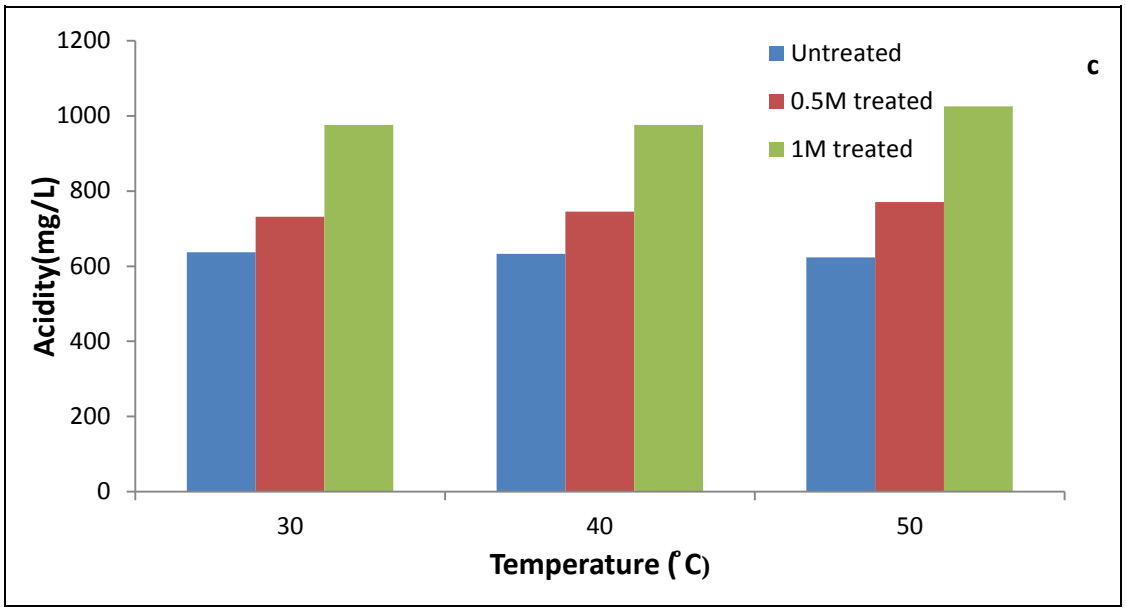
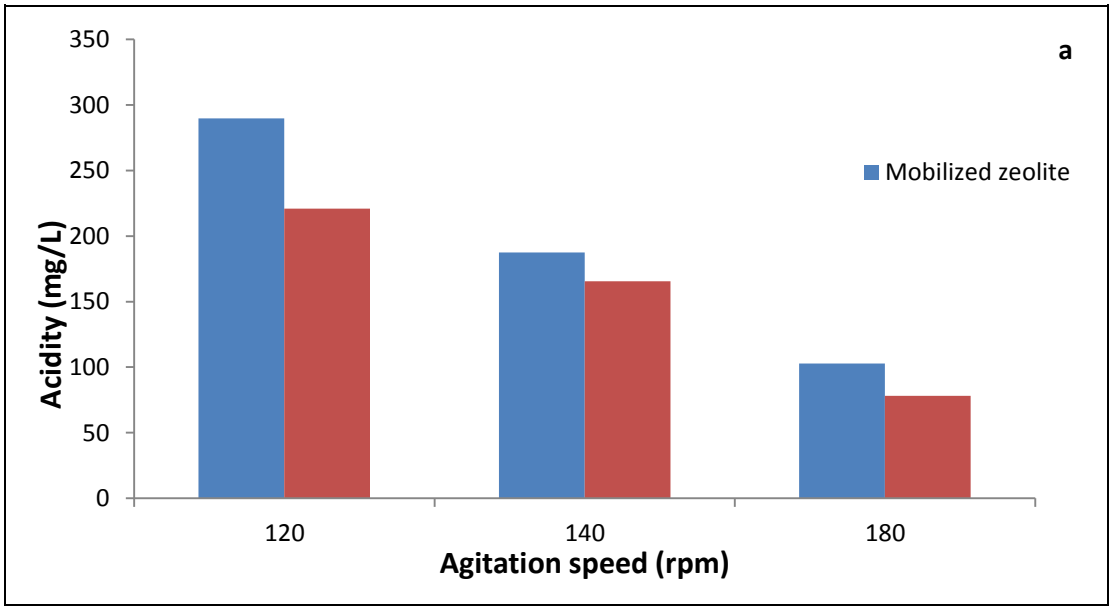


Figure A9: Effect of temperature on solution acidity using (a) zeolite (b) bentonite (c) cassava peel biomass adsorbents



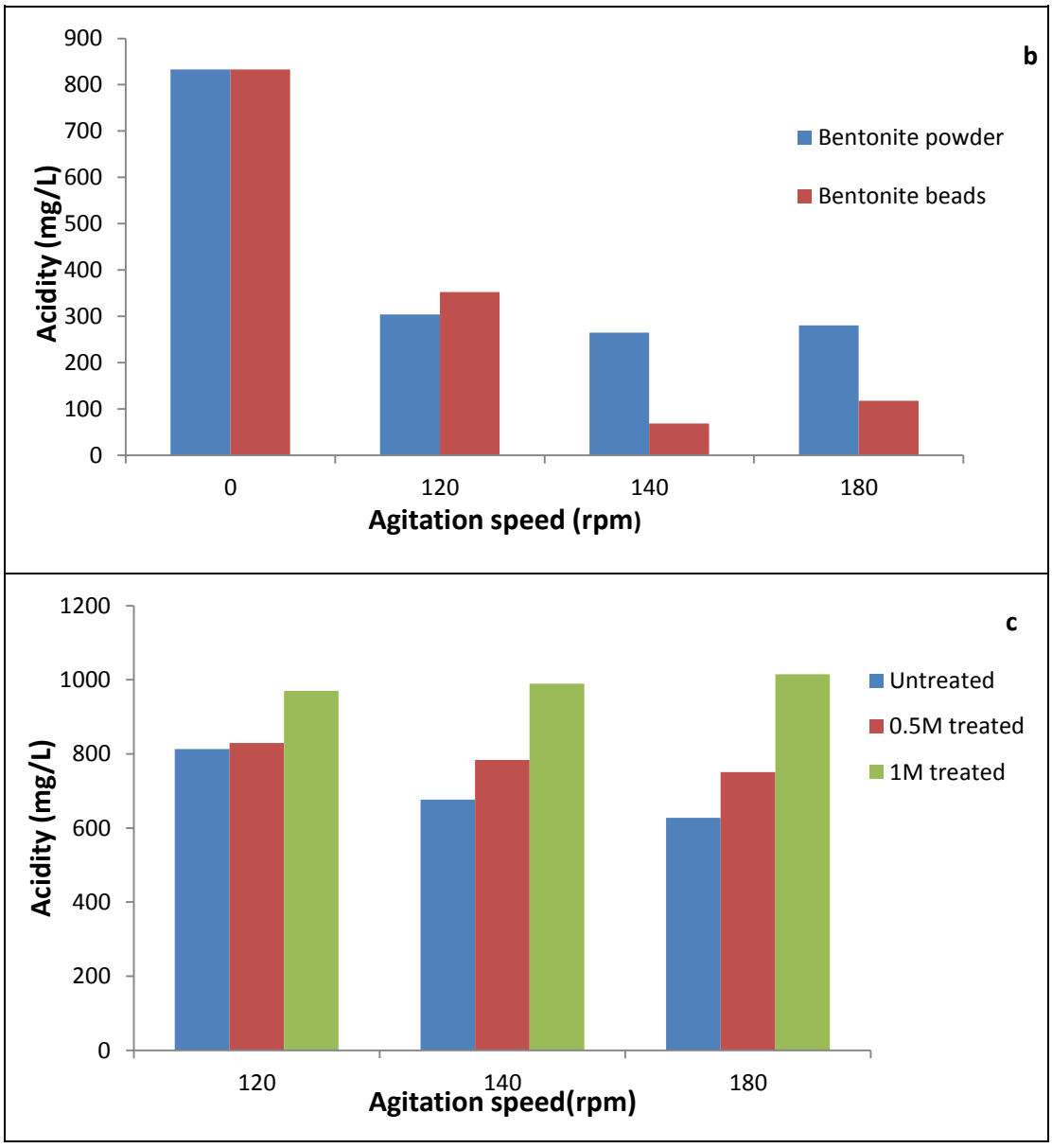
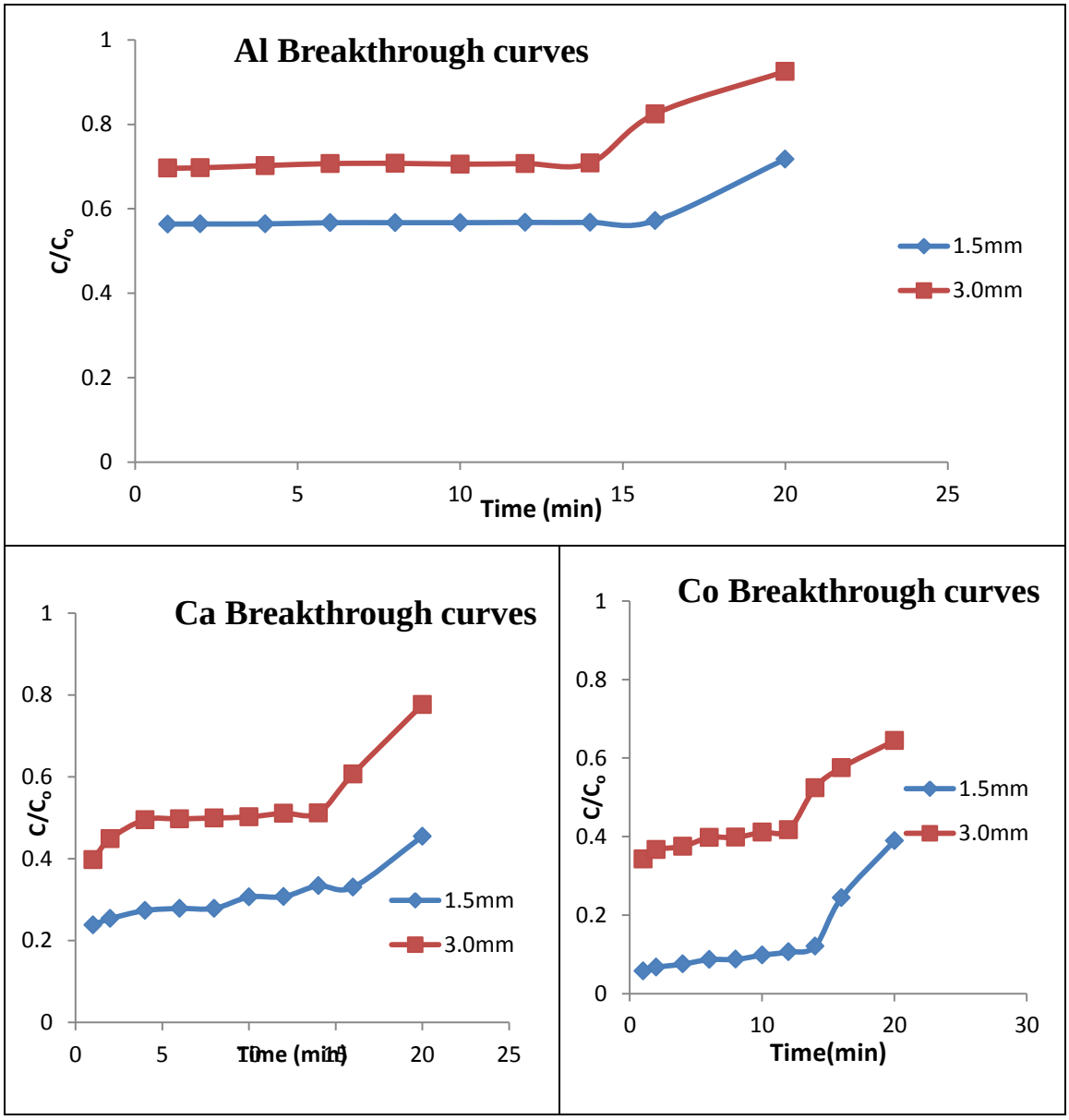


Figure A10: Effect of agitation speed on solution acidity using (a) zeolite (b) bentonite (c) cassava peel biomass adsorbents.

Appendix B

Breakthrough curves for heavy metals in AMD at different biomass bead sizes and using double fixed bed column system



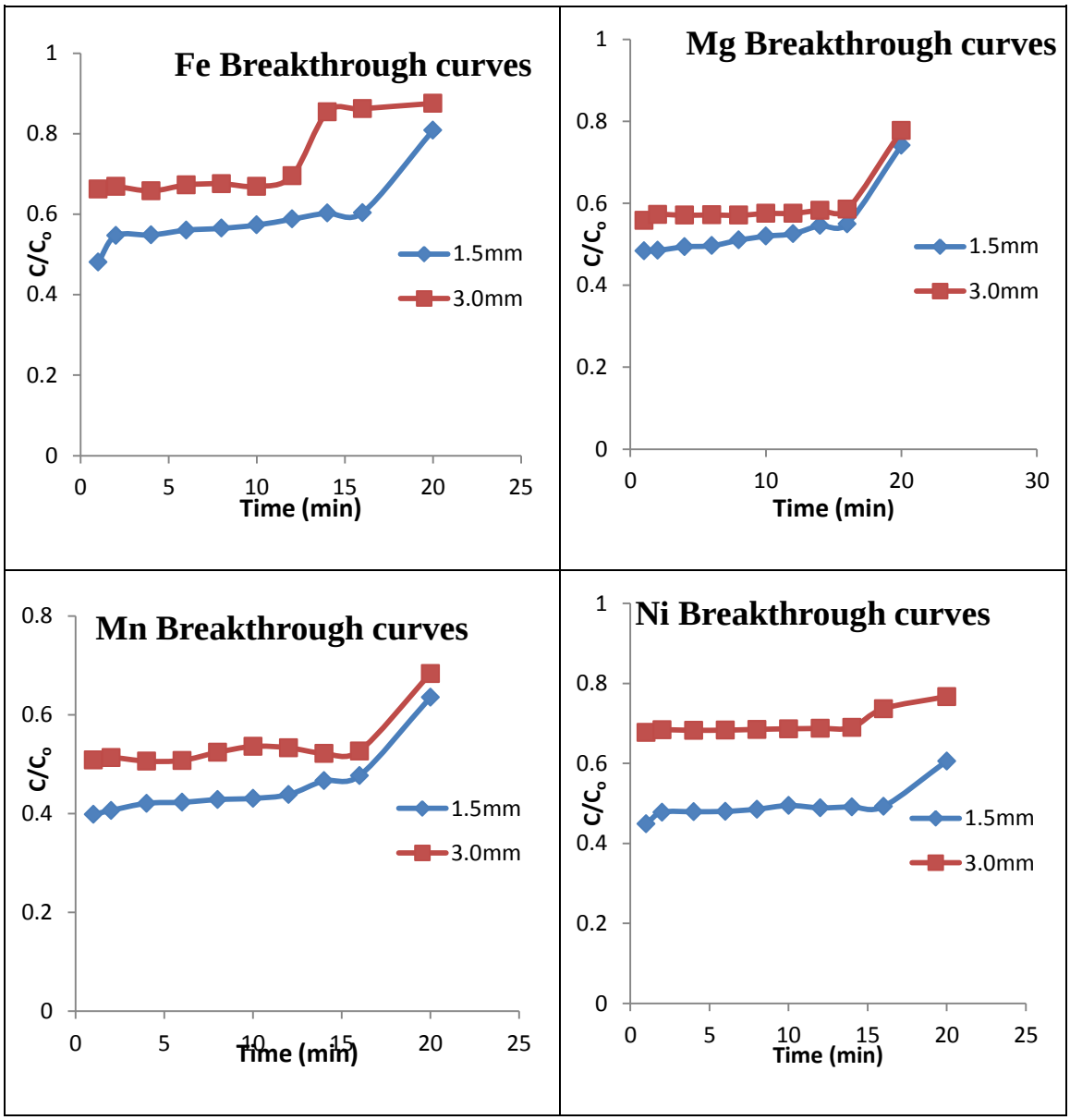
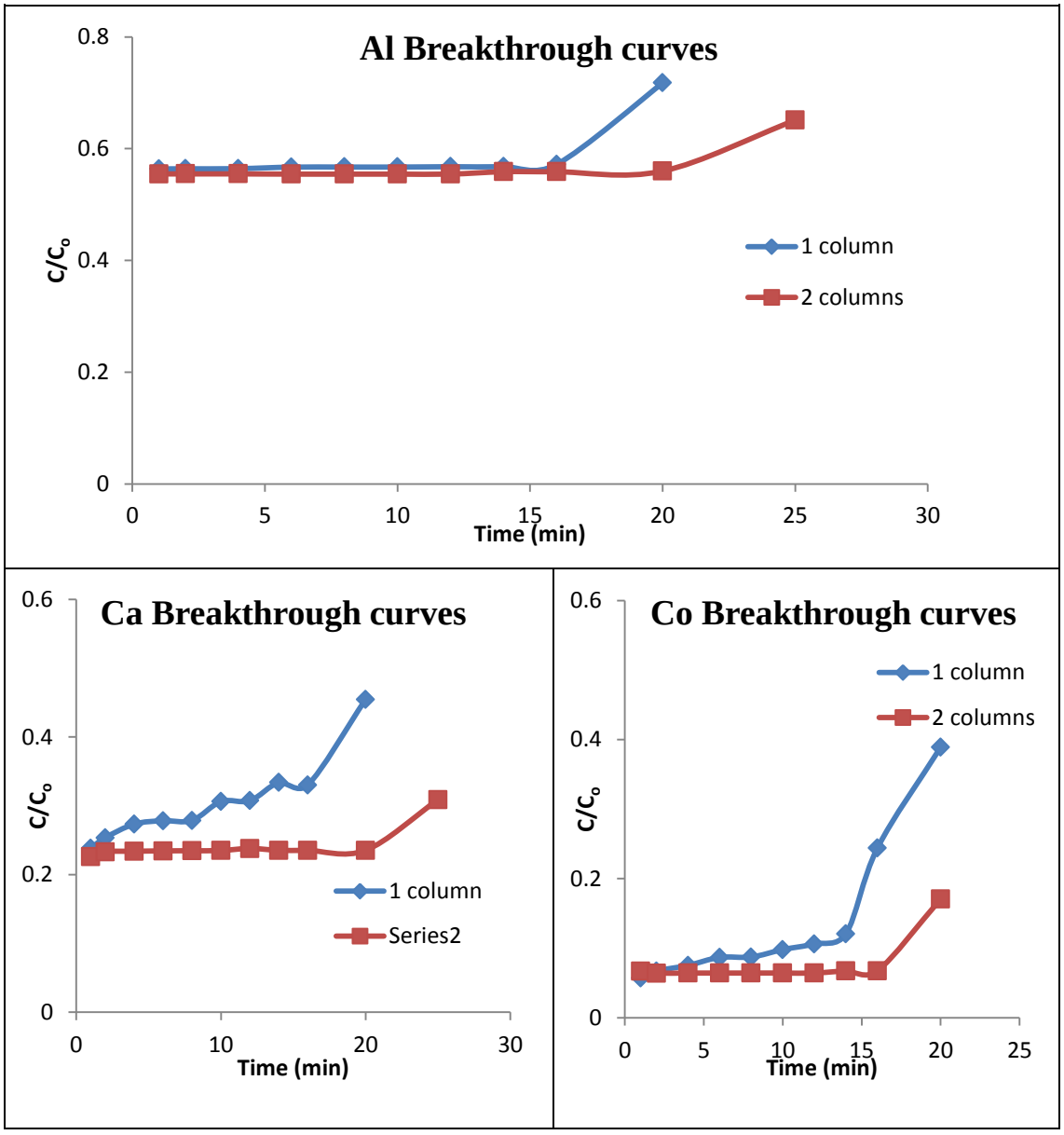


Figure B1: Breakthrough curves for heavy metals in AMD at different biomass bead size (Adsorbent bed height= 45cm, Flow rate =0.89mL/s, Temp. = 25˚C).


Al Breakthrough curves
0.8
0.6
0.4
0.2
0
C/Co
0
5
10
15
20
25
30
Time (min)
1 column
2 columns
Ca Breakthrough curves
0.6
0.4
0.2
0
C/Co
0
10
20
30
Time (min)
1 column
Series2
Co Breakthrough curves
0.6
0.4
0.2
0
C/Co
0
5
10
15
20
25
Time (min)
1 column
2 columns

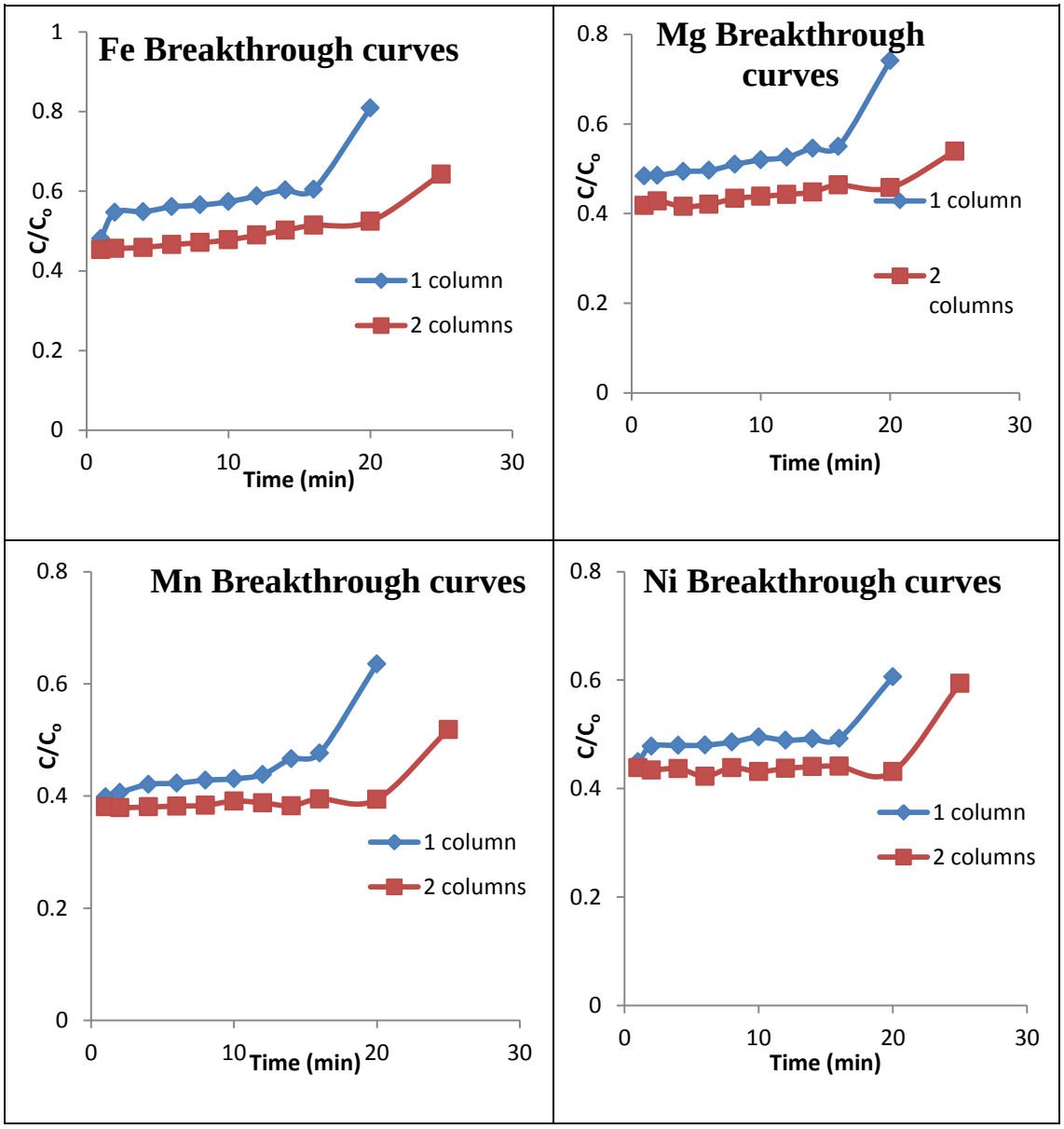


Figure B2: Breakthrough curves for heavy metals in AMD using single and double columns (Adsorbent bed height= 45cm, Flow rate =0.89mL/s, Temp. = 25˚C, adsorbent size= 1.5mm).

Appendix C

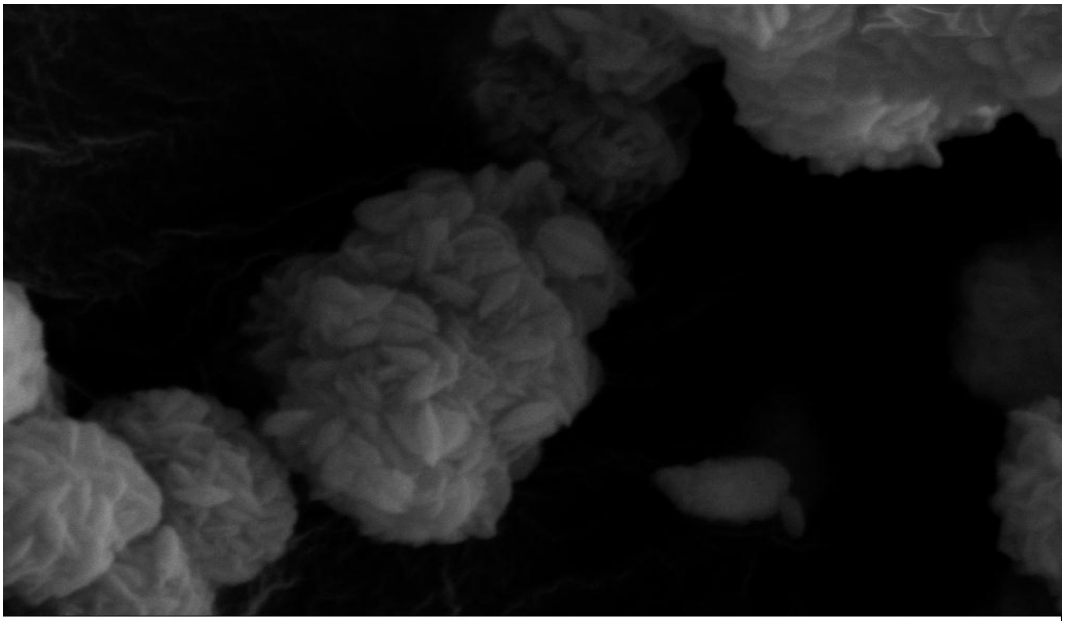


Figure C1: SEM image of iron precipitate formed during evaporation of acid solution.

Calculation of annual raw material requirements

1. $Annual\ CaCl_2\ requirement = \frac{0.2mol}{dm^3} \times \frac{111g}{mol} \times 1800dm^3 \times 48\frac{weeks}{annum} = 1.92t$

   Approximately 2 tons per annum will be required

1. $Annual\ NaCl\ requirement = \frac{0.9}{100} \times 1800dm^3 \times 250 = 4.05t$
2. $Annual\ HNO_3\ requirement = \frac{0.3mol}{dm^3} \times \frac{63g}{mol} \times 1800dm^3 \times 250 = 8.50t$
3. $Annual\ thioglycollic\ acid\ requirement = \frac{1.0mol}{dm^3} \times \frac{92.11g}{mol} \times 1800dm^3 \times 250 = 41t$
4. $Annual\ volume\ of\ resins = \frac{10}{60}hrs \times \frac{1500L}{hr} = 250L$

Total requirement at 44% annual replacement rate = 360L

But density of Dowex MSA resins= 1.06kg/L

$$Annual\ mass\ of\ resins\ required = \ 360L \times 1.06kg/L = 0.3816t$$

Calculation of annual energy requirements

From mass balance 2514.37 kg/h of water need to be vaporized from an initial temperature of 25˚C.

Quantity of energy required = $mC_P\Delta T + ML$

= {(0.69kg/s x 4.187KJ/kg ˚C x (100-25) ˚C**)** + 0.69kg/s x 2260KJ/kg} x 7680hr/ annum

= 13 600 000KWh per year

A total of approximately **14 000MWh** (including the other processes) per year will be required to run the proposed process.

Figure C2: Mass balance of proposed process (Attached separately).